EIGENVALUE DISTRIBUTIONS OF WILSON LOOPS

DISSERTATION
ZUR ERLANGUNG DES DOKTORGRADES
DER NATURWISSENSCHAFTEN (DR. RER. NAT.)
DER NATURWISSENSCHAFTLICHEN FAKULTÄT II – PHYSIK
DER UNIVERSITÄT REGENSBURG

vorgelegt von

Robert Lohmayer

aus

Mühldorf am Inn

2010

Promotionsgesuch eingereicht am: 22. April 2010

Die Arbeit wurde angeleitet von: Prof. Dr. Tilo Wettig

Prüfungsausschuss:

Vorsitzender:	Prof. Dr. Josef Zweck
1. Gutachter:	Prof. Dr. Tilo Wettig
2. Gutachter:	Prof. Dr. Andreas Schäfer
weiterer Prüfer:	Prof. Dr. Thomas Niehaus

Contents

Part I

Introduction

1 Motivation

In 1981, B. Durhuus and P. Olesen had already observed that the eigenvalue density of the untraced Wilson loop matrix associated with a simple non-selfintersecting curve in continuum SU(N) Yang-Mills theory in two Euclidean dimensions undergoes a phase transition[1] in the infinite-N limit as the size of the loop is dilated [1]: The eigenvalues are concentrated around unity for small loops and are uniformly distributed on the unit circle for very large loops. At a critical size of the loop, the gap in the eigenvalue spectrum closes at a point of non-analyticity (derivatives of the eigenvalue density with respect to the area and the angular variable diverge). This transition is unavoidable if confinement occurs and if the Wilson loop matrix is close to the identity for small loops (confinement means that the uniform limit is approached with corrections that are exponentially suppressed in the area enclosed by the loop). The Durhuus-Olesen transition can be viewed as a transition from an ordered or perturbative phase, where the Wilson loop matrix is close to the identity and the spectrum has a gap, to a disordered or non-perturbative phase, where the eigenvalues are randomly distributed over the entire unit circle.

Recently, R. Narayanan and H. Neuberger provided numerical evidence (by extrapolating results from lattice simulations to the continuum) that the eigenvalue distributions of (smeared) SU(N) Wilson loop matrices in three and four Euclidean dimensions also undergo a transition at a critical loop size at large N which is very similar to the Durhuus-Olesen transition of the two-dimensional case. The hypothesis formulated (and tested partly with numerical means) in Ref. [2] states not only that a non-analyticity in the eigenvalue density at a critical loop size occurs in two, three, and four spacetime dimensions but also that the transitions in all these dimensions belong to the same universality class, which means that close to the critical scale, the complicated dependence on the loop shape in three and four dimensions at large but finite N enters only through a finite number of non-universal parameters, which are coefficients of sub-leading terms (to the infinite-N result) of the form N^{ν_i} with a few universal exponents ν_i.

The universal nature of this transition might allow for relating perturbative calculations to non-perturbative models in four spacetime dimensions by requiring smooth matches between small, critical, and large scales. The basic idea would be to consider an observable like, e.g., the extremal zero of the average characteristic polynomial associated to the Wilson loop matrix, and to perform a perturbative calculation in the regime below the transition point. On the other hand, something beyond ordinary field theory would be needed for very large loops. In this case, it might be possible to describe the observable by an effective string theory model, defined in terms of a dimensional string tension. To relate this parameter to the perturbative scale, it is then necessary to join the corresponding regimes over the crossover which separates them. The situation simplifies at large N, when the crossover sharpens and finally becomes a phase transition. If the transition (and

[1] The Durhuus-Olesen transition is not a real phase transition (there are no discontinuities in the partition function and its derivatives); we nevertheless use this terminology to refer to the non-analytic properties of the eigenvalue density.

the manner how the infinite-N limit is approached near the transition point) is indeed universal, and in the same universality class as the Durhuus-Olesen transition in two spacetime dimensions, the scale dependence near the critical scale would be known up to a few non-universal constants. Requiring smooth matches between calculations at small, critical, and large scales could then relate the string tension to the perturbative scale Λ_{QCD}.

To parametrize the crossover, separating small and large scales, one has to work out the details of the two-dimensional case first. In part II of this thesis, we present exact results for the eigenvalue distribution (in two dimensions) at arbitrary finite N. Three different density functions, which all reduce to the known eigenvalue density at infinite N but differ at finite N, are compared to each other at finite N, and the infinite-N limit of these functions is studied by performing saddle-point approximations of associated integral representations.

Due to the very special properties of pure SU(N) gauge theory in two Euclidean dimensions, the universality class of the Durhuus-Olesen transition may be defined in terms of a simple multiplicative random matrix model, which can be viewed as a matrix generalization of the multiplicative random walk on the unitary group. In part III, we relax the unitarity constraint and study a multiplicative random complex matrix model, which is similar to the one introduced by Gudowska-Nowak et al. in Ref. [3], where it was shown that the model leads to an infinite-N phase transition. By combining analytical and numerical methods, we confirm that the domain of non-vanishing eigenvalue density undergoes a topological change, from being simply connected to multiply connected, at a critical point. Furthermore, by introducing additional parameters in the probability distribution of the complex matrix factors, we can smoothly interpolate between the original model and the cases where the individual factors in the product are Hermitian or unitary. This generalization allows for establishing a connection of the topological transition in the complex case to the Durhuus-Olesen transition found in the unitary case. In both cases, the infinite-N transition occurs when the effective number of factors (depending both on the true number of factors and the deviation from the identity matrix for each individual factor) exceeds a certain critical value. Motivating physics applications for this study would be more general gauge theories or special regularization prescriptions making complex matrix valued Wilson loop operators natural observables (e.g., by introducing an extra scalar field with a mass much heavier than the QCD scale in the definition of the Wilson loop operator, cf. part III). If the situation for ordinary gauge theories, where the Wilson loop matrix is unitary, generalizes to the complex case, the multiplicative random complex matrix model might capture the universal features of large-N transitions occurring in these complex field theory models in observables that are related to products of many sufficiently decorrelated matrices close to the identity matrix.

Part IV is somewhat unrelated to the other parts of the thesis. In this last part, we study the entanglement entropy which is obtained by tracing out the degrees of freedom residing inside an imaginary sphere for a free massless scalar field in four-dimensional Euclidean spacetime. At leading order, this entropy is proportional to the area of the sphere, a result which is similar to the area law found for the intrinsic entropy of a black hole. Since existing analytical calculations of subleading terms rely on some non-trivial assumptions (e.g., the replica trick), we determine the next order correction to the area law in four dimensions, a logarithmic term which might be universal, by numerical means.

2 Basic concepts of group theory

In this introductory section, we review the basic concepts of group theory, "the study of symmetry" [4], which is of fundamental importance to a wide range of physical applications. The following discussion of finite groups and continuous Lie groups is based on Refs. [4, 5, 6]. All proofs are omitted.

2.1 Basic definitions

A *group* G is a set of elements g_1, g_2, etc., for which a law of composition (in the following called "multiplication") is given so that the "product" $g_1 g_2$ of any two elements is well-defined and which satisfies the following conditions:

- If g_1 and g_2 are elements of the set, then the product $g_1 g_2$ is an element of the set, too.
- Multiplication is associative, i.e., $g_1(g_2 g_3) = (g_1 g_2) g_3$.
- The set contains an element e, called the *identity*, such that $ge = eg = g$ for every element $g \in G$.
- If g_1 is in the set, then so is an element g_2 such that $g_1 g_2 = g_2 g_1 = e$. The element g_2 is called the *inverse* of g_1 and is denoted by $g_2 = g_1^{-1}$.

Although we usually refer to the law of composition as "multiplication", this does not necessarily imply ordinary multiplication. (Consider, for example, the set of integers, which form a group under the composition law of ordinary addition.)

Two elements g_1, g_2 are said to *commute* with each other if $g_1 g_2 = g_2 g_1$. If all the elements of a group commute with one another, the group is called *Abelian*.

If the number of group elements is finite, the group is said to be *finite*, and the number of its elements is called the *order* of the group. Otherwise, the group is said to be *infinite*.

If a subset $H \subseteq G$ forms a group under the same law of multiplication that defines the group G, H is said to be a *subgroup* of the group G. Every group has two trivial subgroups, the identity element and the whole group itself.

An element $g_1 \in G$ is said to be *conjugate* to the element $g_2 \in G$ if there is an element $g_3 \in G$ such that $g_3 g_2 g_3^{-1} = g_1$. It is obvious that if g_1 is conjugate to g_2, then g_2 is conjugate to g_1. Furthermore, if g_1 is conjugate to g_2, and g_2 is conjugate to g_3, then g_3 is conjugate to g_1. This means that we have a relation between elements which fulfills the requirements of an equivalence relation. Therefore, it can be used to separate the group into *conjugacy classes* of elements which are conjugate to one another.

A subgroup $H \subseteq G$ is called *invariant* or *self-conjugate* if $ghg^{-1} \in H$ for every $h \in H$ and $g \in G$.

2.2 Representations and characters

A *representation* of a group G is a mapping Γ of the elements of G onto a set of invertible linear operators, acting on a vector space V, with the following properties:

- $\Gamma(e) = \mathbf{1}$, where $\mathbf{1}$ is the identity operator which leaves all vectors in V unchanged.
- $\Gamma(g_1 g_2) = \Gamma(g_1)\Gamma(g_2)$, i.e., the group multiplication law is mapped onto the natural multiplication of the linear operators.

We call Γ a *faithful* representation if the mapping is injective, i.e., if $\Gamma(g_1) = \Gamma(g_2)$ implies that $g_1 = g_2$ for all $g_1, g_2 \in G$.

If the dimensionality of the *representation space* V is n, we say that Γ is an *n-dimensional representation* of the group G. After choosing a basis in the n-dimensional space V, the linear operators can be described by their matrix representatives and we obtain a mapping of the group G on a group of $n \times n$ matrices $\Gamma(G)$, which we call a *matrix representation* of G. When we deal with several different representations, we use superscripts to distinguish among them, e.g., $\Gamma^{(\mu)}(G)$.

A representation Γ is called a *unitary representation* if the matrices $\Gamma(g)$ are unitary for all $g \in G$, i.e., $\Gamma(g)^{-1} = \Gamma(g)^\dagger$ (the symbol $\dagger$ denotes transposition and complex conjugation).

If we change the basis in the vector space V, the matrices $\Gamma^{(\mu)}(g)$ are replaced by matrices $\Gamma^{(\nu)}(g) = S\Gamma^{(\mu)}(g)S^{-1}$ with some invertible matrix S. Those transformed matrices also provide a representation of the group, which is equivalent to the original representation $\Gamma^{(\mu)}$ (although the matrices may look different). One can show that every representation of a finite group is equivalent to a unitary representation.

The trace of a matrix $\Gamma^{(\mu)}(g)$ is invariant under a change of basis due to the cyclic invariance of the trace, $\mathrm{Tr}(AB) = \mathrm{Tr}(BA)$. For group representations, the trace $\sum_{i=1}^{n} \Gamma_{ii}^{(\mu)}(g)$ is called the *character* of g in the representation $\Gamma^{(\mu)}$ and is denoted by

$$\chi^{(\mu)}(g) = \sum_{i=1}^{n} \Gamma_{ii}^{(\mu)}(g)\,. \tag{2.1}$$

Equivalent representations obviously have the same set of characters. Furthermore, elements which are conjugate to each other have the same character, i.e., the same number is assigned to all the elements in a given conjugacy class of the group G. If the group has m classes K_i, $i = 1, \ldots, m$, each representation $\Gamma^{(\mu)}$ can be described by a set of m numbers $\chi_i^{(\mu)}$ ($\chi^{(\mu)}(g) = \chi_i^{(\mu)}$ for all $g \in K_i$).

A representation Γ is called *reducible* if there is an invariant subspace $U \subset V$ under Γ (with $\dim(U) < \dim(V)$), i.e., for every $g \in G$, $u \in U$ we have $\Gamma(g)u \in U$. The representation Γ is said to be *irreducible* if it is not reducible, i.e., if V does not have any invariant subspaces under Γ. If Γ is equivalent to a representation in which all the matrices have block diagonal form (the $\Gamma^{(i)}(g)$ below are square matrices)

$$\Gamma(g) = \begin{pmatrix} \Gamma^{(1)}(g) & 0 & \ldots \\ 0 & \Gamma^{(2)}(g) & \ldots \\ \vdots & \vdots & \ddots \end{pmatrix}, \tag{2.2}$$

we call Γ a *fully reducible* representation. A representation Γ in block diagonal form is said to be the *direct sum* of the subrepresentations $\Gamma^{(i)}$,

$$\Gamma = \Gamma^{(1)} \oplus \Gamma^{(2)} \oplus \ldots\,. \tag{2.3}$$

By transforming a fully reducible representation to block diagonal form (with maximum number of blocks), we are decomposing the original representation into a direct sum of its irreducible components.

For unitary representations, reducibility implies full reducibility, which means that for finite groups, reducible representations always decompose into a sum of irreducible representations.

Considering all non-equivalent irreducible representations of a finite group G of order N, one can prove that the quantities $\Gamma_{ij}^{(\mu)}(g)$, for fixed μ, i, j, form an N-dimensional

vector such that

$$\sum_{g\in G}\Gamma^{(\mu)}_{ij}(g)\Gamma^{(\nu)}_{kl}(g^{-1}) = \frac{N}{n_\mu}\delta_{\mu\nu}\delta_{il}\delta_{jk}\,, \tag{2.4}$$

where n_μ is the dimension of the representation $\Gamma^{(\mu)}$. In the derivation of this orthogonality relation, one has to make use of the so-called *rearrangement theorem*: If $f(g)$ is a function defined on the group, then

$$\sum_{g\in G} f(g) = \sum_{g\in G} f(gh) \qquad \forall h \in G\,. \tag{2.5}$$

For unitary representations, Eq. (2.4) reads

$$\sum_{g\in G}\Gamma^{(\mu)}_{ij}(g)\Gamma^{(\nu)*}_{lk}(g) = \frac{N}{n_\mu}\delta_{\mu\nu}\delta_{il}\delta_{jk}\,. \tag{2.6}$$

This means that every irreducible representation $\Gamma^{(\mu)}$ leads to n_μ^2 vectors $\Gamma^{(\mu)}_{ij}(g)$, $1 \le i,j \le n_\mu$, which are orthogonal to each other and to all the vectors $\Gamma^{(\nu)}_{ij}(g)$ obtained from non-equivalent irreducible representations. Since the number of orthogonal vectors cannot exceed N, the dimension of the space, we have

$$\sum_\mu n_\mu^2 \le N\,, \tag{2.7}$$

where the sum is over all non-equivalent irreducible representations. Equation (2.7) evidently implies that the number of non-equivalent irreducible representations of a finite group is finite.

Setting $i = j$ and $k = l$ in Eq. (2.4) and summing over all i and k leads to orthogonality relations for the characters,

$$\frac{1}{N}\sum_{g\in G}\chi^{(\mu)}(g)\chi^{(\nu)}(g^{-1}) = \delta_{\mu\nu}\,, \tag{2.8}$$

or, if the representation is unitary,

$$\frac{1}{N}\sum_{g\in G}\chi^{(\mu)}(g)\chi^{(\nu)*}(g) = \delta_{\mu\nu}\,. \tag{2.9}$$

Hence, the characters of independent irreducible representations are orthogonal to each other. Furthermore, they are constant on conjugacy classes, and one can show that they form a complete basis for all functions that are constant on conjugacy classes. This has an important consequence: The number of inequivalent irreducible representations is equal to the number of conjugacy classes.

For any finite group of order N, we can define an N-dimensional vector space by taking the group elements themselves to form an orthonormal basis g_1, g_2,...,g_N of the vector space. If we now define

$$\Gamma(g_1)g_2 = g_1 g_2\,, \tag{2.10}$$

we obtain an N-dimensional representation Γ of the group which is referred to as the *regular representation*.

Using the orthogonality relation of the characters, one finds that the number of times each irreducible representation is contained in the regular representation is equal to the dimension of the irreducible representation (this implies that we can replace Eq. (2.7) by a strict equality).

2.3 Group algebra

Consider again the N-dimensional vector space constructed from the elements g of a finite group G of order N. An element x of this vector space can be written as

$$x = \sum_g x_g g \,, \tag{2.11}$$

where the coefficients x_g are the coordinates of the vector x in the basis which is obtained by taking the group elements themselves as basis vectors. We can use the multiplication law of the group to define the product of two vectors $x = \sum_g x_g g$ and $y = \sum_h y_h h$, which is contained in the space,

$$z = xy = \sum_{g,h} x_g y_h gh = \sum_f \left(\sum_g x_g y_{g^{-1}f} \right) f = \sum_f \left(\sum_h x_{fh^{-1}} y_h \right) f \,. \tag{2.12}$$

This linear vector space, which is closed under the multiplication law induced by the multiplication law of the group, is called the *group algebra* A.

Any representation of the group G immediately leads to a representation of the algebra A in the following way: If $x = \sum_g x_g g$, we simply take

$$\Gamma(x) = \sum_g x_g \Gamma(g) \,. \tag{2.13}$$

Similarly, any representation of the algebra gives a representation of the group. Furthermore, if one of these representations is reducible (or irreducible), then so is the other.

A *subalgebra* $B \subset A$ is a vector space which is contained in the algebra A and which is closed under the law of multiplication of A. If a subalgebra B has the property that $ab \in B$ for all elements $a \in A$ and $b \in B$, it is referred to as a *left ideal*. If the left ideal B in turn does not contain subalgebras which are left ideals, B is called *minimal* and provides an irreducible representation of the algebra A.

Since the regular representation is fully reducible, the algebra A is given by a direct sum of minimal left ideals B_i, i.e.,

$$A = B_1 \oplus B_2 \oplus \ldots \oplus B_k \,. \tag{2.14}$$

This means that any element $a \in A$ is uniquely expressible as the sum of elements of the ideals B_i,

$$a = a_1 + a_2 + \ldots + a_k \,, \qquad a_i \in B_i \,. \tag{2.15}$$

Only the element 0 is common to the subalgebras B_i. Since the unit element e of the group G is an element of the group algebra A, it decomposes into

$$e = e_1 + e_2 + \ldots + e_k \,, \qquad e_i \in B_i \,. \tag{2.16}$$

Multiplying this equation with a and comparing with Eq. (2.15), we see that

$$a_i = a e_i \,, \qquad 1 \leq i \leq k \,. \tag{2.17}$$

The resolution of the unit element e into its parts $e_i \in B_i$ leads to generators of the ideals B_i since $ae_i \in B_i$ for all $a \in A$ and $a_i e_i = a_i$ for all $a_i \in B_i$. The elements e_i are *idempotent*, i.e., $e_i^2 = e_i$, and in addition $e_i e_j = 0$ for $i \neq j$. If e_i generates a minimal left ideal, e_i is called a *primitive* idempotent.

Furthermore, any idempotent element of the group algebra generates a left ideal, giving a representation which is contained in the regular representation. In the next section, we will use this relation to construct all irreducible representations of the so-called symmetric group.

2.4 The symmetric group

The permutations of degree n, denoted by

$$\begin{pmatrix} 1 & 2 & \dots & n \\ p_1 & p_2 & \dots & p_n \end{pmatrix}, \tag{2.18}$$

form the *symmetric group* S_n, which is of central importance for both mathematics and physics. Acting with the above permutation on an ordered set of n elements brings the first element to position p_1, the second element to position p_2, etc. ($1 \leq p_i \leq n$, $p_i \neq p_j$ for $i \neq j$). The order of S_n is $n!$.

Any element of S_n can be written in terms of *cycles*. A cycle is a cyclic permutation of a subset and is written as a set of numbers in parentheses, indicating the set of elements that is cyclically permuted, e.g., the cycle (3468) of S_8 takes $3 \to 4 \to 6 \to 8 \to 3$ and can be viewed as an abbreviation (omitting unpermuted symbols) for the permutation

$$(3468) \equiv \begin{pmatrix} 1 & 2 & 3 & 4 & 5 & 6 & 7 & 8 \\ 1 & 2 & 4 & 6 & 5 & 8 & 7 & 3 \end{pmatrix}. \tag{2.19}$$

Each element of S_n can be written as a product of disjoint cycles (involving each integer from 1 to n in exactly one cycle), e.g.,

$$\begin{pmatrix} 1 & 2 & 3 & 4 & 5 & 6 & 7 & 8 \\ 2 & 5 & 4 & 6 & 1 & 8 & 7 & 3 \end{pmatrix} = (3468)(251)(7)\,. \tag{2.20}$$

An arbitrary element of S_n has k_j j-cycles (a j-cycle permutes j elements), such that

$$\sum_{j=1}^{n} j k_j = n\,. \tag{2.21}$$

Since the disjoint cycles have no elements in common, they commute with each other, and the order in which we write the cycles is irrelevant. A 2-cycle is called a *transposition*.

On the other hand, any permutation can be written as a product of transpositions (having elements in common), e.g.,

$$(123) = (13)(12)\,, \tag{2.22}$$

where we use the convention that the product $g_1 g_2$ of two permutations is obtained by applying first the permutation g_2 to a set of n elements, which are afterwards permuted according to g_1. A j-cycle is equal to a product of $j-1$ transpositions. If a permutation can be decomposed into an even (resp. odd) number of transpositions, the permutation is called even (resp. odd).

It is easy to see that conjugate elements have the same cycle structure. For any $g \in S_n$, conjugation with a transposition $(p_1 p_2)$ just interchanges the numbers p_1 and p_2 in the (disjoint) cycle decomposition of g, e.g.,

$$(34)^{-1}\,((123)(45))\,(34) = (124)(35)\,. \tag{2.23}$$

Since all elements of S_n can be decomposed into transpositions, the conjugacy classes of S_n consist of all possible permutations with a particular cycle structure. This means that they can be identified by the integers k_j, the number of j-cycles. The number of different permutations in a conjugacy class is given by

$$\frac{n!}{\prod_j j^{k_j} k_j!} \tag{2.24}$$

because changing the order between cycles and cyclic order within a cycle is irrelevant.

Therefore, each conjugacy class of S_n corresponds to a partition $(\lambda) = (\lambda_1, \lambda_2, \ldots, \lambda_m)$ of n given by a set of positive integers λ_i with

$$\lambda_1 \geq \lambda_2 \geq \ldots \geq \lambda_m\,, \qquad \sum_{i=1}^{m} \lambda_i = n\,. \tag{2.25}$$

Two partitions (λ) and (μ) are equal if $\lambda_i = \mu_i$ for all i. It is useful to associate to the partition (λ) of n a diagram, consisting of r rows with λ_i boxes in the i-th row (starting with λ_1 boxes in the top row). A diagram of this form is called a *Young diagram*. The partition (λ) corresponds to the conjugacy class of permutations which can be decomposed into m (disjoint) cycles of length λ_1, λ_2, ..., λ_m. For example, the conjugacy class of S_{11} which contains permutations consisting of a 4-cycle, two 3-cycles, and a 1-cycle is identified with the diagram

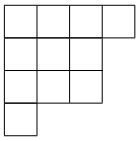

. (2.26)

Since the number of conjugacy classes is equal to the number of irreducible representations, the diagrams are in one-to-one correspondence with the irreducible representations of S_n. The Young diagrams can be used to construct the irreducible representations by identifying appropriate subspaces of the regular representation of S_n, which contains all irreducible representations.

For any partition (λ) of n, we draw the corresponding Young diagram and insert the numbers from 1 to n into the diagram in any order (this is called a *Young tableau*). A Young tableau is said to be a *normal* Young tableau if the numbers from 1 to n are inserted in increasing order, first from left to right, then from top to bottom. For each Young diagram there is only one normal Young tableau. If the numbers in a Young tableau increase from left to right in each row and from top to bottom in each column (the numbers do not necessarily have to be ordered), the tableau is called a *standard* Young tableau. A normal Young tableau is, e.g.,

1	2
3	4

, (2.27)

whereas

1	3
2	4

(2.28)

is another standard Young tableau obtained from the same diagram.

For a fixed tableau, a horizontal permutation h is a permutation which interchanges only symbols in the same row, a vertical permutation v interchanges only symbols in the same column. We now construct two elements of the group algebra of S_n, the so-called symmetrizer s and the anti-symmetrizer a,

$$s = \sum_h h\,, \qquad a = \sum_v \delta_v v\,, \tag{2.29}$$

where the sum is over all horizontal, resp. vertical permutations, and δ_v is the parity of the permutation v ($\delta_v = 1$ if v is even, $\delta_v = -1$ if v is odd). Then one can show that the *Young operator*

$$y = as \tag{2.30}$$

is essentially idempotent, i.e., idempotent up to a normalization constant, and generates a left ideal which provides an irreducible representation of S_n. Different tableaux obtained from the same diagram give equivalent irreducible representations. On the other hand, representations corresponding to different diagrams are inequivalent.

Therefore, the Young operators corresponding to normal Young tableaux generate all inequivalent irreducible representations of S_n. The regular representation can be completely decomposed into irreducible representations by using all Young operators corresponding to standard Young tableaux.

Consider, e.g., $n = 3$: The standard Young tableaux are

$$\begin{array}{|c|c|c|}\hline 1&2&3\\\hline\end{array}\,,\quad \begin{array}{|c|c|}\hline 1&2\\\hline 3\\\cline{1-1}\end{array}\,,\quad \begin{array}{|c|c|}\hline 1&3\\\hline 2\\\cline{1-1}\end{array}\,,\quad \begin{array}{|c|}\hline 1\\\hline 2\\\hline 3\\\hline\end{array}\,, \tag{2.31}$$

and the corresponding Young operators are given by

$$y_1 = \sum_{p\in S_n} p = e + (12) + (13) + (23) + (123) + (132)\,, \tag{2.32}$$

$$y_2 = (e - (13))(e + (12)) = e + (12) - (13) - (123)\,, \tag{2.33}$$

$$y_3 = (e - (12))(e + (13)) = e + (13) - (12) - (132)\,, \tag{2.34}$$

$$y_4 = \sum_{p\in S_n} \delta_p p = e - (12) - (13) - (23) + (123) + (132)\,. \tag{2.35}$$

These operators are essential idempotent and the resolution of the unit element into primitive idempotents is found to be

$$e = \frac{1}{6}y_1 + \frac{1}{6}y_4 + \frac{1}{3}y_2 + \frac{1}{3}y_3\,. \tag{2.36}$$

The Young operators y_1 and y_4 each generate a one-dimensional irreducible representation of S_n (the identity representation and the alternating representation), which are inequivalent. The two-dimensional irreducible representations generated by y_2 and y_3 are equivalent. This is in agreement with the general result that the number of times an irreducible representation is contained in the regular representation is equal to its dimensionality (cf. Sec. 2.2).

2.5 Lie groups

In the next sections, we will consider infinite groups G, where the group elements $g \in G$ depend continuously on a finite set of real parameters $\alpha_1,\ \alpha_2, \ldots, \alpha_r$,

$$g = g(\alpha_1, \alpha_2, \ldots, \alpha_r) \equiv g(\alpha)\,. \tag{2.37}$$

Two group elements $g(\alpha)$ and $g(\alpha')$ are said to be close if the distance $\|\alpha - \alpha'\|$ in the parameter space is small. The multiplication law is

$$g(\alpha)g(\alpha') = g(\alpha'') \tag{2.38}$$

with

$$\alpha''_i = f_i(\alpha_1, \ldots, \alpha_r; \alpha'_1, \ldots, \alpha'_r)\,, \qquad 1 \le i \le r\,. \tag{2.39}$$

Let the identity element $e \in G$ correspond to the parameters $\alpha^0 = (\alpha_1^0, \ldots, \alpha_r^0)$. Every $g(\alpha) \in G$ must have an inverse $g^{-1} \in G$, corresponding to some point $\bar{\alpha} = (\bar{\alpha}_1, \ldots, \bar{\alpha}_r)$ in the space of parameters which has to fulfill

$$f_i(\alpha_1, \ldots, \alpha_r; \bar{\alpha}_1, \ldots, \bar{\alpha}_r) = f_i(\bar{\alpha}_1, \ldots, \bar{\alpha}_r; \alpha_1, \ldots, \alpha_r) = \alpha_i^0 \,. \tag{2.40}$$

If these equations can be inverted, i.e.,

$$\bar{\alpha}_i = h_i(\alpha_1, \ldots, \alpha_r; \alpha_1^0, \ldots, \alpha_r^0) \,, \tag{2.41}$$

and if the functions h_i and f_i are analytic functions for all i, then the group is called a *Lie group*. A *compact* Lie group is described by parameters α_i which vary over finite and closed intervals.

An example for a Lie group is the general linear group $\mathrm{GL}(n, \mathbb{C}) \equiv \mathrm{GL}(n)$, the group of all non-singular linear transformations in an n-dimensional complex vector space. The *defining* (or *fundamental*) representation is given by complex $n \times n$ matrices M with $\det M \neq 0$, the multiplication law is just ordinary matrix multiplication.

The unitary groups $\mathrm{U}(n)$ and $\mathrm{SU}(n)$ are subgroups of $\mathrm{GL}(n)$, obtained by the restriction

$$UU^\dagger = U^\dagger U = \mathbf{1} \,, \tag{2.42}$$

where $\mathbf{1}$ denotes the n-dimensional identity matrix. This matrix equation leads to n^2 equations for the $2n^2$ variables which parametrize the matrix elements of the complex $n \times n$ matrix. Consequently, an element of the unitary group $\mathrm{U}(n)$ is determined by n^2 real parameters. For $\mathrm{SU}(n)$, we have in addition the requirement $\det U = 1$, which leads to a parametrization in terms of $n^2 - 1$ real variables.

For finite groups, the rearrangement theorem, Eq. (2.5), is of central importance. For an infinite group, the sum over group elements has to be replaced by an integral over the parameters α_i. The rearrangement theorem can be generalized to infinite groups if one can define an invariant integration measure, the so-called *Haar measure*,

$$d\mu(g) \equiv d\mu(\alpha_1, \ldots, \alpha_r) d\alpha_1 \cdots d\alpha_r \,, \tag{2.43}$$

such that (for any function f defined on the group and any $h \in G$)

$$\int_G d\mu(g) f(g) = \int_G d\mu(g) f(gh) = \int_G d\mu(g) f(hg) \,, \tag{2.44}$$

where the integral is over the entire parameter space of the group G. Since this has to hold for an arbitrary function f, the Haar measure has to fulfill

$$d\mu(g) = d\mu(gh) = d\mu(hg) \,, \qquad \forall\ g, h \in G \,. \tag{2.45}$$

It turns out that an invariant Haar measure exists for all compact Lie groups, such as $\mathrm{U}(N)$ and $\mathrm{SU}(N)$. For these groups, every matrix representation is equivalent to a unitary representation, and the matrix elements of the irreducible representations obey the orthogonality relation (similar to Eq. (2.6) for finite groups)

$$\int_G d\mu(g) \Gamma^{(\nu)}(g)_{ij} \Gamma^{(\sigma)*}(g)_{kl} = \frac{\delta_{\nu\sigma}\delta_{ik}\delta_{jl}}{n_\nu} \,\mathrm{vol}(G) \,, \tag{2.46}$$

where $\mathrm{vol}(G) = \int_G d\mu(g)$, and n_ν is the dimension of the representation $\Gamma^{(\nu)}$.

Consequently, the orthogonality relation for characters reads

$$\int_G d\mu(g)\chi^{(\nu)}(g)\chi^{(\sigma)*}(g) = \delta_{\nu\sigma}\,\mathrm{vol}(G)\,. \tag{2.47}$$

Usually, we use the normalization $\mathrm{vol}(G) = 1$.

Many properties of Lie groups can be related to the properties of group elements which are close to the identity (infinitesimal transformations). It is useful to parametrize these elements in such a way that $\alpha_i = 0$, for all $1 \leq i \leq r$, corresponds to the identity element, $g(\alpha = 0) = e$. If we have an n-dimensional (faithful) representation Γ of the group, the matrices are parametrized in the same way,

$$\Gamma(g(\alpha))|_{\alpha=0} \equiv \Gamma(\alpha)|_{\alpha=0} = \mathbf{1}\,. \tag{2.48}$$

At least in some neighborhood of the identity, we can then use the exponential parametrization

$$\Gamma(\alpha) = e^{i\sum_{j=1}^{r}\alpha_j S_j}\,. \tag{2.49}$$

The matrices S_j are called *generators* of the Lie group and are defined through

$$S_j = -i\frac{\partial}{\partial\alpha_j}\Gamma(\alpha)|_{\alpha=0}\,. \tag{2.50}$$

For unitary representations, the generators are Hermitian, i.e., $S_j^\dagger = S_j$.

By multiplying infinitesimal elements, one finds that the commutator of two generators must be expressible as a linear combination of all the generators,

$$[S_i, S_j] = \sum_{k=1}^{r} c_{ij}^k S_k\,, \tag{2.51}$$

where the coefficients $c_{ij}^k = -c_{ji}^k$ are called *structure constants* of the Lie group. This means that the generators form an algebra under commutation, the so-called *Lie algebra*, which is entirely determined by the structure constants. The commutation relations of the Lie algebra completely specify the group multiplication law of the associated Lie group sufficiently close to the identity. The structure constants are purely imaginary if there is any unitary representation of the algebra.

The structure constants themselves generate a representation of the Lie algebra, the *adjoint representation*, since the $r \times r$ matrices T_i with elements $(T_i)_{kj} = c_{ij}^k$ fulfill the commutator relation (2.51) of the algebra.

A subset of commuting generators which is as large as possible is called a *Cartan subalgebra*. These generators, called Cartan generators, can be diagonalized simultaneously. The number of independent Cartan generators is called the *rank* of the Lie group.

A Lie group is called *simple* if it does not have any non-trivial invariant subgroup. If it does not have any Abelian non-trivial invariant subgroup, the group is called *semisimple*. For every semisimple Lie group of rank m, there exists a set of m *Casimir operators* which are polynomials in the generators and commute with all the generators of the Lie algebra. Every semisimple Lie group has $m \geq 1$ and there is at least one Casimir operator in the form of a polynomial of degree two,

$$C_2 = \sum_{i,j=1}^{r} g^{ij} S_i S_j\,, \tag{2.52}$$

where g^{ij} is the inverse of the symmetric Cartan metric tensor

$$g_{ij} = \sum_{k,l=1}^{r} c_{il}^{k} c_{jk}^{l} , \qquad \sum_{k=1}^{r} g^{ik} g_{kj} = \delta_{ij} . \tag{2.53}$$

The necessary and sufficient condition for a Lie algebra to be semisimple is that $\det g \neq 0$. The Casimir operator C_2 is called the quadratic Casimir operator.

Since an operator which commutes with all the generators must be a multiple of the identity operator, each Casimir operator has a fixed numerical value in a given irreducible representation. Therefore, those values can be used to label the non-equivalent irreducible representations.

For every compact semisimple Lie group, such as SU(n), there exists a basis for the Lie algebra (a set of generators $\tilde{S}_i = A_{ij} S_j$, with A a real non-singular matrix) for which $g_{ij} = \delta_{ij}$. In this basis, the structure constants c_{ij}^{k} are antisymmetric under any interchange of indices and

$$C_2 = \sum_{i=1}^{r} \tilde{S}_i \tilde{S}_i . \tag{2.54}$$

2.6 Irreducible tensors

Consider a group G of linear transformations in an n-dimensional (complex) vector space V_n (the group G may be a faithful matrix representation of some abstract group). The transformation $g \in G$ transforms $v \in V_n$ into v',

$$v'_i = g_{ij} v_j , \tag{2.55}$$

where the sum over repeated indices is implied.

A tensor of rank r is a quantity T which is described by n^r components $T_{i_1 i_2 \ldots i_r}$ in a given coordinate basis and transforms like the product of r vectors,

$$T'_{i_1 i_2 \ldots i_r} = g_{i_1 j_1} g_{i_2 j_2} \cdots g_{i_r j_r} T_{j_1 j_2 \ldots j_r} . \tag{2.56}$$

It is convenient to abbreviate the above equation by

$$T'_{(i)} = g_{(i)(j)} T_{(j)} . \tag{2.57}$$

The transformation g on V_n induces a transformation $g \otimes g \otimes \ldots \otimes g$ (with r factors g) in the space of r-th-rank tensors and therefore leads to an n^r-dimensional representation of G acting on V_n^r. In general, this representation will be reducible.

Let us first consider the general linear group GL(n) of all non-singular linear transformations in n-dimensional space. We will turn to the subgroups U(n) and SU(n) later.

Consider a tensor T of rank r. To each permutation

$$p = \begin{pmatrix} 1 & 2 & \ldots & r \\ p_1 & p_2 & \ldots & p_r \end{pmatrix} \equiv \begin{pmatrix} 1 & 2 & \ldots & r \\ 1' & 2' & \ldots & r' \end{pmatrix} \tag{2.58}$$

of the symmetric group S_r we associate an operator $\hat{p}$ which acts on the indices of the tensor T,

$$(\hat{p}T)_{i_1 i_2 \ldots i_r} = T_{i'_1 i'_2 \ldots i'_r} , \qquad (\hat{p}T)_{(i)} = T_{(p(i))} . \tag{2.59}$$

Since the tensor transformation (2.57) is bisymmetric, i.e.,

$$g_{(p(i))(p(j))} = g_{i'_1 j'_1} g_{i'_2 j'_2} \cdots g_{i'_r j'_r} = g_{i_1 j_1} g_{i_2 j_2} \cdots g_{i_r j_r} = g_{(i)(j)} , \tag{2.60}$$

it commutes with the permutation operator $\hat{p}$,

$$(\hat{p}T')_{(i)} = (T')_{(p(i))} = g_{(p(i))(p(j))}T_{(p(j))} = g_{(i)(j)}(\hat{p}T)_{(j)} \,. \tag{2.61}$$

Therefore, the tensors of rank r which have a particular symmetry (with respect to the permutation operators) transform among themselves under the transformation (2.57). The entire space of r-th-rank tensors is reducible into subspaces consisting of tensors of different symmetry type, associated to different Young diagrams with r boxes.

To generate tensors of a certain symmetry type, we can act with the Young operator $\hat{y} = \hat{a}\hat{s}$ (associated to a Young tableau with r boxes, cf. Eq. (2.30)) on the indices $i_1, i_2, \ldots, i_r$ of a general r-th-rank tensor.

Consider, e.g., a general tensor $R_{i_1 i_2 i_3}$ of rank 3. For $r = 3$, there are three symmetry classes, corresponding to the three Young diagrams

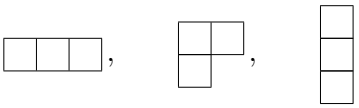 (2.62)

The first (resp. last) class consists of tensors which are completely symmetric (resp. antisymmetric) in all three indices. To construct a tensor $T_{i_1 i_2 i_3}$ belonging to the second symmetry class, we can use the symmetrizer and anti-symmetrizer

$$s = e + (12) \,, \qquad a = e - (13) \tag{2.63}$$

of the Young tableau

 (2.64)

and obtain

$$T_{i_1 i_2 i_3} = R_{i_1 i_2 i_3} + R_{i_2 i_1 i_3} - R_{i_3 i_2 i_1} - R_{i_2 i_3 i_1} \,. \tag{2.65}$$

For the general linear group $\mathrm{GL}(n)$, the matrix elements are not subject to any restrictive conditions, and the only method of reducing the tensor space is the symmetrization process. Therefore, the r-th-rank tensors of a given symmetry are irreducible tensors with respect to $\mathrm{GL}(n)$, i.e., they form a basis for an irreducible representation of $\mathrm{GL}(n)$.

If the Young diagram contains more than n rows, there will always be at least two indices in the first column which assume the same value, which means that all the tensors of this symmetry type are identically equal to zero (since the irreducible tensors constructed in this way are antisymmetric in the indices appearing in the same column). On the other hand, every symmetry type corresponding to a diagram with n rows or less is realized, i.e., there exist non-zero tensors of all such symmetry types. If we consider all possible Young diagrams (with less than $n + 1$ rows), the associated tensors form a complete set in the sense that all irreducible representations of the group, with representation matrices that are homogeneous polynomials in the elements g_{ij}, are counted once. Therefore, we can label the inequivalent irreducible representations with Young diagrams (corresponding to the symmetry class of tensors which generates the representation).

To decompose a general r-th-rank tensor into a sum of tensors of definite symmetry type, we can use the decomposition of the identity element of S_r into primitive idempotents. Up to numerical factors, those are the Young operators corresponding to the standard Young tableaux of r boxes (cf. Sec. 2.4).

Let us once again consider the example $r = 3$. The identity $e \in S_3$ decomposes into four primitive idempotents, cf. Eq. (2.36),

$$e = \frac{1}{6}y_1 + \frac{1}{3}y_2 + \frac{1}{3}y_3 + \frac{1}{6}y_4\,, \tag{2.66}$$

and the general tensor R can be decomposed into tensors of definite symmetry,

$$R = \frac{1}{6}\hat{y}_1 R + \frac{1}{3}\hat{y}_2 R + \frac{1}{3}\hat{y}_3 R + \frac{1}{6}\hat{y}_4 R\,. \tag{2.67}$$

The tensors $\hat{y}_2 R$ and $\hat{y}_3 R$ belong to the same symmetry class (the standard tableaux are obtained from the same diagram), they generate irreducible representations of $\mathrm{GL}(n)$ which are equivalent. If we label the irreducible representations of $\mathrm{GL}(n)$ with the corresponding Young diagrams, the decomposition of the product representation, on the space of tensors of rank 3, into irreducible representations reads

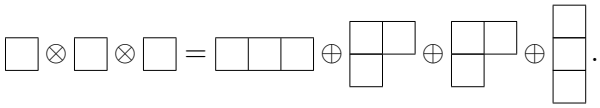

(2.68)

The dimensionality of an irreducible representation of $\mathrm{GL}(n)$ constructed in this way is determined by the number of independent components of tensors of definite symmetry type corresponding to a Young diagram $(\lambda) = (\lambda_1, \ldots, \lambda_n)$. For a given diagram, the number of independent tensor components is equal to the number of standard tableaux which can be formed. (We can insert any of the numbers $1, 2, \ldots, n$ in each of the r boxes. In a standard tableaux, the numbers do not decrease from left to right in a row and always increase from top to bottom). The general result is

$$\dim_n(\lambda) = \left(\prod_{i=1}^{n-1} \frac{1}{i!}\right) \det\left((\lambda_i + n - i)^{n-j}\right)_{i,j=1,\ldots,n}\,, \tag{2.69}$$

which can be restated as

$$\dim_n(\lambda) = \prod_{i,j} \frac{n + j - i}{h_{ij}}\,, \tag{2.70}$$

where in the last equation the product is over all boxes of the Young diagram (λ) (i (resp. j) labels rows (resp. columns)) and h_{ij} is the so-called hook index of the box at position (i, j). If the i-th row of the diagram has λ_i boxes, and the j-th column consists of γ_j boxes, then $h_{ij} = 1 + \lambda_i - i + \gamma_j - j$.

The irreducible representations of $\mathrm{GL}(n)$ remain irreducible when we go to certain subgroups of $\mathrm{GL}(n)$, such as $\mathrm{U}(n)$ or $\mathrm{SU}(n)$. ($\mathrm{O}(n)$, for example, does not remain irreducible.)

The reason for this is the following: In the fundamental representation, the Lie algebra of $\mathrm{U}(n)$ consists of the Hermitian $n \times n$ matrices. If we choose a basis of n^2 matrices $T_i = T_i^\dagger$ in the Lie algebra, then the elements of the Lie algebra of $\mathrm{U}(n)$ are all linear combinations $\sum_{i=1}^{n^2} \alpha_i T_i$ of these basis elements with real coefficients α_i. On the other hand, linear combinations with complex coefficients would give the Lie algebra of $\mathrm{GL}(n)$. Consider now some representation Γ of the basis elements. If the representation is reducible for $\mathrm{U}(n)$, there is a basis in which the matrices $\sum_i \alpha_i \Gamma(T_i)$ are in reduced form for all real values of α_i. This means that a certain set of linear forms in the α_i vanishes for all real values of α_i. If this is the case, those linear forms must vanish for all complex values of α_i, which implies that the representation is reducible for $\mathrm{GL}(n)$, too.

Although the irreducible representations of GL(n) remain irreducible for U(n) and SU(n), these representations may not be independent for these subgroups of GL(n).

If we have a representation Γ of GL(n) corresponding to the Young diagram $(\lambda) = (\lambda_1, \ldots, \lambda_n)$ and construct a new representation Γ' by adjoining s columns of length n to (λ), Γ' corresponds to the diagram $(\lambda') = (\lambda_1 + s, \ldots, \lambda_n + s)$. The single modification of the representation matrices is that they are all multiplied by the common factor $(\det(g))^s$ (for the transformation (2.56)),

$$\Gamma'(g) = (\det(g))^s \, \Gamma(g) \, . \tag{2.71}$$

If we are dealing with SU(n), we have $\det(g) = 1$ and the irreducible representations Γ and Γ' are equivalent.

A very useful application of the correspondence between Young diagrams and irreducible representations of GL(n), U(n), and SU(n) is the decomposition of direct products into irreducible representations.

Consider two irreducible representations $\Gamma^{(\lambda)}$ and $\Gamma^{(\mu)}$ corresponding to Young diagrams (λ) and (μ). The graphical rule for decomposing the product representation $\Gamma^{(\lambda)} \otimes \Gamma^{(\mu)}$ into irreducible representations is the following: In the Young diagram of the second factor, assign the number i to all boxes in the i-th row. Attach these boxes to the Young diagram of the first factor (starting with boxes from the first row, then continuing with the second row, etc.), such that the resulting diagram is still an allowed Young diagram (i.e., the length of the rows does not increase from top to bottom and the number of rows does not exceed n) and no two i's appear in the same column. After all boxes have been added, read the numbers in the final diagram from right to left, starting in the first row, then continuing in the second, etc. At any point in this sequence, there must not be more i's than $(i-1)$'s. If two diagrams generated in this way have the same form, they are counted as different contributions to the decomposition only if the distribution of the i's is different.

Let us return to the example of tensors of rank 3. According to these rules, we find

$$\square \otimes \boxed{1} = \square\boxed{1} \oplus \begin{array}{|c|}\hline \\ \hline 1 \\ \hline \end{array} \, , \tag{2.72}$$

$$\square \otimes \boxed{1}\boxed{1} = \square\boxed{1}\boxed{1} \oplus \begin{array}{|c|c|}\hline \\ \hline 1 \\ \hline \end{array}\!\!\begin{array}{|c|}\hline 1 \\ \hline \end{array} \, , \tag{2.73}$$

$$\square \otimes \begin{array}{|c|}\hline 1 \\ \hline 2 \\ \hline \end{array} = \begin{array}{|c|c|}\hline \\ \hline 2 \\ \hline \end{array}\!\!\begin{array}{|c|}\hline 1 \\ \hline \end{array} \oplus \begin{array}{|c|}\hline \\ \hline 1 \\ \hline 2 \\ \hline \end{array} \, , \tag{2.74}$$

which results in

$$\square \otimes \square \otimes \square = \square\square\square \oplus \begin{array}{|c|c|}\hline \\ \hline \\ \hline \end{array}\!\!\begin{array}{|c|}\hline \\ \hline \end{array} \oplus \begin{array}{|c|c|}\hline \\ \hline \\ \hline \end{array}\!\!\begin{array}{|c|}\hline \\ \hline \end{array} \oplus \begin{array}{|c|}\hline \\ \hline \\ \hline \\ \hline \end{array} \tag{2.75}$$

in agreement with the decomposition in Eq. (2.68).

3 Basic concepts of quantum field theory

Units $\hbar = c = 1$ and the convention that repeated indices are summed over are used throughout the following sections of this thesis. In Minkowski space, we use the metric tensor $g_{\mu\nu} = g^{\mu\nu} = \mathrm{diag}(+1, -1, -1, -1)$. The scalar product of two four-vectors $x^\mu = (x^0, \vec{x})$ and $y^\mu = (y^0, \vec{y})$ is denoted with $x{\cdot}y$ and given by $x{\cdot}y = x^\mu y_\mu = x^\mu y^\nu g_{\mu\nu}$. Operators in quantum mechanics (and field operators in the operator formulation of quantum field theory) are usually labeled with hats, e.g., $\hat{p}$ denotes the momentum operator in one-dimensional quantum mechanics. This overview is based on Refs. [7, 8, 9, 10, 11, 12].

3.1 Path integral formulation of quantum mechanics

In the Schrödinger representation of ordinary quantum mechanics, the amplitude for a particle to propagate from an initial point q_i at time t_i to a final point q_f at time $t_f = t_i + T$ in one space dimension is given by $\langle q_f | \, e^{-i\hat{H}T} \, | q_i \rangle$, where the Dirac bra and ket notation is used, and $\hat{H} = H_0(\hat{p}) + V(\hat{x})$ with $H_0(\hat{p}) = \hat{p}^2/2m$ denotes the Hamiltonian operator for a massive particle in a potential V. Following the standard procedure, we divide the time interval T into n segments of length $\tau = T/n$ and use the completeness relation $\int dq \, |q\rangle \langle q| = \mathbf{1}$ to write the transition amplitude as

$$\langle q_f | \, e^{-i\hat{H}T} \, | q_i \rangle = \left(\prod_{k=1}^{n-1} \int dq_k \right) \langle q_f | \, e^{-i\hat{H}\tau} \, | q_{n-1} \rangle \, \langle q_{n-1} | \, e^{-i\hat{H}\tau} \, | q_{n-2} \rangle \cdots \langle q_1 | \, e^{-i\hat{H}\tau} \, | q_i \rangle \; . \tag{3.1}$$

Approximating $e^{i\tau(\hat{H}_0 + \hat{V})} = e^{i\tau\hat{H}_0} e^{i\tau\hat{V}} e^{\tau^2/2[\hat{H}_0, \hat{V}]} = e^{i\tau\hat{H}_0} e^{i\tau\hat{V}} + \mathcal{O}\left(\tau^2\right)$, inserting again complete sets of states $\int dp \, |p\rangle \langle p| = \mathbf{1}$, and finally taking the limit $n \to \infty$ leads to the famous *path integral representation* of the transition amplitude due to Dirac and Feynman [8]

$$\langle q_f | \, e^{-i\hat{H}T} \, | q_i \rangle = \int_{q(t_i)=q_i}^{q(t_f)=q_f} [Dq(t)] \exp\left(i \int_{t_i}^{t_f} dt L[\dot{q}, q] \right) \, , \tag{3.2}$$

where the integral over paths is defined as

$$\int [Dq(t)] = \lim_{n \to \infty} \left(\frac{m}{2\pi i \tau} \right)^{\frac{n}{2}} \prod_{k=1}^{n-1} \int dq_k \, , \tag{3.3}$$

and $L\left(\dot{q}, q\right) = \frac{1}{2} m \dot{q}^2 - V(q)$ denotes the Lagrangian. This fundamental result means that the above transition amplitude is given by an integral over all possible paths $q(t)$ fulfilling the boundary conditions $q(t_i) = q_i$ and $q(t_f) = q_f$. The contribution of each individual path is proportional to $e^{iS[q]}$, where $S[q] = \int_{t_i}^{t_f} dt L[\dot{q}, q]$ is the classical action of the path under consideration.

Let us now switch to the Heisenberg picture[2] of quantum mechanics, where the states $|\psi, t\rangle_{_H} \equiv e^{i\hat{H}t} \, |\psi\rangle_{_S}$ are by construction time independent and the operators are defined as $\hat{A}_{_H}(t) \equiv e^{i\hat{H}t} \hat{A}_{_S} e^{-i\hat{H}t}$ and therefore evolve with time. Using the Heisenberg representation, the above result can be restated as

$${}_{_H}\langle q_f, t_f | q_i, t_i \rangle_{_H} = \int_{q(t_i)=q_i}^{q(t_f)=q_f} [Dq(t)] e^{iS[q]} \, . \tag{3.4}$$

[2]States and operators in the Heisenberg picture are labeled by the subscript H, in contrast to the subscript S, which we use for the Schrödinger representation from now on.

Inserting into this path integral a factor of $q(t_m)$ with $t_i < t_m < t_f$ yields

$$\int_{q(t_i)=q_i}^{q(t_f)=q_f} [Dq(t)] e^{iS[q]} q(t_m) = \int_{-\infty}^{\infty} d\tilde{q} \left(\int_{q(t_i)=q_i}^{q(t_m)=\tilde{q}} [Dq(t)] \exp\left[i \int_{t_i}^{t_m} dt L(\dot{q}, q) \right] \right) \tilde{q} \times \left(\int_{q(t_m)=\tilde{q}}^{q(t_f)=q_f} [Dq(t)] \exp\left[i \int_{t_m}^{t_f} dt L(\dot{q}, q) \right] \right) \tag{3.5}$$

because of

$$\int_{q(t_i)=q_i}^{q(t_f)=q_f} [Dq(t)] = \int_{-\infty}^{\infty} d\tilde{q} \int_{q(t_i)=q_i}^{q(t_m)=\tilde{q}} [Dq(t)] \int_{q(t_m)=\tilde{q}}^{q(t_f)=q_f} [Dq(t)] \tag{3.6}$$

and

$$\int_{t_i}^{t_f} dt L = \int_{t_i}^{t_m} dt L + \int_{t_m}^{t_f} dt L \,. \tag{3.7}$$

However, the terms in parentheses in Eq. (3.5) are just the path integral expressions for the transition amplitudes ${}_H\langle \tilde{q}, t_m | q_i, t_i \rangle_H$ and ${}_H\langle q_f, t_f | \tilde{q}, t_m \rangle_H$. Therefore, the insertion of the factor $q(t)$ in the path integral results in [9]

$$\begin{aligned} \int_{q(t_i)=q_i}^{q(t_f)=q_f} [Dq(t)] e^{iS[q]} q(t_m) &= \int_{-\infty}^{\infty} d\tilde{q}\ {}_H\langle \tilde{q}, t_m | q_i, t_i \rangle_H\ \tilde{q}\ {}_H\langle q_f, t_f | \tilde{q}, t_m \rangle_H \\ &= \int_{-\infty}^{\infty} d\tilde{q}\ {}_H\langle q_f, t_f |\, \hat{q}_H(t_m)\, | \tilde{q}, t_m \rangle_H\ {}_H\langle \tilde{q}, t_m | q_i, t_i \rangle_H \\ &= {}_H\langle q_f, t_f |\, \hat{q}_H(t_m)\, | q_i, t_i \rangle_H \ . \end{aligned} \tag{3.8}$$

Repeating the above arguments for the insertion of n factors $q(t_1)$, $q(t_2)$, ..., $q(t_n)$ at times $t_i < t_k < t_f$ $(k = 1, ..., n)$ finally leads to

$$\int_{q(t_i)=q_i}^{q(t_f)=q_f} [Dq(t)]\, e^{iS[q]} q(t_1) \cdots q(t_n) = {}_H\langle q_f, t_f |\, T\left\{ \hat{q}_H(t_1) \cdots \hat{q}_H(t_n) \right\} | q_i, t_i \rangle_H \tag{3.9}$$

with the *time-ordered product* $T\left\{ \hat{q}_H(t_1) \cdots \hat{q}_H(t_n) \right\} = \hat{q}_H(t'_1) \cdots \hat{q}_H(t'_n)$, where the times t'_k are obtained by permuting the times t_k such that $t'_1 > \cdots > t'_n$ [9].

3.2 Quantum field theory: path integral quantization of scalar fields

Quantum field theory (QFT) is needed when the two great physics innovations of the last century, special relativity and quantum mechanics, are confronted simultaneously and a new set of phenomena arises, particles can be created and particles can be annihilated [8]. Wave equations, whether they are relativistic or not, cannot describe processes in which the number and the type of particles change, as in almost all reactions of nuclear and particle physics. Changing the viewpoint from wave equations, where one quantizes a single particle in an external classical potential, to QFT, where one identifies the particles with the modes of a field and quantizes the field itself, a proper resolution of that difficulty is possible. This procedure is also known as second quantization. Quantum field theory, the synthesis of quantum mechanics and special relativity, can be regarded as one of the great achievements of modern physics [9].

3.2.1 Green's functions

The path integral formulation of quantum mechanics in one dimension, presented in the previous section, remains still valid for a multi-dimensional space with coordinates q_j instead of the single coordinate q if $\int [Dq(t)]$ is replaced simply by $\int \prod_j [Dq_j(t)]$. Therefore, the extension from quantum mechanics to the field theory for a scalar field $\phi(x) \equiv \phi(\vec{x}, t)$ in 3+1 dimensions is rather straightforward, at least at a formal level [9]. The field $\phi(x)$ in quantum field theory simply takes the role of the coordinates $q_j(t)$. It is important to remember that in QFT, $\vec{x}$ is just a label (just like j in q_j), not a dynamical variable. In complete analogy to the path integral formulation of quantum mechanics (cf. Eq. (3.4)), the probability amplitude for a transition between an initial field configuration $\phi_i(\vec{x})$ at time t_i and a second configuration $\phi_f(\vec{x})$ at a later time t_f is given by

$$ {}_H\langle \phi_f(\vec{x}, t_f) | \phi_i(\vec{x}, t_i) \rangle_H = \int_{\phi(\vec{x},t_i)=\phi_i(\vec{x})}^{\phi(\vec{x},t_f)=\phi_f(\vec{x})} [D\phi\,(\vec{x}, t)] \exp\left(i \int_{t_i}^{t_f} dt \int d^3x\, \mathcal{L}[\phi] \right) , \tag{3.10} $$

where $\int [D\phi\,(\vec{x}, t)]$ denotes the integration over all field configurations satisfying the given boundary conditions and the Lagrangian occurring in the exponential is written as $L = \int d^3x \mathcal{L}[\phi]$ [9]. The Lagrangian density[3] $\mathcal{L}$, which is a functional of the field $\phi(x)$ and its spacetime derivatives, may be considered as the most fundamental specification of a quantum field theory [7]. The functional integral can be used to calculate correlation functions, called Green's functions, such as

$$ G(x_1, x_2) \equiv \langle \Omega |\, T \left\{ \hat{\phi}_H(x_1) \hat{\phi}_H(x_2) \right\} | \Omega \rangle \ , \tag{3.11} $$

where the notation $|\Omega\rangle$ is used to denote the ground state (the vacuum) of the theory under consideration. Physically, this function can be interpreted as the amplitude for the propagation of a particle or excitation between spacetime points x_1 and x_2 [7]. To derive a functional formula for such correlation functions, it is convenient to start with the functional integral

$$ O(x_1, x_2) \equiv \int_{\phi(\vec{x},-T)=\phi_i(\vec{x})}^{\phi(\vec{x},T)=\phi_f(\vec{x})} [D\phi(x)] \phi(x_1) \phi(x_2) \exp\left(i \int_{-T}^{T} dt \int d^3x\, \mathcal{L}[\phi] \right) , \tag{3.12} $$

where the boundary conditions on the integral are $\phi(\vec{x}, -T) = \phi_i(\vec{x})$ and $\phi(\vec{x}, T) = \phi_f(\vec{x})$. Similarly to the procedure in the previous section, the functional integral can be split up into parts, with the times t_1 and t_2 automatically falling in order: If, for example, $-T < t_1 = x_1^0 < t_2 = x_2^0 < T$, then

$$ \begin{aligned} \int [D\phi(x)] = \int [D\phi_1(\vec{x})] \int [D\phi_2(\vec{x})] & \int_{\phi(\vec{x},-T)=\phi_i(\vec{x})}^{\phi(\vec{x},t_1)=\phi_1(\vec{x})} [D\phi(x)] \int_{\phi(\vec{x},t_1)=\phi_1(\vec{x})}^{\phi(\vec{x},t_2)=\phi_2(\vec{x})} [D\phi(x)] \\ & \times \int_{\phi(\vec{x},t_2)=\phi_2(\vec{x})}^{\phi(\vec{x},T)=\phi_f(\vec{x})} [D\phi(x)] \, . \end{aligned} \tag{3.13} $$

In addition to the initial time $-T$ and the final time T, the main functional integral $\int [D\phi(x)]$ is now constrained at the two intermediate times t_1 and t_2, too. Using Eq. (3.10),

[3] In field theory, we often refer to the density $\mathcal{L}$ simply as "the Lagrangian".

this decomposition leads to

$$\begin{aligned} O(x_1,x_2) &= \int [D\phi_1(\vec{x})] \int [D\phi_2(\vec{x})] \phi_1(\vec{x}_1)\phi_2(\vec{x}_2)\, {}_H\langle \phi_f, T|\phi_2, t_2\rangle_H \\ &\quad \times {}_H\langle \phi_2, t_2|\phi_1, t_1\rangle_H\, {}_H\langle \phi_1, t_1, \phi_i, -T\rangle_H \\ &= \int [D\phi_1(\vec{x})] \int [D\phi_2(\vec{x})]\, {}_H\langle \phi_f, T|\hat{\phi}_H(x_2)|\phi_2, t_2\rangle_H \\ &\quad \times {}_H\langle \phi_2, t_2|\hat{\phi}_H(x_1)|\phi_1, t_1\rangle_H\, {}_H\langle \phi_1, t_1, \phi_i, -T\rangle_H \ . \end{aligned} \tag{3.14}$$

With the help of the completeness relation $\int [D\phi_j]\, |\phi_j\rangle \langle \phi_j| = \mathbf{1}$, the integrals over the intermediate states can be performed and we obtain

$$\begin{aligned} O(x_1,x_2) &= {}_H\langle \phi_f, T|\, T\left\{ \hat{\phi}_H(x_1)\hat{\phi}_H(x_2) \right\} |\phi_i, -T\rangle_H \\ &= {}_S\langle \phi_f|\, e^{-i\hat{H}T} T \left\{ \hat{\phi}_H(x_1)\hat{\phi}_H(x_2) \right\} e^{-i\hat{H}T}\, |\phi_i\rangle_S \ . \end{aligned} \tag{3.15}$$

Assuming that the initial and final states have some overlap with the vacuum, the ground state $|\Omega\rangle$ is projected out from $|\phi_i\rangle$ and $|\phi_f\rangle$ in the limit $T \to \infty(1 - i\varepsilon)$, i.e., the limit $T \to \infty$ is considered for a time integral along a contour that is slightly rotated in the complex plane, $t \to t(1 - i\varepsilon)$. The limit $\varepsilon \to 0$ can then be taken at the end of the calculation [7]. A decomposition into eigenstates $|n\rangle$ of $\hat{H}$ results in

$$\lim_{T\to\infty(1-i\varepsilon)} e^{-i\hat{H}T}\, |\phi_i\rangle = \lim_{T\to\infty(1-i\varepsilon)} \sum_n e^{-iE_nT}\, |n\rangle \langle n|\phi_i\rangle = \lim_{T\to\infty(1-i\varepsilon)} \langle \Omega|\phi_i\rangle\, e^{-iE_0T}\, |\Omega\rangle \tag{3.16}$$

due to $\lim_{T\to\infty(1-i\varepsilon)} e^{-i(E_n-E_0)T} = 0$ for $E_n - E_0 > 0$. The overlap $\langle \Omega|\phi_i\rangle$ as well as the phase factor e^{-iE_0T} cancel if $O(x_1, x_2)$ is divided by a quantity which is identical to Eq. (3.12) up to the insertion of the two field factors $\phi(x_1)$ and $\phi(x_2)$. Hence, the two-point Green's function (3.11) can be expressed as [7]

$$G(x_1,x_2) = \lim_{T\to\infty(1-i\varepsilon)} \frac{\int [D\phi(x)]\phi(x_1)\phi(x_2) \exp\left(i\int_{-T}^{T} d^4x\, \mathcal{L}[\phi] \right)}{\int [D\phi(x)] \exp\left(i\int_{-T}^{T} d^4x\, \mathcal{L}[\phi] \right)} \tag{3.17}$$

with $\int_{-T}^{T} d^4x \equiv \int_{-T}^{T} dt \int d^3x$. For higher correlation functions, the above steps can be repeated successively, leading to

$$\begin{aligned} G(x_1,...,x_n) &\equiv \langle \Omega|\, T\left\{ \hat{\phi}_H(x_1)\cdots\hat{\phi}_H(x_n) \right\} |\Omega\rangle \\ &= \lim_{T\to\infty(1-i\varepsilon)} \frac{\int [D\phi(x)]\phi(x_1)\cdots\phi(x_n) \exp\left(i\int_{-T}^{T} d^4x\, \mathcal{L}[\phi] \right)}{\int [D\phi(x)] \exp\left(i\int_{-T}^{T} d^4x\, \mathcal{L}[\phi] \right)} \ . \end{aligned} \tag{3.18}$$

This equation allows for the derivation of the Feynman rules for a scalar field theory and can be considered as the basic formula which connects the path integral formalism to the operator formalism of quantum field theory [9].

3.2.2 Generating functionals

One method for computing correlation functions is based on the so-called *generating functional*, defined as

$$Z[J] \equiv \int [D\phi(x)] \exp\left[i\int d^4x \left(\mathcal{L}[\phi] + J(x)\phi(x) \right) \right] , \tag{3.19}$$

where a source term $J(x)\phi(x)$ is added to $\mathcal{L}$ in the exponent [7]. With the functional derivative $\frac{\delta}{\delta J(x)}$, which obeys the basic axiom

$$\frac{\delta}{\delta J(x)} J(y) = \delta(x-y)\,, \tag{3.20}$$

the n-point function is given by

$$G(x_1,\ldots,x_n) = (Z[J=0])^{-1}\left(-i\frac{\delta}{\delta J(x_1)}\right)\cdots\left(-i\frac{\delta}{\delta J(x_n)}\right) Z[J]\Big|_{J=0}\,. \tag{3.21}$$

This formula proves beneficial because $Z[J]$ can be rewritten, at least in a free field theory, in a very explicit form.

For a non-interacting real-valued scalar field of mass m, the Lagrangian density is given by $\mathcal{L}_0[\phi] = \frac{1}{2}\partial_\mu\phi\partial^\mu\phi - \frac{1}{2}m^2\phi^2$. In classical field theory, the principle of least action leads to the Euler-Lagrange equation of motion for the field ϕ,

$$\partial_\mu\left(\frac{\partial\mathcal{L}}{\partial(\partial_\mu\phi)}\right) - \frac{\partial\mathcal{L}}{\partial\phi} = 0\,. \tag{3.22}$$

For the non-interacting scalar field this equation reads

$$\left(\partial^\mu\partial_\mu + m^2\right)\phi = 0\,, \tag{3.23}$$

which is the well-known Klein-Gordon equation for the classical field ϕ.

Integrating by parts and introducing a convergence factor $i\varepsilon$ in the functional integral (which corresponds to the rotation of the time integral in the complex plane), the exponent in Eq. (3.19) can be replaced by

$$i\int d^4x\,(\mathcal{L}_0[\phi] + J(x)\phi(x)) = i\int d^4x\left(\frac{1}{2}\phi(x)\left(-\partial^2 - m^2 + i\varepsilon\right)\phi(x) + J(x)\phi(x)\right)\,. \tag{3.24}$$

Performing a shift of variables, symbolically written as $\phi \to \phi - \left(-\partial^2 - m^2 + i\varepsilon\right)^{-1} J$, the generating functional of the free scalar field is simply [7]

$$Z[J] = Z[J=0]\exp\left(-\frac{1}{2}\int d^4x d^4y J(x) D_F(x-y) J(y)\right) \tag{3.25}$$

with the well-known Feynman propagator

$$D_F(x-y) = \int\frac{d^4k}{(2\pi)^4} e^{ik\cdot(x-y)}\frac{i}{k^2 - m^2 + i\varepsilon}\,, \tag{3.26}$$

which is a solution of

$$\left(-\partial^2 - m^2 + i\varepsilon\right) D_F(x-y) = i\delta(x-y)\,. \tag{3.27}$$

Now we can use Eqs. (3.21) and (3.25) to calculate all correlation functions of the free scalar theory. Obviously, the two-point function is

$$G(x_1,x_2) = D_F(x_1-x_2)\,. \tag{3.28}$$

The next non-vanishing Green's function, the four-point function, is given by

$$\begin{aligned} G(x_1,x_2,x_3,x_4) = {} & D_F(x_1-x_2)D_F(x_3-x_4) + D_F(x_1-x_3)D_F(x_2-x_4) \\ & + D_F(x_1-x_4)D_F(x_2-x_3) \end{aligned} \tag{3.29}$$

in agreement with Wick's theorem, which in general states that if n is even, the n-point function is a sum of products of two-point functions [10],

$$G(x_1, ..., x_n) = \sum_{\text{permutations } p} G(x_{p_1}, x_{p_2}) \cdots G(x_{p_{n-1}}, x_{p_n}) \,, \tag{3.30}$$

where the sum is over all permutations that give inequivalent contributions (i.e., there are $n!/(2^{\frac{n}{2}} \left(\frac{n}{2}\right)!)$ terms in the sum). From Eq. (3.21), it is evident that the n-point correlation function vanishes if n is odd.

3.2.3 Euclidean field theory

Instead of adding the convergence factor $\exp\left(-\frac{1}{2}\varepsilon \int d^4x\phi^2\right)$, which corresponds to the Feynman prescription for the propagator in Eq. (3.26), the theory can be rotated to Euclidean space to ensure the convergence of the path integral [9]. This means that the time integration is not only slightly tipped into the complex plane, but rotated through an angle of $\frac{\pi}{2}$ completely onto the imaginary axis. If the time coordinate is taken to be purely imaginary,

$$t \equiv x^0 = -ix^4 \equiv -it_{_E} \,, \quad x^4 \in \mathbb{R} \,, \tag{3.31}$$

the spacetime metric for the coordinates x^1, x^2, x^3, x^4 is a Euclidean one. In Minkowski space, the scalar product between two vectors $x = (x^0, x^1, x^2, x^3)$ and $y = (y^0, y^1, y^2, y^3)$ is defined by

$$x \cdot y \equiv x^\mu y_\mu = g_{\mu\nu} x^\mu y^\nu = x^0 y^0 - x^1 y^1 - x^2 y^2 - x^3 y^3 \tag{3.32}$$

with the metric tensor $g_{\mu\nu} = \text{diag}(+1, -1, -1, -1)$. Therefore, the Wick rotation of the time coordinate yields

$$x \cdot y = -x^4 y^4 - x^1 y^1 - x^2 y^2 - x^3 y^3 \equiv -x_{_E} y_{_E} \,, \tag{3.33}$$

where $x_{_E} y_{_E}$ denotes the Euclidean scalar product between the vectors $x_{_E} \equiv (x^1, x^2, x^3, x^4)$ and $y_{_E} \equiv (y^1, y^2, y^3, y^4)$. Since Eq. (3.31) implies

$$d^4x = dt d^3x = -i dt_{_E} d^3x \equiv -i(d^4x)_{_E} \qquad \text{and} \qquad \frac{\partial}{\partial t} = i \frac{\partial}{\partial t_{_E}} \,, \tag{3.34}$$

the action of the free scalar field reads

$$\begin{aligned} S &= \frac{1}{2} \int d^4x \left((\partial_t \phi)^2 - \left(\vec{\nabla}\phi\right)^2 - m^2\phi^2 \right) = -\frac{i}{2} \int (d^4x)_{_E} \left(-(\partial_{t_{_E}} \phi)^2 - \left(\vec{\nabla}\phi\right)^2 - m^2\phi^2 \right) \\ &\equiv i \int (d^4x)_{_E} \mathcal{L}_{_E} \equiv i S_{_E} \end{aligned} \tag{3.35}$$

with the Euclidean action $S_{_E}$. Then the path integral over Euclidean field configurations $\phi(x_{_E})$ is well-defined because the Euclidean action is positive definite and therefore the factor $e^{iS} = e^{-S_E}$ ensures convergence [9]. Furthermore, the transition to imaginary times produces a close connection between field theory and statistical physics since the Euclidean functional integral can be regarded as a probability system weighted by a Boltzmann distribution e^{-S_E}. This is the basis for Monte Carlo simulations, e.g., in lattice quantum chromodynamics (see below).

Analogously to Eqs. (3.19) and (3.21), Euclidean correlation functions can be calculated from the Wick-rotated generating functional

$$Z_{_E}[J] = \int D\phi(x) \exp\left(-\int (d^4x)_{_E} \left(\mathcal{L}_{_E} - J\phi \right) \right) \,, \tag{3.36}$$

which for instance leads to

$$G_{_E}((x_1)_{_E},(x_2)_{_E}) = \int \frac{(d^4k)_{_E}}{(2\pi)^4} \frac{e^{ik_{_E}\left((x_1)_{_E}-(x_2)_{_E}\right)}}{k_{_E}^2+m^2} \tag{3.37}$$

for the two-point function [7]. The correlation functions in Minkowski space can then be obtained by analytic continuation of the Euclidean correlation functions, provided that these obey a positivity condition which is called Osterwalder-Schrader positivity or reflection positivity [11]. In analogy to statistical mechanics, the Euclidean generating functional $Z_{_E}$ is also often referred to as the *partition function*.

3.3 Quantum chromodynamics

The most natural candidate for a model of the strong interactions is the non-Abelian gauge theory with gauge group SU(N) coupled to spin-$\frac{1}{2}$ particles in the fundamental representation of the gauge group. In the case of $N = 3$, the particles are known as *quarks* and the theory is called *quantum chromodynamics* (QCD). The gauge theory with the Abelian U(1) gauge group is known as *quantum electrodynamics* (QED) [7].

Although free quarks have not been observed in nature, there is strong experimental evidence that hadronic matter is made of these elementary particles. Baryons, such as protons and neutrons, are bound states of three quarks, whereas mesons, such as pions, are composed of a quark and an antiquark. In the non-Abelian gauge theory of QCD, the gauge bosons (called *gluons*) mediate the strong force between quarks just like the photon (the gauge boson of the Abelian U(1) gauge theory) mediates the electromagnetic force between electrically charged particles. In analogy to electrodynamics, a "color" charge is assigned to quarks (and gluons), which is responsible for the strong interactions (hence the name quantum chromodynamics). The fact that quarks are observed in nature only in bound states and cannot be isolated is known as *confinement*. It is generally believed that the non-Abelian nature of the gauge interaction in QCD is responsible for quark confinement. The expectation is that the quarks are sources of chromoelectric flux which is concentrated within narrow tubes (or strings) [12]. This is in contrast to QED, where the electromagnetic field lines connecting a pair of opposite charges are allowed to spread out in space. If the chromoelectric flux is confined to narrow tubes, the energy is not allowed to spread and the potential of a quark-antiquark pair increases with its spatial separation, as long as vacuum polarization effects do not screen the color charge. If the energy stored in the string is sufficient to produce real quark pairs, the system will lower its energy by breaking the string and going over into a new hadronic state [12].

In contrast to QED, QCD has the remarkable property of *asymptotic freedom*, which means that the effective coupling vanishes at short distances (or high energies) and increases with increasing distance. Therefore, perturbative QCD is only applicable at short distances, where the quarks behave like free particles. On the other hand, the formulation of gauge theories on a discretized spacetime, known as lattice gauge theory, allows for the study of the long distance (or low energy) properties of QCD, such as its confining behavior.

3.3.1 Free fermionic Lagrangian

The Lagrangian density of free quark fields can be written as [7]

$$\mathcal{L}_{\text{Dirac}} = \sum_{\text{flavors } f} \bar{\psi}_f(x)\left(i\gamma^\mu\partial_\mu - m_f\right)\psi_f(x)\,, \tag{3.38}$$

where the sum runs over all quark flavors f under consideration[4], and the quark fields $\psi_f(x) \equiv \psi_{f\nu c}(x)$ also have, in addition to the flavor index f, a Dirac spinor index ν and an SU(N) color index c (usually, we consider fermions in the fundamental representation of the gauge group, i.e., $c = 1, \ldots, N$). However, for the sake of simplicity, the summations over spinor and color indices are not written out explicitly in Eq. (3.38) as well as in almost all of the following expressions. In the following, we will consider only a single-flavor field $\psi(x)$ with mass m.

The gamma matrices γ^μ, which act on the spinor indices of the fermionic field, obey the anticommutation relations

$$\{\gamma^\mu, \gamma^\nu\} \equiv \gamma^\mu\gamma^\nu + \gamma^\nu\gamma^\mu = 2g^{\mu\nu}\mathbf{1}\,. \tag{3.39}$$

The classical Euler-Lagrange equations (for a single quark flavor) derived from $\mathcal{L}_{\text{Dirac}}$ read

$$(i\gamma^\mu\partial_\mu - m)\,\psi = 0\,, \qquad -i\partial_\mu\bar{\psi}\gamma^\mu - m\bar{\psi} = 0\,. \tag{3.40}$$

The first equation is the famous Dirac equation, the second just its Hermitian-conjugate form (with $\bar{\psi} = \psi^\dagger\gamma^0$). By acting with $(-i\gamma^\mu\partial_\mu - m)$ on the Dirac equation, we see that it implies the Klein-Gordon equation

$$\left(\partial^\mu\partial_\mu + m^2\right)\psi = 0\,, \tag{3.41}$$

due to the anticommutation relation (3.39).

3.3.2 Functional integrals for fermion fields

To use functional methods to compute correlation functions for fermionic fields, which obey canonical anticommutation relations, the fields must be represented by anticommuting numbers, also called Grassmann numbers (cf. App. D). A Grassmann field $\psi(x)$ is a function of spacetime whose values are Grassmann numbers. It can be defined in terms of any complete set of ordinary orthonormal basis functions $f_i(x)$ with anticommuting coefficients ψ_i,

$$\psi(x) = \sum_i \psi_i f_i(x)\,. \tag{3.42}$$

To describe Dirac fermions, we have to choose a basis of four-component spinors $f_i(x)$. This allows for the evaluation of fermionic correlation functions with functional integral methods. The two-point function (for a single flavor), e.g., is given by

$$\langle\Omega|\,T\left\{\hat{\psi}_{\scriptscriptstyle H}(x_1)\hat{\bar{\psi}}_{\scriptscriptstyle H}(x_2)\right\}|\Omega\rangle = \lim_{T\to\infty(1-i\varepsilon)} \frac{\int[D\bar{\psi}][D\psi]\exp\left(i\int d^4x\mathcal{L}_{\text{Dirac}}[\bar{\psi},\psi]\right)\psi(x_1)\bar{\psi}(x_2)}{\int[D\bar{\psi}][D\psi]\exp\left(i\int d^4x\mathcal{L}_{\text{Dirac}}[\bar{\psi},\psi]\right)}\,, \tag{3.43}$$

where $\bar{\psi}$ and ψ are treated as independent integration variables. Here, the time-ordering operator acting on two spinor-fields is defined with an additional minus sign,

$$T\left\{\hat{\psi}_{\scriptscriptstyle H}(x)\hat{\bar{\psi}}_{\scriptscriptstyle H}(y)\right\} = \Theta(x^0-y^0)\hat{\psi}_{\scriptscriptstyle H}(x)\hat{\bar{\psi}}_{\scriptscriptstyle H}(y) - \Theta(y^0-x^0)\hat{\bar{\psi}}_{\scriptscriptstyle H}(y)\hat{\psi}_{\scriptscriptstyle H}(x)\,. \tag{3.44}$$

As for the scalar field, the limits on the time integrals lead to an $i\varepsilon$-term in the Feynman propagator,

$$\langle\Omega|\,T\left\{\hat{\psi}_{\scriptscriptstyle H}(x_1)\hat{\bar{\psi}}_{\scriptscriptstyle H}(x_2)\right\}|\Omega\rangle = S_F(x_1-x_2) = \int\frac{d^4k}{(2\pi)^4}\frac{ie^{-ik\cdot(x_1-x_2)}}{\not{k}-m+i\varepsilon}\,, \tag{3.45}$$

[4]There are six known quark flavors: up, down, charm, strange, top, bottom.

where $\not{k} = k^\mu \gamma_\mu$. Higher correlation functions are again obtained according to Wick's theorem.

Similar to the scalar field theory, the Feynman rules for the Dirac theory can be derived from the generating functional

$$Z[\bar{\eta},\eta] = \int [D\bar{\psi}][D\psi] \exp\left(i \int d^4x \left[\bar{\psi} \left(i\not{\partial} - m \right) \psi + \bar{\eta}\psi + \bar{\psi}\eta \right] \right) , \tag{3.46}$$

where $\eta(x)$ and $\bar{\eta}(x)$ are Grassmann-valued source fields. Shifting the integration variables $\psi(x)$ and $\bar{\psi}(x)$ leads to

$$Z[\bar{\eta},\eta] = Z[0,0] \exp\left(- \int d^4x d^4y \, \bar{\eta}(x) S_F(x-y) \eta(y) \right) . \tag{3.47}$$

Correlation functions can be obtained by differentiating Z with respect to the sources η and $\bar{\eta}$, e.g.,

$$\langle \Omega | \, T \left\{ \hat{\psi}_H(x_1) \hat{\bar{\psi}}_H(x_2) \right\} | \Omega \rangle = Z[0,0]^{-1} \left(-i \frac{\delta}{\delta \bar{\eta}(x_1)} \right) \left(i \frac{\delta}{\delta \eta(x_2)} \right) Z[\bar{\eta},\eta] \big|_{\bar{\eta},\eta=0} . \tag{3.48}$$

3.3.3 Local gauge invariance

Since the Dirac Lagrangian, defined in Eq. (3.38), is diagonal in color space, it is invariant under global SU(N) transformations[5]. Every element g of SU(N) can be written in the form (cf. Sec. 2.5)

$$g = e^{i\alpha_i t_i} , \tag{3.49}$$

where a summation over the repeated index i from 1 to $N^2 - 1$ is implied. In the defining (or fundamental) representation, g is an $N \times N$ matrix that satisfies

$$g^\dagger g = \mathbf{1} , \qquad \det g = 1 . \tag{3.50}$$

The generators t_i are traceless, Hermitian, and satisfy the commutation relations

$$[t_i, t_j] = i f_{ijk} t_k \tag{3.51}$$

with completely antisymmetric and real structure constants f_{ijk} (cf. Sec. 2.5). Usually, the generators are normalized by requiring

$$\mathrm{Tr}\,\{t_i t_j\} = \frac{1}{2} \delta_{ij} . \tag{3.52}$$

The density $\mathcal{L}_{\mathrm{Dirac}}$ is invariant under global transformations of the form

$$\psi(x) \to \psi'(x) = h\psi(x) , \qquad \bar{\psi}(x) \to \bar{\psi}'(x) = \bar{\psi}(x) h^{-1} , \qquad h \in \mathrm{SU}(N) , \tag{3.53}$$

where g acts only on the SU(N) color indices of the fields ψ and $\bar{\psi}$ (i.e., g commutes with the gamma matrices γ^μ which act on the spinor indices of ψ and $\bar{\psi}$).

The present belief is that so-called *local gauge symmetries* (h becomes spacetime dependent) may dictate all particle interactions [13]. In analogy to the principle of general covariance in Einstein's theory of general relativity, the concept of local gauge invariance was introduced by H. Weyl for the theory of electromagnetism; an extension to non-Abelian gauge groups was achieved by Yang and Mills. Local gauge transformations correspond to

[5] A global transformation is a transformation (in the internal space) that is spacetime independent.

an x-dependent change of basis and therefore should, according to the Naheinformationsprinzip, not affect the physics [11]. For that reason, the Lagrangian density is required to be invariant under this kind of transformations. The derivative term $\bar{\psi}(x)\partial_\mu\psi(x)$ obviously spoils invariance under transformations with spacetime dependent matrices $h(x)$. Invariance under these transformations can be achieved by introducing a *covariant derivative* D_μ such that $\bar{\psi}(x)D_\mu\psi(x)$ becomes invariant. This can be realized by introducing a new field, the *gauge field* $A_\mu(x)$.

The covariant derivative is defined as

$$D_\mu = \partial_\mu - iA_\mu(x) \tag{3.54}$$

with gauge field $A_\mu(x) = A^i_\mu(x)t_i$ (we do not distinguish between upper and lower color indices). This derivative is both a differential operator and a matrix in the internal SU(N) color space. The fermionic part of the full QCD Lagrangian density is obtained by replacing the ordinary derivative ∂_μ in the Dirac Lagrangian (3.38) by D_μ. In the case of QCD ($N = 3$), the eight fields $A^i_\mu(x)\,(i = 1, ..., 8)$ are called gluons. The Lagrangian density

$$\mathcal{L}^{\mathrm{F}}_{\mathrm{QCD}} = \bar{\psi}(x)\left(i\gamma^\mu D_\mu - m\right)\psi(x)\,, \tag{3.55}$$

which contains the interaction term $\bar{\psi}\gamma^\mu A_\mu\psi$, is then invariant under the *local gauge transformation*

$$\psi(x) \to \psi'(x) = h(x)\psi(x)\,, \tag{3.56}$$

$$\bar{\psi}(x) \to \bar{\psi}'(x) = \bar{\psi}(x)h^{-1}(x)\,, \tag{3.57}$$

$$A_\mu(x) \to A'_\mu(x) = h(x)A_\mu(x)h^{-1}(x) - i\left(\partial_\mu h(x)\right)h^{-1}(x) \tag{3.58}$$

with $h(x) \in \mathrm{SU}(N)$. The transformation law for the gauge field is obtained from the requirement that the covariant derivative of ψ transforms exactly in the same way as the field ψ itself,

$$D_\mu\psi(x) \to D'_\mu\psi'(x) = \left(\partial_\mu - iA'_\mu(x)\right)\psi'(x) = h(x)\left(\partial_\mu - iA_\mu(x)\right)\psi(x)\,, \tag{3.59}$$

which leads to the invariance of the Lagrangian.

A dynamics for the gauge field itself is generated by the gauge-invariant *Yang-Mills Lagrangian* [11]

$$\mathcal{L}_{\mathrm{YM}} = -\frac{1}{2g^2}\,\mathrm{Tr}\left\{F_{\mu\nu}(x)F^{\mu\nu}(x)\right\} \tag{3.60}$$

with a coupling constant g (interaction terms in the Lagrangian are of order g or g^2 if the field variables are rescaled according to $A^i_\mu \to gA^i_\mu$). The antisymmetric field strength tensor $F_{\mu\nu}(x) = F^i_{\mu\nu}(x)\,t_i$ can be defined through the commutator of two covariant derivatives,

$$F_{\mu\nu}(x) = i\left[D_\mu, D_\nu\right] = \partial_\mu A_\nu(x) - \partial_\nu A_\mu(x) - i\left[A_\mu(x), A_\nu(x)\right]\,. \tag{3.61}$$

In terms of the components $F^i_{\mu\nu}(x)$, this equations reads

$$F^i_{\mu\nu}(x) = \partial_\mu A^i_\nu(x) - \partial_\nu A^i_\mu(x) + f_{ijk}A^j_\mu(x)A^k_\nu(x)\,. \tag{3.62}$$

The definition of the field strength tensor through covariant derivatives immediately leads to the transformation law

$$F_{\mu\nu}(x) \to h(x)F_{\mu\nu}(x)h^{-1}(x)\,. \tag{3.63}$$

Due to the cyclic invariance of the trace, $\mathcal{L}_{\rm YM}$ is invariant under this kind of transformations.

The gauge field with its Yang-Mills action $S_{\rm YM} = \int d^4x \mathcal{L}_{\rm YM}$ may also be considered on its own, without being coupled to quark fields. Since $S_{\rm YM}$ involves triple and quartic interactions of the fields A^i_μ, the pure gauge sector of QCD describes a highly non-trivial interacting theory, called pure Yang-Mills theory.

3.3.4 Functional integrals for gauge fields

Since the Yang-Mills Lagrangian is invariant under local gauge transformations, some degrees of freedom of the gauge field are unphysical because they can be adjusted arbitrarily by gauge transformations. This means that the functional integral over a gauge field must be defined carefully and that subtle aspects of this construction can introduce new ingredients into the quantum theory [7].

To quantize pure gauge theory, we have to define the functional integral

$$Z = \int [DA(x)] e^{iS_{\rm YM}[A]} = \int [DA(x)] \exp\left[i \int d^4x \left(-\frac{1}{4g^2} (F^i_{\mu\nu}(x))^2 \right) \right] , \tag{3.64}$$

where the measure is taken to be invariant under local gauge transformations. For both Abelian and non-Abelian gauge fields, the Lagrangian remains unchanged along the directions in the space of field configurations which correspond to local gauge transformations. Hence, the functional integral is badly defined because we are redundantly integrating over a continuous infinity of physically equivalent field configurations. A method for dealing with this redundancy was invented by Faddeev and Popov and works in the following way: The integration over physically equivalent gauge configurations is constrained by imposing a gauge fixing condition, $G_i(A) = 0$, at each spacetime point (i is a color index). To this end, the identity

$$1 = \Delta_{\rm FP}(A) \int [Dh(x)] \delta \left(G_i \left(A^h \right) \right) , \tag{3.65}$$

which is basically the definition of the Faddeev-Popov determinant $\Delta_{\rm FP}$, is inserted into the path integral [10]. Here A^h denotes the gauge field which is obtained from the field A through the local gauge transformation (3.58) with $h(x) = \exp\left(i\alpha(x)\right) = \exp\left(i\alpha_j(x) t_j\right)$,

$$A^h_\mu(x) = e^{i\alpha(x)} A_\mu(x) e^{-i\alpha(x)} - i \left(\partial_\mu e^{i\alpha(x)} \right) e^{-i\alpha(x)} , \tag{3.66}$$

whose infinitesimal form is given by

$$A^\alpha_\mu(x) = A_\mu(x) + i \left[\alpha(x), A_\mu(x) \right] + \partial_\mu \alpha(x) , \tag{3.67}$$

$$\left(A^\alpha\right)^i_\mu(x) = A^i_\mu(x) + f_{ijk} \alpha_k(x) A^j_\mu(x) + \partial_\mu \alpha_i(x) = A^i_\mu + \left(D_\mu \alpha\right)_i , \tag{3.68}$$

where D_μ is a covariant derivative acting on a field in the adjoint representation of the gauge group. In the adjoint representation, the matrix elements of the generators are given by the structure constants, $(t^{\rm adj}_j)_{ik} = i f_{ijk}$, cf. Sec. 2.5, and therefore

$$\left(\partial_\mu - i A^j_\mu t^{\rm adj}_j \right)_{ik} = \delta_{ik} \partial_\mu + f_{ijk} A^j_\mu . \tag{3.69}$$

The integration measure is given by a product of Haar measures at each spacetime point,

$$[Dh(x)] = \prod_x d\mu(h(x)) , \tag{3.70}$$

where $d\mu(h)$ is the invariant Haar measure of SU(N), cf. Sec. 2.5. Similarly, the delta functional in Eq. (3.65) is given by a product of delta functions at each spacetime point. Since $d\mu(h) = d\mu(hh')$, the Faddeev-Popov determinant is invariant under local gauge transformations,

$$\begin{aligned}\Delta_{\mathrm{FP}}\left(A^h\right)^{-1} &= \int [Dh'(x)]\delta\left(G_i\left(A^{hh'}\right)\right) = \int [Dh^{-1}h''(x)]\delta\left(G_i\left(A^{h''}\right)\right) \\ &= \int [Dh''(x)]\delta\left(G_i\left(A^{h''}\right)\right) = \Delta_{\mathrm{FP}}(A)^{-1}\,. \end{aligned} \tag{3.71}$$

Inserting the identity (3.65) into the functional integral (3.64) and interchanging the order of integration (over h and A) leads to

$$Z = \int [Dh(x)] \int [DA(x)] e^{iS_{\mathrm{YM}}[A]} \Delta_{\mathrm{FP}}\left(A\right) \delta\left(G_i\left(A^h\right)\right)\,. \tag{3.72}$$

We can now change the integration variable from A to $A^{h^{-1}}$ and use that

$$S_{\mathrm{YM}}\left[A^h\right] = S_{\mathrm{YM}}\left[A\right]\,, \qquad \left[DA^h(x)\right] = \left[DA(x)\right]\,, \qquad \Delta_{\mathrm{FP}}\left(A^h\right) = \Delta_{\mathrm{FP}}(A)\,, \tag{3.73}$$

which results in

$$Z = \left(\int [Dh(x)]\right) \int [DA(x)] e^{iS_{\mathrm{YM}}[A]} \Delta_{\mathrm{FP}}\left(A\right) \delta\left(G_i\left(A\right)\right)\,. \tag{3.74}$$

In this expression, the group integration $\int [Dh(x)]$ has been factored out and may therefore be ignored. It only leads to an (infinite) normalization constant which is fortunately irrelevant for the computation of correlation functions. The correct expression for Z is therefore given by [10]

$$Z = \int [DA(x)] e^{iS_{\mathrm{YM}}[A]} \Delta_{\mathrm{FP}}\left(A\right) \delta\left(G_i\left(A\right)\right)\,. \tag{3.75}$$

Let us consider, e.g., the generalized Lorentz gauge condition [7]

$$G_i(A(x)) = \partial^\mu A^i_\mu(x) - \omega_i(x) \tag{3.76}$$

with an arbitrary function $\omega_i(x)$. Equation (3.75) holds for any $\omega_i(x)$, so it remains valid if we replace the right hand side by any normalized linear combination involving different functions $\omega_i(x)$. We can therefore integrate over $\omega_i(x)$ with a Gaussian weight function and obtain (up to an irrelevant normalization factor)

$$\begin{aligned} Z &= \int [D\omega_i(x)] e^{-i\int d^4x \frac{1}{2\xi g^2}\omega_i(x)\omega_i(x)} \int [DA(x)] e^{iS_{\mathrm{YM}}[A]} \Delta_{\mathrm{FP}}\left(A\right) \delta\left(\partial^\mu A^i_\mu(x) - \omega_i(x)\right) \\ &= \int [DA(x)] e^{-i\int d^4x \frac{1}{2\xi g^2}\left(\partial^\mu A^i_\mu(x)\right)^2} e^{iS_{\mathrm{YM}}[A]} \Delta_{\mathrm{FP}}\left(A\right)\,. \end{aligned} \tag{3.77}$$

To compute the Faddeev-Popov determinant, it is sufficient to consider the infinitesimal gauge transformation (3.67). In analogy to the properties of delta functions of a finite number of integration variables,

$$1 = \int d\vec{x}\, \delta(\vec{g}(\vec{x})) \det\left|\frac{\partial \vec{g}}{\partial \vec{x}}\right|\,, \tag{3.78}$$

the Faddeev-Popov determinant is given by the functional determinant [10]

$$\Delta_{\mathrm{FP}}(A) = \det \left| \frac{\delta G_i(A^\alpha(x))}{\delta \alpha_j(y)} \right|_{G=0} . \tag{3.79}$$

The generalized Lorentz gauge condition (3.76) leads to

$$\frac{\delta G_i(A^\alpha(x))}{\delta \alpha_l(y)} = \partial^\mu \left(\delta_{il} \partial_\mu + f_{ijl} A^j_\mu(x) \right) \delta(x-y) = \partial^\mu (D_\mu)_{il} \delta(x-y) . \tag{3.80}$$

For an Abelian gauge theory, such as QED, $\Delta_{\mathrm{FP}}(A)$ is independent of A (the structure constants are zero) and the Faddeev-Popov determinant can be treated as just another overall normalization factor. In the non-Abelian case however, the functional determinant contributes new terms to the Lagrangian. The determinant can be represented as a functional integral over new anticommuting fields (called Faddeev-Popov ghosts) belonging to the adjoint representation [7]

$$\det \left(\partial^\mu D_\mu \right) = \int [D\bar{c}(x)][Dc(x)] e^{i \int d^4x \mathcal{L}_{\mathrm{ghost}}[c(x), \bar{c}(x)]} \tag{3.81}$$

with Lagrangian

$$\begin{aligned} \mathcal{L}_{\mathrm{ghost}}[c(x), \bar{c}(x)] &= \bar{c}_i(x) \left(-\delta_{ik} \partial^2 - f_{ijk} \partial^\mu A^j_\mu(x) \right) c_k(x) \\ &= \bar{c}_i(x) \left(-\delta_{ik} \partial^2 - f_{ijk} \left[\left(\partial^\mu A^j_\mu(x) \right) + A^j_\mu(x) \partial^\mu \right] \right) c_k(x) . \end{aligned} \tag{3.82}$$

Although the scalar ghost fields are treated as anticommuting, the violation of the spin-statistics connection is acceptable because they are not associated with physical particles. Nevertheless, we can treat these excitations as additional particles in the computation of Feynman diagrams.

The final Lagrangian, including quark fields and all of the effects of the Faddeev-Popov gauge fixing procedure, is given by [7]

$$\mathcal{L} = -\frac{1}{4g^2} \left(F^i_{\mu\nu} \right)^2 - \frac{1}{2\xi} \left(\partial^\mu A^i_\mu \right)^2 + \bar{\psi}(i \not{D} - m)\psi + \bar{c}_i \left(-\partial_\mu D^\mu_{ik} \right) c_k . \tag{3.83}$$

Correlation functions can be computed in perturbation theory by splitting the Lagrangian into terms which are quadratic in the fields on one side and into interaction terms which contain more than two field variables on the other side. If we rescale the gauge fields by $A \to gA$ (and change the parameter $\xi \to g^2 \xi$), all the terms in the Lagrangian that are not quadratic in the fields are proportional to the coupling constant g.

In perturbation theory, one first computes the "free" propagators, which are obtained from the quadratic terms in the Lagrangian just as in a free theory (this corresponds to setting $g = 0$). Expanding $\exp(i \int d^4x \mathcal{L})$ in powers of g, these propagators can be used to take the effects of the interaction terms into account in a systematic way (assuming that the coupling is small), and correlation functions of the full theory are obtained in a series in g (which needs to be renormalized, cf. Sec. 3.5.6). The Lagrangian resulting from the gauge-fixing procedure is in fact only meaningful in perturbation theory since the gauge-fixing condition does not always have a unique solution (in the space of gauge fields that are equivalent up to gauge transformations). This ambiguity, first noted by Gribov, is related to the property that there exist gauge fields for which the operator $\partial_\mu D^\mu$ has vanishing eigenvalues, cf. Ref. [14].

Computing correlation functions in perturbation theory is somehow an unnatural act since it involves splitting the highly symmetric Lagrangian into two parts. The alternative proposed by Wilson is to violate Lorentz invariance rather than gauge invariance

and to study gauge field theories on a discrete lattice of spacetime points, cf. Sec. 3.5. Lattice gauge theory provides the only known regularization scheme which is entirely non-perturbative.

The quadratic terms in the gauge field A are diagonal in the internal color space; therefore the free gauge-field propagator in SU(N) gauge theory is basically the same as in the Abelian U(1) case (QED). The quadratic action can be written as (after rescaling the fields)

$$\begin{aligned} S_{\text{quad}}[A] &= -\int d^4x \left(\frac{1}{4} \left(\partial_\mu A^i_\nu - \partial_\nu A^i_\mu\right) \left(\partial^\mu A^\nu_i - \partial^\nu A^\mu_i\right) + \frac{1}{2\xi} \left(\partial^\mu A^i_\mu\right) \left(\partial^\nu A^i_\nu\right) \right) \\ &= \frac{1}{2} \int d^4x A^i_\mu(x) \delta_{ij} \left(g^{\mu\nu}\partial^2 - \left(1 - \xi^{-1}\right) \partial^\mu \partial^\nu \right) A^j_\nu(x) \,. \end{aligned} \tag{3.84}$$

In complete analogy to scalar field theory (cf. Sec. 3.2), the free gauge-field propagator

$$D^{jk}_{\nu\sigma}(x-y) = \left\langle A^j_\nu(x) A^k_\sigma(y) \right\rangle = \int [DA(x)]\, A^j_\nu(x) A^k_\sigma(y) e^{iS_{\text{quad}}[A]} \tag{3.85}$$

is found by inverting the differential operator in the Lagrangian. By Fourier transforming, we find that a solution of

$$\delta_{ij} \left(g^{\mu\nu}\partial^2 - \left(1 - \xi^{-1}\right) \partial^\mu \partial^\nu \right) D^{jk}_{\nu\sigma}(x-y) = i \delta^\mu_\sigma \delta_{ik} \delta(x-y) \tag{3.86}$$

is given by

$$D^{jk}_{\nu\sigma}(x-y) = \delta_{jk} \int \frac{d^4k}{(2\pi)^4} \frac{-i}{k^2 + i\varepsilon} \left(g_{\nu\sigma} + (\xi - 1) \frac{k_\nu k_\sigma}{k^2} \right) e^{ik(x-y)} \,, \tag{3.87}$$

where the $i\varepsilon$-term in the denominator arises exactly as in the scalar case [7]. The Faddeev-Popov method guarantees that correlation functions of gauge-invariant operators are independent of the value of ξ. The choice $\xi = 0$ is called Landau gauge, Feynman gauge corresponds to setting $\xi = 1$.

In a similar way, the quadratic terms of the ghost Lagrangian lead to the free ghost-field propagator [7]

$$\langle c_i(x) \bar{c}_j(y) \rangle = \delta_{ij} \int \frac{d^4k}{(2\pi)^4} \frac{i}{k^2 + i\varepsilon} e^{ik(x-y)} \,. \tag{3.88}$$

The Faddeev-Popov gauge fixing procedure can be carried over to Euclidean Yang-Mills theory without complication. In this case, the starting point is the Lagrangian $\mathcal{L}_{_E} = \frac{1}{4g^2} \left(F^i_{\mu\nu}\right)^2$, where $F_{\mu\nu}$ is the Euclidean field strength tensor. The Euclidean action is obtained by integrating over the Euclidean spacetime, $S_{_E} = \int d^4x_{_E} \mathcal{L}_{_E}$, cf. Sec. 3.2.3. After fixing the gauge, correlation functions are obtained from the generating functional

$$Z_{_E}[J] = \int [DA(x)]\, e^{-\frac{1}{g^2}\int d^4x_{_E} \left(\frac{1}{4} \left(F^i_{\mu\nu}\right)^2 + \frac{1}{2\xi} \left(\partial_\mu A^i_\mu\right)^2 \right) + i \int d^4x_{_E} J_\mu A_\mu - S^{\text{ghost}}_E} \,. \tag{3.89}$$

The free gauge-field propagator in Euclidean spacetime is obtained from the quadratic terms in the Lagrangian and is found to be

$$\left(D_{_E}\right)^{jk}_{\nu\sigma}(x-y) = \delta_{jk} \int \frac{d^4k}{(2\pi)^4} \left(\frac{\delta_{\nu\sigma}}{k^2} + (\xi - 1) \frac{k_\nu k_\sigma}{\left(k^2\right)^2} \right) e^{ik(x-y)} \,, \tag{3.90}$$

where the integral is over Euclidean momenta (and the fields have again been rescaled by $A \to gA$). A position space representation of the propagator can be obtained by

performing the Euclidean momentum integration. The general result in d-dimensional Euclidean spacetime is given by (cf. App. A)

$$(D_E)^{jk}_{\mu\nu}(x-y) = \delta_{jk}\frac{\Gamma\left(\frac{d}{2}-1\right)}{4\pi^{\frac{d}{2}}}\left(\frac{1+\xi}{2}\delta_{\mu\nu}+\frac{1-\xi}{2}(d-2)\frac{x_\mu x_\nu}{x^2}\right)\frac{1}{(x^2)^{\frac{d}{2}-1}}\,. \tag{3.91}$$

3.4 Wilson loops

In the previous section, we have introduced the covariant derivative to achieve invariance under local gauge transformations. This derivative can be regarded as a consequence of the concept of parallel transport (inspired from the theory of general relativity). If we allow for local transformations of the fields ψ with spacetime dependent $h(x)$, fields at different spacetime points are measured with respect to different basis systems in the internal SU(N) symmetry space. The gauge field in the covariant derivative has to be introduced in order to compare $\psi(x+dx)$ with the value $\psi(x)$ would have if it were transported from x to $x+dx$, keeping the axes (in the internal space) fixed.

3.4.1 Wilson lines

Consider now a path $x(s)$ in four-dimensional spacetime, which continuously connects two points $x_0 = x(0)$ and $x_1 = x(1)$. We associate to the spacetime curve the so-called *Wilson line*, which is a curve-dependent element of the gauge group SU(N) and is defined as [7]

$$W(x_1,x_0) = P\left\{\exp\left(i\int_0^1 ds\, A_\mu(x(s))\dot{x}^\mu(s)\right)\right\} \tag{3.92}$$

with $\dot{x}^\mu(s) = \frac{dx^\mu}{ds}$. In this definition, the symbol P denotes the path-ordering operator, which is defined analogously to the time-ordering operator introduced in Sec. 3.1. This means that the Wilson line is defined as the power-series expansion of the exponential with the integrands ordered in such a way that higher values of s stand to the left. For the $(n+1)$-th term in the expansion, we get n non-commuting factors $A_{\mu_1}(x(s_1))$, $A_{\mu_2}(x(s_2))$,..., $A_{\mu_n}(x(s_n))$ (the s_i's are the integration variables parametrizing the curve). These can be ordered in $n!$ ways, which leads to the cancellation of the factorial that we get from the exponential series, i.e.,

$$\begin{aligned} &P\left\{\frac{1}{n!}\left(i\int_0^1 ds\, A_\mu(x(s))\dot{x}^\mu(s)\right)^n\right\} \\ &\quad = i^n\int_0^1 ds_1\int_0^{s_1} ds_2\int_0^{s_2} ds_3\cdots\int_0^{s_{n-1}} ds_n\, A(s_1)A(s_2)A(s_3)\cdots A(s_n) \end{aligned} \tag{3.93}$$

with the abbreviation $A(s_i) = \dot{x}^\mu(s_i)A_\mu(x(s_i))$. If we do not fix the endpoint at $x(1)$ but consider instead $W(x(t),x_0)$ with $0\le t\le 1$ and assume that it is a continuous function of the parameter t, we see from Eq. (3.93) that this Wilson line fulfills the differential equation

$$\frac{d}{dt}W(x(t),x_0) = i\dot{x}^\mu(t)A_\mu(x(t))W(x(t),x_0)\,, \tag{3.94}$$

which can be rewritten as

$$\dot{x}^\mu(t)D_\mu W(x(t),x_0) = 0\,. \tag{3.95}$$

By changing the parametrization of the integration domain (restricted to $s_1 \geq s_2 \geq \ldots \geq s_n$) in Eq. (3.93),

$$\int_0^1 ds_1 \int_0^{s_1} ds_2 \int_0^{s_2} ds_3 \cdots \int_0^{s_{n-1}} ds_n = \int_0^1 ds_n \int_{s_n}^1 ds_{n-1} \cdots \int_{s_3}^1 ds_2 \int_{s_2}^1 ds_1 \,, \tag{3.96}$$

we find a similar differential equation for $W(x_1, x(t))$,

$$W(x_1, x(t)) \underbrace{\left(\overleftarrow{\partial}_\mu + iA_\mu(x(t))\right)}_{=\overleftarrow{D}_\mu} \dot{x}^\mu(t) = 0 \,. \tag{3.97}$$

The covariant backward derivative $\overleftarrow{D}_\mu$ has the property that the local gauge transformations (3.57) and (3.58) result in

$$\bar{\psi}(x) \left(\overleftarrow{\partial}_\mu + iA_\mu(x)\right) \to \bar{\psi}(x) \left(\overleftarrow{\partial}_\mu + iA_\mu(x)\right) h^{-1}(x) \,. \tag{3.98}$$

To determine the behavior of W under local gauge transformations, we transform the gauge field according to Eq. (3.58). It is obvious that Eqs. (3.95) and (3.97) have to hold also for the transformed variables, i.e.,

$$\dot{x}^\mu(t) D'_\mu W'(x(t), x_0) = 0 \qquad \text{and} \qquad W'(x_1, x(t)) \overleftarrow{D'}_\mu \dot{x}^\mu(t) = 0 \,, \tag{3.99}$$

where the covariant derivatives D'_μ and $\overleftarrow{D'}_\mu$ are built from the transformed field A'_μ. The transformation law for W then follows from the transformation of the covariant derivatives (cf. Eqs. (3.59) and (3.98)),

$$W(x_1, x_0) \to W'(x_1, x_0) = h(x_1) W(x_1, x_0) h^{-1}(x_0) \,. \tag{3.100}$$

This implies that

$$W(x_1, x_0)\psi(x_0) \to W'(x_1, x_0)\psi'(x_0) = h(x_1) W(x_1, x_0)\psi(x_0) \,, \tag{3.101}$$

which is just the transformation law of a field at the spacetime point x_1. Obviously, the combination $\bar{\psi}(x_1) W(x_1, x_0)\psi(x_0)$ is invariant under local gauge transformations. The Wilson line $W(x_1, x_0)$ compensates for the different transformations at different spacetime points x_1 and x_0 (corresponding to a local change of basis in the internal symmetry space). It can be viewed as a parallel transporter for the field ψ along the curve $x(s)$, allowing for the comparison of fields at different points in spacetime by converting the transformation law at point x_0 to that at x_1.

3.4.2 Closed Wilson lines: Wilson loops

If $x(s)$ describes a closed curve C in spacetime, i.e., $x(0) = x(1)$, the Wilson line is called a *Wilson loop*[6],

$$W_C(x_0, x_0) = P\left\{\exp\left(i \int_0^1 ds\, A_\mu(x(s)) \dot{x}^\mu(s)\right)\right\} = P\left\{\exp\left(i \oint_C A_\mu(x) dx^\mu\right)\right\} . \tag{3.102}$$

[6]Note that in the literature, the term "Wilson loop" often refers to the trace of the Wilson line around a closed path. Here, we usually use the term "Wilson loop" for the untraced matrix. We often refer to the size of the underlying spacetime curve C simply as "the size of the loop".

If the field $\psi(x)$ is transported around the closed curve C, it accumulates a non-trivial SU(N) "phase factor" given by the Wilson loop matrix W_C.

Under local gauge transformations, the Wilson loop transforms according to

$$W_C(x_0, x_0) \to W'_C(x_0, x_0) = h(x_0) W_C(x_0, x_0) h^{-1}(x_0)\,, \tag{3.103}$$

which means that the trace of the Wilson loop is a non-local, gauge-invariant observable,

$$\mathrm{Tr}\left\{W'_C(x_0, x_0)\right\} = \mathrm{Tr}\left\{h(x_0) W_C(x_0, x_0) h^{-1}(x_0)\right\} = \mathrm{Tr}\left\{W_C(x_0, x_0)\right\}\,. \tag{3.104}$$

For an infinitesimal transport along a straight line from x to $x + dx$, the Wilson line can be approximated by

$$W(x + dx, x) \approx e^{iA_\mu(x)dx^\mu} = 1 + iA_\mu(x)dx^\mu + \dots\,. \tag{3.105}$$

Requiring the transformation law $W(x + dx, x) \to W'(x + dx, x) = h(x + dx)W(x + dx, x)h^{-1}(x)$ for the infinitesimal Wilson line results in

$$\left(1 + iA'_\mu(x)dx^\mu\right) = \left(h(x) + \partial_\nu h(x)dx^\nu\right)\left(1 + iA_\mu(x)dx^\mu\right) h^{-1}(x) \tag{3.106}$$

and we recover the transformation law for the gauge field given in Eq. (3.58).

Let us now consider an infinitesimal Wilson loop associated to an infinitesimal square in spacetime with corners at x, $x + \varepsilon$, $x + \varepsilon + \delta$, $x + \delta$ (with infinitesimal four vectors ε and δ). The parallel transport along the sides of the square, from x to $x + \delta$ to $x + \delta + \varepsilon$ to $x + \varepsilon$ and back to x, is given by

$$\begin{aligned} W_\square(x, x) &= W(x, x + \varepsilon)W(x + \varepsilon, x + \varepsilon + \delta)W(x + \varepsilon + \delta, x + \delta)W(x + \delta, x) \\ &\approx e^{-iA_\mu(x)\varepsilon^\mu} e^{-iA_\mu(x+\varepsilon)\delta^\mu} e^{iA_\mu(x+\delta)\varepsilon^\mu} e^{iA_\mu(x)\delta^\mu}\,. \end{aligned} \tag{3.107}$$

By making use of the relation

$$e^{\varepsilon B} e^{\varepsilon C} = e^{\varepsilon(B+C) + \frac{\varepsilon^2}{2}[B,C]} + \mathcal{O}(\varepsilon^3) \tag{3.108}$$

and by expanding the fields around the point x, we obtain

$$W_\square(x, x) \approx e^{i(\partial_\mu A_\nu(x) - \partial_\nu A_\mu(x) - i[A_\mu(x), A_\nu(x)])\delta^\mu\varepsilon^\nu} = e^{iF_{\mu\nu}(x)d\sigma^{\mu\nu}} \tag{3.109}$$

with the infinitesimal area element $d\sigma^{\mu\nu} = \delta^\mu\varepsilon^\nu$. The field strength tensor $F_{\mu\nu}$ can be interpreted as the curvature tensor of the internal symmetry space (in analogy to general relativity).

3.4.3 Divergences in perturbation theory

Expanding the path-ordered exponential in Eq. (3.102) in powers of A_μ leads to a perturbative expansion for Wilson loops (rescaling the fields by $A \to gA$ immediately leads to an expansion in powers of the coupling constant). We will now study the divergences occurring in calculations of expectation values of Wilson loops in perturbation theory. For simplicity, let us first consider the Abelian gauge group U(1). In the Abelian case, the fields commute and therefore path ordering becomes irrelevant. With

$$\mathcal{A} = \oint_C A_\mu(x)dx^\mu \tag{3.110}$$

we obtain, according to Wick's theorem,

$$\left\langle e^{ig\mathcal{A}}\right\rangle = \sum_{n=0}^{\infty} \frac{(ig)^{2n}}{(2n)!} \left\langle \mathcal{A}^{2n}\right\rangle = \sum_{n=0}^{\infty} \frac{\left(-g^2\right)^n}{2^n n!} \left\langle \mathcal{A}^2\right\rangle^n = e^{-\frac{g^2}{2}\left\langle \mathcal{A}^2\right\rangle}, \tag{3.111}$$

which means that we have to compute only a single expectation value. It is instructive to perform this calculation for a circular curve in four-dimensional Euclidean spacetime with a sharp momentum cut-off in the Fourier representation of the gauge-field propagator, i.e., the integral (3.90) is restricted to $k^2 < \Lambda^2$ (all quantities in this section are Euclidean; the subscript E is omitted). We parametrize the circle of radius R by

$$x_\mu(s) = R(\cos(2\pi s), \sin(2\pi s), 0, 0), \tag{3.112}$$

which leads to

$$\dot{x}_\mu(s)\dot{x}_\mu(t) = (2\pi R)^2 \cos(2\pi(s-t)). \tag{3.113}$$

In Feynman gauge ($\xi = 1$), the expectation value (3.111) is obtained from

$$\left\langle \mathcal{A}^2\right\rangle = \int_0^1 ds \int_0^1 dt\, \dot{x}_\mu(s)\dot{x}_\nu(t)\delta_{\mu\nu} \int_{k^2<\Lambda^2} \frac{d^4k}{(2\pi)^4} \frac{1}{k^2} e^{ik(x(s)-x(t))}. \tag{3.114}$$

Integrating over the momentum components perpendicular to the plane of the circular curve (the components k_3 and k_4 in the parametrization (3.112)),

$$\int_0^{\sqrt{\Lambda^2-k_1^2-k_2^2}} \frac{dk_\perp}{2\pi} \frac{k_\perp}{k_\perp^2 + k_1^2 + k_2^2} = \frac{1}{2\pi} \log \frac{\Lambda}{\sqrt{k_1^2+k_2^2}}, \tag{3.115}$$

and using polar coordinates for the remaining components ($k_1 = \kappa\cos\alpha$, $k_2 = \kappa\sin\alpha$) results in

$$\begin{aligned}\left\langle \mathcal{A}^2\right\rangle &= \int_0^1 ds \int_0^1 dt \int_0^\Lambda \kappa d\kappa \int_0^{2\pi} \frac{d\alpha}{2\pi} R^2 \log\left(\frac{\Lambda}{\kappa}\right) \cos(2\pi(s-t)) e^{i\kappa R(\cos(\alpha-2\pi s)-\cos(\alpha-2\pi t))} \\ &= \int_0^{2\pi} \frac{d\phi_1}{2\pi} \int_0^{2\pi} \frac{d\phi_2}{2\pi} \int_0^\Lambda \kappa d\kappa R^2 \log\left(\frac{\Lambda}{\kappa}\right) \cos(\phi_1-\phi_2)\, e^{i\kappa R(\cos\phi_1 - \cos\phi_2)}. \end{aligned} \tag{3.116}$$

Changing the integration variable from κ to $x = \kappa/\Lambda$ and using the integral representation of the Bessel function,

$$iJ_1(z) = \int_0^{2\pi} \frac{d\phi}{2\pi} e^{iz\cos\phi} \cos\phi, \tag{3.117}$$

leads to

$$\left\langle \mathcal{A}^2\right\rangle = -\Lambda R \int_0^1 dx \left(\sqrt{x\Lambda R}\, J_1(x\Lambda R)\right)^2 \log x. \tag{3.118}$$

Making use of the asymptotic form of the Bessel functions for large arguments $x \gg \frac{1}{\Lambda R}$,

$$J_n(x\Lambda R) \approx \sqrt{\frac{2}{\pi x \Lambda R}} \cos\left(x\Lambda R - \left(n+\frac{1}{2}\right)\frac{\pi}{2}\right), \tag{3.119}$$

one finds that the expectation value is linearly divergent in the momentum cut-off $\Lambda \gg \frac{1}{R}$,

$$\left\langle \mathcal{A}^2\right\rangle = c(\Lambda R) + \text{subleading terms}, \tag{3.120}$$

where c is a numerical constant. This divergence is usually referred to as the *perimeter divergence*, cf. Ref. [15]. It appears independently of the shape of the curve and occurs also for non-Abelian gauge groups (see below).

Reducing the number of spacetime dimensions from four to three reduces the divergence to a logarithmic one. In this case, we have to replace the integral (3.115) over the momentum components perpendicular to the plane of the curve by (using again $\kappa^2 = k_1^2 + k_2^2$)

$$\int_0^{\sqrt{\Lambda^2-\kappa^2}} \frac{dk_\perp}{2\pi} \frac{1}{k_\perp^2 + \kappa^2} = \frac{1}{2\pi\kappa} \int_0^{\sqrt{\Lambda^2-\kappa^2}/\kappa} \frac{dx}{x^2+1} = \frac{1}{2\pi\kappa} \arctan\sqrt{\frac{\Lambda^2}{\kappa^2} - 1}\,. \tag{3.121}$$

This results in

$$\left\langle \mathcal{A}^2 \right\rangle = R \int_0^1 dx \, \arctan\left(\sqrt{x^{-2}-1}\right) \frac{1}{x} \left(\sqrt{x\Lambda R}\, J_1(x\Lambda R)\right)^2 , \tag{3.122}$$

which is only logarithmically divergent for $\Lambda R \to \infty$.

In two spacetime dimensions only the integrals over k_1 and k_2 are left, resulting in

$$\left\langle \mathcal{A}^2 \right\rangle = 2\pi R^2 \int_0^1 \frac{dx}{x} \left(J_1(x\Lambda R)\right)^2 , \tag{3.123}$$

which remains finite in the infinite-Λ limit.

For non-Abelian Wilson loops, it was shown by Dotsenko and Vergeles in Ref. [16] that after introducing a regularization, the average of the trace of a Wilson loop W_C which corresponds to a smooth non-selfintersecting contour C in four Euclidean dimensions is of the form

$$\langle \operatorname{Tr} W_C \rangle = e^{-L(C)\Lambda} W_{\text{ren}}(C)\,, \tag{3.124}$$

where Λ is some ultraviolet cutoff and $L(C)$ is the length of the spacetime curve C. The factor $W_{\text{ren}}(C)$ is a functional of C and contains only logarithmic divergences. It is a finite function of the renormalized coupling constant (cf. Sec. 3.5.6) for smooth curves. (For curves with cusps, additional logarithmic divergences appear that depend on the various cusp-angles and therefore cannot be absorbed in the renormalization of the coupling constant.) Since the Wilson loop expectation value can be related to the static quark potential (see Sec. 3.5.5), the perimeter divergence can be interpreted as a mass renormalization of a heavy test quark.

3.5 Quantum field theory on a lattice

As mentioned before, lattice field theory provides a regularization scheme which is entirely non-perturbative. The basic idea is to violate Lorentz invariance rather than gauge invariance and to study gauge field theories on a discrete lattice of spacetime points. This lattice formulation of field theory is in close analogy with a statistical mechanics system and allows for studying various physical observables with numerical Monte Carlo simulations.

In lattice field theory, the Euclidean formulation of quantum field theory is taken as the starting point for all kinds of fields [11]. Since only Euclidean quantities appear in the following, the subscript E is omitted from now on. Moreover, the convention that repeated Lorentz indices are summed with the Euclidean metric $g^E_{\mu\nu} = (+,+,+,+)$, e.g., $x_\mu x_\mu = \sum_{\mu=1}^4 (x^\mu)^2$ is used.

3.5.1 Matter fields

In the case of quantum mechanics, the path integral is defined as a limit of a finite dimensional integral resulting from a discretization of time. This approach can be carried over to field theory by regarding the functional integral as a limit of a well-defined integral over the discretized Euclidean spacetime [11]. For this purpose, a hypercubic lattice

$$H_4 = a\mathbb{Z}^4 = \{x | x_\mu/a \in \mathbb{Z}\} \tag{3.125}$$

with lattice constant a is introduced. The scalar field $\phi(x)$ is then defined on the lattice points $x \in H_4$. Lattice forward and backward derivatives are given by the finite difference operations

$$\begin{aligned} \Delta_\mu \phi(x) &= \frac{1}{a}\left(\phi(x+\mu) - \phi(x)\right) , \\ \bar{\Delta}_\mu \phi(x) &= \frac{1}{a}\left(\phi(x) - \phi(x-\mu)\right) , \end{aligned} \tag{3.126}$$

where $\mu \equiv a\hat{\mu}$ is a vector of length a in the direction indicated by the index $\mu \in \{1,2,3,4\}$. With the lattice d'Alembert operator

$$\Box = -\bar{\Delta}_\mu \Delta_\mu \, , \tag{3.127}$$

which acts on functions defined on the lattice points as

$$\Box\phi(x) = \sum_{\mu=1}^{4} \frac{1}{a^2}\left(2\phi(x) - \phi(x+\mu) - \phi(x-\mu)\right) , \tag{3.128}$$

the lattice action of the free scalar field can be chosen as [11]

$$S[\phi] = \frac{1}{2} \sum_{x,y \in H_4} a^4 \phi(x) \left(\Box + m^2\right)_{x,y} \phi(y) \tag{3.129}$$

with the matrix

$$\left(\Box + m^2\right)_{x,y} = m^2 \delta_{xy} + \sum_{\mu=1}^{4} \frac{1}{a^2}\left(2\delta_{xy} - \delta_{y,x+\mu} - \delta_{y,x-\mu}\right) . \tag{3.130}$$

Since a field configuration on the lattice is defined by the values that the field takes at the lattice sites, the integration measure $D\phi(x)$ in functional integrals can be taken to be the discrete product $D\phi(x) = \prod_{x \in H_4} d\phi(x)$. Thus, the generating functional for the discretized theory is given by

$$Z[J,a] = \int \prod_{x \in H_4} d\phi(x) \exp\left(-S[\phi] + a^4 \sum_{x \in H_4} J(x)\phi(x)\right) , \tag{3.131}$$

which reduces to the generating functional (3.36) for the continuum theory in the limit $a \to 0$ [11]. Due to the fact that the multiple integral is of Gaussian form, the functional $Z[J,a]$ can be easily calculated, resulting in

$$Z[J,a] = Z[0,a] \exp\left(\frac{1}{2} \sum_{x,y \in H_4} a^8 J(x) D(x,y) J(y)\right) . \tag{3.132}$$

Here, the lattice propagator $D(x,y)$ is given by the matrix inverse of $a^4(\Box + m^2)_{x,y}$, i.e., by the solution of the equation

$$\sum_{y\in H_4} a^4(\Box + m^2)_{x,y} D(y,z) = \delta_{xz}\,, \tag{3.133}$$

which can be obtained by Fourier transformation. Since the coordinates x_μ are restricted to multiples of the lattice spacing a, the Fourier decomposition of $D(x,y)$ is given by

$$D(x,y) = \int_{-\pi/a}^{\pi/a} \frac{d^4p}{(2\pi)^4} e^{ip(x-y)} \tilde{D}(p)\,, \tag{3.134}$$

where the momentum integration is restricted to the so-called Brillouin zone of the hypercubic lattice $BZ_H \equiv \left[-\frac{\pi}{a}, \frac{\pi}{a}\right]^4$. Together with the Fourier representation of the Kronecker delta on the H_4 lattice,

$$\delta_{xy} = \frac{a^4}{(2\pi)^4} \int_{-\pi/a}^{\pi/a} d^4p\, e^{ip(x-y)}\,, \tag{3.135}$$

this leads to [11]

$$\tilde{D}(p) = \frac{a^2}{\sum_{\mu=1}^4 2\left(1-\cos(ap_\mu)\right) + (am)^2} = \frac{a^2}{\sum_{\mu=1}^4 4\sin^2\left(\frac{a}{2}p_\mu\right) + (am)^2} \tag{3.136}$$

for the propagator in momentum space. In the limit $a \to 0$, one finds

$$\lim_{a\to 0} \tilde{D}(p) = \frac{1}{p^2 + m^2}\,, \tag{3.137}$$

and we see that the two point Green's function (3.37) is recovered in the continuum limit.

3.5.2 Gauge fields

Similarly to the continuum theory, gauge fields on the lattice are needed to achieve invariance under local gauge transformations. To this end, covariant lattice differentiation is introduced, which in turn is again related to the concept of parallel transport. Since lattice derivatives always involve fields on neighboring lattice sites, the lattice gauge field is defined on the links of the lattice, in contrast to matter fields which are defined on lattice points. For a lattice site $x \in H_4$ and a neighboring point $x + a\hat{\mu} \in H_4$ in the direction $\mu \in \{1,2,3,4\}$, the corresponding link (x,μ) is the straight path form x to $x + a\hat{\mu}$. The associated link variable $U_\mu(x)$ is an element of the gauge group $\mathrm{SU}(N)$, e.g., $U_\mu(x) \in \mathrm{SU}(3)$ for lattice QCD with three colors. The collection of all link variables is then called the lattice gauge field [11].

In addition to the lattice gauge field, the Euclidean lattice action of QCD depends on the quark fields $\psi_{f\nu c}(x) \equiv \psi_f(x)$ and $\bar{\psi}_{f\nu c}(x) \equiv \bar{\psi}_f(x)$ defined on the sites of the lattice. However, the lattice formulation of a fermionic field theory is far from being unique. Two basic types, which are often used, are the Wilson formulation on one hand and the Kogut-Susskind or staggered formulation on the other hand. In the case of Wilson fermions, the quark-field-dependent part of the lattice action reads

$$S_F^W = \sum_{x\in H_4} \left(\bar{\psi}_f(x)\psi_f(x) - K_f \sum_{\mu=\pm 1}^{\pm 4} \bar{\psi}_f(x+a\hat{\mu})\left(r_f - \gamma_\mu\right) U_\mu(x)\psi_f(x) \right) \tag{3.138}$$

with the flavor-dependent Wilson fermion parameter r_f and the hopping parameter K_f, which determine the different quark masses. The Euclidean gamma matrices $\gamma_\mu \equiv -\gamma_{-\mu}$

are Hermitian and satisfy the anticommutation relations $\{\gamma_\mu, \gamma_\nu\} = 2\delta_{\mu\nu}$. Link variables on negative-direction links are defined by $U_{-\mu}(x+\mu) \equiv U_\mu^\dagger(x)$ [11]. The action (3.138) is then invariant under the following local transformations

$$\psi(x) \to h(x)\psi(x)\,, \qquad \bar{\psi}(x) \to \bar{\psi}(x)h^{-1}(x)\,, \tag{3.139}$$

$$U_\mu(x) \to h(x+a\hat{\mu})U_\mu(x)h^{-1}(x)\,, \qquad U_\mu^\dagger(x) \to h(x)U_\mu^\dagger(x)h^{-1}(x+a\hat{\mu})\,, \tag{3.140}$$

where $h(x)$ is an element of SU(N). The link variable $U_\mu(x)$ corresponds to a Wilson line $W(x+a\hat{\mu}, x)$ in the continuum theory (cf. Sec. 3.4.1); it can be viewed as a parallel transporter for the field ψ from a lattice point x to its neighboring point $x+a\hat{\mu}$.

Clearly, the pure gauge field lattice action should be gauge-invariant, too. The simplest gauge-invariant quantity involving only the lattice gauge field is the trace of a path-ordered product of link variables along an elementary square, called plaquette. These are the smallest closed loops on the lattice, consisting of four links between lattice points x, $x+a\hat{\mu}$, $x+a\hat{\mu}+a\hat{\nu}$, $x+a\hat{\nu}$. The associated plaquette variable

$$\begin{aligned} W_{\mu\nu}(x) &\equiv U_{-\nu}(x+a\hat{\nu})U_{-\mu}(x+a\hat{\nu}+a\hat{\mu})U_\nu(x+a\hat{\mu})U_\mu(x) \\ &= U_\nu^\dagger(x)U_\mu^\dagger(x+a\hat{\nu})U_\nu(x+a\hat{\mu})U_\mu(x) = W_{\nu\mu}^\dagger(x) \end{aligned} \tag{3.141}$$

corresponds to a parallel transport for the field ψ from the initial point x to $x+a\hat{\mu}$ to $x+a\hat{\mu}+\nu$ to $x+a\hat{\nu}$ and back to x. With respect to the enclosed area, the plaquette variable is the smallest possible realization of a Wilson loop on the lattice. It transforms under local gauge transformations according to Eq. (3.140) like

$$W_{\mu\nu}(x) \to h(x)W_{\mu\nu}(x)h^{-1}(x)\,. \tag{3.142}$$

The pure gauge field action proposed by Wilson is [12]

$$S_G^W[U] = \frac{2}{g^2}\sum_{x\in H_4}\sum_{\mu<\nu}\mathrm{Tr}\left[\mathbf{1} - \frac{1}{2}\left(W_{\mu\nu}(x) + W_{\mu\nu}(x)^\dagger\right)\right]\,. \tag{3.143}$$

This choice for the gauge field action is far from being unique, it can be systematically improved to approximate the continuum action to higher orders in the lattice spacing.

Since the lattice link variables correspond to infinitesimal Wilson lines as $a \to 0$, we introduce the parametrization (cf. Eq. (3.105))

$$U_\mu(x) = e^{iaA_\mu(x)}\,, \qquad A_\mu(x) = A_\mu^j(x)t_j \tag{3.144}$$

in order to study the naive continuum limit $a \to 0$ (where we assume that $A_\mu(x)$ is weakly fluctuating). The leading terms of an expansion of $W_{\mu\nu}(x)$ in powers of the lattice constant a then follow immediately from the result for the infinitesimal Wilson loop in the continuum, cf. Eq. (3.109),

$$\sum_{\mu<\nu}\mathrm{Tr}\left[\mathbf{1} - \frac{1}{2}\left(W_{\mu\nu}(x) + W_{\mu\nu}(x)^\dagger\right)\right] = \sum_{\mu<\nu}\frac{a^4}{2}\,\mathrm{Tr}\left(F_{\mu\nu}(x)^2\right) + \mathcal{O}(a^5)\,, \tag{3.145}$$

with the field strength tensor $F_{\mu\nu}$ defined in Eq. (3.61). Therefore, the Wilson action reduces to the (Euclidean) Yang-Mills action in the continuum limit $a \to 0$, where $a^4\sum_x \to \int d^4x$. Since the fermionic part of the lattice action S_F^W possesses the desired naive continuum limit, too, the lattice theory is able to describe QCD in this limit [12].

3.5.3 Partition function and Monte Carlo methods

Having constructed a lattice action which possesses the correct naive continuum limit, we can now define the quantum theory by specifying the path integral expression from which correlation functions may be computed [12]. The partition function of a pure lattice gauge theory is given by

$$Z = \int \left(\prod_{x,\nu} d\mu(U_\nu(x)) \right) e^{-\beta S[U]} , \tag{3.146}$$

where $d\mu(U)$ is the Haar measure of the gauge group and $\beta = 2N/g^2$ has been factored out from the pure gauge action (3.143),

$$S[U] = \sum_{x \in H_4} \sum_{\mu<\nu} \frac{1}{N} \operatorname{Tr} \left[\mathbf{1} - \frac{1}{2} \left(W_{\mu\nu}(x) + W_{\mu\nu}(x)^\dagger \right) \right] . \tag{3.147}$$

Obviously, the integration measure $\prod_{x,\nu} d\mu(U_\nu(x))$ is invariant under local gauge transformations.

The partition function Z, which characterizes vacuum effects in the quantum theory, is analogous to a partition function in statistical mechanics at an inverse temperature β. Physical observables are obtained from ensemble averages of the form

$$\langle O[U] \rangle = Z^{-1} \int \left(\prod_{x,\nu} d\mu(U_\nu(x)) \right) e^{-\beta S[U]} O[U] , \tag{3.148}$$

where $O[U]$ is a gauge-invariant functional of the link variables $U_\mu(x)$.

The lattice quantization of gauge theories is performed in a way that preserves the compactness of the gauge group. On a lattice of finite size, the integral over the gauge group is finite. Therefore, the lattice formulation offers the possibility of non-perturbative quantization of gauge theories without fixing a gauge [17]. Nevertheless, it is often convenient in perturbative lattice calculations to fix the gauge. In analogy to the continuum theory, this can be achieved by using the standard Faddeev-Popov method (cf. Sec. 3.3.4). An alternative gauge fixing procedure on the lattice is described in the next section.

A very powerful method for practical non-perturbative calculations of observables in lattice gauge theories is the numerical Monte Carlo method. Since the number of integration variables is very large, it is hopeless to calculate the partition function (3.146) and associated averages exactly for arbitrary values of the coupling. The idea of the Monte Carlo method is to calculate those integrals numerically by using statistical methods. It is applied not to sequential integrals over the link variables, but rather to the multiple integral as a whole, which can be viewed as a sum over states of a statistical system.

The simplest case of a Monte Carlo integration would be to generate field configurations randomly in the space of field variables (a configuration is determined by the values of all the link variables on the lattice). Since the integrand in the path-integral is sharply peaked at some specific configurations (in the vicinity of minima of the action $S[U]$), this method would be very inefficient [11]. An efficient way of computing the ensemble average is provided by the technique of importance sampling [12]. The idea is to generate a sample of n configurations $C_1, \ldots, C_n$ with a probability distribution given by the Boltzmann factor $e^{-\beta S(C_j)}$. If the sample constitutes a representative set of configurations, then averages of the form (3.148) can be approximated by the arithmetic mean

$$\langle O[U] \rangle \approx \frac{1}{n} \sum_{j=1}^{n} O[C_j] . \tag{3.149}$$

If the n configurations are statistically independent, then the error of this approximation will be of the order $1/\sqrt{n}$ [12].

In numerical simulations, the set of sample configurations is prepared in a sequence by repeated application of an update algorithm which creates a new configuration from the previous ones. Usually, one is interested in the case where the configurations are generated in a Markov process (the sequence is then called a Markov chain), i.e., the updating is a stochastic process where the probability for generating a configuration C_j depends only on the previous configuration C_{j-1} and is independent of all the other configurations $C_1, \ldots, C_{j-2}$ in the chain. It is assumed that the transition $C_{j-1} \to C_j$ happens with a transition probability $P(C_{j-1} \to C_j)$ which satisfies the condition of strong ergodicity,

$$P(C \to C') > 0\,, \tag{3.150}$$

for any pair of configurations C and C' [11]. One can show that for a Markov process to sample the distribution $e^{-S(C)}$, it is sufficient that the transition probability satisfies the detailed balance condition

$$e^{-\beta S(C)} P(C \to C') = e^{-\beta S(C')} P(C' \to C)\,. \tag{3.151}$$

This requirement does not determine the transition probability uniquely, and one can use this freedom to adapt the update algorithm to the problem one is studying in order to increase the efficiency of numerical simulations [12]. Two popular algorithms are the heat-bath algorithm and the Metropolis algorithm.

3.5.4 Gauge fixing

Although the lattice formulation of gauge theories offers the possibility of non-perturbative quantization without fixing a gauge, it nevertheless may sometimes be advantageous to work with a fixed gauge. On the lattice, there is a way of fixing the gauge such that some link variables are set equal to prescribed values, which does not introduce any non-trivial Jacobian or Faddeev-Popov ghosts [11].

We consider a set L of links (x, μ) that does not contain any closed loops. We would like to fix the values of the corresponding link variables $U_\mu(x)$ according to

$$U_\mu(x) = \tilde{U}_\mu(x)\,, \qquad (x, \mu) \in L\,. \tag{3.152}$$

This is possible since for any given lattice gauge field configuration, there is a local gauge transformation

$$U_\mu(x) \to U'_\mu(x) = h(x + a\hat{\mu}) U_\mu(x) h^{-1}(x) \tag{3.153}$$

such that

$$U'_\mu(x) = \tilde{U}_\mu(x)\,, \qquad \forall\ (x, \mu) \in L\,. \tag{3.154}$$

For any function f of the link variables which is invariant under local gauge transformations, the expectation value of f can be written as [11]

$$\langle f \rangle = \frac{1}{Z} \int \left(\prod_{x,\mu} d\mu(U_\mu(x)) \right) f[U] e^{-\beta S[U]} = \frac{1}{Z} \int \left(\prod_{(x,\mu) \in L} d\mu(U_\mu(x)) \right) F[U|_L]\,, \tag{3.155}$$

where

$$F[U|_L] = \int \left(\prod_{(x,\mu)\notin L} d\mu(U_\mu(x)) \right) f[U] e^{-\beta S[U]} \tag{3.156}$$

is a function of the link variables corresponding to the links $(x,\mu) \in L$,

$$U|_L = \{U_\mu(x) \mid (x,\mu) \in L\} \; . \tag{3.157}$$

Since f and S are both invariant under the local gauge transformation (3.153), we obtain

$$F[U|_L] = \int \left(\prod_{(x,\mu)\notin L} d\mu(U_\mu(x)) \right) f[U'] e^{-\beta S[U']} \, . \tag{3.158}$$

We can now change the integration variables from U to U'. Due to the invariance of the Haar measure, $d\mu(U) = d\mu(U')$, we find that

$$F[U|_L] = F[U'|_L] = F[\tilde{U}] \tag{3.159}$$

is a constant [11]. This finally results in

$$\langle f \rangle = \frac{1}{Z} F[\tilde{U}] = \frac{1}{Z} \int \left(\prod_{(x,\mu)\notin L} d\mu(U_\mu(x)) \right) f[\bar{U}] e^{-\beta S[\bar{U}]} \, , \tag{3.160}$$

where

$$\bar{U}_\mu(x) = \begin{cases} U_\mu(x) & \text{for } (x,\mu) \notin L \, , \\ \tilde{U}_\mu(x) & \text{for } (x,\mu) \in L \, . \end{cases} \tag{3.161}$$

This means that in calculations of expectation values of gauge-invariant functions, one may fix the link variables on L to arbitrary prescribed values. One example of such a gauge fixing is the temporal gauge, where on an infinite lattice one chooses $U_4(x) = \mathbf{1}$ for all x. A complete gauge fixing is achieved by fixing the link variables on a maximal set of links without closed loops [11].

3.5.5 Wilson loops and confinement

Let us consider first the Euclidean formulation of continuum gauge theories and a rectangular curve $C_{R,T}$ with sides of lengths R and T in Euclidean spacetime (R is associated with space, T with time). One can show that the energy of the gauge field in the presence of two static color sources (a quark and an antiquark), separated by a distance R, is related to the large T behavior of the Wilson loop (in the fundamental representation of the gauge group) corresponding to the curve $C_{R,T}$,

$$W_{C_{R,T}} = P e^{i \oint_{C_{R,T}} dx_\mu A_\mu} \, , \tag{3.162}$$

cf. Sec. 3.4. The static quark-antiquark potential $V(R)$ (including self-energy contributions) is obtained from [11]

$$\left\langle \operatorname{Tr} W_{C_{R,T}} \right\rangle \overset{T\to\infty}{\propto} e^{-TV(R)} \tag{3.163}$$

so that

$$V(R) = -\lim_{T\to\infty} \frac{1}{T} \log \left\langle \operatorname{Tr} W_{C_{R,T}} \right\rangle . \tag{3.164}$$

The expectation value is computed with respect to the Euclidean Yang-Mills action, cf. Sec. 3.3.4,

$$\left\langle \operatorname{Tr} W_{C_{R,T}} \right\rangle = \frac{1}{Z_E} \int [DA(x)] \operatorname{Tr} W_{C_{R,T}} e^{-S_E^{\mathrm{YM}}[A]} . \tag{3.165}$$

The coefficient

$$\sigma = \lim_{R\to\infty} \frac{1}{R} V(R) = -\lim_{R,T\to\infty} \frac{1}{RT} \log \left\langle \operatorname{Tr} W_{C_{R,T}} \right\rangle \tag{3.166}$$

is called the string tension [11]. If the limits $R \to \infty$ and $T \to \infty$ lead to a finite, non-zero result for the string tension σ, the static quark-antiquark potential asymptotically rises linearly with the separation R,

$$V(R) \overset{R\to\infty}{\propto} \sigma R , \tag{3.167}$$

which results in a constant force between widely separated color sources. This behavior is called static quark confinement [11]. In this case, large Wilson loops obey the area law

$$\left\langle \operatorname{Tr} W_{C_{R,T}} \right\rangle \overset{R,T\to\infty}{\propto} e^{-\sigma A} , \tag{3.168}$$

where $A = RT$ is the area of the rectangular spacetime curve that defines the Wilson loop. It is customarily assumed that quarks are confined if an area law holds for loops of large area in pure gauge theory [17]. This suspected relation is referred to as the Wilson loop criterion, which is often used to distinguish different phases, with and without quark confinement. Consequently, the associated string tension is used as an order parameter in many numerical and analytical investigations of lattice gauge theories [11].

Within the continuum formulation, the path integral has only a formal meaning. To define it rigorously, we have to use the lattice versions of the above equations. The lattice version of the Wilson loop defined in Sec. 3.4 is given by an ordered product of link variables $U_\mu(x)$ around a closed contour on the spacetime lattice. A contour C on the lattice can be specified by its initial point x and by the n directions μ_i of the links which form the contour (μ_i may be both positive or negative). If the contour is closed, we have $\sum_{i=1}^{n} \mu_i = 0$. The Wilson loop associated to the closed contour is defined by

$$W_C = U_{\mu_n}(x + \mu_1 + \mu_2 + \ldots \mu_{n-1}) \cdots U_{\mu_2}(x + \mu_1) U_{\mu_1}(x) . \tag{3.169}$$

The smallest closed contour (with non-zero area) is given by an elementary square of the lattice, the associated Wilson loop is the plaquette variable defined in Eq. (3.141), which is used to construct the gauge field action.

The energy of a static quark-antiquark pair measured in lattice units is related to the expectation value of a rectangular Wilson loop on the lattice. Let $\hat{R}$ be the number of links in the space direction and $\hat{T}$ the number of links in the time direction, then the expression analogous to Eq. (3.164) is [12]

$$\hat{V}(\hat{R}) = -\lim_{\hat{T}\to\infty} \frac{1}{\hat{T}} \log \left\langle \operatorname{Tr} W_{C_{\hat{R},\hat{T}}} \right\rangle . \tag{3.170}$$

This relation allows for the computation of the static interquark potential on the lattice using numerical methods [11]. To determine the physical potential $V(R)$, one has to take the appropriate continuum limit of the lattice version (3.170), cf. Sec. 3.5.6.

When $\hat{V}(\hat{R})$ is determined from Monte Carlo simulations where both $\hat{R}$ and $\hat{T}$ are not very large, the potential is not expected to be of the form $\hat{V} = \hat{\sigma}\hat{R}$. In this case, self-energy contributions, which are proportional to the perimeter $\hat{R} + \hat{T}$ of the curve, will compete with the area term in

$$\left\langle \operatorname{Tr} W_{C_{\hat{R},\hat{T}}} \right\rangle = e^{-\hat{\sigma}\hat{R}\hat{T} - \hat{\alpha}\left(\hat{R}+\hat{T}\right)+\hat{\beta}} \,. \tag{3.171}$$

The string tension $\hat{\sigma}$ (in lattice units) can be extracted from so-called Creutz ratios,

$$\gamma(\hat{R},\hat{T}) = -\log \frac{\left\langle \operatorname{Tr} W_{C_{\hat{R},\hat{T}}} \right\rangle \left\langle \operatorname{Tr} W_{C_{\hat{R}-1,\hat{T}-1}} \right\rangle}{\left\langle \operatorname{Tr} W_{C_{\hat{R},\hat{T}-1}} \right\rangle \left\langle \operatorname{Tr} W_{C_{\hat{R}-1,\hat{T}}} \right\rangle} \tag{3.172}$$

where the perimeter terms are eliminated [12].

In two spacetime dimensions, the partition function factorizes and one finds that an exact area law holds for all couplings and all (unitary) gauge groups, cf. Sec. 4.

In a four-dimensional spacetime, however, the situation is more complicated. A linearly rising quark-antiquark potential (up to distances where dynamical fermions might screen the interaction) cannot be generated in perturbation theory. Since there is no way to calculate the potential analytically, one has to rely on numerical methods. However, ignoring vacuum polarization effects (in the absence of dynamical fermions) analytic results can be obtained in the strong coupling regime. In analogy to the high temperature expansion in statistical mechanics, one expands the exponential $e^{-\beta S[U]}$ in the partition function in powers of the inverse coupling β. In the leading order of this approximation, one finds that QCD confines quarks since the expectation value of the trace of the Wilson loop exhibits an area law behavior [12]. However, the same result is obtained in the strong coupling approximation for the Abelian U(1) gauge theory, where it is known that the potential is given by the Coulomb law and where we do not expect confinement in the continuum. It can be shown that the lattice U(1) gauge theory possesses a weak coupling Coulomb phase, and it has been confirmed in numerical simulations that the strong coupling regime is separated from the weak coupling regime by a phase transition. Therefore, it is necessary to check if the confining property of QCD persists into the small coupling regime [12]. Although it has not (yet) been possible to analytically relate the strong coupling limit of QCD to perturbative weak coupling results, the hope (based on numerical evidence) is that no such phase transition exists for non-Abelian SU(N) gauge theories and confinement survives in the weak coupling regime [18].

In the strong coupling limit, the flux lines connecting the quark-antiquark pair are squeezed into narrow tubes (strings) along the shortest path joining the pair. This string is not allowed to fluctuate for $g \to \infty$, $\beta \to 0$. Fluctuations may, however, destroy confinement when one studies the continuum limit. In two spacetime dimensions, the persistence of confinement in the continuum limit is not surprising since in one space dimension there is no way the string can fluctuate. In real QCD, however, there is no a priori reason why confinement could not be lost in the continuum limit $g \to 0$, $\beta \to \infty$ [12]. Up to now, this question can only be answered with the help of numerical lattice simulations. Although the linear rising potential in pure non-Abelian SU(N) gauge theories could be established as a numerical fact, it is not yet known how the theory results in the formation of flux tubes with constant energy density [18].

3.5.6 Renormalization and continuum limit

From a modern point of view, quantum field theory may be regarded as an effective low energy theory, which is valid as long as gravitational effects can be neglected. Going to higher and higher energies, it is expected that it will ultimately turn out to be an approximation to a theory whose identity is not yet known. Since quantum field theory is only valid up to some energy range, ultraviolet divergences occur in most calculations and a renormalization procedure is needed to deal with these infinities, cf. Refs. [7, 8, 11, 12]. Quantum field theories for which all UV divergences can be absorbed in a finite number of physical parameters are called *renormalizable*. In this case, perturbation theory can give well-defined predictions. We consider only such renormalizable theories in the following discussion.

The renormalization program in continuum perturbation theory, where functional integrals are expressed in terms of a power series in the coupling constant, consists of two essential parts. First, the renormalization of Green's functions requires the regularization (i.e., a prescription for handling infinities which occur in the calculation) of the corresponding Feynman integrals in momentum space to make them ultraviolet finite. These integrals then strongly depend on one or more parameters (e.g., a momentum cut-off, Pauli-Villars masses, dimensional regularization parameters; in the following collectively labeled by the expression "cut-off") which are introduced in the regularization process. Afterwards, the second step in the renormalization procedure consists in defining renormalized Green's functions, which approach a finite limit as the ultraviolet cut-off is removed. This involves that the bare parameters of the theory, such as coupling constants and masses, become cut-off dependent. Usually, a set of renormalization conditions, which simply state that physical quantities – such as the coupling strength measured at some momentum transfer and particle masses – are to be held fixed as the regularization parameters are removed, is imposed to determine the dependence of the bare quantities on the cut-off.

On the other hand, the cut-off dependence can also be eliminated by introducing a renormalized coupling g_R which depends on the bare coupling g, a renormalization scale μ and a cut-off M. By inverting the functional dependence of g_R on g, observables, which at first depend on the bare coupling and the regularization parameter, can then be given as functions of g_R and μ instead of g and M. Different regularization prescriptions lead to different definitions for the renormalized coupling, which is a physical quantity that can be related to experiment.

In continuum Yang-Mills theory with non-Abelian gauge group SU(N), a scale Λ occurs in this process, which determines how the renormalized coupling constant g_R, defined, e.g., as the value of the three or four-gluon vertex function at some momentum scale μ, changes with μ (g_R is therefore called a running coupling constant). The relation between g_R and μ, which ensures that physics does not depend on the choice of the renormalization point μ, is given by the Callan-Symanzik β-function

$$\beta(g_R) = \mu \frac{\partial g_R}{\partial \mu} \,. \tag{3.173}$$

In two-loop order, the first two coefficients in a power series expansion of this function are found to be

$$\beta(g_R) = -\beta_0\, g_R^3 - \beta_1\, g_R^5 + \mathcal{O}\left(g_R^7\right) \qquad \text{with} \quad \beta_0 = \frac{11}{3}\frac{N}{16\pi^2}\,, \quad \beta_1 = \frac{34}{3}\left(\frac{N}{16\pi^2}\right)^2 \,. \tag{3.174}$$

Integration of $\mu \frac{\partial g_R}{\partial \mu} = -\beta_0\, g_R^3 - \beta_1\, g_R^5$ yields

$$\frac{1}{\mu} = \frac{1}{\Lambda} \exp\left(-\frac{1}{2\beta_0\, g_R^2} - \frac{\beta_1}{2\beta_0^2} \log\left(\beta_0\, g_R^2\right)\right) \left(1 + \mathcal{O}\left(g_R^2\right)\right) \tag{3.175}$$

with an integration constant Λ. This scale provides a convenient way of parametrizing the coupling constant, presuming that a regularization scheme is specified. Dimensional quantities obtained with different regularization prescriptions can be compared if the relation between the corresponding Λ-parameters is known. In the case of quantum chromodynamics ($N = 3$) with N_f flavors of massless quarks, the values of the first two coefficients (which are prescription independent) are

$$\beta_0 = \frac{1}{16\pi^2}\left(11 - \frac{2}{3}N_f\right), \qquad \beta_1 = \frac{1}{(16\pi^2)^2}\left(102 - \frac{38}{3}N_f\right). \tag{3.176}$$

Since $\beta_0 > 0$ (as long as $N_f < \frac{11}{2}N$), the renormalized coupling constant is driven to $g_R \to 0$ in the limit $\mu \to \infty$, which is the property of asymptotic freedom. Due to this behavior of QCD, the related scale Λ_{QCD} can be measured in deep inelastic scattering processes, where its value is found to be of the order of 200 MeV.

In the lattice approach, the renormalization program can be formulated without reference to perturbation theory. The regularization simply consists in introducing a spacetime lattice at the level of the functional integral, which actually corresponds to defining rigorously what is meant by such an integral. Studying the continuum limit, i.e., removing the lattice structure, then constitutes the second step of the renormalization program. Within the perturbative framework, the usage of a lattice corresponds to a particular way of regularizing Feynman integrals. Although momentum integration is restricted to the Brillouin zone, i.e., momentum space integrals are cut off at a momentum of the order of the inverse lattice spacing, the lattice regularization does not amount to the naive introduction of a momentum cut-off because integrands of Feynman integrals are also modified in a non-trivial way and new vertices arise, which have no analogue in the continuum formulation.

It is no surprise that in general the bare parameters of the lattice theory have to depend on the lattice spacing a since by decreasing a the number of lattice points and links within a fixed physical volume becomes larger and larger. Therefore, the bare parameters must be tuned to the lattice constant if physics is to remain the same.

The lattice action is of course required to reduce to the correct expression in the naive continuum limit $a \to 0$, however, this is not sufficient to ensure that the quantum theory has a continuum limit corresponding to QCD or some other field theory. In the continuum limit, masses measured in lattice units must vanish if physical masses are to be finite. This implies that correlation lengths measured in lattice units must diverge, i.e., the continuum field theory can only be realized at a critical point of the statistical mechanical system described by the lattice partition function.

In pure gauge theory, the only parameter is the bare coupling constant g, which is a dimensionless quantity that does not have any direct physical meaning. For some observable Θ with mass dimension d_Θ, the corresponding lattice quantity $\hat{\Theta}$ may in principle be determined numerically depending on the bare parameters, which in the simplest case is just the coupling constant g. If g is changed with a in an appropriate way, the existence of a continuum limit implies that

$$\Theta(g(a), a) = \left(\frac{1}{a}\right)^{d_\Theta} \hat{\Theta}(g(a)) \xrightarrow{a\to 0} \Theta_{\mathrm{phys}}\,. \tag{3.177}$$

Therefore, the functional dependence of g on a can be determined for small lattice spacing if the relation between $\hat{\Theta}$ and g is known. As $a \to 0$, $g(a)$ approaches the critical coupling g^*, where correlation lengths on the lattice diverge. For sufficiently small a, this procedure does not depend on the observable under consideration. In this limit, the function $g(a)$ is

universal, which ensures the finiteness of any observable. On the other hand, this means that any observable, e.g., the static quark-antiquark potential, can be used to determine $g(a)$. The desired function can be obtained by integrating

$$\beta_{\mathrm{Lat}}(g) = -a\frac{\partial g}{\partial a}\,, \tag{3.178}$$

where β_{Lat} denotes the lattice β-function which can be determined in perturbation theory. In the two-loop approximation, it is found to be

$$\beta_{\mathrm{Lat}}(g) = -\beta_0\, g^3 - \beta_1\, g^5 + \mathcal{O}\left(g^7\right)\,, \tag{3.179}$$

where β_0 and β_1 have the same values as those appearing in the series of the continuum β-function given above. Therefore, the connection between the bare coupling g and the lattice constant a is given by

$$a = \exp\left(-\int^g \frac{dg'}{\beta_{\mathrm{Lat}}(g')}\right) = \frac{1}{\Lambda_{\mathrm{Lat}}}\exp\left(-\frac{1}{2\beta_0 g^2} - \frac{\beta_1}{2\beta_o^2}\log\left(\beta_0 g^2\right)\right)\left(1+\mathcal{O}\left(g^2\right)\right) \tag{3.180}$$

or

$$\frac{1}{g^2} = \beta_0 \log\left(\frac{1}{a^2\Lambda_{\mathrm{Lat}}^2}\right) + \frac{\beta_1}{\beta_0}\log\log\left(\frac{1}{a^2\Lambda_{\mathrm{Lat}}^2}\right) + O\left(\frac{1}{\log a^2\Lambda_{\mathrm{Lat}}^2}\right)\,, \tag{3.181}$$

where the lattice scale parameter Λ_{Lat} emerges as an integration constant. Being dimensionful, Λ_{Lat} provides a scale which survives in the continuum limit. For the comparison of lattice calculations with experimental data, it is necessary to know the value of Λ_{Lat} in MeV units. This value can be determined, for example, from a Monte Carlo calculation of the string tension (defined as the coefficient of the linearly rising part of the quark-antiquark potential for large separations) and is found to be of the order of a few MeV. The fact that the process of renormalization introduces a scale with dimension of a mass into the quantized theory, even though the classical field theory is scale invariant and does not contain any mass scale, is called dimensional transmutation.

3.6 Large-N expansion

The only truly free parameter of pure SU(N) gauge theory is the number of colors N, which led 't Hooft to the non-obvious suggestion to use $1/N$ as an expansion parameter of the theory, see Ref. [19]. This approach was motivated by statistical mechanics, where an expansion in the inverse number of field components is a standard method for non-perturbative investigations [20].

The idea is to think of the SU(N) theory as being the same as the SU(∞) theory up to corrections in inverse powers of N. Although this leads to an expansion around a much simpler theory, it is not simple enough to be solved analytically. For pure gauge theory, the expansion parameter is $1/N^2$ and diagrams of perturbation theory are rearranged according to their topology. Lattice methods have been used to confirm numerically that large-N gauge theories are linearly confining at low temperature and that SU(3) is really close to SU(∞) for many basic physical quantities, e.g., the lightest glueball masses, the deconfining temperature, and the string tension [21].

In the following, we will consider Euclidean Yang-Mills theory in the large-N limit (the subscript E is dropped, all quantities are Euclidean). This short overview is mainly based on Ref. [20] (and original references therein).

3.6.1 Planar diagrams

For a systematic large-N expansion, it is convenient to use the matrix element representation of the gauge field,

$$A_\mu^{ij}(x) = \sum_{a=1}^{N^2-1} A_\mu^a(x)\,(t^a)_{ij}\ , \tag{3.182}$$

where the sum is over the Hermitian generators t^a of the gauge group, see Sec. 3.3.3. The free propagator for the matrix elements A_μ^{ij} is obtained from the standard gauge-field propagator for the A_μ^a components, which is of the form (cf. Eq. (3.91))

$$\left\langle A_\mu^a(x) A_\nu^b(x) \right\rangle = \delta^{ab} D_{\mu\nu}(x)\,. \tag{3.183}$$

For the SU(N) gauge group, the generators in the fundamental representation obey the completeness condition

$$\sum_{a=1}^{N^2-1} (t^a)_{ij}\,(t^a)_{kl} = \frac{1}{2}\left(\delta^{il}\delta^{kj} - \frac{1}{N}\delta^{ij}\delta^{kl}\right)\ . \tag{3.184}$$

If we choose U(N) instead of SU(N), the second term proportional to $1/N$ does not occur in this relation. In the large-N expansion of SU(N) gauge theories, this second term can be omitted, which means that the infinite-N limits for theories with gauge groups U(N) and SU(N) lead to identical results. In this limit, the free propagator is in both cases of the form (in Sec. 3.3.4, the fields have been rescaled by $A \to gA$, making the propagator g-independent)

$$\left\langle A_\mu^{ij}(x) A_\nu^{kl}(y) \right\rangle \propto g^2 \delta^{il}\delta^{kj}\,. \tag{3.185}$$

This propagator can be represented by a double line,

$$\left\langle A_\mu^{ij}(x) A_\nu^{kl}(y) \right\rangle = \begin{array}{c} i \longrightarrow l \\ j \longleftarrow k \end{array}\ , \tag{3.186}$$

one oriented line for each Kronecker delta (the arrows represent the direction of the propagation of the independent complex fields A_μ^{ij} for $i > j$, for the real fields A_μ^{ii} the arrows are irrelevant). The three- and four-gluon vertices, generated by the Yang-Mills action $S = \frac{1}{2g^2}\int d^dx\,\mathrm{Tr}\,F_{\mu\nu}F_{\mu\nu}$, are proportional to g^{-2} and include Kronecker deltas, which are connecting incoming with outgoing arrows. This means that all diagrams of perturbation theory can be rewritten in the double-line notation, which is very convenient to estimate the orders of $1/N$ associated with perturbation theory diagrams: Since each sum over an independent color index results in a factor of N, we have to associate a factor of N with each closed index loop.

't Hooft's idea was to change the order of summation of diagrams of perturbation theory using $1/N$ rather than the coupling g as the expansion parameter. The large-N limit of the theory is non-trivial if the limit is taken at fixed *'t Hooft coupling* $\lambda = g^2N$. This means that the coupling constant has to approach zero in the infinite-N limit according to

$$g^2 \propto \frac{1}{N}\,. \tag{3.187}$$

Consider for example the one-loop correction to the gluon propagator in Fig. 1. The relative contribution of this diagram to the gluon propagator is proportional to g^2N (a factor of $(g^2)^6$ for three additional propagators, a factor of $(g^2)^{-4}$ for two vertices, and a factor of N for the closed index line).

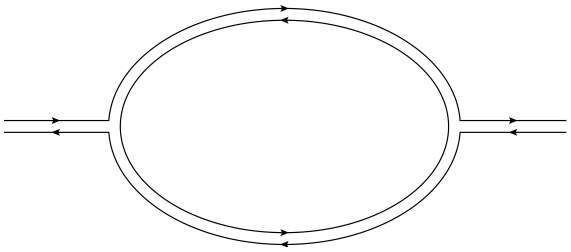

Figure 1: One-loop diagram in double-line notation with one closed index line.

Let us consider next the diagrams depicted in Fig. 2 and Fig. 3. The diagram in Fig. 2 has six three-gluon vertices and three closed index lines. The relative contribution of this diagram therefore is

$$\text{Diag. } 2 \propto \left(g^2\right)^9 \left(g^{-2}\right)^6 N^3 = \left(g^2 N\right)^3 \propto 1\,. \tag{3.188}$$

The diagram in Fig. 3 has also six three-gluon vertices, but only one closed index line. Hence, its relative contribution is found to be

$$\text{Diag. } 3 \propto \left(g^2\right)^9 \left(g^{-2}\right)^6 N = \frac{1}{N^2} \left(g^2 N\right)^3 \propto \frac{1}{N^2}\,. \tag{3.189}$$

The diagram in Fig. 2 is a *planar* diagram, i.e., it can be drawn on a sheet of paper without crossing any lines. This is obviously not the case for the third diagram, which can be drawn without line-crossing only on a surface with a hole, such as a torus, which is a surface of genus one. The genus of a connected orientable surface is the maximum number of cuttings along non-selfintersecting closed simple curves which leave the resultant manifold connected (intuitively, it is the number of "handles" of the surface).

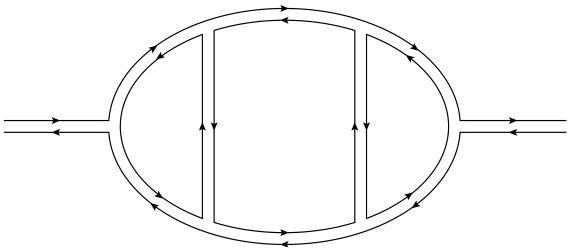

Figure 2: A planar diagram with three closed index lines (resulting in a factor of N^3).

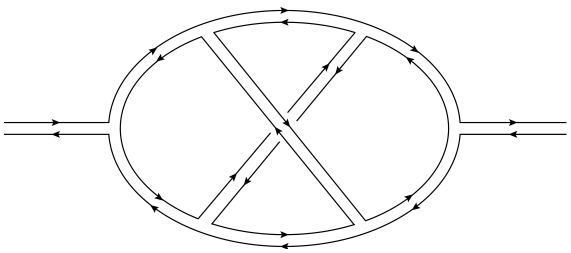

Figure 3: A non-planar diagram with only one closed index line (resulting in a factor of N).

The general formula for the relative order of the contribution of a diagram which can be drawn without line-crossing on a surface of genus n is

$$\text{genus-}n \text{ diagram} \propto N^{-2n} \,. \tag{3.190}$$

This means that a remarkable simplification of the perturbative expansion occurs in the infinite-N limit (i.e., $N \to \infty$ for fixed $\lambda = g^2 N$), the expansion in inverse powers of N arranges the diagrams according to their topological structure. In this limit, only diagrams corresponding to planar surfaces in index space, which are associated with surfaces of genus zero, survive. Therefore, the expansion is also referred to as the *topological expansion* or *genus expansion*. This simplifies the theory considerably since the number of planar graphs grows exponentially with the number of vertices, while the number of all diagrams (planar and non-planar) grows factorially.

Virtual quark loops can be easily included in the systematic large-N expansion. In the so-called *'t Hooft limit*, the number of quark flavors N_f is kept fixed as $N \to \infty$. In this case, fermion loops are suppressed in the large-N limit compared to gluon loops since $NN_f \ll N^2$. Diagrams with l quark loops are suppressed by

$$\text{genus-}n \text{ diagram with } l \text{ quark loops} \propto N^{-2n-l} \,. \tag{3.191}$$

Physical quantities associated with the fermionic sector of large-N QCD can therefore be computed using fermionic observables in a gauge background generated using the pure gauge action [22].

3.6.2 Factorization of expectation values

An important property of QCD in the large-N limit is that expectation values of products of gauge-invariant quantities, which involve an averaging over the color indices (e.g. in a trace), factorize. The simplest operator of this type in pure gauge theory is $\frac{1}{N} \operatorname{Tr} F_{\mu\nu}^2(x)$, which has an expectation value of order 1. The diagrams for the average of a product of two such operators split into a factorized part (gluons are emitted and absorbed by the same operator) and a connected part, which turns out to be suppressed by $1/N^2$. Correlations between the operators are suppressed, and the expectation value indeed factorizes at large N,

$$\left\langle \frac{1}{N} \operatorname{Tr}\left(F_{\mu\nu}^2(x)\right) \frac{1}{N} \operatorname{Tr}\left(F_{\rho\sigma}^2(y)\right) \right\rangle = \left\langle \frac{1}{N} \operatorname{Tr}\left(F_{\mu\nu}^2(x)\right) \right\rangle \left\langle \frac{1}{N} \operatorname{Tr}\left(F_{\rho\sigma}^2(y)\right) \right\rangle + \mathcal{O}\left(N^{-2}\right) \,. \tag{3.192}$$

This factorization property holds for a general set of gauge-invariant operators $O_1, \ldots O_n$,

$$\langle O_1 \cdots O_n \rangle = \langle O_1 \rangle \cdots \langle O_n \rangle + \mathcal{O}\left(N^{-2}\right) \,. \tag{3.193}$$

Factorization holds to all orders of perturbation theory and to all orders of the strong coupling expansion in the lattice theory. Furthermore, it can be confirmed non-perturbatively by using the Makeenko-Migdal loop equations (see below).

A natural interpretation of the factorization property is that the theory possesses a semiclassical nature in the large-N limit. In this limit, with $g^2 N \propto 1$, the Yang-Mills action is of order N^2 since $1/g^2 \propto N$ and the trace leads to an additional factor of N. This property may allow for a saddle-point approach at large N. The idea, due to Witten, is that there might be one particular (infinite-dimensional) field configuration which determines the expectation values of all observables in the infinite-N limit, see Refs. [23, 24]. This is similar to the classical limit $\hbar \to 0$, where functional integrals are

more and more dominated by solutions of the classical equations of motions as $\hbar$ decreases. Since the integration measure in functional integrals depends also exponentially on N^2, the saddle point equation for Yang-Mills theory at large-N differs from the classical one (which is determined exclusively by the Lagrangian). The solution of the saddle-point equation in the large-N limit is usually referred to as the *master field*. In fact, it is more reasonable to speak about a *master gauge orbit* since the solution can be determined by the saddle-point equation only up to a gauge transformation. This would preserve the factorization of gauge-invariant observables, which are given by their values at the master field orbit in the infinite-N limit. The Poincaré invariance of vacuum expectation values implies that there must exist a gauge in which the master field is spacetime independent, i.e., the solution of large-N QCD would be determined by four infinite-dimensional matrices A_μ. However, the conjecture about the existence of only one solution of the saddle-point equation may be too restrictive. If several solutions exist, which are not related by gauge transformations, an additional averaging over these solutions is needed. This averaging then would have to preserve the factorization property of expectation values of gauge-invariant observables. For this case, it has been proposed to think of an operator-valued master field in some Hilbert space (sometimes referred to as the master field in the weak sense) or to describe the master field using the concept of free random variables of non-commutative probability theory, cf. Ref. [25].

3.6.3 Loop equations

The loop-space approach to QCD was motivated by the lattice formulation of non-Abelian gauge theories and based on the fact that all observables can be expressed at large N through expectation values of Wilson loops. Since selfintersecting loops are not independent, it has not been possible to reformulate continuum QCD at finite N in terms of Wilson loops at the level of the functional integral. The reformulation for large N has been achieved by Migdal and Makeenko in terms of Schwinger-Dyson or loop equations [20, 26]:

It turns out that an equation of motion for traces of Wilson loop matrices

$$\Phi(C) = \frac{1}{N} \operatorname{Tr} W_C = \frac{1}{N} \operatorname{Tr} P e^{i \oint_C A_\mu(x) dx_\mu} \tag{3.194}$$

can be represented completely in loop space,

$$\partial_\mu^x \frac{\delta}{\delta \sigma_{\mu\nu}(x)} \langle \Phi(C) \rangle = \lambda \oint_C dy_\nu \delta(x-y) \left\langle \Phi(C_{yx}) \Phi(C_{xy}) - \frac{1}{N^2} \Phi(C) \right\rangle . \tag{3.195}$$

For two points x and y on C, the contours C_{yx} and C_{xy} are the parts of the original contour C from x to y and from y to x, respectively. Due to the presence of the delta function on the RHS of Eq. (3.195), these contours are always closed (but x and y can be associated with different values of the variable which parametrizes the contour). The differential operators in the loop space, which consists of arbitrary continuous closed loops, are obtained by infinitesimal variations of a given loop. The area derivative of a loop functional $F(C)$ is defined by the infinitesimal difference

$$\frac{\delta F(C)}{\delta \sigma_{\mu\nu}(x)} = \frac{1}{|\delta \sigma_{\mu\nu}|} \left[F(C + \delta C_{\mu\nu}(x)) - F(C) \right] , \tag{3.196}$$

where $C + \delta C_{\mu\nu}(x)$ denotes the loop which is obtained by attaching the infinitesimal rectangular loop $\delta C_{\mu\nu}(x)$ in the x_μ-x_ν-plane at point x to the original loop C. The

infinitesimal area element associated with the loop $\delta C_{\mu\nu}(x)$ is denoted by $\delta\sigma_{\mu\nu}$. Similarly, the path derivative is defined by

$$\partial_\mu^x F(C) = \frac{1}{|\delta x_\mu|}\left[F(C+\delta C_\mu(x)) - F(C)\right] , \tag{3.197}$$

where $C+\delta C_\mu(x)$ is obtained by shifting the point x on the contour C along an infinitesimal path, of length $|\delta x_\mu|$, in the μ-direction.

Obviously, the loop equation (3.195) is not closed since it couples one-loop averages to two-loop averages. However, expectation values factorize in the large-N limit, i.e.,

$$\langle\Phi(C_{yx})\Phi(C_{xy})\rangle = \langle\Phi(C_{yx})\rangle\,\langle\Phi(C_{xy})\rangle + \mathcal{O}\left(\frac{1}{N^2}\right) , \tag{3.198}$$

resulting in

$$\partial_\mu^x \frac{\delta}{\delta\sigma_{\mu\nu}(x)}\langle\Phi(C)\rangle = \lambda \oint_C dy_\nu \delta(x-y)\,\langle\Phi(C_{yx})\rangle\,\langle\Phi(C_{xy})\rangle + \mathcal{O}\left(\frac{1}{N^2}\right) , \tag{3.199}$$

which is a closed equation for the Wilson loop average in the infinite-N limit. This equation is often referred to as the Makeenko-Migdal loop equation.

As already mentioned, the factorization property can be derived from a chain of loop equations, which in general couple n-loop averages to $(n-1)$-loop averages and $(n+1)$-loop averages. Similar to Eq. (3.195), the number of colors N enters explicitly, revealing the "semiclassical" nature of the large-N expansion. The generalized chain of loop equations possesses the factorized solution

$$\langle\Phi(C_1)\Phi(C_2)\ldots\Phi(C_n)\rangle = \langle\Phi(C_1)\rangle\,\langle\Phi(C_2)\rangle\ldots\langle\Phi(C_n)\rangle \tag{3.200}$$

in the infinite-N limit, provided that the one-loop average $\langle\Phi(C)\rangle$ solves Eq. (3.199) [20].

4 Pure gauge theories in two spacetime dimensions

QCD in two spacetime dimensions became popular after 't Hooft's suggestion [27] to use it as a simplified model for four-dimensional QCD. At first glance, gauge theories in two spacetime dimensions seem to be rather trivial since there are no transverse degrees of freedom in two dimensions, and the evaluation of most observables can be reduced to finite-dimensional integrals. The Coulomb potential is linear in two dimensions and the theory is confining for both weak and strong coupling [28].

4.1 Factorization of the partition function

In two Euclidean dimensions, the partition function (3.146) of pure lattice gauge theory is (up to an irrelevant constant) given by

$$Z = \int \left(\prod_{x,\nu} d\mu(U_\nu(x)) \right) e^{\frac{1}{g^2} \sum_x \mathrm{Tr}\left(W_{12}(x) + W_{12}(x)^\dagger\right)} . \tag{4.1}$$

Both the action and the integration measure are invariant under local gauge transformations, cf. Eq. (3.140),

$$U_\mu(x) \to h(x + a\hat{\mu}) U_\mu(x) h^{-1}(x) , \qquad U_\mu^\dagger(x) \to h(x) U_\mu^\dagger(x) h^{-1}(x + a\hat{\mu}) , \tag{4.2}$$

where $h(x)$ is an element of the gauge group.

On an infinite lattice the option of making a gauge choice can be used to set all link variables in the time direction equal to the identity, $U_2(x) = \mathbf{1}$ for all x, cf. Sec. 3.5.4. This gauge corresponds to the temporal gauge, $A_2 = 0$, in the continuum theory. In this gauge, the action in two spacetime dimensions reads

$$S = -\frac{1}{g^2} \sum_x \mathrm{Tr} \left(W_{12}(x) + W_{12}(x)^\dagger \right) \tag{4.3}$$

with

$$W_{12}(x) = U_2^\dagger(x) U_1^\dagger(x + a\hat{2}) U_2(x + a\hat{1}) U_1(x) = U_1^\dagger(x + a\hat{2}) U_1(x) . \tag{4.4}$$

We see that the remaining non-trivial link variables $U_1(x_1, x_2)$ are only coupled to link variables $U_1(x_1, x_2')$ at the same x_1 coordinate ($x = (x_1, x_2)$). In two dimensions, this gauge choice hence has the remarkable effect of decoupling all link variables in the orthogonal space direction (with different x_1 coordinate) and the partition function factorizes [14].

After fixing $U_2(x) = \mathbf{1}$ for all x, there is still a remaining symmetry corresponding to gauge transformations $\tilde{h}(x_1, x_2)$ that are independent of x_2, $\tilde{h}(x_1, x_2) = \tilde{h}(x_1, x_2') \equiv \tilde{h}(x_1)$, $\forall x_2, x_2'$, since the effect of those transformations is

$$U_2(x_1, x_2) \to \tilde{h}(x_1, x_2 + a) U_2(x_1, x_2) \tilde{h}^{-1}(x_1, x_2) = \tilde{h}(x_1) \mathbf{1} \tilde{h}^{-1}(x_1) = \mathbf{1} = U_2(x_1, x_2) . \tag{4.5}$$

This remaining gauge freedom can be used to fix all link variables $U_1(x_1, x_2)$ for one specific value of x_2, e.g., at $x_2 = \infty$ [22],

$$U_1(x_1, x_2)|_{x_2 = \infty} = \mathbf{1} . \tag{4.6}$$

After this gauge choice, the only remaining symmetry is a global symmetry, a gauge transformation according to Eq. (3.140) with $h(x) = h$ being spacetime independent.

If we now successively change the remaining integration variables from $U_1(x)$ to $W(x)$ according to

$$U_1(x) = U_1(x + a\hat{2})W(x)\,, \tag{4.7}$$

the plaquette variables in terms of the new variables $W(x)$ read

$$W_{12}(x) = U_1^\dagger(x + a\hat{2})U_1(x) = U_1^\dagger(x + a\hat{2})U_1(x + a\hat{2})W(x) = W(x) \tag{4.8}$$

and the partition function becomes [22]

$$Z = \int \left(\prod_x d\mu(W(x))\right) e^{\frac{1}{g^2}\sum_x \mathrm{Tr}\left(W(x)+W^\dagger(x)\right)} = \prod_x \int d\mu(W(x)) e^{\frac{1}{g^2}\,\mathrm{Tr}\left(W(x)+W^\dagger(x)\right)}\,, \tag{4.9}$$

i.e., the partition function factorizes and the plaquette variables are independent and identically distributed. This factorization is a very special property of pure gauge theory in two spacetime dimensions.

The integrand in Eq. (4.9) is invariant under the transformation

$$W(x) \to V(x)W(x)V^\dagger(x) \tag{4.10}$$

for any $V(x)$ being an element of the gauge group. This is just how an ordinary plaquette variable would transform under local gauge transformations. However, if we use Eq. (4.7) as a definition of $W(x)$, we see that the transformation (4.10) can be viewed as a gauge transformation only if $V(x)$ is spacetime independent. This is equivalent to the above statement that keeping the gauge choices $U_2(x_1, x_2) = \mathbf{1}$ and $U_1(x_1, x_2)|_{x_2=\infty} = \mathbf{1}$ restricts the remaining gauge symmetry to a global one.

For unitary gauge groups of order N (SU(N) or U(N)), one can use the orthogonality relation of the matrix elements (in the fundamental representation of the group), cf. Eq. (2.46),

$$\int d\mu(V) V_{ij} V_{kl}^\dagger = \frac{1}{N}\delta_{il}\delta_{jk}\,, \tag{4.11}$$

together with the global invariance to compute expectation values of single plaquette variables. The orthogonality of the matrix elements results in

$$\int d\mu(V) \left(VWV^\dagger\right)_{ij} = \int d\mu(V) V_{ik} W_{kl} V_{lj}^\dagger = W_{kl}\frac{1}{N}\delta_{ij}\delta_{kl} = \delta_{ij}\frac{1}{N}\,\mathrm{Tr}\,W\,. \tag{4.12}$$

Due to the factorization of the partition function, we obtain

$$\begin{aligned}\left\langle (W_{12}(y))_{ij} \right\rangle &= \frac{1}{Z}\int \left(\prod_x d\mu\left(U_1(x)\right)\right) \left(U_1^\dagger(y + a\hat{2})U_1(y)\right)_{ij} e^{\frac{1}{g^2}\sum_x \mathrm{Tr}\left(U_1^\dagger(x+a\hat{2})U_1(x)+h.c.\right)} \\ &= \frac{\int d\mu(W) W_{ij} e^{\frac{1}{g^2}\,\mathrm{Tr}\left(W+W^\dagger\right)}}{\int d\mu(W) e^{\frac{1}{g^2}\,\mathrm{Tr}\left(W+W^\dagger\right)}} = \frac{\int d\mu(W) d\mu(V) \left(VWV^\dagger\right)_{ij} e^{\frac{1}{g^2}\,\mathrm{Tr}\left(W+W^\dagger\right)}}{\int d\mu(W) e^{\frac{1}{g^2}\,\mathrm{Tr}\left(W+W^\dagger\right)}} \\ &= \delta_{ij}\frac{1}{N}\left\langle \mathrm{Tr}\,W\right\rangle_{\mathrm{sp}}\,,\end{aligned} \tag{4.13}$$

where the last expectation value can be taken with respect to the single plaquette partition function

$$z = \int d\mu(W) e^{\frac{1}{g^2}\,\mathrm{Tr}\left(W+W^\dagger\right)}\,, \tag{4.14}$$

$$\left\langle \mathrm{Tr}\,W\right\rangle_{\mathrm{sp}} = \frac{1}{z}\int d\mu(W)\,\mathrm{Tr}\,(W)\, e^{\frac{1}{g^2}\,\mathrm{Tr}\left(W+W^\dagger\right)}\,. \tag{4.15}$$

This means that $\langle W(x)\rangle$ is proportional to the identity matrix with a spacetime independent proportionality constant. Hence, the two-dimensional gauge theory is reduced to a single integral, which characterizes the one-plaquette world [28].

4.2 Exact area law for Wilson loops

Let us now consider a rectangular curve on the two-dimensional lattice with corners at x, $x + n_1 a\hat{1}$, $x + n_2 a\hat{2}$, and $x + n_1 a\hat{1} + n_2 a\hat{2}$, i.e., the number of links in the time direction is n_2 and the number of links in the space direction is n_1. In the temporal gauge, the corresponding Wilson loop matrix is given by

$$\begin{aligned} W_{n_1,n_2}(x) = {} & U_1^\dagger(x + n_2 a\hat{2}) \cdots U_1^\dagger(x + n_2 a\hat{2} + (n_1-2)a\hat{1}) U_1^\dagger(x + n_2 a\hat{2} + (n_1-1)a\hat{1}) \\ & \times U_1(x + (n_1-1)a\hat{1}) U_1(x + (n_1-2)a\hat{1}) \cdots U_1(x + a\hat{1}) U_1(x) \,. \end{aligned} \tag{4.16}$$

The effect of the variable changes according to Eq. (4.7) is

$$\begin{aligned} U_1(x_0) &= U_1(x_0 + a\hat{2}) W(x_0) = U_1(x_0 + 2a\hat{2}) W(x_0 + a\hat{2}) W(x_0) = \ldots \\ &= U_1(x_0 + n_2 a\hat{2}) W(x_0 + (n_2-1)a\hat{2}) W(x_0 + (n_2-2)a\hat{2}) \cdots W(x_0) \,. \end{aligned} \tag{4.17}$$

Setting $x_0 = x + (n_1 - 1)a\hat{1}$ and averaging over $W(x_0 + ja\hat{2})$, $j = 0, \ldots, n_2 - 1$, we obtain

$$\langle W_{n_1,n_2}(x)\rangle = \langle W_{n_1-1,n_2}(x)\rangle \left(\langle W\rangle_{\mathrm{sp}}\right)^{n_2} \tag{4.18}$$

by using that $\langle W\rangle \propto \mathbf{1}$. Repeating the above steps for $x_0 = x + (n_1 - l)a\hat{1}$, $l = 2, \ldots, n_1$, we finally obtain

$$\langle W_{n_1,n_2}(x)\rangle = \left(\langle W\rangle_{\mathrm{sp}}\right)^{n_1 n_2} \tag{4.19}$$

and

$$\left\langle \frac{1}{N} \operatorname{Tr} W_{n_1,n_2}(x) \right\rangle = \frac{1}{N} \operatorname{Tr} \left(\langle W\rangle_{\mathrm{sp}}\right)^{n_1 n_2} = \left(\left\langle \frac{1}{N} \operatorname{Tr} W \right\rangle_{\mathrm{sp}} \right)^{n_1 n_2} \tag{4.20}$$

due to $\langle W\rangle_{\mathrm{sp}} = \frac{1}{N} \langle \operatorname{Tr} W\rangle_{\mathrm{sp}} \mathbf{1}$. This means that the area law is exact in two-dimensional gauge theories for all unitary groups and for all values of the coupling constant. In the lattice formulation of a pure gauge theory, the potential rises linearly with the separation of a static quark-antiquark pair. The charged pair is confined due to the two-dimensional nature of the problem. In two dimensions, the field energy cannot spread out in space, there is no way that the flux lines connecting the quark and antiquark can fluctuate [12].

4.2.1 Abelian case

Let us now calculate the single plaquette expectation value for the Abelian U(1) gauge theory. In this case, the integrals in Eqs. (4.14) and (4.15) reduce to one-dimensional integrals over an angular variable θ, parametrizing the group U(1) through $W = e^{i\theta}$. With $b = g^{-2}$, we obtain

$$z = \int_{-\pi}^{\pi} \frac{d\theta}{2\pi} e^{b\left(e^{i\theta} + e^{-i\theta}\right)} = \int_{-\pi}^{\pi} \frac{d\theta}{2\pi} e^{2b\cos(\theta)} \,, \tag{4.21}$$

$$\begin{aligned} \langle \operatorname{Tr} W\rangle_{\mathrm{sp}} &= \frac{1}{z} \int_{-\pi}^{\pi} \frac{d\theta}{2\pi} e^{i\theta} e^{b\left(e^{i\theta} + e^{-i\theta}\right)} = \frac{1}{z} \int_{-\pi}^{\pi} \frac{d\theta}{2\pi} \cos(\theta) e^{2b\cos(\theta)} \\ &= \frac{1}{2z} \frac{\partial}{\partial b} z = \frac{1}{2} \frac{\partial}{\partial b} \log z \,. \end{aligned} \tag{4.22}$$

Since the modified Bessel functions of integer order have the integral representations [29]

$$I_n(z) = \int_{-\pi}^{\pi} \frac{d\theta}{2\pi} e^{z\cos\theta} \cos(n\theta) \,, \tag{4.23}$$

the above result can be written as

$$z = I_0(2b) \,, \qquad \langle \mathrm{Tr}\, W \rangle_{\mathrm{sp}} = \frac{I_1(2b)}{I_0(2b)} \,. \tag{4.24}$$

Hence, for the gauge group U(1), Eq. (4.20) reads

$$\langle \mathrm{Tr}\, W_{n_1,n_2}(x) \rangle = \left(\frac{I_1(2b)}{I_0(2b)} \right)^{n_1 n_2} \,. \tag{4.25}$$

With $\hat{R} = n_1$ and $\hat{T} = n_2$, we can read off the static quark-antiquark potential in units of the lattice spacing from Eq. (3.170),

$$\hat{V}(\hat{R}) = -\lim_{\hat{T}\to\infty} \frac{1}{\hat{T}} \log \left\langle \mathrm{Tr}\, W_{\hat{R},\hat{T}} \right\rangle = -\hat{R} \log \left(\frac{I_1(2b)}{I_0(2b)} \right) = \hat{R}\hat{\sigma} \tag{4.26}$$

with lattice string tension

$$\hat{\sigma} = \log \left(\frac{I_0(2b)}{I_1(2b)} \right) \geq 0 \,. \tag{4.27}$$

To determine the physical potential $V(R)$, we have to take the continuum limit of Eq. (4.26). Since QED in two spacetime dimensions is superrenormalizable (the coupling constant in the continuum theory has the dimension of a mass), a simple rescaling of the lattice variables with the lattice spacing a is sufficient [12]. By studying the naive continuum limit of the lattice action, one finds that the coupling constant in physical units, g_p, is related to g by

$$g_p = \frac{1}{a} g \,, \qquad b(a) = \frac{1}{g_p^2 a^2} \,. \tag{4.28}$$

The lattice coupling g is dimensionless and therefore g_p has the correct dimension of a mass. The physical potential $V(R)$ has the dimension of inverse length, so we have to rescale $\hat{V}$ with the inverse lattice spacing, $V = \hat{V}/a$. Furthermore, we have to replace $\hat{R}$ by R/a. Therefore, the physical potential should be calculated as the following limit [12],

$$V(R, g_p) = \lim_{a\to 0} \frac{1}{a} \hat{\sigma}(b(a)) \frac{R}{a} \,, \tag{4.29}$$

where the physical coupling constant g_p has to be kept fixed. In the continuum limit, $b(a)$ diverges and we can use the following asymptotic expansions for $I_1(b)$ and $I_0(b)$ which are valid for large b,

$$I_0(2b) = \frac{e^{2b}}{\sqrt{4\pi b}} \left(1 + \frac{1}{16b} + \mathcal{O}\left(b^{-2}\right) \right) \,, \tag{4.30}$$

$$I_1(2b) = \frac{e^{2b}}{\sqrt{4\pi b}} \left(1 - \frac{3}{16b} + \mathcal{O}\left(b^{-2}\right) \right) \,, \tag{4.31}$$

leading to

$$\begin{aligned} \frac{1}{a^2} \hat{\sigma}(b(a)) &= \frac{1}{a^2} \log \left(1 + \frac{1}{16b(a)} + \frac{3}{16b(a)} + \mathcal{O}\left(b(a)^{-2}\right) \right) = \frac{1}{a^2} \left(\frac{1}{4} g_p^2 a^2 + \mathcal{O}\left(a^4\right) \right) \\ &= \frac{1}{4} g_p^2 + \mathcal{O}\left(a^2\right) \,. \end{aligned} \tag{4.32}$$

For the physical potential, we obtain

$$V(R) = \frac{1}{4} g_p^2 R \,, \tag{4.33}$$

which is the classical energy (in one space dimension) of a pair of opposite charges separated by a distance R. As mentioned before, the persistence of confinement in the continuum limit ($g \to 0$) is not surprising because the field energy cannot spread out in space since there is only one spatial dimension [12].

4.2.2 Non-Abelian case: Gross-Witten singularity

This result generalizes to unitary gauge groups of higher order. The integral in Eq. (4.14) can be performed with $W \in \mathrm{U}(N)$ for any arbitrary N. The integrand only depends on the eigenvalues $e^{i\alpha_j}$, $j = 1, \ldots, N$, of W. In this case, the group integral reduces to an integral over the N angles α_j,

$$z = \int_{-\pi}^{\pi} \left(\prod_{i=1}^{N} d\alpha_i \right) \prod_{i<j} \left| e^{i\alpha_i} - e^{i\alpha_j} \right| e^{\frac{2}{g^2} \sum_{j=1}^{N} \cos \alpha_j} \,, \tag{4.34}$$

up to an irrelevant constant, since the unitary matrix W can be parametrized as $W = S \,\mathrm{diag}(e^{i\alpha_1}, \ldots, e^{i\alpha_N}) S^\dagger$ with $S \in \mathrm{U}(N)$ and

$$d\mu(W) \propto d\mu(S) \left(\prod_{i=1}^{N} d\alpha_i \right) \prod_{i<j} \left| e^{i\alpha_i} - e^{i\alpha_j} \right| \,, \tag{4.35}$$

cf. Ref. [28]. All integrals can be evaluated in terms of modified Bessel functions and the result is found to be [30]

$$z = \det M \,, \qquad M_{ij} = I_{i-j}\,(2bN) \,, \quad i, j = 1, \ldots, N \,, \tag{4.36}$$

with $b = \frac{1}{Ng^2} = \frac{\beta}{2N^2}$. Similar to the Abelian case, the continuum limit at fixed N is obtained by taking $b \to \infty$. The continuum limit of the large-N gauge theory suggested by 't Hooft is obtained if we first take $N \to \infty$ at fixed b and then take $b \to \infty$. In the limit $N \to \infty$, the gauge groups $\mathrm{U}(N)$ and $\mathrm{SU}(N)$ become equivalent [28]. In the large-N limit, one can approximate the single plaquette partition function $z(b, N)$ by using the method of steepest descent. The stationary equation for the angles α_j is given by [28]

$$2b \sin(\alpha_i) = \frac{1}{N} \sum_{j \neq i} \cot \left(\frac{\alpha_i - \alpha_j}{2} \right) . \tag{4.37}$$

Since the integrand in the definition of the single plaquette partition function (4.14) is invariant under $W \to SWS^\dagger$, all expectation values will reduce to integrals over the eigenvalues of W and can be evaluated in the large-N limit by substituting the angles α_i by the solutions of Eq. (4.37) because the integral is dominated by a stationary point and expectation values factorize in the large-N limit.

In the large-N limit, one can replace the saddle point equations (4.37) by their continuum version by introducing a non-decreasing function $\alpha(x)$ with $0 \leq x \leq 1$ such that $\alpha_j = \alpha(j/N)$, which leads to [28]

$$2b \sin \alpha(x) = \mathcal{P} \int_0^1 dy \cot \left(\frac{\alpha(x) - \alpha(y)}{2} \right) , \tag{4.38}$$

where $\mathcal{P}$ refers to the principal value of the integral. One can then define a density of eigenvalues by

$$\rho(\alpha) = \frac{dx}{d\alpha}\,, \qquad \int_{-\alpha_c}^{\alpha_c} d\alpha\rho(\alpha) = \int_0^1 dx = 1\,, \tag{4.39}$$

where the eigenvalues are allowed to lie in the region $|\alpha| \leq \alpha_c$ with $\alpha_c \leq \pi$ [28]. Equation (4.38) then becomes an equation for ρ,

$$2b\sin\alpha = \mathcal{P}\int_{-\alpha_c}^{\alpha_c} d\beta\rho(\beta)\cot\left(\frac{\alpha-\beta}{2}\right)\,. \tag{4.40}$$

Its solution is found to be [22, 28]

$$\rho(\alpha) = \begin{cases} \frac{2b}{\pi}\sqrt{\frac{1}{2b} - \sin^2\left(\frac{\alpha}{2}\right)}\cos\left(\frac{\alpha}{2}\right) & \text{for } b \geq \frac{1}{2} \text{ and } |\alpha| \leq \alpha_c = 2\arcsin\sqrt{\frac{1}{2b}}\,, \\ \frac{1}{2\pi}\left(1 + 2b\cos(\alpha)\right) & \text{for } b \leq \frac{1}{2} \text{ and } |\alpha| \leq \alpha_c = \pi\,. \end{cases} \tag{4.41}$$

At infinite N, the lattice theory undergoes a phase transition (the "Gross-Witten transition") at $b = \frac{1}{2}$, separating the lattice weak and strong coupling limits. The transition occurs at the point where the eigenvalues of the elementary plaquette variable W fill the whole unit circle. It is found to be a third-order phase transition since the third derivative of the free energy $F \propto b^{-1}\log z$ w.r.t. b^{-1} (which plays the role of a temperature) is discontinuous at the critical value of the coupling $b^{-1} = 2$, whereas both the first and the second derivative are continuous, cf. Ref. [28].

However, the continuum theory does not exhibit this phase transition, which is an artefact of the Wilson lattice gauge action and absent in other lattice formulations of pure gauge theories [31]. This means that in order to obtain the correct continuum limit of the large-N theory, one has to keep $b > \frac{1}{2}$, where $\rho(\alpha)$ has a finite support around $\alpha = 0$ not covering the whole unit circle [22].

4.3 Probability distribution for the Wilson loop matrix

4.3.1 Character expansion and continuum limit

The basic idea of the character expansion method is to make use of the fact that the pure gauge part of the lattice action belongs to the general type

$$S[U] = \beta\sum_p F(W_p)\,, \tag{4.42}$$

where the W_p's are the plaquette variables (one has to choose a convention for the orientation of the plaquettes p entering the sum) and $F(W_p)$ is some real valued function which is invariant under gauge transformations, $F\left(hW_ph^{-1}\right) = F(W_p)$ for each element h of the gauge group. Since the contribution of a single plaquette to the partition function, $e^{-\beta F(W_p)}$, is a class function on the group, it can be expanded in terms of characters of irreducible representations (cf. Sec. 2.2) as follows [12]

$$z(W_p) = e^{-\beta F(W_p)} = \sum_\nu \lambda_\nu(\beta)\chi^{(\nu)}(W_p)\,, \tag{4.43}$$

where the sum is over all irreducible representations of the gauge group and $\chi^{(\nu)}$ is the character corresponding to the irreducible representation $\Gamma^{(\nu)}$. Wilson's choice for the

gauge action is given by the real part of the character in the fundamental representation, $F(W_p) \propto \mathrm{Re}\,\chi^{(\mathrm{fund})}(W)$, cf. Sec. 3.5.2.

Due to the orthogonality relations of the characters, cf. Eq. (2.47), the coefficients λ_ν are determined by

$$\lambda_\nu(\beta) = \int d\mu(W)\chi^{(\nu)*}(W)e^{-\beta F(W)}\,. \tag{4.44}$$

Since $F(W)$ is a real class function, complex conjugate representations contribute with the same weight in the expansion (4.43) [12].

Assuming that the function $F(W)$ has only one absolute minimum located at the identity element $\mathbf{1}$ (this requirement is needed to recover the Yang-Mills action in the continuum limit), the main contribution to the integral in Eq. (4.44) comes from the vicinity of the identity as $\beta \to \infty$. Therefore, to lowest order, λ_ν is proportional to the dimension of the irreducible representation $\Gamma^{(\nu)}$, $\gamma_\nu \propto \chi^{(\nu)}(\mathbf{1}) = d_\nu$. Taking into account the next order in β^{-1}, one finds that

$$\lambda_\nu \approx b_1 d_\nu x^{c(\nu)} \qquad \text{with} \qquad \log x = -\frac{b_2}{\beta} + \mathcal{O}\left(\beta^{-2}\right)\,, \tag{4.45}$$

with two constants b_1 and b_2 that depend on the choice of $F(U)$ (b_1 leads to an irrelevant additive term in the action and b_2 can be absorbed in a redefinition of β) [32]. In the limit $\beta \to \infty$, the integration in Eq. (4.44) can be performed by the method of steepest descent. The first contribution then comes from a quadratic form for $F(W)$ and the exponent $c(\nu)$ can be identified with the value of the quadratic Casimir operator in the representation ν, see Ref. [32],

$$c(\nu) = C_2(\nu)\,. \tag{4.46}$$

4.3.2 Lattice action in terms of the heat kernel on the group manifold

As mentioned before, the gauge action proposed by Wilson is not the only possible choice. Motivated by the above character expansion, the *heat kernel action* is defined in terms of [11]

$$z_{\mathrm{hk}}(W_p) = e^{-S_{\mathrm{hk}}(W_p)} = \frac{K\left(W_p, \frac{\bar{g}^2}{2}\right)}{K\left(\mathbf{1}, \frac{\bar{g}^2}{2}\right)}\,, \tag{4.47}$$

where the coupling constant is denoted by $\bar{g}$ (we reserve the symbol g for the coupling in Wilson's action) and

$$K(W,t) = \sum_\nu d_\nu \chi^{(\nu)}(W)e^{-tC_2(\nu)}\,. \tag{4.48}$$

The sum is again over all irreducible representations $\Gamma^{(\nu)}$ of the gauge group G. The heat kernel $K(W,t)$ is a solution of the heat equation on the gauge group,

$$\frac{\partial}{\partial t}K(W,t) = \Delta_G K(W,t)\,, \tag{4.49}$$

where Δ_G is the Laplace-Beltrami operator on the group G. For the Abelian U(1) gauge group, the heat kernel action is known as Villain's action [11]. From the previous discussion, it is evident that the heat kernel action reproduces the Yang-Mills action in the

classical continuum limit because the small g behavior is the same as for Wilson's action. However, it turns out that for this alternative choice of the gauge action, there is no Gross-Witten singularity in two dimensions. If one accepts the idea of universality, the continuum limit of the lattice theory should be independent of the details of the interaction Lagrangian [31]. The Gross-Witten singularity is just a lattice artefact special to Wilson's choice for the action.

The heat kernel on a compact Lie group can be given explicitly in terms of periodic Gaussians in the invariant angles parametrizing the eigenvalues of W, $W = Se^{i\Phi}S^\dagger$, $\Phi = \mathrm{diag}(\phi_1, \ldots, \phi_N)$ (with $\sum_i \phi_i = 0$ for SU(N)). The heat kernel K is a function of $(\phi_1, \ldots, \phi_N)$ only and is given by [31]

$$K\left(W, \frac{\bar{g}^2}{2}\right) = \mathcal{N} \sum_{\{l\}=-\infty}^{\infty} \prod_{i<j} \frac{\phi_i - \phi_j + 2\pi(l_i - l_j)}{2\sin\left(\frac{1}{2}\left[\phi_i - \phi_j + 2\pi(l_i - l_j)\right]\right)} e^{-\frac{1}{\bar{g}^2}\sum_{j=1}^N (\phi_j + 2\pi l_j)^2}, \quad (4.50)$$

where the irrelevant constant $\mathcal{N}$ does not depend on ϕ and the sum is over all integers $l_1, \ldots, l_N$ (with the constraint $\sum_j l_j = 0$ for SU(N)).

When W is close to the identity in the weak coupling limit, the sum is dominated by the $l_1 = \ldots = l_N = 0$ term and all other terms are exponentially suppressed. Using the expansion

$$\frac{\phi}{2\sin\frac{\phi}{2}} = 1 + \frac{\phi^2}{24} + \mathcal{O}(\phi^4) = e^{\frac{\phi^2}{24} + \mathcal{O}(\phi^4)} \quad (4.51)$$

and

$$\prod_{i<j} e^{\frac{1}{24}(\phi_i - \phi_j)^2} = e^{\frac{N}{24}\sum_{i=1}^N \phi_i^2 - \frac{1}{24}\left(\sum_{i=1}^N \phi_i\right)^2} \quad (4.52)$$

results in [31]

$$K\left(W, \frac{\bar{g}^2}{2}\right) \overset{\Phi\to 0}{\approx} \mathcal{N} e^{-\left(\frac{1}{\bar{g}^2} - \frac{N}{24}\right)\sum_{j=1}^N \phi_j^2} \quad (4.53)$$

for SU(N) where $\sum_j \phi_j = 0$.

For Wilson's choice for the SU(N) gauge action, a weak coupling expansion near the identity leads to (cf. Sec. 3.5.2)

$$e^{\frac{1}{g^2}\mathrm{Tr}\left(e^{i\Phi} + e^{-i\Phi} - 2\cdot\mathbf{1}\right)} \overset{\Phi\to 0}{\approx} e^{\frac{1}{g^2}\mathrm{Tr}\left(-\frac{1}{2}\Phi^2 - \frac{1}{2}\Phi^2\right)} = e^{-\frac{1}{g^2}\sum_{j=1}^N \phi_j^2}. \quad (4.54)$$

Therefore, we see that the coupling constants $\bar{g}$ and g are related by [11]

$$\frac{1}{g^2} = \frac{1}{\bar{g}^2} - \frac{N}{24}, \qquad \bar{g}^2 = g^2 \frac{1}{1 + \frac{Ng^2}{24}}. \quad (4.55)$$

If we take the limit $g \to 0$ at fixed N, this results in $\bar{g} = g + \mathcal{O}(g^3)$.

4.3.3 Migdal's recursion

As we have seen in the discussion of the general character expansion of the single plaquette contribution to the partition function, every suitable lattice action (that reduces to the Yang-Mills action in the naive continuum limit) will lead to the heat kernel form in the limit of vanishing coupling constant. In the special case of two spacetime dimensions,

using the heat kernel action from the beginning proves to be very useful since the action is exactly self-reproducing. This property is discussed below (based on Ref. [33]).

Migdal's idea was to use the character expansion to derive an effective action for the doubled lattice cell (a hypercube with edge length $2a$) by joining 2^d neighboring plaquettes (in d spacetime dimensions) and integrating over all internal link variables. Carrying out this integration over the whole volume results in a lattice with doubled lattice spacing and an associated effective action replacing the original one. By repeating this procedure, all the fields are gradually integrated out (this is referred to as *Migdal's recursion*). In Ref. [33], the correlation functional z_{2a} is defined as

$$z_{2a} = \int \left(\prod_{\text{all internal links } (x,\nu)} d\mu(U_\nu(x)) \right) \left(\prod_{i=1}^{2^d} z(W_i) \right) , \tag{4.56}$$

where $i = 1, \ldots, 2^d$ labels the neighboring plaquettes with corresponding plaquette variables W_i and $z(W_p)$ is the contribution of a single plaquette variable W_p to the partition function $Z = \prod_{\text{plaquettes } p} z(W_p)$. The logarithm of z_{2a} then determines the effective action of the doubled cell.

In general, all possible loop products around the surface of the enlarged hypercube with edge length L will contribute to the functional z_L. In dimensions higher than two, one can derive only approximate recursion equations relating these functionals for different L [33]. In the special case of $d = 2$, the situation is much simpler since every link is common to only two neighboring plaquettes on the two-dimensional lattice.

Let us now consider two neighboring plaquettes p_1 and p_2 on a two-dimensional spacetime lattice, cf. Fig. 4. To determine the correlation functional z_{12} of the joint lattice cell $p_1 + p_2$ (which defines an effective action for the doubled plaquette), one has to compute the integral

$$z_{12}(V_1, V_2) = \int d\mu(U) z(V_1 U) z(U^\dagger V_2) \tag{4.57}$$

over the common link variable U. The plaquette variables are parametrized as $W_{p_1} = V_1 U$, $W_{p_2} = U^\dagger V_2$, where V_1 and V_2 are products of three link variables, corresponding to the remaining links of the two plaquettes p_1 and p_2. This integral can be performed by using the character expansion (4.44). Since we are only interested in the continuum limit, we can choose the heat kernel action from the beginning and set $z = z_{\text{hk}}$, cf. Eq. (4.47).

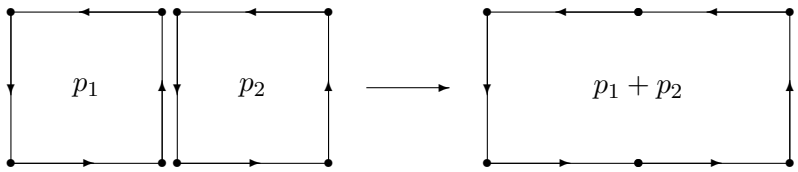

Figure 4: Two neighboring plaquettes p_1 and p_2 are combined to a larger cell, the common link variable of the corresponding plaquette variables is integrated out.

The integral in Eq. (4.57) can be computed by making use of the generalized orthogonality relations of the group characters [12],

$$\int d\mu(V) \chi^{(\nu_1)}(V_1 V) \chi^{(\nu_2)}(V^\dagger V_2) = \frac{\delta_{\nu_1 \nu_2}}{d_{\nu_1}} \chi^{(\nu_1)}(V_1 V_2) \, . \tag{4.58}$$

Ignoring the irrelevant normalization factor $K(\mathbf{1}, t)$, which cancels in computations of expectation values, we obtain

$$\begin{aligned} z_{12}(V_1, V_2) &= \int d\mu(U) \sum_{\nu_1} \sum_{\nu_2} d_{\nu_1} d_{\nu_2} \chi^{(\nu_1)}(V_1 U) \chi^{(\nu_2)}(U^\dagger V_2) e^{-\frac{1}{2}\bar{g}^2 C_2(\nu_1)} e^{-\frac{1}{2}\bar{g}^2 C_2(\nu_2)} \\ &= \sum_{\nu} d_\nu \chi^{(\nu)}(V_1 V_2) \left(e^{-\frac{1}{2}\bar{g}^2 C_2(\nu)} \right)^2 . \end{aligned} \tag{4.59}$$

The product $W_{12} = V_1 V_2$ is just a Wilson loop corresponding to the perimeter curve of the joint cell $p_1 + p_2$. We see that the form of the correlation functional reproduces itself when two lattice cells are joined together, the coefficients in the character expansion just get multiplied. This rule does not depend on the size and form of the two cells that are joined together. If, e.g., two cells c_1 and c_2 (that are each composed of more than one elementary plaquette) have two links in common, the Wilson loops along the perimeters of the cells can be parametrized by $W_1 = V_1 U_b U_a$ and $W_2 = V_2 U_a^\dagger U_b^\dagger$, where V_1 and V_2 are independent products of link variables. The correlation functional follows from the integral

$$\begin{aligned} \int d\mu(U_a) d\mu(U_b) \chi^{(\nu_1)}(V_1 U_b U_a) \chi^{(\nu_2)}(U_b^\dagger V_2 U_a^\dagger) &= \int d\mu(U_b) \frac{\delta_{\nu_1 \nu_2}}{d_{\nu_1}} \chi^{(\nu_1)}(V_1 U_b U_b^\dagger V_2) \\ &= \frac{\delta_{\nu_1 \nu_2}}{d_{\nu_1}} \chi^{(\nu_1)}(V_1 V_2) , \end{aligned} \tag{4.60}$$

where $V_1 V_2$ is again the Wilson loop around the perimeter of the joint cell $c_1 + c_2$. This result obviously holds for an arbitrary number of common link variables that are integrated out.

The z-functional for a region R, with area $A_R = na^2$, that is obtained by joining n neighboring elementary plaquettes and integrating over all internal link variables is therefore given by

$$z_R\left(W_{\partial R}\right) = \sum_{\nu} d_\nu \chi^{(\nu)}(W_{\partial R}) e^{-\frac{1}{2}\bar{g}^2 a^{-2} A_R C_2(\nu)} , \tag{4.61}$$

where $W_{\partial R}$ denotes the Wilson loop along the boundary of R.

In order to compute the expectation value of $\chi^{(\nu)}(W_{\partial R})$, we have to integrate over all the link variables on the lattice (weighted with the action $e^{-S[U]}$). We can first integrate over the link variables inside R, which leads to $z_R\left(W_{\partial R}\right)$, and then integrate over the link variables outside R, which results in $z_{\bar{R}}(W_{\partial R}^\dagger)$. Since the external region $\bar{R}$ has infinite area, only the trivial representation with $C_2 = 0$ contributes in the sum over irreducible representations, resulting in $z_{\bar{R}} = 1$. Due to the invariance of the Haar measure, the remaining integrals over link variables on the boundary of R result in a single integral over the product matrix $W_{\partial R}$, such that [33]

$$\left\langle \chi^{(\nu)}(W_{\partial R}) \right\rangle = \frac{\int d\mu(W) \chi^{(\nu)}(W) z_R(W)}{\int d\mu(W) z_R(W)} = d_\nu e^{-\frac{1}{2}\bar{g}^2 a^{-2} A_R C_2(\nu)} \tag{4.62}$$

due to $z_R(W) = z_R(W^\dagger)$ and $\int d\mu(W) z_R(W) = 1$ (only the trivial representation contributes).

In the continuum limit $a \to 0$, $\bar{g}$ has to go to zero such that $\bar{g}/a = g_p$ remains finite. This means that a properly normalized probability distribution (with respect to the Haar measure) for Wilson loops, corresponding to closed non-selfintersecting spacetime curves

enclosing an area A_R, is given by

$$\mathcal{P}(W) = \sum_\nu d_\nu \chi^{(\nu)}(W) e^{-\frac{1}{2} g_p^2 A_R C_2(\nu)} \,. \tag{4.63}$$

Note that there is no dependence on the shape of the spacetime curve, only the enclosed area A_R enters (through the dimensionless product $g_p^2 A_R$).

We see that the lattice formulation in terms of the heat kernel action is exactly equivalent to the continuum theory (the initial probability distribution for an elementary plaquette variable in Eq. (4.47) has exactly the same form as Eq. (4.63)), but the above result for the probability distribution of Wilson loops in the continuum limit does of course not depend on the initial choice for the lattice gauge action.

4.4 Durhuus-Olesen transition

It was shown by Durhuus and Olesen in Ref. [1] that the eigenvalue density of a Wilson loop matrix W associated with a simple non-selfintersecting loop in two-dimensional Euclidean continuum SU(N) Yang-Mills theory undergoes a "phase transition" in the infinite-N limit as the size of the loop is dilated (remember that "the size of the Wilson loop" refers to the size of the underlying spacetime curve). This transition is not a real phase transition since the partition function and expectation values of traces of arbitrary powers of W are perfectly analytical. We nevertheless use the term "phase transition" (or "Durhuus-Olesen phase transition") to refer to the non-analyticity in the eigenvalue density observed by Durhuus and Olesen.

At finite N, the N eigenvalues of the unitary Wilson loop matrix W_C, corresponding to a curve C in two-dimensional spacetime, are of the form $e^{i\alpha_j}$, $j = 1, \ldots, N$, and can be identified with points on the unit circle in the complex plane. A natural definition of an average eigenvalue density for Wilson loops corresponding to a fixed curve C is given by

$$\rho_C(\theta) = \frac{2\pi}{N} \sum_{j=1}^{N} \langle \delta_{2\pi} \left(\theta - \alpha_j(W_C)\right) \rangle \,, \tag{4.64}$$

where $\delta_{2\pi}$ denotes the 2π-periodized delta function with normalization[7]

$$\int_{-\pi}^{\pi} d\theta \, \delta_{2\pi}(\theta) = 1 \,. \tag{4.65}$$

In the following, only curves without selfintersections are considered. We have seen in the previous section that averaging over the gauge fields with the usual Yang-Mills action in two Euclidean dimensions produces a probability distribution for the loop matrix, which, according to Eq. (4.63), depends only on the area of the underlying spacetime curve. Therefore, the average density ρ_C depends only on the area enclosed by the curve C, too.

At infinite N, the domain of non-vanishing eigenvalue density on the unit circle has a gap centered at $\theta = \pm\pi$ for small loops, which probe short-distance perturbative physics. Durhuus and Olesen observed that as the size of the loop is increased, the region of non-vanishing eigenvalue density expands from a small arc on the unit circle to encompassing the entire unit circle for large loops, which probe large-distance non-perturbative physics. The transition occurs at a critical area where the gap in the spectrum just closes. After the gap is eliminated, the distribution becomes more and more uniform with further

[7] Note that this definition of the eigenvalue density differs from the one in Ref. [1] by a normalization factor of 2π.

increasement of the loop size. Confinement means that the uniform limit is approached with a correction that goes to zero exponentially with the area enclosed by the underlying spacetime curve. The Durhuus-Olesen transition can be viewed as a transition from an ordered phase, where W is close to the identity matrix (the spectrum has a gap), to a disordered phase, where the eigenvalues are randomly distributed on the unit circle (the spectrum is uniform).

4.4.1 Complex Burgers equation from loop equations

Starting from the Makeenko-Migdal loop equation (cf. Eq. (3.199)), it is shown in Ref. [34] that the eigenvalue density of the Wilson loop operator has to satisfy

$$\partial_\mu^x \frac{\delta \rho_C(\theta)}{\delta \sigma_{\mu\nu}(x)} = \frac{\lambda}{\pi} \oint_C dy_\nu \delta(x-y) \frac{\partial}{\partial \theta} \left[\rho_C(\theta) \mathcal{P} \int_{-\infty}^{\infty} d\phi \frac{\rho_C(\phi)}{\theta - \phi} \right] \tag{4.66}$$

in the infinite-N limit ($\mathcal{P}$ denotes the principal value of the integral). It is convenient to introduce the Hilbert-transform (for complex θ)

$$f_C(\theta) = \frac{1}{4\pi} \int_{-\pi}^{\pi} d\phi \rho_C(\phi) \cot\left(\frac{\theta - \phi}{2}\right) = \frac{1}{2\pi} \int_{-\infty}^{\infty} d\phi \frac{\rho_C(\phi)}{\theta - \phi}\,, \tag{4.67}$$

where the representation

$$\cot(z) = \sum_{n=-\infty}^{\infty} \frac{1}{z - n\pi} \tag{4.68}$$

has been used ($\rho_C(\theta)$ is periodic, $\rho_C(\theta) = \rho_C(\theta + 2\pi n)\ \forall n \in \mathbb{Z}$). In the limit $\mathrm{Im}\,\theta \to 0^-$, we obtain

$$f_C(\theta) = \frac{1}{2\pi} \mathcal{P} \int_{-\infty}^{\infty} d\phi \frac{\rho_C(\phi)}{\theta - \phi} + \frac{i}{2} \rho_C(\theta)\,. \tag{4.69}$$

In the above equation, there is a choice of sign for the imaginary part, depending on whether $f(\theta)$ is defined to be analytic in the lower or upper complex half-plane. In the present choice, f is analytic for $\mathrm{Im}\,\theta \leq 0$. Equation (4.66) can then be rewritten as

$$\partial_\mu^x \frac{\delta f_C(\theta)}{\delta \sigma_{\mu\nu}(x)} = 2\lambda \oint_C dy_\nu \delta(x-y) f_C(\theta) \frac{\partial f_C(\theta)}{\partial \theta}\,. \tag{4.70}$$

In two dimensions, $\rho_C(\theta)$ depends on the curve C only through the area A_C enclosed by C if the curve is taken to be a simple curve without selfintersections. Therefore, the same is true for the function $f_C(\theta)$. In fact, we know from Eq. (4.63) that it depends only on the dimensionless area (the area in units of the 't Hooft coupling)

$$t = \lambda A_C\,. \tag{4.71}$$

This leads to the following simple differential equation for the (complex) function $f_C(\theta) \equiv f(\theta, t)$ that determines $\rho_C(\theta) \equiv \rho(\theta, t)$, cf. Ref. [1],

$$\frac{\partial f(\theta,t)}{\partial t} + f(\theta,t) \frac{\partial f(\theta,t)}{\partial \theta} = 0\,. \tag{4.72}$$

This equation is known as the complex Burgers equation (in the inviscid limit). When f is real, the equation has a simple flow interpretation and the solutions are, in general, of the shock-wave type. While the real Burgers equation appears in condensed matter

physics, statistical physics, fluid dynamics, and also in vehicle traffic models, its complex generalization is relevant, e.g., to the free random variables calculus and models for quasi-geostrophic processes (describing, e.g., the dynamics of the mixture of cold and hot air), see Ref. [35] and references therein. In fluid dynamics, the variable t is associated with time, θ is a coordinate, and f plays the role of a velocity field.

Solutions of Eq. (4.72) can be obtained by using the method of characteristics, for both real and complex f. If the function $f(\theta, t)$ is given for an initial area $t = t_0$ by

$$f(\theta, t_0) = f_{t_0}(\theta)\,, \tag{4.73}$$

then a solution of Eq. (4.72) is given by

$$f(\theta, t) = f_{t_0}\left(\xi(\theta, t)\right)\,, \tag{4.74}$$

where the function $\xi(\theta, t)$ has to solve

$$\xi(\theta, t) = \theta - (t - t_0) f_{t_0}\left(\xi(\theta, t)\right)\,. \tag{4.75}$$

Once $\xi(\theta, t)$ has been found, we obtain for $t > t_0$

$$f(\theta, t) = f_{t_0}\left(\xi(\theta, t)\right) = \frac{\theta - \xi(\theta, t)}{t - t_0}\,, \tag{4.76}$$

and for real φ, from Eq. (4.69),

$$\rho(\varphi, t) = 2\,\mathrm{Im}\, f(\varphi - i0^+, t) = -\frac{2}{t - t_0}\,\mathrm{Im}\,\xi(\varphi - i0^+, t)\,. \tag{4.77}$$

By differentiating Eq. (4.75) w.r.t. t and θ, which results in

$$\frac{\partial \xi}{\partial \theta} = \frac{1}{1 + (t - t_0) f'_{t_0}(\xi)}\,, \qquad \frac{\partial \xi}{\partial t} = \frac{-f_{t_0}(\xi)}{1 + (t - t_0) f'_{t_0}(\xi)} \tag{4.78}$$

with $f'_{t_0}(\xi) = \partial_\xi f_{t_0}(\xi)$, we see that $f_{t_0}(\xi)$ is indeed a solution of the Burgers equation (4.72) due to

$$\frac{\partial f_{t_0}(\xi)}{\partial t} + f_{t_0}(\xi)\frac{\partial f_{t_0}(\xi)}{\partial \theta} = f'_{t_0}(\xi)\left(\frac{\partial \xi}{\partial t} + f_{t_0}(\xi)\frac{\partial \xi}{\partial \theta}\right) = 0\,. \tag{4.79}$$

If the function f is real, the phenomenon of shock waves may occur when the partial derivatives in Eq. (4.78) develop singularities, which happens if the denominator vanishes at a "time" $t = t_0 - 1/f'_{t_0}(\xi(\theta, t))$. In the complex case, these singularities are of course absent as long as $f'_{t_0}(\xi)$ has a non-vanishing imaginary part [1].

Requiring that the Wilson loop matrix is equal to the identity matrix for a loop of zero area, $W(t = 0) = \mathbf{1}$, the initial spectral density is given by

$$\rho(\theta, 0) = \rho_0(\theta) = 2\pi\delta_{2\pi}(\theta)\,, \tag{4.80}$$

resulting in

$$f(\theta, 0) = f_0(\theta) = \frac{1}{2}\cot\left(\frac{\theta}{2}\right)\,. \tag{4.81}$$

Equation (4.75) then leads to the implicit equation

$$\xi = \theta - \frac{t}{2}\cot\left(\frac{\xi}{2}\right) \tag{4.82}$$

determining $\xi(\theta,t)$. For this initial condition, Eqs. (4.74) and (4.75) read

$$f(\theta,t) = \frac{1}{2}\cot\left(\frac{\xi(\theta,t)}{2}\right), \qquad \xi(\theta,t) = \theta - tf(\theta,t), \tag{4.83}$$

which implies that the function $f(\theta,t)$ has to be a solution of

$$f(\theta,t) = \frac{1}{2}\cot\left(\frac{\theta - tf(\theta,t)}{2}\right). \tag{4.84}$$

4.4.2 Numerical solution – phase transition in the spectral density

It was first shown in Ref. [1] that any initial eigenvalue distribution $\rho_{t_0}(\theta)$, at initial area $t = t_0$, develops into a uniform distribution as t increases,

$$\rho(t,\theta) \overset{t\to\infty}{\to} 1. \tag{4.85}$$

This means that the infinite-N version of Yang-Mills theory in two spacetime dimensions always shows a disordered behavior (with a uniform distribution of the eigenvalues of the Wilson loop matrix) for large areas, independent of the distribution for finite areas. This situation is also expected in a confining phase in higher dimensions (cf. Sec. 4.4.6 below). Furthermore, Durhuus and Olesen observed that the partial derivatives of $\rho(\theta,t)$ w.r.t. θ and t diverge at a critical angle $|\theta| = \theta_c(t) \leq \pi$ if t is below a critical value $t < t_c$, where $\theta_c(t_c) = \pi$. For $t < t_c$, the spectral density vanishes for $\theta_c < |\theta| \leq \pi$, whereas the density is always non-zero for $t > t_c$, cf. Figs. 12 and 13 below. A transition from an "ordered phase" to a "disordered phase" occurs at a point of non-analyticity for a critical value of the area $t = t_c$. For the initial distribution given in Eq. (4.81), the critical size, at which the phase transition in the spectral distribution occurs, is found to be $t_c = 4$.

To study the Durhuus-Olesen transition in the eigenvalue density, let us now analyze the solutions of the complex Burgers equation with the initial condition (4.81) at zero area ($t = 0$). Using the method of characteristics, we have to find solutions of Eq. (4.82), where ξ and θ are complex numbers. We choose $\operatorname{Im}\theta \leq 0$ and are interested in the limit $\operatorname{Im}\theta \to 0^-$, which determines the eigenvalue density through Eq. (4.77).

Following the analysis presented in Ref. [35], we decompose Eq. (4.82) into two real equations. With $\theta = \varphi + i\eta$, $\varphi,\eta \in \mathbb{R}$ and $\xi = x + iy$, $x,y \in \mathbb{R}$, we obtain

$$\varphi = x + t\,\frac{e^{-y}\sin(x)}{1 + e^{-2y} - 2e^{-y}\cos(x)} = x + \frac{t}{2}\,\frac{\sin(x)}{\cosh(y) - \cos(x)}, \tag{4.86a}$$

$$\eta = y + \frac{t}{2}\,\frac{e^{-2y} - 1}{1 + e^{-2y} - 2e^{-y}\cos(x)} = y - \frac{t}{2}\,\frac{\sinh(y)}{\cosh(y) - \cos(x)}. \tag{4.86b}$$

If we treat x and y as parameters, the characteristics $\varphi(t)$ and $\eta(t)$ form a family of straight lines in the φ-η-plane. To construct the solution of the complex Burgers equation, it is not enough to consider only the case $\eta = 0$ since characteristics that start at $y = 0$ stay at $\eta = 0$ as t increases, but move away from this point as soon as a small imaginary part is present, cf. Ref. [35]. In the following, we consider only the case $\eta \leq 0$ and $0 \leq \varphi \leq \pi$ (the density is even in φ, $\rho(\varphi,t) = \rho(-\varphi,t)$). To construct solutions, we have to invert the relations $\varphi(x,y;t)$, $\eta(x,y;t)$ and determine $x(\varphi,\eta;t)$, $y(\varphi,\eta;t)$. This can be done only with numerical means.

It is instructive to investigate the shape of the curves of constant η and φ in the x-y-plane for different values of t. Figures 5 and 6 show plots of such curves for $\varphi = 2.0$ and $\eta = -0.05$, resp. $\eta = -10^{-5}$. For a fixed value of t, intersection points of the curves of constant φ and η correspond to solutions (x,y) of Eq. (4.86).

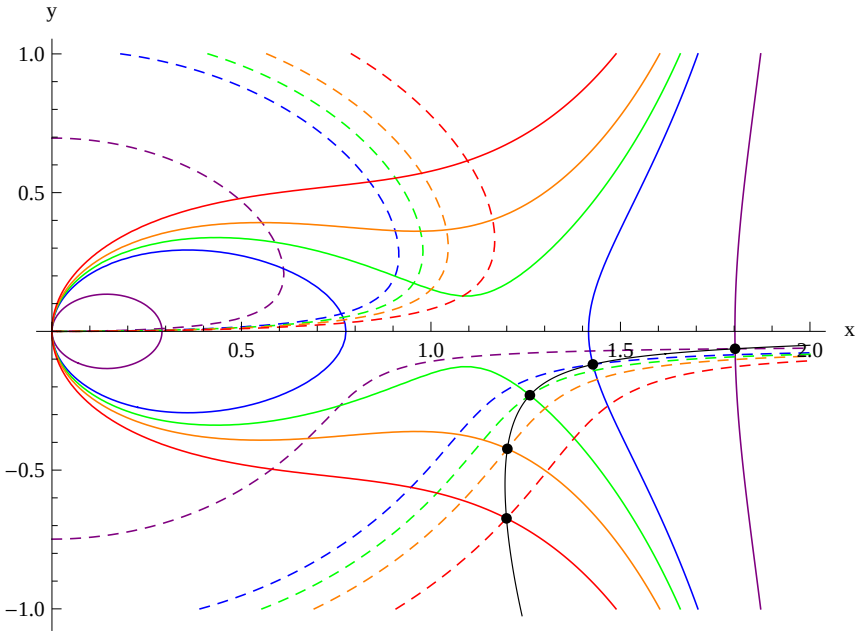

Figure 5: Plot of curves of constant $\varphi = 2.0$ (solid) and constant $\eta = -0.05$ (dashed) in the x-y-plane for $t = 0.5$ (purple), $t = 1.0$ (blue), $t = 1.12$ (green), $t = 1.25$ (orange), $t = 1.5$ (red). The intersection points of dashed and solid curves (with identical color) correspond to solutions of Eq. (4.86). Those intersection points which are smoothly connected (as t increases) to the correct starting point at $t = 0$ are marked with black dots. With increasing t, these solutions move along the thin black line (cf. also Fig. 8 below).

We observe that for given $\eta < 0$, φ and $t > 0$, there are in general two solutions (x, y) (with $0 \leq x \leq \pi$), one with $y > 0$ and a second one with $y < 0$. However, it turns out that only the latter fulfills the initial condition (4.81) as $t \to 0$. The two solutions are smoothly connected (with varying t) to two different solutions at small t, which can be obtained in analytical form. At $t = 0$, one solution of Eq. (4.86) is given by $x_1(\varphi, \eta; 0) = \varphi$ and $y_1(\varphi, \eta; 0) = \eta$ (assuming that the denominator does not vanish for these values of x and y). This solution obviously leads to the correct initial function,

$$f(\theta, t = 0) = \frac{1}{2} \cot\left(\frac{x_1(\varphi, \eta; 0) + i y_1(\varphi, \eta; 0)}{2}\right) = \frac{1}{2} \cot\left(\frac{\theta}{2}\right) = f_0(\theta)\,. \tag{4.87}$$

For small t, a second solution of Eq. (4.86) is given by

$$x_2(\varphi, \eta; t) = \frac{\varphi}{\varphi^2 + \eta^2} t + \mathcal{O}(t^2)\,, \qquad y_2(\varphi, \eta; t) = -\frac{\eta}{\varphi^2 + \eta^2} t + \mathcal{O}(t^2)\,. \tag{4.88}$$

With $x_2, y_2 \to 0$ for $t \to 0$, it follows from the characteristics, cf. Eq. (4.82), that

$$\frac{1}{2} \cot\left(x_2 + i y_2\right) \to \frac{\varphi + i\eta}{t} \qquad \text{for } t \to 0\,, \tag{4.89}$$

i.e., the solution diverges for all φ and η in the limit $t \to 0$. As t increases, $y(\varphi, \eta; t)$ does not change sign, therefore we can discard all solutions with $y > 0$ since those solutions emerge from the "wrong" small-t solution (x_2, y_2). Note that there are infinitely many additional solutions with either $x < 0$ or $x > \pi$ which we do not have to consider for $0 \leq \varphi \leq \pi$.

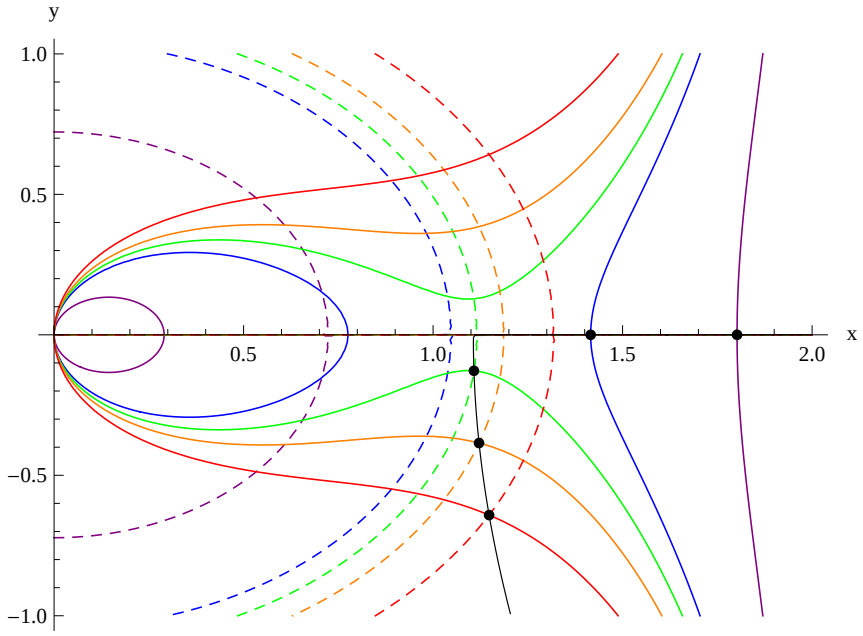

Figure 6: Plot of the same curves as in Fig. 5, the single difference is that here $\eta = -10^{-5}$. The curves of constant η (for fixed t) touch each other at a point on the x-axis in the limit $\eta \to 0$, the combined curve is then symmetric w.r.t. reflection at the x-axis.

Let us now analyze how the solutions $(x(\varphi, \eta; t), y(\varphi, \eta; t))$ that are smoothly connected to $(x_1 = \varphi, y_1 = \eta)$ at $t = 0$ evolve with increasing t for fixed φ and fixed $\eta < 0$.

Figure 7 shows some examples of curves $x(\varphi, \eta; t)$ and $y(\varphi, \eta; t)$ as functions of t, for a single value of φ and some values of $\eta < 0$. Figure 8 shows a plot of the same curves in the x-y-plane. These are the curves on which the solutions (in the x-y-plane) move with increasing t, which are also plotted in Figs. 5 and 6, for $\eta = -0.05$ and $\eta = -10^{-5}$.

The generic feature is that the derivatives w.r.t. t become discontinuous, for both $x(\varphi, \eta; t)$ and $y(\varphi, \eta; t)$, in the limit $\eta \to 0^-$ at some critical area $t_d(\varphi)$ with $t_d(\pi) = t_c = 4$. In this limit, $y(\varphi, \eta \to 0^-; t)$ approaches zero for $t < t_d(\varphi)$ but remains non-zero for $t > t_d(\varphi)$. There are no discontinuities as long as η remains non-zero. Since $\mathrm{Im}\, \xi = y$ in the limit $\eta \to 0^-$ determines the eigenvalue density through Eq. (4.77), this leads to a transition in the density at the angle φ for $t = t_d(\varphi)$: $\rho(\varphi, t) = 0$ as long as $t < t_d(\varphi)$ and $\rho(\varphi, t) > 0$ for $t > t_d$. The transition point $t_d(\varphi)$ increases monotonically with $\varphi \leq \pi$. The eigenvalue density is non-zero for all angles φ for $t > t_d(\pi) = t_c = 4$, the gap in the eigenvalue density closes at $\varphi = \pm\pi$ for $t = t_c = 4$. (This value for t_c is not a numerical result; we will show below that the transition occurs exactly at $t = 4$.)

It is also instructive to plot the curves of constant η and φ in the x-y-plane for a single value of t and various values of φ. Figures 9, 10, and 11 show examples of such curves for $t = 2$, $t = 4$, and $t = 5$. Solutions of Eq. (4.86) at a given value of t are again given by the intersection points of lines of constant φ and η. We are interested only in the case $\eta \to 0^-$ since those solutions determine the eigenvalue density, cf. Eq. (4.77). Furthermore, we have to consider only those curves of constant $\eta = 0$ which have $y < 0$ as long as η is non-zero. These curves are referred to as $(\eta = 0^-)$-curves in the following. (Recall that for small but non-zero η, we have two curves of constant η, one with $y < 0$ and one with $y > 0$. In the limit $\eta \to 0^-$, these two curves have a common point $(x_c, y_c = 0)$ (for $t \leq 4$). Points on the x-axis with $0 \leq x \leq x_c$ lead to $\eta = 0$, but those points originate from the

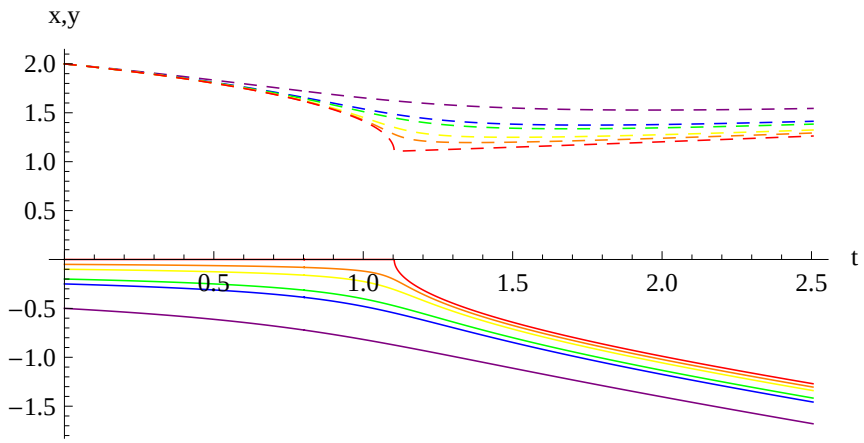

Figure 7: Evolution of the solutions $x(\varphi, \eta; t)$ (dashed) and $y(\varphi, \eta; t)$ (solid) starting at $t = 0$ from $x = \varphi = 2.0$ and $y = \eta$ with $\eta = -0.5$ (purple), $\eta = -0.25$ (blue), $\eta = -0.2$ (green), $\eta = -0.1$ (yellow), $\eta = -0.05$ (orange), and $\eta = -10^{-5}$ (red).

curve of constant η with $y > 0$ when η is non-zero, cf. Figs. 5 and 6.)

For $t > t_c$, the curve of constant $\eta = 0^-$ does not intersect the x-axis, cf. Fig. 11. All curves of constant φ intersect the $(\eta = 0^-)$-curve at non-zero y, which means that the eigenvalue density is non-zero for all φ. For $t < t_c = 4$, a part of the curve $\eta = 0^-$ lies on the x-axis (parametrizing the curve as $y = y(x)$, we have $y(x) < 0$ for $0 \leq x < x_c$ and $y(x) = 0$ for $x_c \leq x \leq \pi$), cf. Fig 9. The eigenvalue density vanishes for values of $\varphi > \varphi_c(t)$ leading to intersection points with the $(\eta = 0^-)$-curve at $y = 0$. For $t = t_c = 4$, this happens only at $\varphi = \pi$.

The density $\rho(\varphi, t)$ is basically determined by the t-dependent location of the curves of constant $\eta = 0^-$ in the x-y-plane. A point (x_0, y_0) on such a curve for a given value of t determines the spectral density at the angle $\varphi_0 = \varphi(x_0, y_0; t)$ to be $\rho(\varphi_0, t) = -2y_0/t$. The map from (x_0, y_0) to φ_0 is explicitly given by Eq. (4.86). Figures 12 and 13 show numerical results for $\rho(\varphi, t)$.

4.4.3 Edge of the spectrum – analytical results

The location of the edge $\varphi_c(t)$ of the spectrum for $0 < t \leq 4$ can be obtained by expanding Eq. (4.86) for small y and setting $\eta = 0$, which leads to

$$y = \frac{t}{2} \frac{y}{1 - \cos(x)} \,. \tag{4.90}$$

For small but non-zero y, the solution is

$$\cos(x_c) = 1 - \frac{t}{2} \,, \qquad x_c(t) = \arccos\left(1 - \frac{t}{2}\right) \,, \tag{4.91}$$

which exists for $t \leq 4$. This is the point where the $(\eta = 0^-)$-curve with $y < 0$ falls on the $(y = 0)$-axis.

The angle $\varphi_c(t)$, where the transition from zero to non-zero $\rho(\varphi, t)$ occurs, is therefore given by

$$\varphi_c(t) = x_c(t) + t \sin(x_c(t)) \frac{1}{2 - 2\cos(x_c(t))} = \arccos\left(1 - \frac{t}{2}\right) + \sqrt{t\left(1 - \frac{t}{4}\right)} \,. \tag{4.92}$$

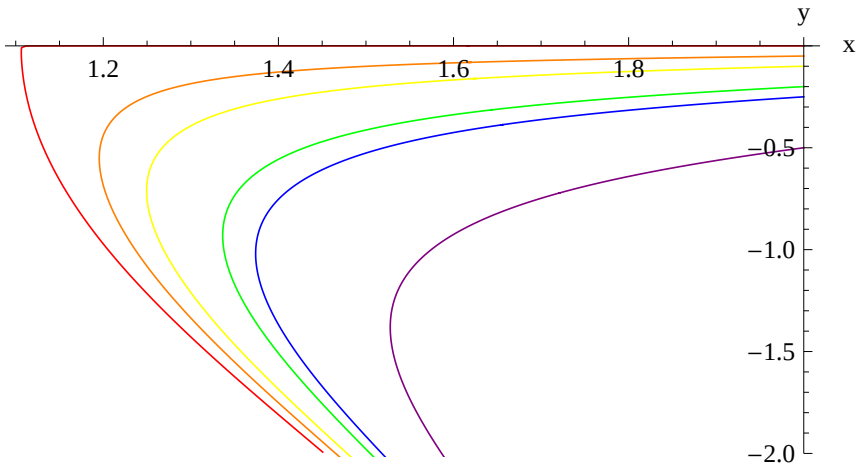

Figure 8: Plot of the curves of Fig. 7 in the x-y-plane (parameters and color-coding are identical). The curve for $\eta = -0.05$ (resp. $\eta = -10^{-5}$) is also plotted in Fig. 5 (resp. Fig. 6).

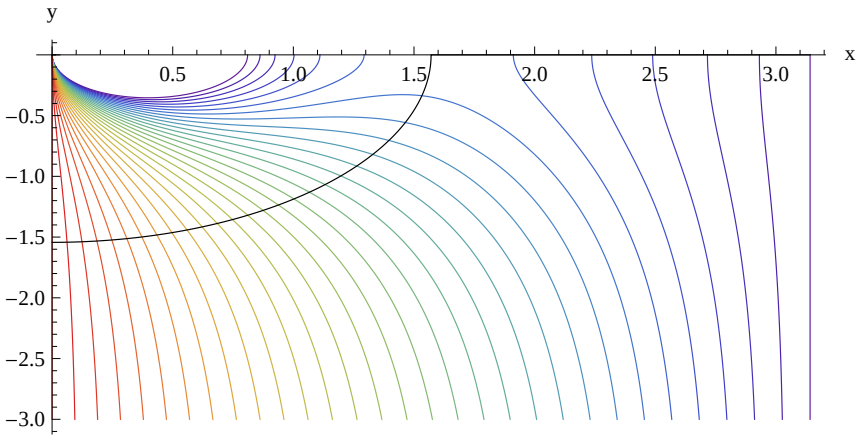

Figure 9: Plot of lines of constant $\eta = -10^{-10}$ (black) and constant $\varphi = \frac{j\pi}{30}$, $j = 0, \ldots, 30$ (colored lines; $\varphi = 0$ in red and $\varphi = \pi$ in purple) at $t = 2$.

A plot of $\varphi_c(t)$ is included in Fig. 37 below.

For $t > 4$, the curve of constant $\eta = 0^-$ intersects the axis $x = \pi$ at a non-zero y-value, which is implicitly given by

$$y_s = \frac{t}{2} \tanh\left(\frac{y_s}{2}\right) . \tag{4.93}$$

The solution $y_s < 0$ determines $\rho(\pi, t) = -\frac{2}{t} y_s$. For large t, $y_s \to -t/2$ and $\rho(\pi, t) \to 1$.

Taking the limit $t \to 4$ from above leads to $y_s \to 0$. We can therefore expand Eq. (4.93) in y_s for $t \approx 4$ which leads to

$$y_s^2 \approx 12 \frac{t-4}{t} \approx 3(t-4) . \tag{4.94}$$

This results in (with $t > 4$)

$$\rho(\pi, t \approx 4) \approx \frac{1}{2} \sqrt{3(t-4)} , \tag{4.95}$$

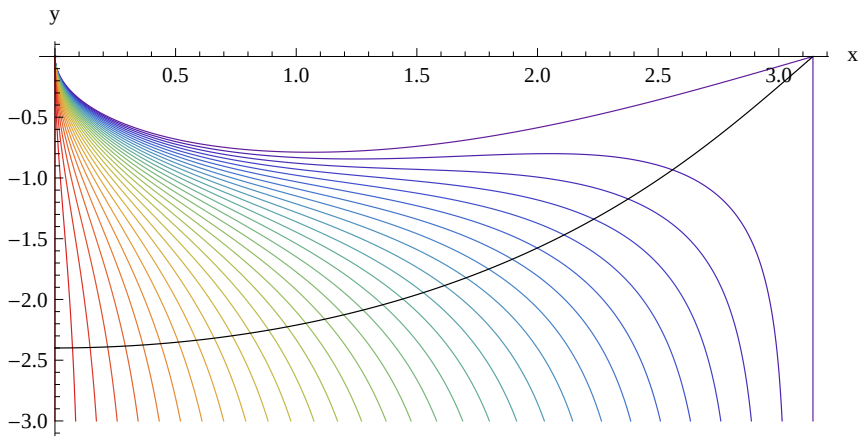

Figure 10: Plot of lines of constant $\eta = -10^{-10}$ (black) and constant $\varphi = \frac{j\pi}{30}$, $j = 0, \ldots, 30$ (colored lines; $\varphi = 0$ in red and $\varphi = \pi$ in purple) at $t = 4$.

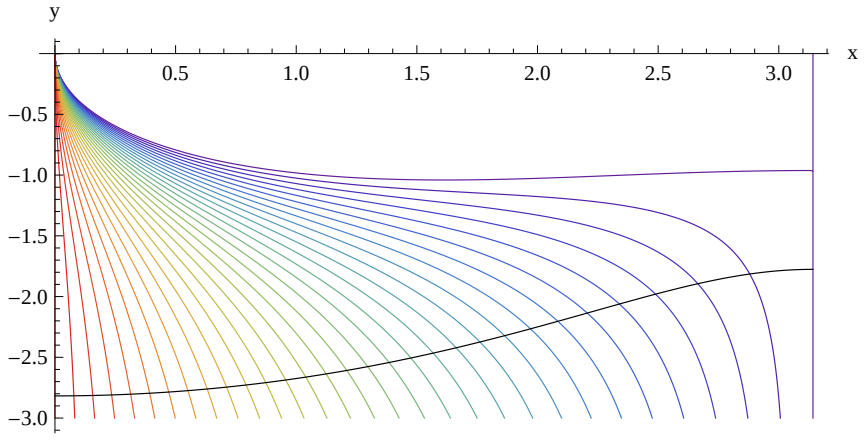

Figure 11: Plot of lines of constant $\eta = -10^{-10}$ (black) and constant $\varphi = \frac{j\pi}{30}$, $j = 0, \ldots, 30$ (colored lines; $\varphi = 0$ in red and $\varphi = \pi$ in purple) at $t = 5$.

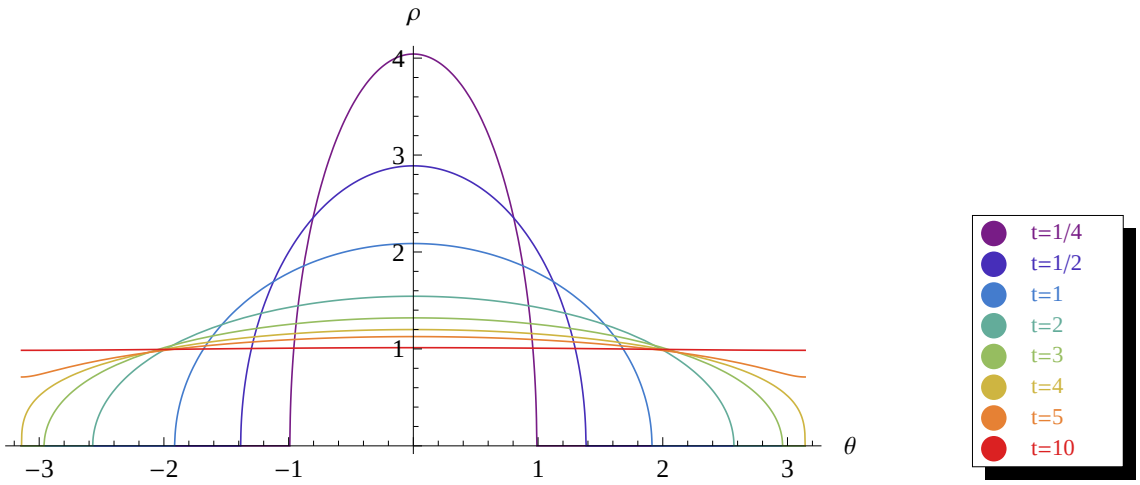

Figure 12: Plots of $\rho(\theta, t)$ (computed numerically) as a function of θ for various values of t. For $t > t_c = 4$, the spectral density is non-zero in the entire interval. For $t < t_c$, the partial derivative w.r.t. θ is singular at the critical angle $\theta_c(t)$ ($\theta_c(t_c) = \pi$).

confirming that the derivative $\partial_t \rho(\pi, t)$ is singular at the transition point $t = t_c = 4$. Figure 14 shows a plot of the full numerical result for $\rho(\pi, t)$ together with the above approximation which is valid for $t \approx 4$.

When we set $\eta = 0$, the construction of the solution of the Burgers equation from the characteristics fails at the point $(x_c(t), y = 0)$, cf. Eq. (4.91), because

$$f_0'(x_c(t)) = -\frac{1}{4\sin^2\left(\frac{x_c}{2}\right)} = -\frac{1}{2(1-\cos(x_c))} = -\frac{1}{t}\,, \tag{4.96}$$

and the partial derivatives in Eq. (4.78) become singular, which means that the mapping between θ and ξ is no longer one-to-one. In fact, we have already observed that $(x_c(t), y = 0)$ is a common point of two different curves of constant η in the limit $\eta \to 0$. This singularity is absent as long as we keep $\eta \neq 0$.

In the vicinity of the singularity, one can construct the solution of the Burgers equation analytically, which leads to an analytical expression for the eigenvalue density near the edge of the spectrum ($\varphi \approx \varphi_c(t)$) for $t \leq 4$, cf. Ref. [35]. To this end, we expand $f_0(\xi)$ in $\xi - \xi_c = \xi - x_c$

$$f_0(\xi) = f_0(\xi_c) + (\xi - \xi_c) f_0'(\xi_c) + \frac{1}{2}(\xi - \xi_c)^2 f_0''(\xi_c) + \frac{1}{6}(\xi - \xi_c)^3 f_0'''(\xi_c) + \mathcal{O}\left((\xi - \xi_c)^4\right)\,. \tag{4.97}$$

Equation (4.82) then leads to

$$\theta = \xi + t f_0(\xi) = \varphi_c + \frac{t}{2}(\xi - \xi_c)^2 f_0''(\xi_c) + \frac{t}{6}(\xi - \xi_c)^3 f_0'''(\xi_c) + \mathcal{O}\left((\xi - \xi_c)^4\right)\,. \tag{4.98}$$

With Eq. (4.91), we find

$$\frac{t}{2} f_0''(\xi_c) = \sqrt{\frac{1}{t} - \frac{1}{4}} = f_0(\xi_c)\,, \qquad \frac{t}{6} f_0'''(\xi_c) = \frac{1}{6} - \frac{1}{t}\,. \tag{4.99}$$

For $t = 4$, the second derivative vanishes and we have $\xi_c = x_c = \pi = \varphi_c$, which leads to

$$\theta \approx \pi - \frac{1}{12}(\xi - \pi)^3\,. \tag{4.100}$$

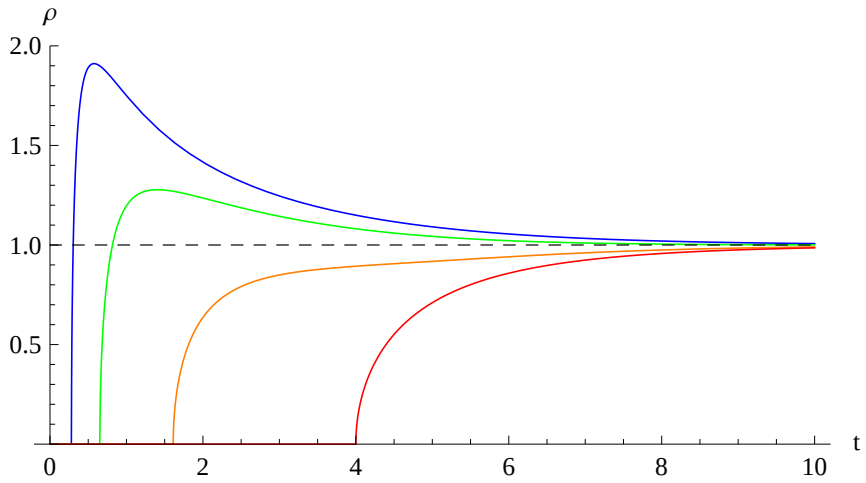

Figure 13: Plots of $\rho(\theta, t)$ (computed numerically) as a function of t for $\theta = \frac{\pi}{3}$ (blue), $\theta = \frac{\pi}{2}$ (green), $\theta = \frac{3}{4}\pi$ (orange), and $\theta = \pi$ (red). For large t, the density approaches the uniform limit $\rho(\theta, t) \to 1$ for all θ (indicated by the horizontal dashed line). The partial derivative w.r.t t is singular at the transition points from zero to non-zero eigenvalue density for each value of θ. For $\theta = \pi$, the transition occurs at $t = t_c = 4$.

We are interested in solutions with $\theta = \varphi$ real, $\varphi \leq \pi$, and $0 \leq \mathrm{Re}\,\xi \leq \pi$, $\mathrm{Im}\,\xi < 0$. For this case, we obtain

$$\pi - \xi = e^{i\frac{\pi}{3}} \left(12(\pi - \varphi)\right)^{\frac{1}{3}} , \tag{4.101}$$

which leads to

$$\mathrm{Im}\,\xi = -\sin\left(\frac{\pi}{3}\right) \left(12(\pi - \varphi)\right)^{\frac{1}{3}} . \tag{4.102}$$

For $t = 4$ and φ close to π (with $\varphi \leq \pi$), the eigenvalue density to leading order in $(\pi - \varphi)$ is therefore given by

$$\rho(\varphi, t = 4) = \frac{1}{2}\sin\left(\frac{\pi}{3}\right) \left(12(\pi - \varphi)\right)^{\frac{1}{3}} = \frac{\sqrt{3}}{4} 12^{\frac{1}{3}} (\pi - \varphi)^{\frac{1}{3}} . \tag{4.103}$$

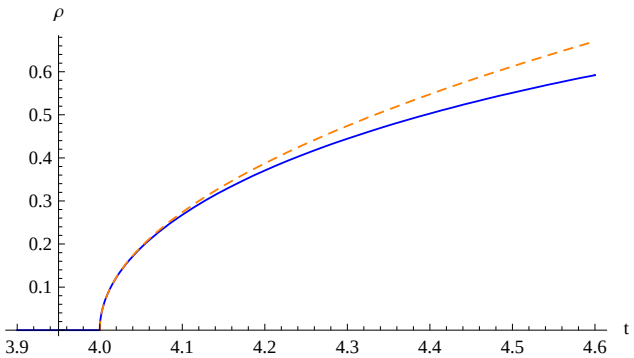

Figure 14: Plot of the numerical result for the eigenvalue density $\rho(\pi, t)$ (solid blue curve) together with the analytical approximation for $t \approx 4$ given in Eq. (4.95) (dashed orange curve).

The derivative $\partial_\varphi \rho$ is singular at the angle $\varphi_c(t=4) = \pi$. Figure 15 shows plots of the full numerical result for $\rho(\varphi, t=4)$ together with the above approximation valid for φ close to π.

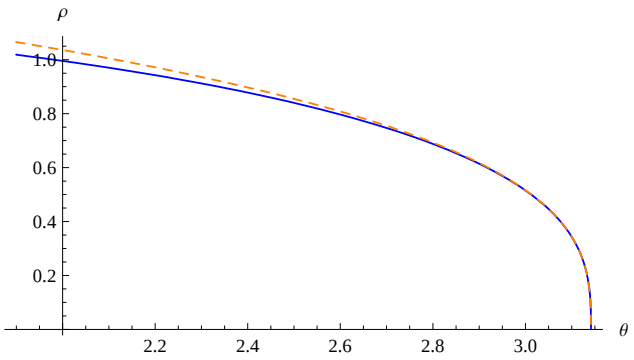

Figure 15: Plot of the numerical result for the eigenvalue density $\rho(\theta, 4)$ (solid blue curve) at the edge of the spectrum, together with the analytical approximation for θ close to π given in Eq. (4.103) (dashed orange curve).

A similar behavior occurs also for $t < 4$, the derivative $\partial_\varphi \rho$ is singular at the angle $\varphi_c(t)$, but the exponent is different. In this case, we can ignore the third-order term in Eq. (4.98) and obtain

$$\theta = \varphi_c + (\xi - \xi_c)^2 \sqrt{\frac{1}{t} - \frac{1}{4}}\,. \tag{4.104}$$

We are interested in solutions for $\theta = \varphi \in \mathbb{R}$, $\varphi < \varphi_c$ with $\operatorname{Re}\xi \leq \xi_c = x_c \in \mathbb{R}$ and $\operatorname{Im}\xi \leq 0$. This leads to

$$\xi_c - \xi = i \frac{\sqrt{\varphi_c - \varphi}}{\left(\frac{1}{t} - \frac{1}{4}\right)^{\frac{1}{4}}}\,. \tag{4.105}$$

Due to

$$\operatorname{Im}\xi = -\frac{\sqrt{\varphi_c - \varphi}}{\left(\frac{1}{t} - \frac{1}{4}\right)^{\frac{1}{4}}}\,, \tag{4.106}$$

the eigenvalue density $\rho(\varphi, t)$ near the edge $\varphi_c(t)$, where the transition from non-zero to zero density occurs for $t < 4$, is given by

$$\rho(\varphi, t) = \frac{2}{t\left(\frac{1}{t} - \frac{1}{4}\right)^{\frac{1}{4}}} \sqrt{\varphi_c - \varphi} \tag{4.107}$$

to leading order in $\varphi_c - \varphi$.

4.4.4 Moments in analytic form

In contrast to the spectral density $\rho(\theta, t)$, the moments

$$w_n(t) = \left\langle \frac{1}{N} \operatorname{Tr}\left[(W_t)^n\right] \right\rangle \tag{4.108}$$

are available in analytic form. Here, W_t denotes a Wilson loop matrix corresponding to a simple curve enclosing the dimensionless area t. The matrix $(W_t)^n$ corresponds to a Wilson loop obtained from traversing a simple curve (of area t) n times. The relation to the eigenvalue density is

$$w_n(t) = \int_{-\pi}^{\pi} \frac{d\theta}{2\pi} e^{in\theta} \rho(\theta, t)\,, \tag{4.109}$$

$$\rho(\theta, t) = 1 + 2\sum_{n=1}^{\infty} w_n(t) \cos(n\theta)\,. \tag{4.110}$$

This results in (with $\theta \to \theta - i0^+$)

$$f(\theta, t) = i\left(\frac{1}{2} + \sum_{n=1}^{\infty} w_n(t) e^{-in\theta}\right)\,. \tag{4.111}$$

In the special case where the initial condition is given by Eq. (4.81), one can show that the non-linear Burgers equation (4.72) reduces to the linear second order equation [36]

$$\frac{\partial^2 t f(\theta, t)}{\partial t^2} - \left(\frac{1}{t} - \frac{1}{4}\right) \frac{\partial^2 t f(\theta, t)}{\partial \theta^2} = 0\,. \tag{4.112}$$

With Eq. (4.111), this leads to a differential equation for the moments $w_n(t)$,

$$\frac{\partial^2 w_n(t)}{\partial t^2} + \frac{2}{t}\frac{\partial w_n(t)}{\partial t} + \frac{n^2}{4}\left(\frac{4}{t} - 1\right) w_n(t) = 0\,. \tag{4.113}$$

For the boundary condition $w_n(0) = 1$, this equation is solved by

$$w_n(t) = \frac{1}{n} L^1_{n-1}(nt) e^{-\frac{nt}{2}}\,, \tag{4.114}$$

where the L^1's are the Laguerre polynomials of type 1. This is a well-known result for winding Wilson loops in two-dimensional Yang-Mill theory, see Refs. [36, 37, 38].

Although the moments are perfectly analytic and the critical loop size does not represent a phase transition in these observables, they nevertheless encode the critical behavior of the spectral density at $t = t_c = 4$ [39]. The differential equation (4.113) can be interpreted as the radial Schrödinger equation (with zero angular momentum) for the hydrogen atom if the radial variable is identified with the dimensionless area t and the charge is identified with n. The critical area $t_c = 4$ plays the role of the Bohr radius of the atom, $w_n(t)$ oscillates as a function of t for $t < t_c = 4$ (the number of oscillations increases with n) and is exponentially suppressed for $t > t_c$ [36]. The asymptotic behavior of the Laguerre polynomials as a function of n can be studied by using a saddle-point analysis of their integral representations. The result for large n is that $w_n \propto n^{-3/2}$ for $t < t_c$, while the moments are damped exponentially with n for $t > t_c$. Although the moments are analytic, this does not exclude non-analyticities in the eigenvalue density, which is given by an infinite sum over moments, cf. Eq. (4.110).

4.4.5 Universal properties – turbulence and random matrix model

In Ref. [35], it is shown that Eq. (4.96) (with x_c allowed to be complex), which determines the location of the singularities in the construction of the solutions of the complex Burgers equation, also determines the envelope of the characteristics $(\varphi(t), \eta(t))$ when x and y are

treated as parameters, cf. Eq. (4.86). Pointing out a beautiful analogy between the large-N limit of two-dimensional Yang-Mills theory and the limiting procedure from wave optics to geometric optics ($\frac{1}{2N}$ is associated with a wavelength λ), Blaizot and Nowak observe that the complex characteristics, which are given by straight lines, play the role of classical rays of light. In this analogy, the singularities in the solutions of the Burgers equation correspond to so-called caustics (with infinite intensity in the $\lambda \to 0$ limit) in geometric optics.

By restricting θ to $\theta = \pi + i\eta$ (with η being real) the eigenvalue density at π can be analyzed with the help of a real Burgers equation. Introducing a finite viscosity $\nu = \frac{1}{2N}$ in this equation (cf. also [40] and Sec. 5.5 below), it is furthermore observed that finite-viscosity scaling leads to the same critical exponents as finite-λ scaling of wave packets in optics. Therefore, Blaizot and Nowak argue that the finite-N critical scaling of the eigenvalue density of the Wilson loop matrix could belong to the same universality class as the scaling of interference patterns in wave optics.

We have seen in the previous sections that the complex Burgers equation provides a unique solution which connects the initial Wilson loop eigenvalue density at $t = 0$ ($\rho(\theta, t = 0) = 2\pi\delta_{2\pi}(\theta)$) to the uniform limit for $t \to \infty$. It is explicitly shown in Refs. [35, 41] that this solution is not stable under backward evolution for initial conditions (at large t) that deviate only slightly from the generic solution. Blaizot and Nowak argue that the extreme sensitivity on the initial condition is due to a turbulent nature of the disordered (gapless) phase and suggest that the general mechanism for the transition in the eigenvalue density (which occurs also in Yang-Mills theories in higher dimensions, cf. Sec. 4.4.6 below) is determined by the occurrence of "spectral shock waves".

In Refs. [35, 42], it is observed that the appearance of inviscid and viscid Burgers equations in the analysis of the eigenvalue distribution of Wilson loops is not surprising since these equations naturally appear in both additive and multiplicative random walks of large matrices. For the Gaussian unitary ensemble, which is extensively studied in random matrix theory, the joint probability distribution for the eigenvalues can be interpreted as the result of an additive random walk performed independently by the matrix elements of a Hermitian matrix. In this case, a viscid Burgers equation with viscosity $1/2N$ is found to be of central importance. Furthermore, the edge of the spectrum of the eigenvalues (which is given by Wigner's famous semicircle) can in a fluid-dynamical picture be related to a shock wave produced by the Burgers equation with the appropriate initial condition. Through this relation, Blaizot and Nowak can recover universal properties of the random matrix model exclusively from the perspective of the theory of turbulence.

Due to the special properties of two-dimensional Yang-Mills theory, the universality class of the Durhuus-Olesen transition in the spectral density may be defined in terms of a simple multiplicative random matrix model introduced by Janik and Wieczorek in Ref. [43]. The model can be viewed as a matrix generalization of the multiplicative random walk and can be interpreted as a multiplicative diffusion process on the unitary group. It can be axiomatized in the language of non-commutative probability [44] and provides a generalization of the familiar law of large numbers; the essential feature making a difference is that one case is commutative and the other is not (cf. also Sec. 10 below).

The model can be defined in the following way: A product matrix W_n is generated by multiplying n independent and identically distributed unitary $N \times N$ matrices $U_j = e^{i\varepsilon H_j}$, $j = 1, \ldots, n$, where the Hermitian and traceless matrices H_j are distributed according to the probability distribution

$$P(H_j) = \mathcal{N} e^{-\frac{N}{2} \operatorname{Tr} H_j^2} . \tag{4.115}$$

In the "continuum limit" $n \to \infty$ and $\varepsilon \to 0$ with $n\varepsilon^2$ kept fixed, the probability distribu-

tion for the product matrix

$$W_n = U_1 U_2 \cdots U_n \tag{4.116}$$

coincides exactly with the probability distribution for the Wilson loop matrix in two-dimensional Yang-Mills theory, given in Eq. (4.63), provided that the parameter $n\varepsilon^2$, which plays the role of a diffusive evolution time in the multiplicative random walk, is identified with the dimensionless area $\lambda A = t$, see Refs. [2, 41]. A generalized form of this model is discussed extensively in Sec. 12 below.

Janik and Wieczorek used free random variable methods, in particular the so-called S-transform method, to determine the eigenvalue density of the product matrix in the limit $N \to \infty$. This approach leads to an implicit equation determining the spectral density which is equivalent to Eq. (4.84) above.

It was furthermore observed in Ref. [43] that a generalization of the probability distribution for the Hermitian matrices given in Eq. (4.115) does not affect the spectral properties of the product matrix; as long as $\langle \operatorname{Tr} H \rangle$ vanishes, these properties are exclusively determined by the second moment $\left\langle \operatorname{Tr} H^2 \right\rangle$ of the random Hermitian matrix.

4.4.6 Universal properties – higher dimensions

It was observed by R. Narayanan and H. Neuberger in Refs. [2, 45] that the eigenvalue density of Wilson loops in pure SU(N) Yang-Mills theory in more than two spacetime dimensions exhibits a critical behavior similar to the Durhuus-Olesen transition found in the two-dimensional case.

The hypothesis formulated in Ref. [2] states not only that a non-analyticity in the eigenvalue density at a critical loop size occurs in two, three, and four Euclidean dimensions, but also that the transitions in these dimensions belong to the same universality class. This means that close to the critical scale, the complicated dependence on the loop shape in three and four dimensions at large but finite N comes in only through a finite number of non-universal parameters, which are coefficients of sub-leading terms (to the infinite-N result) of the form N^{ν_i} with a few universal exponents ν_i.

In higher dimensions, numerical lattice simulations and extrapolations to the continuum limit are needed to study the transition in the eigenvalue density in the continuum theory. In three and four dimensions, perimeter and corner divergences occur (cf. Sec. 3.4.3), which can be eliminated by working with smeared versions of Wilson loops.

To test their hypothesis with lattice simulations, Narayanan and Neuberger used the simplest gauge-invariant observable which reflects the non-analyticity in the eigenvalue density, i.e., the expectation value of the characteristic polynomial (cf. also Sec. 5.5 below),

$$O_N = \left\langle \det(e^{\frac{y}{2}} - e^{-\frac{y}{2}} W) \right\rangle . \tag{4.117}$$

For a family $\mathcal{F}$ of Wilson loops corresponding to closed curves of fixed shape, obtained by dilating a given curve with a dilation parameter m ($x_\mu(s,m) = \frac{1}{m} x_\mu(s)$ parametrizes the curve which is obtained by dilating the original curve $x_\mu(s,1)$), the observable O_N depends on N, the coupling constant $b = \lambda^{-1}$, and the dilation parameter m. The universality hypothesis formulated by Narayanan and Neuberger states that O_N shows critical behavior in the infinite-N limit (with fixed λ) at some critical loop size, i.e., at a critical value m_c of the dilation parameter, and that scaling y and m with powers of N leads to a non-trivial

and universal infinite-N limit in two, three, and four spacetime dimensions according to

$$\lim_{N\to\infty} \mathcal{N}(N,\lambda,\mathcal{F}) O_N \left(y = \left(\frac{4}{3N^3}\right)^{\frac{1}{4}} \frac{\xi}{a_1(\mathcal{F})}, m = m_c \left(1 + (3N)^{-\frac{1}{2}} \frac{\alpha}{a_2(\mathcal{F})}\right)\right) = \zeta(\xi,\alpha) \tag{4.118}$$

with a universal function $\zeta(\xi,\alpha)$. The variables ξ and α are kept fixed as $N \to \infty$, the double scaling limit (both y and m are scaled with appropriate powers of N) is used to zoom into the critical region around the transition point at $y = 0$ and $m = m_c$. In contrast to the universal scaling exponents $\frac{1}{2}$ and $\frac{3}{4}$, the parameters a_1 and a_2 are non-universal since they depend on the shape of the spacetime curve defining the family $\mathcal{F}$ of Wilson loops.

In two dimensions, the probability distribution of W reduces to the simple form given in Eq. (4.63), where the dependence on the curve defining a Wilson loop enters only through the enclosed area ($t = \lambda A$ plays the role of m^{-1}). The expectation value at finite N can be calculated by expanding the determinant in characters of irreducible representations of SU(N) (cf. Sec. 5.5). The universal function $\zeta(\xi,\alpha)$ is obtained by calculating the expectation value in Eq. (4.118) in the two-dimensional case. The result is given in terms of an integral representation (related to the so-called Pearcey integral),

$$\zeta(\xi,\alpha) = \int_{-\infty}^{\infty} du e^{-u^4 - \alpha u^2 + \xi u}\,. \tag{4.119}$$

In two dimensions, the parameters a_1 and a_2 (which are shape dependent in higher dimensions) are given by $a_1 = a_2 = 1$, independent of the shape of the curve (cf. Eqs. (5.58) and (5.59) below).

Using numerical lattice simulations, Narayanan and Neuberger carried out a test of the hypothesis in three dimensions, confirming that the critical exponents $\frac{1}{2}$ and $\frac{3}{4}$ are consistent with the data. In four dimensions, the existence of a transition from a gapless to a gaped phase in the eigenvalue density has been observed numerically, however, the critical exponents have not been tested yet (numerical simulations in three dimensions are cheaper in computation time than those in four dimensions).

It is emphasized in Ref. [45] that the non-analyticity in the eigenvalue density of Wilson loops observed by using the lattice formulation is very different from the Gross-Witten phase transition (a transition similar to the one in the two-dimensional case, cf. Sec. 4.2.2, occurs also in three and four dimensions), which is a lattice artefact of Wilson's action since the location of the transition does not scale with the lattice size. The continuum theory does not exhibit this transition, it is always in the phase where the eigenvalue distribution of the plaquette variable has a gap. The plaquette variable is a Wilson loop with an enclosed area that goes to zero in the continuum limit $b \to \infty$. To study the properties of physical Wilson loops, one has to take the limit $b \to \infty$ while keeping the spacetime extent in physical units fixed (which means that the size of the loop in lattice units diverges). Let us repeat here that the Durhuus-Olesen phase transition refers only to a non-analyticity in the eigenvalue density, there is no non-analyticity in the partition function or expectation values of traces of Wilson loops. The location of the transition point in the lattice formulation scales properly with b, i.e., the transition is a transition of the continuum theory.

Part II

Eigenvalue densities of Wilson loops in 2D SU(N) YM

Since the Durhuus-Olesen phase transition (the non-analyticity in the eigenvalue distribution of the SU(N) Wilson loop matrix, cf. Sec. 4.4) has universal properties shared across dimensions and across analog two-dimensional models [2, 46], a detailed understanding of the transition region in two dimensions will be of relevance to crossovers from weakly to strongly interacting regimes in a wide class of models with symmetry SU(N). Based on previous investigations in Refs. [40, 41, 47], the work carried out in collaboration with Herbert Neuberger and Tilo Wettig and published in Ref. [48] contains several new results in this direction. Following Ref. [48], these results are presented in this part of the thesis.

In the following, we focus on the eigenvalues of the Wilson loop. The associated observables are three different density functions $\rho_N^\ell(\theta)$, with ℓ = asym, sym, true, of the angular variable θ (for the time being, we suppress the loop-size dependence). The three functions have identical limits at infinite N, $\rho_\infty^\ell(\theta) = \rho_\infty(\theta)$. This is the eigenvalue density studied in detail in Sec. 4.4. Let us repeat here that the non-negative function $\rho_\infty(\theta)$ exhibits a transition, the Durhuus-Olesen phase transition, at a critical size of the Wilson loop. At the transition point, a gap centered at $\theta = \pm\pi$, present in the eigenvalue density for small loops, just closes, and derivatives with respect to θ and the dimensionless area variable diverge.

The $\rho_N^\ell(\theta)$ for ℓ = asym, sym are obtained from the logarithmic derivative of $\langle \det{}^k(z - W)\rangle$ for $k = 1$ and -1, respectively, where one needs to take z to $e^{i\theta}$ in a specified manner. Neither of these two functions $\rho_N^\ell(\theta)$ has a natural interpretation at finite N, the interest in these functions mainly stems from them obeying simple partial integro/differential equations which are exactly integrable and already known and studied in Refs. [40, 47]. In the following, we extend the results presented there.

Unlike $\rho_N^\ell(\theta)$ with ℓ = asym or ℓ = sym, $\rho_N^{\text{true}}(\theta)$ literally is the eigenvalue density at finite N, determined by $\langle \operatorname{Tr} \delta(\theta + i \log W)\rangle$, and poses no difficulties of interpretation. It can be obtained from $\langle \det(1 + uW)/(1 - vW)\rangle$ in the limit $-u \to v \to e^{i\theta}$. Explicit expressions for $\rho_N^{\text{true}}(\theta)$ are derived below. As anticipated in Ref. [47], we find no evidence that $\rho_N^{\text{true}}(\theta)$ obeys as simple equations as the $\rho_N^\ell(\theta)$ for $\ell \neq$ true were found to do.

This part of the thesis starts with a general description of $\rho_N^\ell(\theta)$, followed with details for each case. In Sec. 6, we focus on the case ℓ = asym and study the loop-size dependence of the zeros z_j of the average characteristic polynomial (ρ_N^{asym} is completely determined by these zeros). The equations governing the zeros were derived in Ref. [40], and here we work out the approximate solutions for small, intermediate, and large loops. We continue in Sec. 7 with a description of the case ℓ = sym and a saddle-point analysis of the integral representation found in Ref. [47]. A connection to the multiplicative random matrix model of Refs. [3, 49] is pointed out. Exact representations of $\rho_N^{\text{true}}(\theta)$ for arbitrary finite N are derived in Sec. 8. As expected, we do not find a simple direct equation for $\rho_N^{\text{true}}(\theta)$, but we do find a simple equation for $\langle \det(1 + uW)/(1 - vW)\rangle$ and obtain a representation of $\rho_N^{\text{true}}(\theta)$ by a sum. By numerically performing the sum, $\rho_N^{\text{true}}(\theta)$ can be evaluated to any desired accuracy. Furthermore, we derive an integral representation for $\rho_N^{\text{true}}(\theta)$, which is

useful for setting up the $1/N$ expansion of $\rho_N^{\rm true}(\theta)$. We carry out the saddle-point analysis which is the starting point of this expansion. We also show that one can define a natural extension to negative values of N, and in this extension $\rho_N^{\rm true}(\theta) = \rho_{-N}^{\rm true}(\theta)$. We follow this up by a numerically-aided study of the relations between the three $\rho_N^\ell(\theta)$. We compare numerically the densities $\rho_N^{\rm true}(\theta)$ and $\rho_N^{\rm sym}(\theta)$ at the same areas. As $\rho_N^{\rm asym}(\theta)$ is given by a sum of delta functions, its comparison to another $\rho_N^\ell(\theta)$ is less direct. We conjecture, and check numerically, that the location of the N peaks in $\rho_N^{\rm true}(\theta)$ are close to the matching zeros $\theta_j = -i \log z_j$ of the average characteristic polynomial. By "close" we mean that for large N, the distance between a θ_j and the matching peak vanishes faster than the distance between that peak and its adjacent valley.

5 Three densities $\rho_N^\ell(\theta)$ and how they compare

5.1 Convenient definitions of dimensionless area

The dimensionless area variable has to take a slightly different form for the average of the characteristic polynomial and the average of its inverse to obey equations that look simple.

As in Sec. 4.4, we define

$$t = Ag^2N\,, \tag{5.1}$$

where A is the area enclosed by the Wilson loop, g is the Yang-Mills coupling, and the gauge group is SU(N). The standard 't Hooft coupling is given by $\lambda = g^2N$, and t makes it dimensionless. This t appears in $\rho_N^{\rm true}(\theta, t)$, the Durhuus-Olesen transition for infinite N occurs at $t = t_c = 4$ (see Sec. 4.4).

The average characteristic polynomial generates the expectation values of the characters of all antisymmetric representations of the Wilson loop matrix. The appropriate area variable in this case is denoted by

$$\tau = t\left(1 + \frac{1}{N}\right)\,, \tag{5.2}$$

cf. Ref. [47]. Thus, when $\rho_N^{\rm asym}(\theta, \tau)$ is compared to $\rho_N^{\rm true}(\theta, t)$, the $1/N$ correction in t relative to τ has to be taken into account.

The average of the inverse of the characteristic polynomial generates the expectation values of the characters of all symmetric representations of the Wilson loop matrix. The appropriate area variable in this case is denoted by T, with [47]

$$T = t\left(1 - \frac{1}{N}\right)\,. \tag{5.3}$$

When we compare $\rho_N^{\rm sym}(\theta, T)$ to $\rho_N^{\rm true}(\theta, t)$, we have to take into account the $1/N$ correction in t relative to T.

5.2 Averaging over the Wilson loop matrix

We have seen in Sec. 4.3 that two-dimensional Yang-Mills theory is very special. The probability density for the Wilson loop matrix W is given by a simple sum over characters of irreducible representations of SU(N), cf. Eq. (4.63). With $t = Ag^2N$, this equation reads

$$\mathcal{P}_N(W, t) = \sum_r d_r \chi_r(W) e^{-\frac{t}{2N} C_2(r)}\,, \tag{5.4}$$

where the sum is over all distinct irreducible representations r of SU(N) with d_r denoting the dimension of r and $C_2(r)$ denoting the value of the quadratic Casimir on r. $\chi_r(W)$ is the character of W in the representation r and is normalized by $\chi_r(\mathbf{1}) = d_r$.

Averages over W at fixed t are then obtained by integrating over the gauge group SU(N) with the invariant Haar measure dW,

$$\langle \mathcal{O}(W) \rangle = \int dW \mathcal{P}_N(W,t) \mathcal{O}(W) \,. \tag{5.5}$$

The measure is normalized by $\int dW = 1$, and we have in addition $\int dW \mathcal{P}_N(W,t) = 1$. Any class function on SU(N) can be averaged when expanded in characters using character orthogonality (see Sec. 2).

Since each representation is accompanied by its complex conjugate representation in the sum over r in Eq. (5.4), it follows that

$$\langle \mathcal{O}(W) \rangle = \langle \mathcal{O}(W^\dagger) \rangle = \langle \mathcal{O}(W^*) \rangle \,, \tag{5.6}$$

implying identities relating $\langle \det(z - W) \rangle$, $\langle \det(z - W)^{-1} \rangle$, and $\langle \det(1 + uW)/(1 - vW) \rangle$ to the same objects with $z \to 1/z$, $z \to z^*$, $u, v \to 1/u, 1/v$, and $u, v \to u^*, v^*$, respectively.

5.3 General properties of the densities

All densities ρ_N^ℓ are real on the unit circle parametrized by the angle $|\theta| \leq \pi$, even under $\theta \to -\theta$, and depend on the size of the loop. All three are positive distributions in θ, normalized by

$$\int_{-\pi}^{\pi} \frac{d\theta}{2\pi} \rho_N^\ell(\theta) = 1 \,. \tag{5.7}$$

We will see below that the density ρ_N^{asym} summarizes the averages of the characters of W in all totally antisymmetric representations, i.e., single-column Young diagrams. Similarly, ρ_N^{sym} summarizes the averages of the characters of W in all totally symmetric representations, i.e., single-row Young diagrams. The true eigenvalue density ρ_N^{true} summarizes the averages of the traces of all k-wound Wilson loops matrices, $\langle \operatorname{Tr} W^k \rangle$. As we will discuss in Sec. 8, the latter are determined by linear combinations of the averages of the characters of W in representations which we label by (p, q) and whose Young diagrams have the following shape:

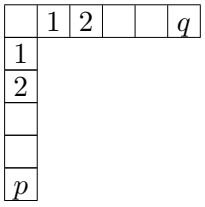

. (5.8)

The density ρ_N^{true} determines $\langle \operatorname{Tr} f(W) \rangle$ for any function f. However, unlike ρ_N^{asym} and ρ_N^{sym}, it has no information about any average of the type $\langle \operatorname{Tr} f(W) \operatorname{Tr} g(W) \rangle$, where the number of trace factors exceeds one. In other words, ρ_N^{true} is the single eigenvalue density and, unlike ρ_N^{asym} and ρ_N^{sym}, contains no information about any higher-point eigenvalue correlations.

We will show below that the density $\rho_N^{\text{true}}(\theta, t)$ is smooth over the unit circle and similar to $\rho_N^{\text{sym}}(\theta, T)$ in this sense but has N peaks adding an oscillatory modulation to the non-oscillatory function $\rho_N^{\text{sym}}(\theta, T)$ (cf. Secs. 5.6 and 9 below). In some sense $\rho_N^{\text{true}}(\theta, t)$ is intermediate between $\rho_N^{\text{asym}}(\theta, \tau)$ and $\rho_N^{\text{sym}}(\theta, T)$ since it can be obtained from the expectation value of the ratio of values of the characteristic polynomial evaluated at

two different values of its argument (ρ_N^{asym} is obtained from $\langle\det(z-W)\rangle$; ρ_N^{sym} is obtained from $\langle\det(z-W)^{-1}\rangle$). The oscillatory behavior is in this sense a remnant of the delta-function structure of $\rho_N^{\text{asym}}(\theta,t)$ (cf. Sec. 5.5 below). For this reason, we expect the peaks of $\rho_N^{\text{true}}(\theta,t)$ to occur at locations close to the matching angles $\theta_j(\tau)$ which parametrize the zeros of the average characteristic polynomial (cf. Eq. (5.27) below). This expectation will be confirmed numerically in Sec. 9.

5.4 True eigenvalue density $\rho_N^{\text{true}}(\theta,t)$ and associated resolvent

Unlike ρ_N^ℓ with $\ell = \text{asym},\ \text{sym}$, the density $\rho_N^{\text{true}}(\theta,t)$ has a natural definition at finite N. It is equivalent to the density that we have introduced in Eq. (4.64): If the eigenvalues of W are $e^{i\alpha_j}$ with $j = 0,1,\ldots,N-1$, we define

$$\rho_N^{\text{true}}(\theta,t) = \frac{2\pi}{N}\sum_j \langle\delta_{2\pi}(\theta-\alpha_j(W))\rangle = \frac{2\pi}{N}\langle\operatorname{Tr}\delta_{2\pi}(\theta+i\log(W))\rangle\,, \tag{5.9}$$

where $\delta_{2\pi}$ denotes the 2π-periodized delta function with normalization

$$\int_{-\pi}^{\pi} d\theta\,\delta_{2\pi}(\theta) = 1\,. \tag{5.10}$$

Given $\rho_N^{\text{true}}(\theta,t)$, we can compute the averages of a specific subset of class functions $F(W)$, namely, those that can be written as

$$F(W) = \frac{1}{N}\sum_j f(\alpha_j(W))\,. \tag{5.11}$$

The obvious formula is

$$\langle F(W)\rangle = \Big\langle \frac{1}{N}\sum_j \int_{-\pi}^{\pi} d\theta f(\theta)\delta_{2\pi}(\theta-\alpha_j(W))\Big\rangle = \int_{-\pi}^{\pi}\frac{d\theta}{2\pi} f(\theta)\rho_N^{\text{true}}(\theta,t)\,. \tag{5.12}$$

The density $\rho_N^{\text{true}}(\theta,t)$ summarizes all the information contained in the entire collection of averages of the type $\langle\operatorname{Tr} f(W)\rangle$. Viewed in this way, it is analogous to $\rho_N^{\text{asym}}(\theta,\tau)$ and $\rho_N^{\text{sym}}(\theta,T)$, which summarize all the information contained in all averages $\langle\chi_r(W)\rangle$, with r denoting all totally antisymmetric and all totally symmetric representations, respectively (cf. Secs. 5.5 and 5.6).

In the following, we show explicitly that the true eigenvalue density can be obtained from the associated resolvent

$$G_{N,\pm}^{\text{true}}(z,t) = \frac{1}{N}\left\langle\operatorname{Tr}\frac{1}{z-W}\right\rangle = \frac{1}{N}\frac{\partial}{\partial z}\langle\log\det(z-W)\rangle\,, \tag{5.13}$$

where the $+$ sign goes with $|z|>1$ and the $-$ sign goes with $|z|<1$ (we can choose G^{true} to be analytic either inside or outside the unit circle). However, using Eq. (5.6) one easily concludes that $G_{N,-}^{\text{true}}$ is completely determined by $G_{N,+}^{\text{true}}$. Clearly, $\rho_N^{\text{true}}(\theta,t)$ determines $G_{N,\pm}^{\text{true}}(z,t)$ since the latter is the average of a single trace. As the resolvent $G_{N,\pm}^{\text{true}}(z,t)$ is determined by an expectation value which belongs to the general type of Eq. (5.12), we obtain

$$G_{N,\pm}^{\text{true}}(z,t) = \int_{-\pi}^{\pi}\frac{d\alpha}{2\pi}\frac{\rho_N^{\text{true}}(\alpha,t)}{z-e^{i\alpha}}\,. \tag{5.14}$$

It is easy to see that the opposite is also true, namely, $G^{\text{true}}_{N,\pm}(z,t)$ determines $\rho^{\text{true}}_N(\theta,t)$. Since $\rho^{\text{true}}_N(\theta,t)$ is a periodic and even function of θ, its Fourier expansion can be written as

$$\rho^{\text{true}}_N(\theta,t) = 1 + \sum_{n=1}^{\infty} \rho_n \cos(n\theta) \qquad \text{with } \rho_n \in \mathbb{R}\,. \tag{5.15}$$

Let us first focus on $G^{\text{true}}_{N,+}(z,t)$. We set $z = e^{i\theta+\varepsilon}$ with $\theta, \varepsilon \in \mathbb{R}$ and $\varepsilon > 0$ and use the expansion in a geometric series

$$\frac{1}{e^{i\theta+\varepsilon} - e^{i\alpha}} = \frac{e^{-i\theta-\varepsilon}}{1 - e^{i(\alpha-\theta)-\varepsilon}} = e^{-i\theta-\varepsilon} \sum_{n=0}^{\infty} e^{in(\alpha-\theta)} e^{-n\varepsilon}\,, \tag{5.16}$$

which leads to

$$\begin{aligned} G^{\text{true}}_{N,+}(e^{i\theta+\varepsilon},t) &= \int_{-\pi}^{\pi} \frac{d\alpha}{2\pi} \left(1 + \sum_{k=1}^{\infty} \rho_k \cos(k\alpha)\right) \sum_{n=0}^{\infty} e^{in\alpha} e^{(n+1)(-\varepsilon-i\theta)} \\ &= e^{-i\theta-\varepsilon} + \sum_{k=1}^{\infty} \frac{1}{2} \rho_k e^{(k+1)(-i\theta-\varepsilon)} \\ &= e^{-(i\theta+\varepsilon)} \left(1 + \frac{1}{2} \sum_{k=1}^{\infty} \rho_k \left(\cos(k\theta) - i\sin(k\theta)\right) e^{-\varepsilon k}\right)\,. \end{aligned} \tag{5.17}$$

By comparison with the Fourier expansion in Eq. (5.15), we see that the density $\rho^{\text{true}}_N(\theta,t)$ is obtained from the resolvent $G^{\text{true}}_{N,+}(z,t)$ through the relation

$$\rho^{\text{true}}_N(\theta,t) = \lim_{\varepsilon\to 0^+} \text{Re}\left[2e^{i\theta+\varepsilon} G^{\text{true}}_{N,+}(e^{i\theta+\varepsilon},t) - 1\right]\,. \tag{5.18}$$

In order to compute $G^{\text{true}}_{N,-}(z,t)$, we set $z = e^{i\theta-\varepsilon}$, again with $\theta, \varepsilon \in \mathbb{R}$ and $\varepsilon > 0$. In this case, making use of

$$\frac{1}{e^{i\theta-\varepsilon} - e^{i\alpha}} = -e^{-i\alpha} \frac{1}{1 - e^{i(\theta-\alpha)-\varepsilon}} = -e^{-i\alpha} \sum_{n=0}^{\infty} e^{in(\theta-\alpha)} e^{-n\varepsilon} \tag{5.19}$$

results in

$$\begin{aligned} G^{\text{true}}_{N,-}(e^{i\theta-\varepsilon},t) &= \int_{-\pi}^{\pi} \frac{d\alpha}{2\pi} \left(1 + \sum_{k=1}^{\infty} \rho_k \cos(k\alpha)\right) \sum_{n=0}^{\infty} (-1) e^{-i(n+1)\alpha} e^{n(i\theta-\varepsilon)} \\ &= -\sum_{k=1}^{\infty} \rho_k \frac{1}{2} e^{(k-1)(i\theta-\varepsilon)} = -e^{-(i\theta-\varepsilon)} \frac{1}{2} \sum_{k=1}^{\infty} \rho_k e^{-\varepsilon k} \left(\cos(k\theta) + i\sin(k\theta)\right)\,, \end{aligned} \tag{5.20}$$

which leads to

$$\rho^{\text{true}}_N(\theta,t) = \lim_{\varepsilon\to 0^+} \text{Re}\left[-2e^{i\theta-\varepsilon} G^{\text{true}}_{N,-}(e^{i\theta-\varepsilon},t) + 1\right]\,. \tag{5.21}$$

It is therefore convenient to introduce the function

$$F^{\text{true}}_{N,\pm}(z,t) = z G^{\text{true}}_{N,\pm}(z,t) - \frac{1}{2} \tag{5.22}$$

since

$$\rho_N^{\mathrm{true}}(\theta,t) = \lim_{\varepsilon\to 0^+} \mathrm{Re}\left[2F_{N,+}^{\mathrm{true}}(e^{i\theta+\varepsilon},t)\right] = \lim_{\varepsilon\to 0^+} \mathrm{Re}\left[-2F_{N,-}^{\mathrm{true}}(e^{i\theta-\varepsilon},t)\right] . \tag{5.23}$$

Equations (5.17) and (5.20) explicitly show that

$$F_{N,-}^{\mathrm{true}}(e^{i\theta-\varepsilon},t) = -F_{N,+}^{\mathrm{true}}(e^{i\theta+\varepsilon},t)^* \tag{5.24}$$

with $\varepsilon > 0$ and $\theta \in \mathbb{R}$. This relation is an immediate consequence of the general properties of the probability distribution of the unitary Wilson loop matrix. Due to $WW^\dagger = \mathbf{1}$, we find with $|z| > 1$ that

$$\begin{aligned} F_{N,-}^{\mathrm{true}}\left(\frac{1}{z^*},t\right) &= \left\langle \frac{1}{z^*N}\,\mathrm{Tr}\,\frac{1}{\frac{1}{z^*}-W} - \frac{1}{2}\right\rangle = \left\langle \frac{1}{zN}\,\mathrm{Tr}\,\frac{1}{\frac{1}{z}-W^\dagger} - \frac{1}{2}\right\rangle^* \\ &= \left\langle \frac{1}{N}\,\mathrm{Tr}\,\frac{W}{W-z} - \frac{1}{2}\right\rangle^* = \left\langle -\frac{z}{N}\,\mathrm{Tr}\,\frac{1}{z-W} + \frac{1}{2}\right\rangle^* = -F_{N,+}^{\mathrm{true}}(z,t)^* . \end{aligned} \tag{5.25}$$

This means that the eigenvalue density is obtained from the difference between $F_{N,-}^{\mathrm{true}}(z,t)$ (which is an analytic function inside the unit circle, $|z| < 1$) and $F_{N,+}^{\mathrm{true}}(z,t)$ (which is an analytic function outside the unit circle, $|z| > 1$) on the unit circle $|z| = 1$ since Eq. (5.23) can be written as

$$\begin{aligned} \rho_N^{\mathrm{true}}(\theta,t) &= \lim_{\varepsilon\to 0^+}\left[F_{N,+}^{\mathrm{true}}(e^{i\theta+\varepsilon},t) + F_{N,+}^{\mathrm{true}}(e^{i\theta+\varepsilon},t)^*\right] \\ &= \lim_{\varepsilon\to 0^+}\left[F_{N,+}^{\mathrm{true}}(e^{i\theta+\varepsilon},t) - F_{N,-}^{\mathrm{true}}(e^{i\theta-\varepsilon},t)\right] . \end{aligned} \tag{5.26}$$

Unlike for $\ell = \mathrm{asym}, \mathrm{sym}$, explicit formulas for $\rho_N^{\mathrm{true}}(\theta,t)$ were unavailable so far. New formulas that apply in this case will be derived in relative detail in Sec. 8.

5.5 The antisymmetric density $\boldsymbol{\rho_N^{\mathrm{asym}}(\theta,\tau)}$

5.5.1 Characteristic polynomial and totally antisymmetric representations

The density $\rho_N^{\mathrm{asym}}(\theta,\tau)$ is constructed from the logarithmic derivative of the average of the characteristic polynomial

$$\psi_{N,\pm}^{\mathrm{asym}}(z,\tau) = \langle \det(z-W)\rangle = \prod_{j=0}^{N-1}(z - z_j(\tau)) . \tag{5.27}$$

It was shown in Ref. [2] that $\psi_{N,\pm}^{\mathrm{asym}}$ has all its roots on the unit circle. This was observed by deriving an integral representation for the average of the characteristic polynomial (see below) and interpreting the integral as the partition function of a classical ferromagnetic spin-$\frac{1}{2}$ system in an external magnetic field determined by z. Since the zeros $z_j(\tau)$ are located on the unit circle, they can be parametrized as $z_j(\tau) = \exp(i\theta_j(\tau))$ with $j = 0,\ldots,N-1$ and $-\pi \le \theta_j \le \pi$. Being a polynomial in z, the function ψ_N^{asym} is analytic in the entire complex plane and the distinction between the cases $|z| > 1$ and $|z| < 1$ is not necessary at this stage (however, it will become relevant for the associated resolvents).

The characteristic polynomial can be expanded in characters of totally antisymmetric representations of SU(N). This is the reason for the label "asym". Parametrizing the eigenvalues of a given Wilson loop matrix by $e^{i\alpha_j}$, $0 \le j \le N-1$, we get [2]

$$\det(z-W) = \prod_{j=0}^{N-1}\left(z - e^{i\alpha_j}\right) = \sum_{k=0}^{N} z^{N-k}(-1)^k \chi_k^{\mathrm{asym}}(W) \tag{5.28}$$

with

$$\chi_k^{\text{asym}}(W) = \sum_{1\le j_1<j_2<\cdots<j_k\le N} e^{i\left(\alpha_{j_1}+\alpha_{j_2}+\ldots+\alpha_{j_k}\right)} \tag{5.29}$$

being the character of the k-fold totally antisymmetric irreducible representation of SU(N), which is associated to a single-column Young diagram with k boxes, cf. Sec. 2.6 ($k = 0$ and $k = N$ correspond to the trivial representation of SU(N)).

This implies that the zeros $e^{i\theta_j(\tau)}$ of the average characteristic polynomial determine the expectation values of all characters of totally antisymmetric representations. By comparing

$$\langle \det(z - W)\rangle = \sum_{k=0}^{N} z^{N-k}(-1)^k \left\langle \chi_k^{\text{asym}}(W)\right\rangle \tag{5.30}$$

with Eq. (5.27), we obtain

$$\left\langle \chi_k^{\text{asym}}(W)\right\rangle = \sum_{1\le j_1<j_2<\cdots<j_k\le N} e^{i\left(\theta_{j_1}(\tau)+\theta_{j_2}(\tau)+\ldots+\theta_{j_k}(\tau)\right)}\,. \tag{5.31}$$

On the other hand, we can use the orthogonality relations of the irreducible characters to compute these expectation values. Using that the probability distribution of the Wilson loop matrix is given by Eq. (5.4), we obtain

$$\begin{aligned}\left\langle \chi_k^{\text{asym}}(W)\right\rangle &= \int dW \chi_k^{\text{asym}}(W)\mathcal{P}_N(W,t) = \int dW \chi_k^{\text{asym}}(W)\mathcal{P}_N(W^\dagger,t)\\ &= \int dW \sum_r d_r e^{-\frac{t}{2N}C_2(r)}\chi_k^{\text{asym}}(W)\chi_r(W^\dagger) = d_k^{\text{asym}} e^{-\frac{t}{2N}C_2^{\text{asym}}(k)}\,.\end{aligned} \tag{5.32}$$

The dimension and the value of the quadratic Casimir operator of a k-fold antisymmetric representation are given by [50]

$$d_k^{\text{asym}} = \binom{N}{k}, \qquad C_2^{\text{asym}}(k) = k(N-k)\left(1+\frac{1}{N}\right)\,. \tag{5.33}$$

With $\tau = t\left(1+\frac{1}{N}\right)$, this results in

$$\left\langle \chi_k^{\text{asym}}(W)\right\rangle = \binom{N}{k} e^{-\frac{\tau}{2N}k(N-k)} \tag{5.34}$$

and consequently [40]

$$\langle \det(z - W)\rangle = \sum_{k=0}^{N} \binom{N}{k} z^{N-k}(-1)^k e^{-\frac{\tau}{2N}k(N-k)}\,. \tag{5.35}$$

5.5.2 Antisymmetric resolvent and density

In analogy to the definition of the true resolvent $G_{N,\pm}^{\text{true}}(z,t)$ in Eq. (5.13), we define the antisymmetric resolvent by

$$G_{N,\pm}^{\text{asym}}(z,\tau) = \frac{1}{N}\frac{\partial}{\partial z}\log\langle \det(z-W)\rangle = \frac{1}{N\psi_{N,\pm}^{\text{asym}}(z,\tau)}\partial_z\psi_{N,\pm}^{\text{asym}}(z,\tau) \tag{5.36}$$

and introduce in addition[8]

$$F_{N,\pm}^{\mathrm{asym}}(z,\tau) = zG_{N,\pm}^{\mathrm{asym}}(z,\tau) - \frac{1}{2} = \frac{1}{N\psi_{N,\pm}^{\mathrm{asym}}(z,\tau)}\left(z\partial_z - \frac{N}{2}\right)\psi_{N,\pm}^{\mathrm{asym}}(z,\tau)\,. \tag{5.37}$$

Note that the antisymmetric resolvent differs from the true resolvent only in the order of the logarithm and the expectation value. In the infinite-N limit, we expect the ordering to become irrelevant due to infinite-N factorization of expectation values, which means that the resolvents and the related densities become equivalent.

Using the parametrization of the average characteristic polynomial (5.27) in terms of its zeros, we find (with $|z|>1$)

$$F_{N,+}^{\mathrm{asym}}(z,\tau) = \frac{z}{N}\sum_{j=0}^{N-1}\frac{1}{z-z_j(\tau)} - \frac{1}{2} \tag{5.38}$$

and

$$\begin{aligned} F_{N,-}^{\mathrm{asym}}\left(\frac{1}{z^*},\tau\right) &= \frac{1}{N}\sum_{j=0}^{N-1}\frac{1}{1-z^*z_j(\tau)} - \frac{1}{2} = \left(\frac{1}{N}\sum_{j=0}^{N-1}\frac{\left(z_j(\tau)^{-1}\right)^*}{\left(z_j(\tau)^{-1}\right)^*-z} - \frac{1}{2}\right)^* \\ &= \left(-\frac{1}{N}\sum_{j=0}^{N-1}\left(\frac{z}{z-z_j(\tau)}-1\right) - \frac{1}{2}\right)^* = -F_{N,+}^{\mathrm{asym}}(z,\tau)^*\,, \end{aligned} \tag{5.39}$$

which holds due to $|z_j(\tau)|=1$, implying $\left(z_j(\tau)^{-1}\right)^* = z_j(\tau)$. The above identity is an immediate consequence of $\det W = 1$ and $\mathcal{P}(W) = \mathcal{P}(W^\dagger)$, resulting in $\psi_{N,\pm}^{\mathrm{asym}}(z,\tau)^* = \psi_{N,\pm}^{\mathrm{asym}}(z^*,\tau)$ and

$$\begin{aligned} \psi_{N,\pm}^{\mathrm{asym}}\left(\frac{1}{z^*},\tau\right) &= \left\langle \det\left(\frac{1}{z^*}-W\right)\right\rangle = \left\langle \left(\frac{1}{z^*}\right)^N \det\left(1-z^*W\right)\det W^\dagger\right\rangle \\ &= \left(\left(-\frac{1}{z}\right)^N \psi_{N,\pm}^{\mathrm{asym}}(z,\tau)\right)^*\,. \end{aligned} \tag{5.40}$$

Relation (5.39) is the analogue of Eq. (5.25) for F_N^{true} and means that we can uniquely define the antisymmetric eigenvalue density by imposing relations between the antisymmetric density and the antisymmetric resolvent which are analogous to the relations between the true density and the true resolvent of Sec. 5.4 (cf. Eqs. (5.23) and (5.26) therein),

$$\begin{aligned} \rho_N^{\mathrm{asym}}(\theta,\tau) &= \lim_{\varepsilon\to 0^+}\mathrm{Re}\left[2F_{N,+}^{\mathrm{asym}}(e^{i\theta+\varepsilon},\tau)\right] = \lim_{\varepsilon\to 0^+}\mathrm{Re}\left[-2F_{N,-}^{\mathrm{asym}}(e^{i\theta-\varepsilon},\tau)\right] \\ &= \lim_{\varepsilon\to 0^+}\left[F_{N,+}^{\mathrm{asym}}(e^{i\theta+\varepsilon},\tau) - F_{N,-}^{\mathrm{asym}}(e^{i\theta-\varepsilon},\tau)\right]\,. \end{aligned} \tag{5.41}$$

The density $\rho_N^{\mathrm{asym}}(\theta,\tau)$ can obviously be expressed in terms of the N zeros $z_j(\tau) = e^{i\theta_j(\tau)}$ of the average characteristic polynomial. With $z = e^{i\theta+\varepsilon}$, $\varepsilon>0$, Eq. (5.38) can be written as

$$F_{N,+}^{\mathrm{asym}}(e^{i\theta+\varepsilon},\tau) = \frac{1}{N}\sum_{j=0}^{N-1}\left(\frac{1}{1-e^{i(\theta_j(\tau)-\theta-\varepsilon)}} - \frac{1}{2}\right) = \frac{1}{N}\sum_{j=0}^{N-1}\left(\frac{1}{2} + \sum_{k=1}^{\infty} e^{ik(\theta_j(\tau)-\theta)}e^{-k\varepsilon}\right)\,, \tag{5.42}$$

[8]The function $F_{N,\pm}^{\mathrm{asym}}(z,\tau)$ is related to the function $\phi^{(N)}(z,\tau)$ defined in Eq. (2.10) of Ref. [48] by $F = -i\phi - 1$. The notation here is similar to the one used in Ref. [51].

which results in

$$\rho_N^{\rm asym}(\theta,\tau) = \lim_{\varepsilon\to 0^+} {\rm Re}\left[2F_{N,+}^{\rm asym}(e^{i\theta+\varepsilon},\tau)\right] = \lim_{\varepsilon\to 0^+}\frac{1}{N}\sum_{j=0}^{N-1}\left(\sum_{k=-\infty}^{\infty} e^{ik(\theta_j(\tau)-\theta)}e^{-\varepsilon|k|}\right)$$
$$= \frac{2\pi}{N}\sum_{j=0}^{N-1}\delta_{2\pi}(\theta-\theta_j(\tau))\,. \tag{5.43}$$

The sum over delta functions will reproduce exactly the averages of the traces of W in all totally antisymmetric representations at arbitrary finite N, simply by setting W equal to ${\rm diag}(e^{i\theta_0(\tau)}, e^{i\theta_1(\tau)}, \ldots, e^{i\theta_{N-1}(\tau)})$, cf. Eq. (5.31). Thus, the entire information of $\rho_N^{\rm asym}(\theta,\tau)$ is contained in the set $\theta_j(\tau)$. It is obvious that given $\rho_N^{\rm asym}(\theta,\tau)$, we can reconstruct $F_{N,\pm}^{\rm asym}(z,\tau)$ and $G_{N,\pm}^{\rm asym}(z,\tau)$,

$$\int_{-\pi}^{\pi}\frac{d\alpha}{2\pi}\frac{\rho_N^{\rm asym}(\alpha,\tau)}{z-e^{i\alpha}} = \frac{1}{N}\sum_{j=0}^{N-1}\frac{1}{z-e^{i\theta_j(\tau)}} = G_{N,\pm}^{\rm asym}(z,\tau)\,. \tag{5.44}$$

This is the analogue of Eq. (5.14) which determines $G_{N,\pm}^{\rm true}(z,t)$ from $\rho_N^{\rm true}(\theta,t)$.

It was observed in Ref. [2] that the infinite-N limit of $\rho_N^{\rm asym}(\theta,\tau)$ reproduces the Durhuus-Olesen result for $\rho_\infty(\theta,\tau)$.

5.5.3 Real Burgers equation and double scaling limit

It was shown in Ref. [40] that the function

$$\tilde F_{N,\pm}^{\rm asym}(y,\tau) = -F_{N,\pm}^{\rm asym}(-e^y,\tau)\,, \tag{5.45}$$

with real y, satisfies the real Burgers equation

$$\frac{\partial}{\partial\tau}\tilde F_{N,\pm}^{\rm asym}(y,\tau) + \tilde F_{N,\pm}^{\rm asym}(y,\tau)\frac{\partial}{\partial y}\tilde F_{N,\pm}^{\rm asym}(y,\tau) = \frac{1}{2N}\frac{\partial^2}{\partial y^2}\tilde F_{N,\pm}^{\rm asym}(y,\tau)\,, \tag{5.46}$$

where $\frac{1}{2N}$ plays the role of a viscosity. This can be seen by writing

$$\tilde F_{N,\pm}^{\rm asym}(y,\tau) = -\frac{1}{N}\frac{\partial}{\partial y}\log\tilde\psi_{N,\pm}^{\rm asym}(y,\tau) \tag{5.47}$$

with[9]

$$\tilde\psi_{N,\pm}^{\rm asym}(y,\tau) = e^{\frac{N}{2}\left(\frac{\tau}{4}-y\right)}(-1)^N\psi_{N,\pm}^{\rm asym}(-e^y,\tau) = \sum_{k=0}^{N}\binom{N}{k}e^{y\left(\frac{N}{2}-k\right)}e^{\frac{\tau}{2N}\left(\frac{N}{2}-k\right)^2}\,, \tag{5.48}$$

which follows from Eq. (5.35). We observe that

$$\frac{\partial}{\partial\tau}\tilde\psi_{N,\pm}^{\rm asym}(y,\tau) = \frac{1}{2N}\frac{\partial^2}{\partial y^2}\tilde\psi_{N,\pm}^{\rm asym}(y,\tau)\,, \tag{5.49}$$

leading to the Burgers equation (5.46) due to

$$\partial_\tau\tilde F = -\frac{1}{N}\left[\frac{1}{\tilde\psi}\partial_\tau\partial_y\tilde\psi - \frac{1}{\tilde\psi^2}\left(\partial_\tau\tilde\psi\right)\left(\partial_y\tilde\psi\right)\right] = -\frac{1}{2N^2}\left[\frac{1}{\tilde\psi}\partial_y^3\tilde\psi - \frac{1}{\tilde\psi^2}\left(\partial_y^2\tilde\psi\right)\left(\partial_y\tilde\psi\right)\right]$$
$$= \frac{1}{2N}\partial_y^2\tilde F - \tilde F\partial_y\tilde F\,. \tag{5.50}$$

[9] $\tilde\psi_{N,\pm}^{\rm asym}(y,\tau)$ is equivalent to the function $q_N(y,\tau)$ defined in Ref. [40].

The initial condition is determined by the requirement that W is given by the identity matrix at zero area. Setting $\tau = 0$ in Eq. (5.48) results in

$$\tilde{\psi}_{N,\pm}^{\mathrm{asym}}(y,0) = \left(e^{\frac{y}{2}} + e^{-\frac{y}{2}}\right)^N = \left(2\cosh\frac{y}{2}\right)^N , \tag{5.51}$$

$$\tilde{F}_{N,\pm}^{\mathrm{asym}}(y,0) = -\frac{1}{2}\frac{e^{\frac{y}{2}} - e^{-\frac{y}{2}}}{e^{\frac{y}{2}} + e^{-\frac{y}{2}}} = -\frac{1}{2}\tanh\frac{y}{2} . \tag{5.52}$$

The initial condition for $\tilde{F}_N^{\mathrm{asym}}$ is N-independent, therefore, the infinite-N limit can be determined by solving the Burgers equation (5.46) in the inviscid limit (i.e., the $1/2N$ term is dropped). In this limit, solutions can be obtained by the method of characteristics, cf. Sec. 4.4.1, leading to the implicit equation

$$\tilde{F}_{\infty,\pm}^{\mathrm{asym}}(y,\tau) = -\frac{1}{2}\tanh\left(\frac{y - \tau\tilde{F}_{\infty,\pm}^{\mathrm{asym}}(y,\tau)}{2}\right) . \tag{5.53}$$

In the infinite-N limit, the initial condition leads to the formation of a "shock" at $y = 0$ when τ reaches the critical value $\tau = 4$, cf. Fig. 16. The solution is smooth in y as long as $\tau < 4$, but at $\tau = 4$, $\partial_y \tilde{F}^{\mathrm{asym}}$ diverges at $y = 0$, and multiple solutions become available for $\tau > 4$, cf. Refs. [15, 40]. The occurrence of a shock in the solution of the inviscid Burgers equation reflects the Durhuus-Olesen phase transition since $\tilde{F}$ is related to the eigenvalue density at $\theta = \pm\pi$ (we have set $z = -e^y = e^{\pm i\pi + y}$ in the definition of $\tilde{F}$ in Eq. (5.45)),

$$\rho_\infty(\pm\pi,\tau) = \lim_{y\to 0^+}\left(-\tilde{F}_{\infty,+}^{\mathrm{asym}}(y,\tau) + \tilde{F}_{\infty,-}^{\mathrm{asym}}(-y,\tau)\right) . \tag{5.54}$$

At infinite N, we have $t = \tau$ and $\rho_\infty(\pm\pi,\tau) = 0$ for $\tau \le 4$, whereas $\rho_\infty(\pm\pi,\tau) > 0$ for $\tau > 4$.

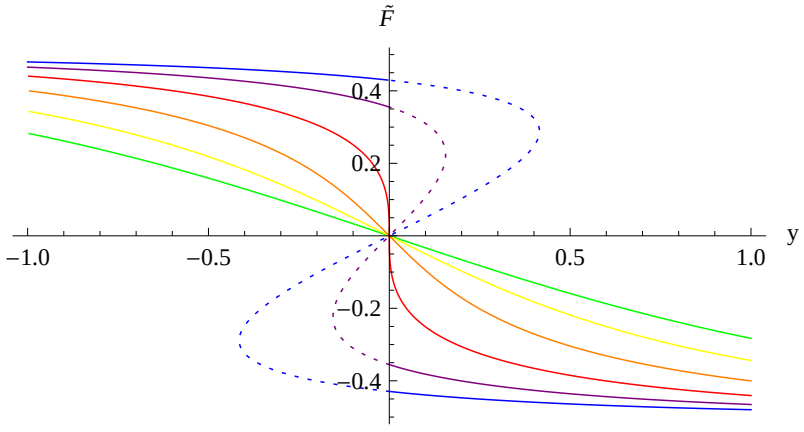

Figure 16: Solutions $\tilde{F}_{\infty,\pm}^{\mathrm{asym}}(y,\tau)$ of Eq. (5.53) for $\tau = 1$ (green), $\tau = 2$ (yellow), $\tau = 3$ (orange), $\tau = 4$ (red), $\tau = 5$ (purple), $\tau = 6$ (blue). The non-analyticity at $y = 0$ for $\tau = 4$ reflects the Durhuus-Olesen phase transition, the discontinuity at $y = 0$ for $\tau > 4$ results in a non-zero eigenvalue density $\rho_\infty(\pi,\tau)$.

Introducing a small viscosity (i.e., making N finite) results in a dissipative regularization eliminating the shock, which is smoothed out in a universal way in the vicinity of the critical point, near $\tau = 4$ and $y = 0$. The behavior in the vicinity of this point can be

studied by scaling both $\tau - 4$ and y with N (cf. also Ref. [35]). The universal exponents can be identified by introducing a Gaussian integral in Eq. (5.48),

$$e^{\frac{\tau}{2N}\left(\frac{N}{2}-k\right)^2} = \sqrt{\frac{N}{2\pi\tau}} \int_{-\infty}^{\infty} dx e^{-\frac{N}{2\tau}x^2 + \left(\frac{N}{2}-k\right)x} , \tag{5.55}$$

separating the terms that are quadratic in the summation variable k. Performing the sum over k then leads to the integral representation [2]

$$\tilde{\psi}_{N,\pm}^{\text{asym}}(y,\tau) = 2^N \sqrt{\frac{N}{2\pi\tau}} \int_{-\infty}^{\infty} e^{-\frac{N}{2\tau}(x-y)^2} e^{N \log\cosh\frac{x}{2}} . \tag{5.56}$$

After expanding

$$\log\cosh\frac{x}{2} = \frac{x^2}{8} - \frac{x^4}{192} + \mathcal{O}(x^6) , \tag{5.57}$$

we see that scaling the variables y, τ, and x with N according to

$$y = \left(\frac{4}{3N^3}\right)^{\frac{1}{4}} \xi , \tag{5.58}$$

$$\frac{1}{\tau} = \frac{1}{4}\left(1 + \frac{\alpha}{\sqrt{3N}}\right) , \tag{5.59}$$

$$x = 2\sqrt{2}\left(\frac{3}{N}\right)^{\frac{1}{4}} u \tag{5.60}$$

and taking the limit $N \to \infty$ with α and ξ kept finite leads to [2]

$$\lim_{N\to\infty} \frac{\sqrt{\pi}}{(3N)^{\frac{1}{4}}\, 2^N} \tilde{\psi}_{N,\pm}^{\text{asym}}(y,\tau) = \int_{-\infty}^{\infty} du\, e^{-u^4 - \alpha u^2 + \xi u} = \zeta(\xi,\alpha) \tag{5.61}$$

with finite-N corrections that go as powers of $1/\sqrt{N}$. It is this function $\zeta(\xi,\alpha)$ that captures the properties of the characteristic polynomial also in higher dimensions, when a similar double scaling limit for y and τ is introduced as described in Sec. 4.4.6.

5.5.4 Equations of motion for the zeros $z_j(\tau)$

In Ref. [40], it was observed that the angles $\theta_j(\tau)$, which parametrize the zeros of the average characteristic polynomial $\psi_{N,\pm}^{\text{asym}}(z,\tau)$, are determined by a set of first-order "equations of motion" in τ. These equations can be derived by inserting the product representation (5.27) into the heat equation (5.49). We evaluate the partial derivatives of $\tilde{\psi}_{N,\pm}^{\text{asym}}(y,\tau)$ at $y = y_k(\tau)$ (complex), such that $e^{y_k(\tau)} = -z_k(\tau)$, by using Eq. (5.27) together with the definition (5.48),

$$\tilde{\psi}_{N,\pm}^{\text{asym}}(y,\tau) = e^{\frac{N}{2}\left(\frac{\tau}{4}-y\right)} \prod_{i=0}^{N-1} \left(e^y + z_i(\tau)\right) , \tag{5.62}$$

$$\partial_\tau \tilde{\psi}_{N,\pm}^{\text{asym}}(y,\tau)\big|_{y=y_k(\tau)} = e^{\frac{N}{2}\left(\frac{\tau}{4}-y_k(\tau)\right)} \dot{z}_k(\tau) \prod_{i\neq k} \left(z_i(\tau) - z_k(\tau)\right) , \tag{5.63}$$

$$\begin{aligned} \partial_y^2 \tilde{\psi}_{N,\pm}^{\text{asym}}(y,\tau)\big|_{y=y_k(\tau)} &= z_k(\tau)(N-1) e^{\frac{N}{2}\left(\frac{\tau}{4}-y_k(\tau)\right)} \prod_{i\neq k} (z_i(\tau) - z_k(\tau)) \\ &\quad + 2 z_k(\tau)^2 e^{\frac{N}{2}\left(\frac{\tau}{4}-y_k(\tau)\right)} \sum_{j\neq k} \prod_{i\neq j,k} \left(z_i(\tau) - z_k(\tau)\right) , \end{aligned} \tag{5.64}$$

where $\dot{z}_k(\tau)=\partial_\tau z_k(\tau)$. The heat equation then results in

$$\frac{\dot{z}_k(\tau)}{z_k(\tau)}=\frac{N-1}{2N}+\frac{1}{2N}\sum_{j\neq k}\frac{2z_k(\tau)}{z_j(\tau)-z_k(\tau)}=\frac{1}{2N}\sum_{j\neq k}\frac{z_j(\tau)+z_k(\tau)}{z_j(\tau)-z_k(\tau)}\,. \tag{5.65}$$

With $z_j(\tau)=e^{i\theta_j(\tau)}$, we obtain

$$\dot{\theta}_k(\tau)=\partial_\tau\theta_k(\tau)=\frac{1}{2N}\sum_{j\neq k}\cot\frac{\theta_k-\theta_j}{2}\,. \tag{5.66}$$

The specific initial condition

$$\theta_j(0)=0 \tag{5.67}$$

is at a singular point of the differential equations. However, once one understands that as τ grows from zero the $\theta_k(\tau)$ spread out, the solution becomes uniquely determined. Throughout the evolution, the derivatives $\dot{\theta}_j$ never change sign. For any $\tau>0$, we have

$$\theta_0(\tau)<\theta_1(\tau)<\ldots<\theta_{N-1}(\tau)\,. \tag{5.68}$$

There is a $\mathbb{Z}_2$ symmetry pairing these angles,

$$\theta_{N-j-1}(\tau)=-\theta_j(\tau)\,. \tag{5.69}$$

If N is odd, Eq. (5.69) yields

$$\theta_{\frac{N-1}{2}}(\tau)=0\,. \tag{5.70}$$

Thus, there are $[N/2]$ pairs of non-zero eigenvalues of opposite signs, implying $\rho_N^{\rm asym}(\theta,\tau)=\rho_N^{\rm asym}(-\theta,\tau)$.

In Sec. 6, we will calculate the behavior of the $\theta_j(\tau)$ at small, critical, and large τ.

5.6 The symmetric density $\boldsymbol{\rho_N^{\rm sym}(\theta,T)}$

5.6.1 Inverse characteristic polynomial and totally symmetric representations

The density $\rho_N^{\rm sym}(\theta,T)$ is constructed from the logarithmic derivative of the average of the inverse characteristic polynomial. We reproduce here the relevant formulas from Ref. [47] in a slightly different notation. In analogy to the definition of $\psi_{N,\pm}^{\rm asym}(z,\tau)$ in Eq. (5.27), we define

$$\psi_{N,\pm}^{\rm sym}(z,T)=\langle\det(z-W)^{-1}\rangle\,, \tag{5.71}$$

where the + sign is again for $|z|>1$, and the − sign is for $|z|<1$. In this case, due to the negative power, one cannot exclude singularities at $|z|=1$ (although Eq. (22) of Ref. [47], which is reproduced in Eq. (5.78) below, shows that these singularities are removable so that $\psi_\pm^{(N)}(z,T)$ can be continued to $|z|=1$). One should think about $\psi_{N,+}^{\rm sym}(z,T)$ and $\psi_{N,-}^{\rm sym}(z,T)$ as two distinct functions. Due to the properties of the probability distribution $\mathcal{P}(W)$, cf. Sec. 5.2, we have $\psi_{N,\pm}^{\rm sym}(z^*,T)=\psi_{N,\pm}^{\rm sym}(z,T)^*$ and the functions $\psi_{N,+}^{\rm sym}$ and $\psi_{N,-}^{\rm sym}$ are simply related to each other by

$$\begin{aligned}\psi_{N,-}^{\rm sym}\left(\frac{1}{z^*},T\right)&=\left\langle\frac{1}{\det\left(\frac{1}{z^*}-W\right)\det W^\dagger}\right\rangle=(-z^*)^N\left\langle\frac{1}{\det\left(z^*-W^\dagger\right)}\right\rangle\\&=\Big((-z)^N\psi_{N,+}^{\rm sym}(z,T)\Big)^*\end{aligned} \tag{5.72}$$

with $|z|>1$.

The label "sym" is due to the fact that the inverse of the determinant can be expanded in characters of totally symmetric representations of SU(N). With $e^{i\alpha_j}$, $0 \le j \le N-1$, parametrizing the N eigenvalues of the matrix W, the character of W in the k-fold totally symmetric representation is given by

$$\chi_k^{\mathrm{sym}}(W) = \sum_{i_1 \ge i_2 \ge \ldots \ge i_k} e^{i\left(\alpha_{i_1}+\alpha_{i_2}+\ldots+\alpha_{i_k}\right)} = \sum_{n_0,n_1,\ldots,n_{N-1}\ge 0,\ \sum_{j=0}^{N-1} n_j = k} e^{i\sum_{j=0}^{N-1} n_j \alpha_j} \,. \quad (5.73)$$

Therefore, we get for $|z| > 1$ (cf. Ref. [47])

$$\begin{aligned} \frac{1}{\det(z-W)} &= \frac{1}{z^N} \prod_{j=0}^{N-1} \frac{1}{1-\frac{e^{i\alpha_j}}{z}} = \frac{1}{z^N} \prod_{j=0}^{N-1} \sum_{n_j=0}^{\infty} \frac{e^{i n_j \alpha_j}}{z^{n_j}} = \frac{1}{z^N} \sum_{n_0,n_1,\ldots,n_{N-1}\ge 0} \frac{e^{i\sum_{j=0}^{N-1} n_j \alpha_j}}{z^{\sum_{j=0}^{N-1} n_j}} \\ &= \frac{1}{z^N} \sum_{k=0}^{\infty} \frac{1}{z^k} \chi_k^{\mathrm{sym}}(W) \,. \end{aligned} \quad (5.74)$$

Similarly, for $|z| < 1$ we have

$$\frac{1}{\det(z-W)} = (-1)^N \sum_{k=0}^{\infty} z^k \chi_k^{\mathrm{sym}}(W^\dagger) \,. \quad (5.75)$$

Since the dimension and the value of the quadratic Casimir operator of the k-fold totally symmetric representation of SU(N) are given by [50]

$$d_k^{\mathrm{sym}} = \binom{N+k-1}{k} \,, \qquad C_2^{\mathrm{sym}}(k) = \left(1-\frac{1}{N}\right) k(N+k) \,, \quad (5.76)$$

averaging over W results in

$$\left\langle \chi_k^{\mathrm{sym}}(W) \right\rangle = \binom{N+k-1}{k} e^{-\frac{T}{2N}k(N+k)} \quad (5.77)$$

with $T = t\left(1-\frac{1}{N}\right)$. This leads to

$$\psi_{N,+}^{\mathrm{sym}}(z,T) = \sum_{k=0}^{\infty} \binom{N+k-1}{k} z^{-N-k} e^{-\frac{T}{2N}k(N+k)} \,, \quad (5.78)$$

$$\psi_{N,-}^{\mathrm{sym}}(z,T) = \sum_{k=0}^{\infty} \binom{N+k-1}{k} (-1)^N z^k e^{-\frac{T}{2N}k(N+k)} \,. \quad (5.79)$$

For $T > 0$, these infinite sums can be analytically extended to all z, except for $z = 0$ for $\psi_{N,+}^{\mathrm{sym}}$ and $z = \infty$ for $\psi_{N,-}^{\mathrm{sym}}$, cf. Ref. [47].

5.6.2 Integral representation

Similar to the antisymmetric case (cf. Eq. (5.55)), an integral representation for $\psi_{N,\pm}^{\mathrm{sym}}$ can be derived by separating the terms that are quadratic in k,

$$e^{-\frac{T}{2N}k(N+k)} = e^{\frac{NT}{8}} e^{-\frac{T}{2N}\left(k+\frac{N}{2}\right)^2} = e^{\frac{NT}{8}} \sqrt{\frac{N}{2\pi T}} \int_{-\infty}^{\infty} dx\, e^{-\frac{N}{2T}x^2 - i\left(k+\frac{N}{2}\right)x} \,. \quad (5.80)$$

Due to

$$\sum_{k=0}^{\infty} \binom{N+k-1}{k} z^{-N-k} = \frac{1}{(z-1)^N} \qquad \text{for } |z| > 1 \,, \quad (5.81)$$

which is just a special case of Eq. (5.74) with $W=\mathbf{1}$, we obtain for $T>0$ and $|z|>1$

$$\begin{aligned}\psi_{N,+}^{\rm sym}(z,T) &= e^{\frac{NT}{8}}\sqrt{\frac{N}{2\pi T}}\int_{-\infty}^{\infty} dx\, e^{-\frac{N}{2T}x^2-i\frac{N}{2}x}e^{iNx}\left(ze^{-ix}-1\right)^N \\ &= e^{\frac{NT}{8}}\sqrt{\frac{N}{2\pi T}}\int_{-\infty}^{\infty} dx\, e^{-\frac{N}{2T}x^2}\left(ze^{-i\frac{x}{2}}-e^{i\frac{x}{2}}\right)^N . \end{aligned} \tag{5.82}$$

It was pointed out in Ref. [47] that this formula exhibits a formal relation to $\langle\det(z-W)\rangle$ under a sign switch of N.

5.6.3 Symmetric resolvent and density

In analogy to the definition of the true resolvent $G_{N,\pm}^{\rm true}(z,t)$ (cf. Eq. (5.13)) and the antisymmetric resolvent $G_{N,\pm}^{\rm asym}(z,\tau)$ (cf. Eq. (5.36)), we now define the symmetric resolvent

$$G_{N,\pm}^{\rm sym}(z,T) = -\frac{1}{N}\frac{\partial}{\partial z}\log\left\langle\frac{1}{\det(z-W)}\right\rangle = -\frac{1}{N\psi_{N,\pm}^{\rm sym}(z,T)}\partial_z\psi_{N,\pm}^{\rm sym}(z,T) \tag{5.83}$$

and also introduce[10]

$$F_{N,\pm}^{\rm sym}(z,T) = zG_{N,\pm}^{\rm sym}(z,T)-\frac{1}{2} = -\frac{1}{N\psi_{N,\pm}^{\rm sym}(z,\tau)}\left(z\partial_z+\frac{N}{2}\right)\psi_{N,\pm}^{\rm sym}(z,\tau)\,. \tag{5.84}$$

Similar to the antisymmetric resolvent, the symmetric resolvent $G_N^{\rm sym}$ differs from the true resolvent only in the order of the logarithm and the expectation value (this is the motivation for the factor of -1 in the above definition of $G_N^{\rm sym}$). In the infinite-N limit, the three resolvents and the related densities become equivalent due to the infinite-N factorization of expectation values. This can be confirmed by performing saddle-point approximations of the integral representations of the resolvents (cf. below).

Due to the relation between $\psi_{N,+}^{\rm sym}$ and $\psi_{N,-}^{\rm sym}$ given in Eq. (5.72), we find (for $|z|>1$)

$$F_{N,-}^{\rm sym}\left(\frac{1}{z^*},T\right) = -F_{N,+}^{\rm sym}(z,T)^*\,. \tag{5.85}$$

This is the analogue of Eq. (5.39) for $F_N^{\rm asym}$ and Eq. (5.25) for $F_N^{\rm true}$. In complete analogy to the definitions of the densities $\rho_N^{\rm true}$ and $\rho_N^{\rm asym}$, we can therefore uniquely define

$$\begin{aligned}\rho_N^{\rm sym}(\theta,T) &= \lim_{\varepsilon\to0^+}\mathrm{Re}\left[2F_{N,+}^{\rm sym}(e^{i\theta+\varepsilon},T)\right] = \lim_{\varepsilon\to0^+}\mathrm{Re}\left[-2F_{N,-}^{\rm sym}(e^{i\theta-\varepsilon},T)\right] \\ &= \lim_{\varepsilon\to0^+}\left[F_{N,+}^{\rm sym}(e^{i\theta+\varepsilon},T)-F_{N,-}^{\rm sym}(e^{i\theta-\varepsilon},T)\right]. \end{aligned} \tag{5.86}$$

Unlike $\rho_N^{\rm asym}(\theta,\tau)$, $\rho_N^{\rm sym}(\theta,T)$ is a smooth function of θ for any finite N and $T>0$. It obeys $\rho_N^{\rm sym}(\theta,T)=\rho_N^{\rm sym}(-\theta,T)$ and is monotonic on each of the segments $(-\pi,0)$ and $(0,\pi)$ with the maximum at $\theta=0$ and the minimum at $\theta=\pm\pi$. The infinite-N critical point is at $T=4$. For $T>4$, $\rho_N^{\rm sym}(\theta,T)$ approaches $\rho_\infty(\theta,T)$ by power corrections in $1/N$ [47]. For $T<4$, $\rho_\infty(\theta,T)$ is zero for $|\theta|>\theta_c(T)$, where $0<\theta_c(T)<\pi$ and $\theta_c(4)=\pi$. In this interval, $\rho_N^{\rm sym}(\theta,T)$ approaches zero by corrections that are exponentially suppressed in N.

[10] The function $F_{N,\pm}^{\rm sym}(z,T)$ is related to the function $\phi_\pm^{(N)}(z,T)$ defined in Eq. (2.22) of Ref. [48] by $F=i\phi$.

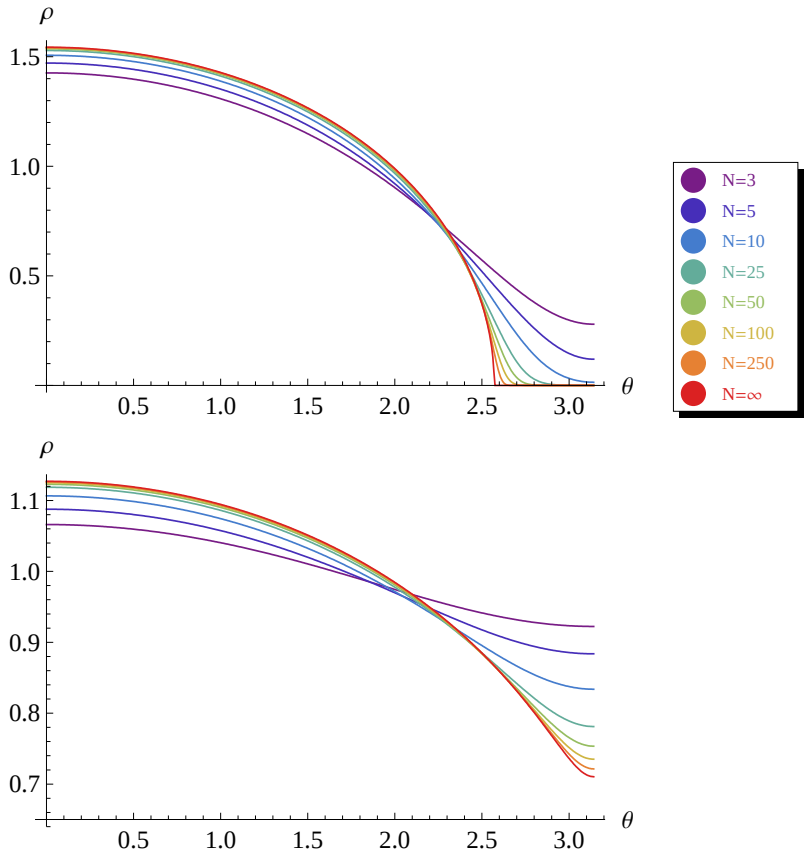

Figure 17: Plots of $\rho_N^{\mathrm{sym}}(\theta,T)$ for $T=2$ (top), $T=5$ (bottom) and $N=3,5,10,25,50,100,250$ together with $\rho_\infty(\theta,T)$.

Due to Eqs. (5.78) and (5.79), $\rho_N^{\mathrm{sym}}(\theta,T)$ has an explicit form in terms of rapidly converging infinite sums:

$$\lim_{\varepsilon\to 0^+} F_{N,+}^{\mathrm{sym}}(e^{i\theta+\varepsilon},T) = \frac{1}{2}+\frac{1}{N}p(\theta,T)\,, \tag{5.87}$$

$$\lim_{\varepsilon\to 0^+} F_{N,-}^{\mathrm{sym}}(e^{i\theta-\varepsilon},T) = -\frac{1}{2}-\frac{1}{N}p^*(\theta,T) \tag{5.88}$$

with

$$p(\theta,T)=\frac{\sum_{k=1}^\infty k\binom{N+k-1}{k}e^{-ik\theta}e^{-T\frac{k(k+N)}{2N}}}{1+\sum_{k=1}^\infty \binom{N+k-1}{k}e^{-ik\theta}e^{-T\frac{k(k+N)}{2N}}} \tag{5.89}$$

results in

$$\rho_N^{\mathrm{sym}}(\theta,T)=1+\frac{p(\theta,T)+p^*(\theta,T)}{N}\,. \tag{5.90}$$

Given $\rho_N^{\mathrm{sym}}(\theta,T)$ with $T>0$, we can reconstruct $F_{N,\pm}^{\mathrm{sym}}(z,T)$ and $\psi_{N,\pm}^{\mathrm{sym}}(z,T)$ on account of the analyticity of $F_{N,\pm}^{\mathrm{sym}}(z,T)$,

$$\int_{-\pi}^{\pi}\frac{d\alpha}{2\pi}\frac{\rho_N^{\mathrm{sym}}(\alpha,T)}{z-e^{i\alpha}}=\left(F_{N,\pm}^{\mathrm{sym}}(z,T)+\frac{1}{2}\right)\frac{1}{z}=G_{N,\pm}^{\mathrm{sym}}(z,T)\,, \tag{5.91}$$

in analogy to Eqs. (5.14) and (5.44).

Equation (5.89) can be evaluated numerically for arbitrary N to any desired precision. In Fig. 17, we show how $\rho_N^{\mathrm{sym}}(\theta, T)$ approaches the infinite-N result $\rho_\infty(\theta, T)$ of Durhuus and Olesen for fixed $T = 2$ and $T = 5$.

In addition to these numerical results, it would be useful to compute analytically the asymptotic expansion of $\rho_N^{\mathrm{sym}}(\theta, T)$ in powers of $1/N$. To achieve this, it is sufficient to expand $\psi_{N,+}^{\mathrm{sym}}(z, T)$ in $1/N$, which is best done by starting from Eq. (5.82). The $1/N$ expansion then comes from an expansion around a single saddle point. This problem will be considered in Sec. 7. The saddle points turn out to be related to the position of the boundary of the eigenvalue domain of the random multiplicative complex matrix ensemble studied in Refs. [3, 49], cf. also Sec. 11 below. In Sec. 9, we will show plots comparing $\rho_N^{\mathrm{sym}}(\theta, T)$ to $\rho_N^{\mathrm{true}}(\theta, t)$.

6 Motion of the zeros $z_j(\tau)$ as a function of τ

In this section, we only consider $\rho_N^{\text{asym}}(\theta,\tau)$ and study the zeros $z_j(\tau) = e^{i\theta_j(\tau)}$, $0 \le j \le N-1$, of the average characteristic polynomial, cf. Eq. (5.27), for small τ, large τ, and near the critical τ.

6.1 $\theta_j(\tau)$ for small τ

6.1.1 Approximate "equations of motion"

By using the expansion

$$\cot\left(\frac{z}{2}\right) = \sum_{n=-\infty}^{\infty} \frac{2}{z-2\pi n}\,, \tag{6.1}$$

we obtain from Eq. (5.66) that

$$\dot\theta_j(\tau) = \partial_\tau \theta_j(\tau) = \frac{1}{N}\sum_{k\neq j}\sum_{n\in\mathbb{Z}} \frac{1}{\theta_j(\tau)-\theta_k(\tau)+2\pi n}\,. \tag{6.2}$$

Rescaling the angles with $\sqrt{N}$, i.e.,

$$\theta_j(\tau) = \frac{\eta_j(\tau)}{\sqrt{N}}\,, \tag{6.3}$$

yields

$$\dot\eta_j(\tau) = \sum_{k\neq j}\sum_{n\in\mathbb{Z}} \frac{1}{\eta_j(\tau)-\eta_k(\tau)+2\pi n\sqrt{N}}\,. \tag{6.4}$$

The initial condition $\theta_j(\tau=0)=0$ indicates that one can neglect to leading order in τ the terms with $n\neq 0$, which leads to the approximate "equations of motion"

$$\dot\eta_j(\tau) \approx \sum_{k\neq j} \frac{1}{\eta_j(\tau)-\eta_k(\tau)}\,. \tag{6.5}$$

In this approximation, periodicity under $\theta_j \to \theta_j + 2\pi$ is lost, making the approximation unreliable when periodicity becomes relevant. This weak-coupling feature is characteristic for models that have compact variables and become disordered at strong couplings.

6.1.2 Solution of the approximate equations

Assigning dimension 1 to τ, we see that the variables $\eta_j(\tau)$ have dimension 1/2. Thus, defining

$$\eta_j(\tau) = \hat\eta_j\sqrt{2\tau} \tag{6.6}$$

makes the $\hat\eta_j$ variables dimensionless and therefore independent of τ. These variables are determined by the equations

$$\hat\eta_j = \sum_{k\neq j}\frac{1}{\hat\eta_j-\hat\eta_k}\,, \qquad 0\le j\le N-1\,. \tag{6.7}$$

The solution of these equations is well-known, see, e.g., Ref. [52, App. A.6]: The $\hat\eta_j$'s are the distinct zeros of the Hermite polynomial $H_N(x)$,

$$H_N(\hat\eta_j) = 0\,, \qquad j=0,\ldots,N-1\,. \tag{6.8}$$

6.1.3 Relation to harmonic oscillator

In the theory of orthogonal polynomials, the zeros of orthogonal polynomials are shown to be the eigenvalues of the Jacobi matrix, which is the appropriately truncated matrix of recurrence coefficients, cf. Ref. [53]. We introduce the matrix a_N, an N-truncated version of the infinite dimensional annihilation operator a, normalized by

$$[a, a^\dagger] = 1\,. \tag{6.9}$$

The truncation is to the space spanned by the harmonic oscillator states $(a^\dagger)^j|0\rangle$ with $j = 0, \ldots, N-1$,

$$a_N = \begin{pmatrix} 0 & \sqrt{1} & 0 & 0 & \cdots & 0 & 0 \\ 0 & 0 & \sqrt{2} & 0 & \cdots & 0 & 0 \\ \vdots & \vdots & \vdots & \vdots & \vdots & \vdots & 0 \\ 0 & 0 & 0 & 0 & \cdots & 0 & \sqrt{N-1} \\ 0 & 0 & 0 & 0 & \cdots & 0 & 0 \end{pmatrix}. \tag{6.10}$$

Then, the matrices a_N satisfy

$$[a_N, a_N^\dagger] = \mathbf{1}_N - N P_{N-1}\,, \tag{6.11}$$

where $P_n = |n\rangle\langle n|$.

Using the recurrence relations of the Hermite polynomials, the Jacobi matrix is found to be $\frac{1}{\sqrt{2}}(a_N + a_N^\dagger)$. Thus, to leading order in τ, the zeros of $\langle \det(z - W)\rangle$ are the same as the zeros of

$$\det\left(z - e^{i\sqrt{\frac{\tau}{N}}(a_N + a_N^\dagger)}\right). \tag{6.12}$$

6.1.4 Largest zeros

Of particular interest are the largest zeros in absolute magnitude. Due to the $\mathbb{Z}_2$ symmetry, cf. Eq. (5.69), they come in a pair of opposite signs. Using a known formula for large N, cf. Ref. [54], we have

$$\hat{\eta}_M = \sqrt{2N} - \frac{1.856}{(2N)^{1/6}} + \ldots\,, \tag{6.13}$$

giving the largest θ_j as

$$\theta_M(\tau) = 2\sqrt{\tau}\left(1 - \frac{1.856}{(2N)^{2/3}} + \ldots\right), \qquad M \equiv N - 1\,. \tag{6.14}$$

We now are in a position to estimate when τ cannot be considered to be small anymore and the approximation first breaks down.

If we set $j = M$ in Eq. (6.2) and choose k so that $\theta_k = -\theta_M$, we see that by keeping only the $n = 0$ term in the sum, we neglected, e.g., the potentially large term

$$\frac{1}{2\theta_M - 2\pi}\,. \tag{6.15}$$

Clearly, ignoring periodicity becomes unacceptable when $\theta_M = \pi$. Therefore, at $N \gg 1$ our small-τ approximation breaks down for

$$2\sqrt{\tau}\left(1 - \frac{1.856}{(2N)^{2/3}}\right) \approx \pi\,. \tag{6.16}$$

In conclusion, the small-τ approximation holds only for

$$\sqrt{\tau} \ll \frac{\pi}{2} \tag{6.17}$$

if $N \gg 1$ but extends further if N is not too large, cf. Fig. 18. Since we know that there is a transition at $\tau = 4$ for infinite N, we see that the small-τ approximation cannot take us all the way to the critical point for $N \gg 1$.

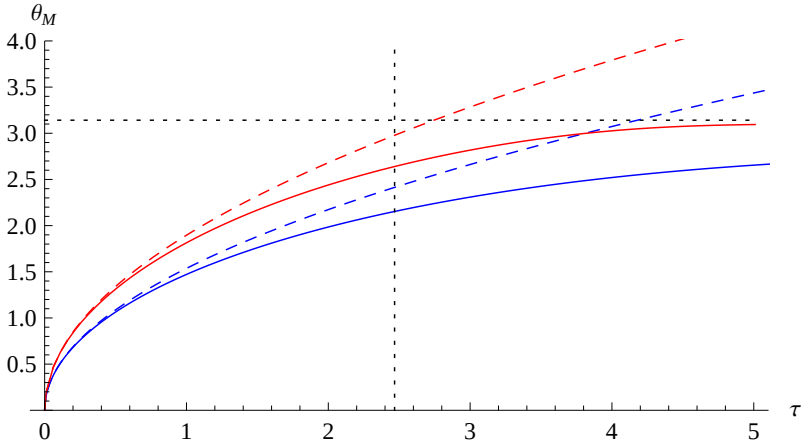

Figure 18: Plots of $\theta_M(\tau)$ as a function of τ for $N = 10$ (blue) and $N = 100$ (red). The solid curves show the exact location of θ_M (computed numerically by using the expansion in Eq. (5.35)), the dashed curves show the corresponding small-τ approximations obtained from Eqs. (6.6) and (6.8) (the largest zero of H_N is computed numerically). The dotted horizontal line corresponds to $\theta_M = \pi$, the dotted vertical line is located at $\tau = \frac{\pi^2}{4}$.

The most important conclusion is that the expansion in scale for small loops yields a spectrum restricted to a finite arc centered at zero angle and that the boundaries of the arc approach their infinite-N limits by a leading term of order $N^{-2/3}$. The same exponent occurs also in the Gaussian ensemble of Hermitian matrices and is connected to universal functions constructed out of Airy functions.

As the scale of the loop grows, the boundaries of the arc expand, until they meet each other at $\theta = \pm\pi$, at which point the small-scale expansion definitely breaks down and the exponent changes (cf. Sec. 6.3).

6.2 $\theta_j(\tau)$ for large τ

6.2.1 The eigenvalues at $\tau = \infty$

The eigenvalues expand away from zero until they stop at $\tau = \infty$, at which point they are equally spaced and contained in the interval $(-\pi, \pi)$. Throughout the expansion, they maintain the sum rule

$$\sum_{j=0}^{N-1} \theta_j(\tau) = 0\,. \tag{6.18}$$

Together with the $\mathbb{Z}_2$ pairing (5.69), this determines their asymptotic limits to be

$$\theta_j(\tau = \infty) = \frac{2\pi}{N}\left(j - \frac{N-1}{2}\right) \equiv \Theta_j\,, \qquad j = 0, \ldots, N-1\,. \tag{6.19}$$

We now prove that the above configuration is an equilibrium point of the equations of motion (5.66), i.e., that the τ-derivatives of the angles $\theta_j(\tau)$ vanish for $\theta_j(\tau) = \Theta_j$, $j = 0, \ldots, N-1$. Since the differential equations can be written as

$$\dot{\theta}_j(\tau) = -\frac{i}{2N} \sum_{k \neq j} \frac{1 + e^{i(\theta_j(\tau) - \theta_k(\tau))}}{1 - e^{i(\theta_j(\tau) - \theta_k(\tau))}}\,, \tag{6.20}$$

we need to show that for each $j = 0, \ldots, N-1$, we have

$$\sum_{k \neq j} \frac{1 + e^{i(\Theta_j - \Theta_k)}}{1 - e^{i(\Theta_j - \Theta_k)}} = 0\,. \tag{6.21}$$

Let us denote by q the N-th roots of unity. A sum over q runs over these N complex numbers. We need to show that

$$A = \sum_{q \neq 1} \frac{1+q}{1-q} = 0\,. \tag{6.22}$$

This would then imply Eq. (6.21) since $\Theta_j - \Theta_k = \frac{2\pi}{N}(j-k)$ and therefore

$$\sum_{k \neq j} f\left(e^{i(\Theta_j - \Theta_k)}\right) = \sum_{q \neq 1} f(q)\,. \tag{6.23}$$

The above equation already implies that the LHS of Eq. (6.21) is independent of j. Dividing by q the numerator and denominator of each term in the sum (6.22) and noticing that the restriction $q \neq 1$ is identical to the restriction $1/q \neq 1$ for the N-th roots of unity q, we get

$$A = \sum_{q \neq 1} \frac{1+q}{1-q} = \sum_{q \neq 1} \frac{q^{-1}+1}{q^{-1}-1} = \sum_{q \neq 1} \frac{q+1}{q-1} = -A = 0\,. \tag{6.24}$$

However, we shall soon need to evaluate other sums over q, and for these a more general procedure is needed. When applied to the present trivial case, this procedure goes as follows: We start from

$$A = \lim_{x \to 1^-} \left[\sum_q \left(\frac{1+xq}{1-xq} \right) - \frac{1+x}{1-x} \right]. \tag{6.25}$$

Next, expanding in a geometric series results in

$$A = \lim_{x \to 1^-} \left[\sum_q (1+xq) \sum_{n=0}^{\infty} x^n q^n - \frac{1+x}{1-x} \right] = \lim_{x \to 1^-} \left[-N + 2 \sum_{n=0}^{\infty} x^n \sum_q q^n - \frac{1+x}{1-x} \right]. \tag{6.26}$$

In order to evaluate $\sum_q q^n$, let us assume first that $e^{2\pi i \frac{n}{N}} \neq 1$. In this case,

$$\sum_q q^n = \sum_{j=0}^{N-1} e^{2\pi i \frac{j}{N} n} = \sum_{j=0}^{N-1} \left(e^{2\pi i \frac{n}{N}} \right)^j = \frac{e^{2\pi i \frac{n}{N} N} - 1}{e^{2\pi i \frac{n}{N}} - 1} = 0\,. \tag{6.27}$$

In the other case, $e^{2\pi i \frac{n}{N}} = 1$, we immediately obtain $\sum_q q^n = N$. Thus, we observe that $\sum_q q^n$ will be zero if n is not a multiple of N, and N otherwise, which results in

$$\begin{aligned} A &= \lim_{x\to 1^-}\left[-N + 2N\sum_{k=0}^{\infty} x^{kN} - \frac{1+x}{1-x}\right] = \lim_{x\to 1^-}\left[-N + \frac{2N}{1-x^N} - \frac{1+x}{1-x}\right] \\ &= \lim_{\varepsilon\to 0^+}\left[-N + \frac{2N}{1-(1-\varepsilon)^N} - \frac{2-\varepsilon}{\varepsilon}\right] = \lim_{\varepsilon\to 0^+}\left[-N + \left(\frac{2}{\varepsilon} + N - 1\right) - \frac{2-\varepsilon}{\varepsilon}\right] = 0\,. \end{aligned} \tag{6.28}$$

This again proves Eq. (6.21). Above, we needed $x < 1$ to perform the expansion in a geometric series, but at the end we can take $x \to 1$. Similar techniques work for all other sums over q that we shall need in the following.

6.2.2 Linearization of the large-τ equation

We now expand around the infinite-τ solution, to see how it is approached. From the exact formula (5.35) for $\langle \det(z - W)\rangle$, we expect the approach to be exponentially rapid with decay constants given by the Casimirs of the antisymmetric representations labeled by k, where $k = 1, \ldots, N-1$. This is $N-1$ non-zero values, not N. The missing value corresponds to a uniform τ-independent shift in all $\theta_j(\tau)$, which is a symmetry of the differential equation. This symmetry would produce a zero mode in the linearized equation, but the mode is eliminated by the sum rule (6.18), which depends also on the initial condition.

To linearize, we set

$$\theta_j(\tau) = \Theta_j + \delta\theta_j(\tau) \tag{6.29}$$

and expand the equation of motion to linear order in $\delta\theta_j(\tau)$. Unlike the initial condition at $\tau = 0$, the set $\{\Theta_j\}$ provides a non-degenerate configuration around which it is straightforward to expand. We find

$$\begin{aligned} \delta\dot{\theta}_j(\tau) &= \frac{1}{2N}\sum_{k\neq j}\cot\left(\frac{\Theta_j - \Theta_k}{2} + \frac{\delta\theta_j(\tau) - \delta\theta_k(\tau)}{2}\right) \\ &= -\frac{1}{4N}\sum_{k\neq j}\frac{1}{\sin^2\left(\frac{\Theta_j-\Theta_k}{2}\right)}\left(\delta\theta_j(\tau) - \delta\theta_k(\tau)\right) + \mathcal{O}\left(\delta\theta^2\right)\,, \end{aligned} \tag{6.30}$$

which can be written as

$$\delta\dot{\theta}_j(\tau) = -\frac{1}{4N}\sum_{k=0}^{N-1} A_{jk}\delta\theta_k(\tau) \tag{6.31}$$

with the matrix A given by

$$A_{jk} = \begin{cases} -\frac{1}{\sin^2\left(\frac{\Theta_j-\Theta_k}{2}\right)} & \text{for } k \neq j\,, \\ \sum\limits_{l\neq j}\frac{1}{\sin^2\left(\frac{\Theta_j-\Theta_l}{2}\right)} & \text{for } k = j\,. \end{cases} \tag{6.32}$$

We need to find the eigenvalues and eigenvectors of this matrix. Note first that A_{jj} does not depend on j and is given by

$$A_{jj} = 4\sum_{q\neq 1}\frac{1}{(1-q)(1-q^{-1})}\,. \tag{6.33}$$

The sum over q can be performed as before. We start from

$$\begin{aligned} A_{jj} &= 4 \lim_{x\to 1^-} \left[\sum_q \frac{xq}{(1-xq)(xq-1)} + \frac{x}{1-x^2} \right] \\ &= 4 \lim_{x\to 1^-} \left[\sum_q (-xq) \sum_{j=0}^{\infty} \sum_{k=0}^{\infty} (xq)^{j+k} + \frac{x}{1-x^2} \right] , \end{aligned} \tag{6.34}$$

then, performing the sum over q leads to

$$A_{jj} = 4 \lim_{x\to 1^-} \left[-N^2 \frac{x^N}{(1-x^N)^2} + \frac{x}{(1-x)^2} \right] = \frac{N^2-1}{3} . \tag{6.35}$$

Hence, the matrix A is a so-called circulant matrix, i.e., it has entries A_{ij} which only depend on $(i-j) \bmod N$. Therefore, A has N eigenvectors $\phi^{(l)}$ with components $\phi^{(l)}_k$, $k, l = 0, \ldots, N-1$, given by

$$\phi^{(l)}_k = \frac{1}{\sqrt{N}} e^{-i\frac{\pi l(N-1)}{N}} e^{i\frac{2\pi l}{N}k} . \tag{6.36}$$

The phases are chosen for later convenience. In order to compute the eigenvalues of A, we have to evaluate the action of A on an eigenvector $\phi^{(l)}$,

$$\begin{aligned} \sum_{k=0}^{N-1} A_{jk} \phi^{(l)}_k &= \frac{e^{-i\frac{\pi l(N-1)}{N}}}{\sqrt{N}} \left(e^{i\frac{2\pi l}{N}j} \frac{N^2-1}{3} - \sum_{k\neq j} \frac{\left(e^{i\frac{2\pi k}{N}}\right)^l}{\sin^2\left(\frac{\pi}{N}(j-k)\right)} \right) \\ &= \phi^{(l)}_j \left(\frac{N^2-1}{3} - 4 \sum_{q\neq 1} \frac{q^l}{(1-q)(1-q^{-1})} \right) , \end{aligned} \tag{6.37}$$

where the sum over q runs again over the N-th roots of unity with $q = 1$ excluded. The sum

$$\xi^{(l)} = -4 \sum_{q\neq 1} \frac{q^l}{(1-q)(1-q^{-1})} \tag{6.38}$$

is performed as before, which results in

$$\xi^{(l)} = -4 \lim_{x\to 1^-} \left(lN \frac{x^N}{1-x^N} - N^2 \frac{x^N}{(1-x^N)^2} + \frac{x^{l+1}}{(1-x)^2} \right) = -\frac{N^2-1}{3} + 2l(N-l) , \tag{6.39}$$

leading to

$$\sum_{k=0}^{N-1} A_{jk} \phi^{(l)}_k = \lambda^{(l)} \phi^{(l)}_j \qquad \text{with} \qquad \lambda^{(l)} = 2l(N-l) . \tag{6.40}$$

Thus, the eigenvalue of A corresponding to the l-th eigenvector $\phi^{(l)}$ is $\lambda^{(l)} = 2l(N-l)$. Obviously, $l = 0$ corresponds to the zero mode which does not contribute to the $\delta\theta_j$, so we are left with $N-1$ contributing modes, labeled by $l = 1, \ldots, N-1$. As expected, the eigenvalues of A come out proportional to the quadratic Casimirs in the l-fold antisymmetric representation, given by

$$C_2^{\text{asym}}(l) = \frac{N+1}{N} l(N-l) . \tag{6.41}$$

The equations of motion (5.66) have the values of the Casimirs encoded in them.

We have found that the solution of the linearized equation of motion (6.31), obeying the initial condition $\delta\theta_k(\tau \to \infty) = 0$, is given by

$$\delta\theta_k(\tau) = \sum_{l=1}^{N-1} c_l \phi_k^{(l)} e^{-\frac{\tau}{2N} l(N-l)} \,. \tag{6.42}$$

It remains to determine the coefficients c_l. Since the leading asymptotic terms at large τ correspond to $l = 1$ and $l = N-1$, we only need c_1 and c_{N-1}.

6.2.3 Constraints on the coefficients

The coefficients c_l are restricted by two quite trivial exact general properties which imply for the $\delta\theta_k(\tau)$ that (cf. Eq. (5.69))

$$\delta\theta_k(\tau) = \delta\theta_k^*(\tau) \,, \qquad \delta\theta_k(\tau) = -\delta\theta_{N-k-1}(\tau) \,. \tag{6.43}$$

These constraints lead to

$$\delta\theta_k(\tau) = \sum_{l=1}^{N-1} \rho_l \sin\left[\frac{2\pi l}{N}(k+1/2)\right] e^{-\frac{\tau}{2N} l(N-l)} \tag{6.44}$$

with real ρ_l and

$$\rho_l = \rho_{N-l} \,. \tag{6.45}$$

Every term in the sum representing $\delta\theta_k(\tau)$ is invariant under $l \to N-l$.

6.2.4 Leading asymptotic behavior

Note first that we have

$$\langle \mathrm{Tr}\, W \rangle = \sum_{j=0}^{N-1} e^{i\theta_j(\tau)} \,, \tag{6.46}$$

which follows from the general result for $\langle \chi_k^{\mathrm{asym}}(W) \rangle$, given in Eq. (5.31), by setting $k = 1$. This is the term proportional to z^{N-1} in the expansion of $\langle \det(z - W) \rangle$ in powers of z.

For the leading asymptotic behavior of the $\theta_k(\tau)$, we only need ρ_1. We can obtain ρ_1 from the exact result

$$\frac{1}{N} \langle \mathrm{Tr}\, W \rangle = e^{-\frac{\tau}{2N}(N-1)} \,, \tag{6.47}$$

which is just Eq. (5.34) for $k = 1$.

Actually, we only need this result at leading order as $\tau \to \infty$. To linear order in $\delta\theta_k$, we get from Eq. (6.46)

$$\langle \mathrm{Tr}\, W \rangle = \sum_{j=0}^{N-1} e^{i(\Theta_j + \delta\theta_j(\tau))} = \sum_{j=0}^{N-1} e^{i\Theta_j} \left(1 + i\delta\theta_j(\tau)\right) = i \sum_{j=0}^{N-1} e^{i\Theta_j} \delta\theta_j(\tau) \tag{6.48}$$

due to $\sum_{j=0}^{N-1} e^{i\Theta_j} = 0$. Keeping only the terms with $l = 0$ and $l = N-1$ in Eq. (6.44) results in

$$\frac{1}{N} \langle \mathrm{Tr}\, W \rangle = -\frac{2i}{N} \rho_1 \sum_{k=0}^{N-1} e^{\frac{2\pi i}{N}(k+1/2)} \sin\left[\frac{2\pi}{N}(k+1/2)\right] e^{-\frac{\tau}{2N}(N-1)} \,. \tag{6.49}$$

Performing the trivial sum over k,

$$\sum_{k=0}^{N-1} e^{\frac{2\pi i}{N}(k+1/2)} \sin\left[\frac{2\pi}{N}(k+1/2)\right] = -\frac{i}{2}\sum_{k=0}^{N-1}\left(e^{\frac{2\pi i}{N}(2k+1)} - 1\right) = \frac{iN}{2}\,, \tag{6.50}$$

we get

$$\frac{1}{N}\langle \mathrm{Tr}\, W\rangle = \rho_1 e^{-\frac{\tau}{2N}(N-1)} \tag{6.51}$$

and therefore, by comparison with Eq. (6.47),

$$\rho_1 = 1\,. \tag{6.52}$$

Hence, as $\tau \to \infty$, we have

$$\delta\theta_k(\tau) \approx 2\sin\left[\frac{2\pi}{N}(k+1/2)\right] e^{-\frac{\tau}{2N}(N-1)} \tag{6.53}$$

or, more completely,

$$\theta_k(\tau) \approx \frac{\pi}{N}(2k+1-N) + 2\sin\left[\frac{2\pi}{N}(k+1/2)\right] e^{-\frac{\tau}{2N}(N-1)}\,. \tag{6.54}$$

Equivalently, we can write

$$\theta_k(\tau) \approx \Theta_k - 2e^{-\frac{\tau}{2N}(N-1)}\sin(\Theta_k)\,. \tag{6.55}$$

For Θ_k negative, the correction is positive, and for Θ_k positive, the correction is negative. This shows that for increasing τ, each eigenvalue is distancing itself from the origin for all k as expected. The correction is largest for eigenvalues in the middle of the upper and lower half of the circle – the eigenvalues here are the last to settle into their infinite-τ destinations, cf. Fig. 19.

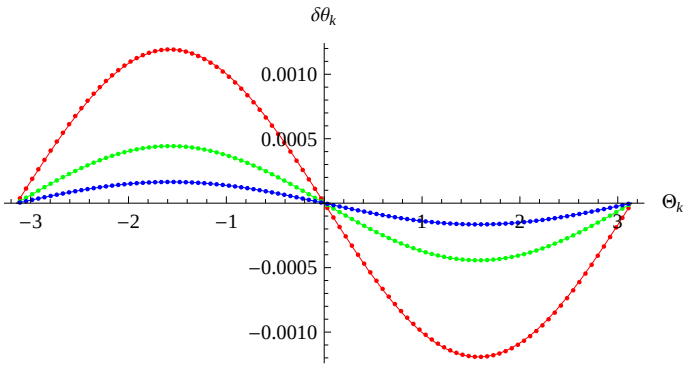

Figure 19: Plots of $\delta\theta_k$ as a function of Θ_k for $N = 100$ and $\tau = 15$ (red), $\tau = 17$ (green), and $\tau = 19$ (blue). The N dots show numerical results, the solid curves are obtained from the corresponding large-τ approximation given by Eq. (6.55).

The large-τ approximation for the extremal zero reads

$$\theta_M(\tau) \approx \pi\left(1 - \frac{1}{N}\right) - 2e^{-\frac{\tau}{2N}(N-1)}\sin\left(\pi\left(1-\frac{1}{N}\right)\right)\,. \tag{6.56}$$

Figure 20 shows a plot of the exact result for $\theta_M(\tau)$ (computed numerically) together with the approximations for small and large τ for $N = 10$.

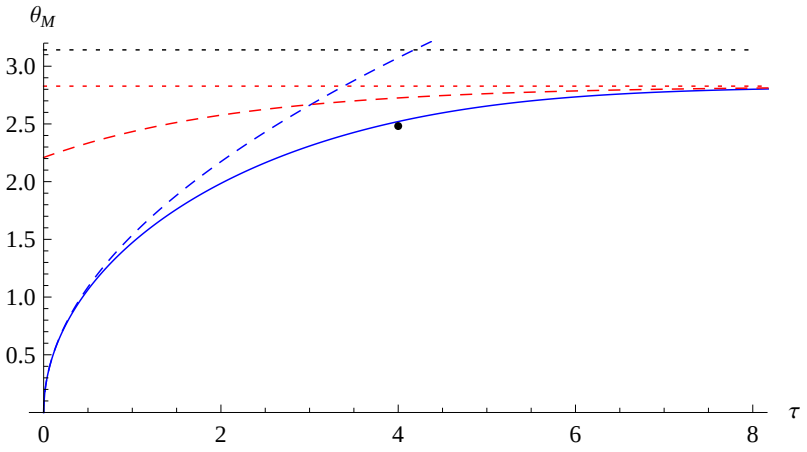

Figure 20: Plot of the numerical result for $\theta_M(\tau)$ for $N = 10$ (solid blue curve) together with the small-τ approximation (blue dashed curve) and the large-τ approximation (red dashed curve). The horizontal red dotted line indicates the infinite-τ location $\Theta_M = \pi\left(1 - \frac{1}{N}\right)$, the horizontal black dotted line is located at $\theta = \pi$. The black dot at $\tau = 4$ shows the result of the critical-τ approximation (6.65) for $N = 10$.

6.3 Extremal $\theta_j(\tau)$ for $\tau \approx 4$ and large N

6.3.1 Universal zeros

In terms of the variable y introduced in Sec. 5.5.3, the zeros corresponding to the angles $\theta_j(\tau)$ mod 2π are determined by

$$\tilde{\psi}^{\text{asym}}_{N,\pm}\left(i(\theta_j(\tau) - \pi), \tau\right) = 0 \tag{6.57}$$

with $\tilde{\psi}^{\text{asym}}_{N,\pm}(y,\tau)$ defined in Eq. (5.48).

At $\tau = 4$, we obtain from the integral representation (5.56) that

$$\tilde{\psi}^{\text{asym}}_{N,\pm}(y,4) = \int_{-\infty}^{\infty} dx\, e^{-\frac{N}{8}(x-y)^2} e^{N\log(2\cosh(x/2))}\,. \tag{6.58}$$

We have seen that the universal form of $\tilde{\psi}^{\text{asym}}_{N,\pm}(y,\tau)$ for large N, $y \approx 0$, and $\tau \approx 4$ is obtained by replacing the $\log(2\cosh(x/2))$ above by its expansion truncated at order x^4, cf. Eq. (5.57),

$$\log\left(\cosh\frac{x}{2}\right) = \frac{x^2}{8} - \frac{x^4}{192}\,. \tag{6.59}$$

Therefore, the "universal zeros" y_*^j are defined by

$$\int_{-\infty}^{\infty} dx\, e^{-\frac{N}{192}(x^4 - 48xy_*^j)} = 0\,. \tag{6.60}$$

6.3.2 Universal numerical values

Zeros of Eq. (6.60) have been investigated in Ref. [55]. If we define

$$\frac{Nx^4}{192} = \mu u^4\,, \qquad \frac{Nxy_*^j}{4} = 4i\mu u\,, \tag{6.61}$$

then

$$y_*^k = \pm i \frac{4\sqrt{2}}{3} \left(\frac{3\mu_k}{N} \right)^{3/4} , \tag{6.62}$$

where the μ_k's ($k = 1, 2, \ldots$) are the zeros of

$$F(\mu) = \int du\, e^{\mu(4iu - u^4)} . \tag{6.63}$$

From Table 1 of Ref. [55], we have the numerical approximations $\mu_1 \approx 0.8221$, $\mu_2 \approx 2.0227$, etc. Various other results concerning the μ_k can be found in Ref. [55]. For the extremal positive zero at $\tau = 4$, we need to look at y_*^1,

$$y_*^1 \approx i \frac{3.711}{N^{3/4}} . \tag{6.64}$$

This gives, for large N, that the zero $z_j(\tau_c)$ (with $\mathrm{Im}\, z_j > 0$) that is closest to -1 is

$$z_M \approx e^{i(\pi - 3.711 N^{-3/4})} . \tag{6.65}$$

The approximation for $\theta_M(4)$ is plotted in Fig. 20 for $N = 10$, together with the approximations for small and large τ. Figure 21 shows a plot of $\theta_M(\tau = 4)$ as a function of N.

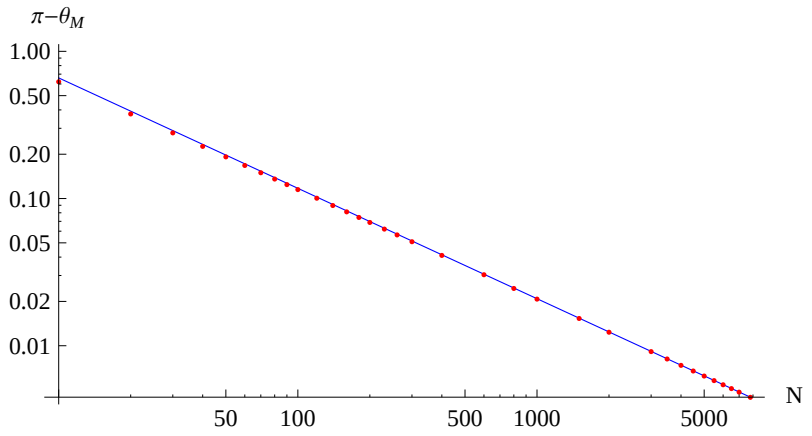

Figure 21: Double-logarithmic plot of $\pi - \theta_M(4)$ as a function of N, between $N = 10$ and $N = 8000$. The red dots show numerical results, which are in good agreement with the critical-τ approximation (blue line) obtained from Eq. (6.65). Furthermore, the numerical results confirm the expectation that the difference between the exact location and the approximation goes as $N^{-\frac{5}{4}}$ (the numerical value of the coefficient of this next order correction is found to be about 0.70).

6.3.3 Double scaling limit

In Eq. (6.58) we have set $\tau = 4$. Alternatively, we can also scale τ with N in the vicinity of the critical point as in Sec. 5.5.3 , according to

$$\tau = \frac{4}{1 + \frac{\alpha}{\sqrt{3N}}} . \tag{6.66}$$

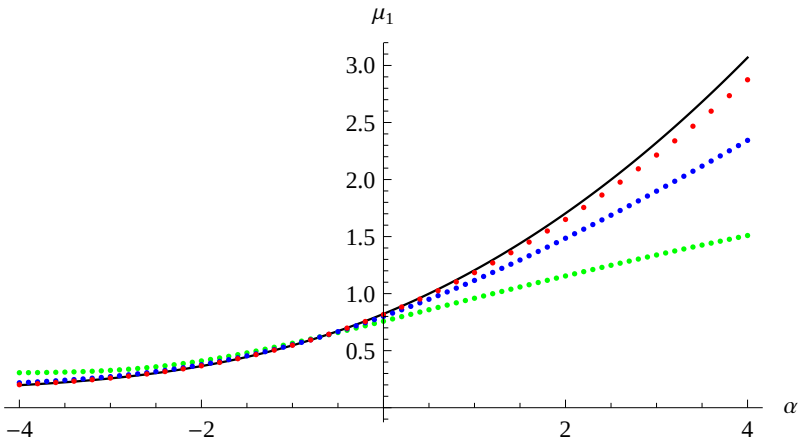

Figure 22: Plots of $\mu_1(\alpha)$, obtained by computing the LHS of Eq. (6.68) numerically at finite N, for $N = 10$ (green dots), $N = 100$ (blue dots), and $N = 2000$ (red dots). The black curve shows the expected result at infinite N, following from Eq. (6.67). We observe that the convergence to the infinite-N limit becomes slower with increasing α.

Then, the leading asymptotic behavior of the zeros y_*^k is again given by Eq. (6.62) if we replace μ_k by $\mu_k(\alpha)$, which are defined to be the zeros of

$$F_\alpha(\mu) = \int du\, e^{\mu\left(4iu - u^4 - \frac{\alpha}{\sqrt{\mu}}u^2\right)} \tag{6.67}$$

with $\mu_k(\alpha = 0) = \mu_k$. Therefore, we obtain for the extremal angle $\theta_M(\tau)$ that

$$\lim_{N\to\infty} \frac{N}{3}\left[\frac{3}{4\sqrt{2}}\left[\pi - \theta_M\left(\tau = \frac{4}{1 + \frac{\alpha}{\sqrt{3N}}}\right)\right]\right]^{\frac{4}{3}} = \mu_1(\alpha) \tag{6.68}$$

with $\mu_1(\alpha = 0) \approx 0.8221$. See Fig. 22 for a plot of $\mu_1(\alpha)$ in the range $-4 \le \alpha \le 4$.

7 Asymptotic expansion of $\rho_N^{\mathrm{sym}}(\theta, T)$

The aim of this section is to construct an asymptotic expansion of $\rho_N^{\mathrm{sym}}(\theta, T)$ in powers of $1/N$. To this end, we perform a saddle-point analysis[11] of the integral in Eq. (5.82), from which $\rho_N^{\mathrm{sym}}(\theta, T)$ can be obtained via Eqs. (5.84) and (5.86). It is sufficient to study only $\psi_{N,+}^{\mathrm{sym}}(z, T)$ because $\psi_{N,-}^{\mathrm{sym}}(z, T)$ can be obtained from Eq. (5.72) once $\psi_{N,+}^{\mathrm{sym}}(z, T)$ is known.

7.1 Saddle-point analysis

For $|z| = 1$, the integrand of Eq. (5.82) has singularities on the real-u axis. We therefore set $z = e^{\varepsilon + i\theta}$, where $\varepsilon > 0$ ensures that $|z| > 1$ but will later be taken to zero. The integrand of Eq. (5.82) can be written as $\exp(-Nf(u, z))$ with

$$f(u, z) = \frac{u^2}{2T} + \log\left(ze^{-i\frac{u}{2}} - e^{i\frac{u}{2}}\right). \tag{7.1}$$

We now look for saddle points of the integrand in the complex-u plane, which we label by $\bar{u} = iTU(\theta, T)$, where $U(\theta, T) = U_r(\theta, T) + iU_i(\theta, T)$ is a complex-valued function of θ and T (of course U depends also on ε as long as we keep $\varepsilon > 0$). In the following, the explicit z-dependence of $f(u, z)$ is often suppressed to simplify the notation, we simply write $f(u) \equiv f(u, z)$. Due to

$$f'(u) \equiv \partial_u f(u, z) = \frac{u}{T} - \frac{i}{2}\,\frac{ze^{-iu} + 1}{ze^{-iu} - 1}\,, \tag{7.2}$$

the saddle-point equation, $f'(iTU) = 0$, turns out to be

$$e^{-TU(\theta,T)}\frac{U(\theta, T) + 1/2}{U(\theta, T) - 1/2} = z = e^{\varepsilon + i\theta}\,. \tag{7.3}$$

For $\varepsilon = 0$, this is Eq. (5.49) in Ref. [49] and is related to the inviscid complex Burgers equation via Eq. (5.44) therein (cf. also Sec. 11.4.3 below). In the present notation, the latter equation has the form

$$\frac{\partial U}{\partial T} + iU\frac{\partial U}{\partial \theta} = 0\,. \tag{7.4}$$

We will show in Sec. 7.2 that the dominating saddle point $U(\theta, T)$ directly determines the infinite-N limit of the density $\rho_N^{\mathrm{sym}}(\theta, T)$. In Sec. 4.4, we have seen that the Durhuus-Olesen result for $\rho_\infty(\theta, t)$ is obtained by solving the inviscid complex Burgers equation (4.72), which is equivalent to Eq. (7.4) (up to factors of i). This already indicates that indeed $\lim_{N\to\infty} \rho_N^{\mathrm{sym}} = \rho_\infty$ as expected, cf. Sec. 7.2.

Taking the absolute value of Eq. (7.3) leads to the equation (for $U_r \neq 0$)

$$U_i^2 = U_r \coth(TU_r + \varepsilon) - U_r^2 - \frac{1}{4}\,. \tag{7.5}$$

For $\varepsilon = 0$, this equation has been investigated also in Ref. [49], cf. Sec. 11.4.3 below. Equation (7.5) describes one or more curves in the complex-U plane on which the saddle points have to lie (for a given value of θ, the saddles are isolated points on these curves).

As long as we keep $\varepsilon > 0$, there are no solutions of Eq. (7.3) with $U_r = 0$. When we set $\varepsilon = 0$, we can expand the RHS of Eq. (7.5) in U_r and obtain at leading order $U_i^2 = 1/T - 1/4$ (cf. also Eq. (11.52) below), which admits real solutions for $T < 4$. These are the points where the curves of solutions intersect the imaginary axis (for $\varepsilon = 0$ and

[11] See App. C for a general description of the saddle-point method.

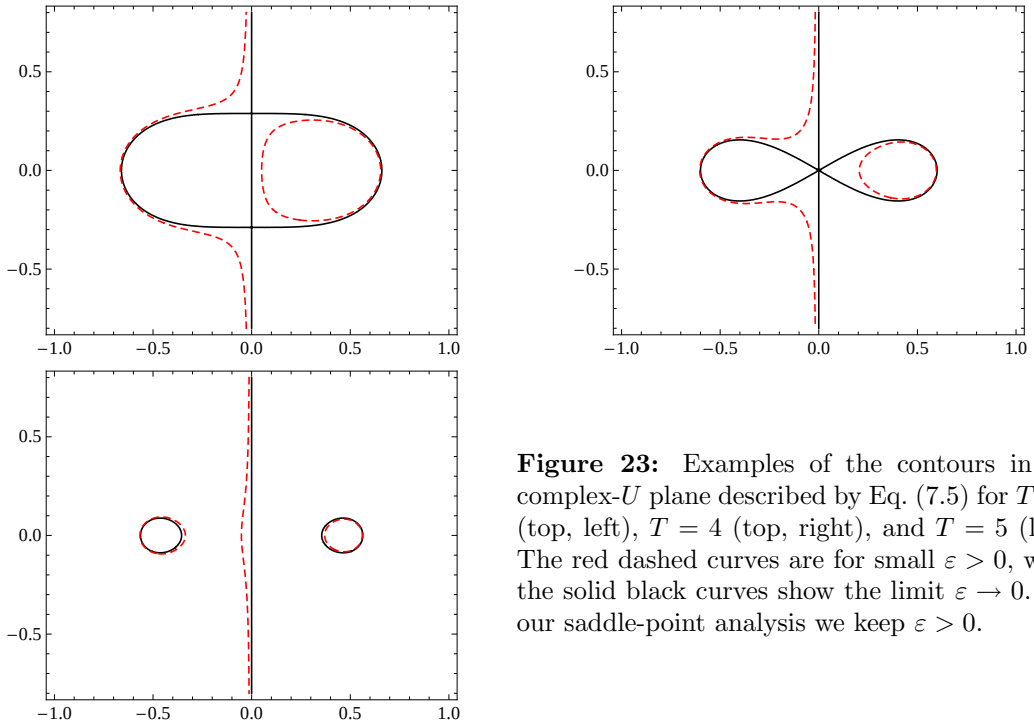

Figure 23: Examples of the contours in the complex-U plane described by Eq. (7.5) for $T = 3$ (top, left), $T = 4$ (top, right), and $T = 5$ (left). The red dashed curves are for small $\varepsilon > 0$, while the solid black curves show the limit $\varepsilon \to 0$. For our saddle-point analysis we keep $\varepsilon > 0$.

$T < 4$). There are no such intersections for $T > 4$. However, when we set $U_r = 0$, the absolute value of the LHS of Eq. (7.3) is equal to one, which means that every point on the imaginary axis provides a solution for some value of θ if we set $\varepsilon = 0$ (see Fig. 23 for some plots).

Here, we keep $\varepsilon > 0$ for the time being. The singularities of the integrand of Eq. (5.82) then all have $U_r < 0$ (they are located between the imaginary axis and those curves of solutions of Eq. (7.5) which are located in the half-plane $U_r < 0$).

In Fig. 23, we show typical examples for the curves described by Eq. (7.5) for $T < 4$, $T = 4$, and $T > 4$, where ε has been chosen sufficiently close to zero. The closed contours always enclose the points $U = 1/2$ or $U = -1/2$. For $T > 4$ and larger ε, the closed contour in the left half-plane would be missing, but right now we are not concerned with this since we are only interested in the limit $\varepsilon \to 0^+$.

Clearly, every solution $U(\theta, T)$ of Eq. (7.3) has to fulfill Eq. (7.5) by construction. On the other hand, every solution of Eq. (7.5) leads to a solution of Eq. (7.3) for one unique value of θ with $-\pi < \theta \leq \pi$ (for a given solution $U_r + iU_i$ of Eq. (7.5), this value of θ is obtained simply by evaluating the LHS of Eq. (7.3)). Analyzing Eq. (7.3) numerically, we find for all values of T that for a given value of θ there is always one (and only one) saddle point on the closed contour in the right half-plane, i.e., with $U_r > 0$. This means that there is a one-to-one mapping from θ (with $-\pi < \theta \leq \pi$) to saddle points on this closed contour, cf. Fig. 24.

Note that we are showing the complex-U plane in Fig. 23, in which the original integration contour corresponds to the imaginary axis. The integration contour can be smoothly deformed to go through the (single) saddle point in the right half-plane along a path of steepest descent. No singularities are crossed since they all have $U_r < 0$. There are also saddle points on the contour(s) in the left half-plane (in fact, there are infinitely many on the open contour), but these need not to be considered. Figure 25 shows an example for the location of the saddle points and the deformation of the integration contour in the

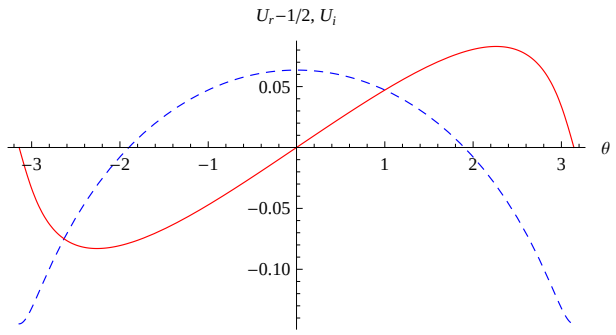

Figure 24: Plot of the solution $U(\theta, T)$ of Eq. (7.3) which is located on the closed contour in the right half plane as a function of θ for $T = 5$ and $\varepsilon = 0$. The dashed blue curve shows $U_r(\theta, 5) - \frac{1}{2}$, the red curve shows $U_i(\theta, 5)$.

complex-u plane.

Once the integration contour has been deformed to go through the saddle point, we can safely take the limit $\varepsilon \to 0^+$. Parametrizing the contour in the vicinity of the saddle point by $u = \bar{u} + xe^{i\beta}$, where x is the new integration variable corresponding to the fluctuations around the saddle and β is the angle which the path of steepest descent makes with the real-u axis, $\psi^{\text{sym}}_{N,+}(e^{i\theta}, T)$ is given, up to exponentially small corrections in N, by

$$\psi^{\text{sym}}_{N,+}(e^{i\theta}, T) = \frac{1}{2^N}\sqrt{\frac{N}{2\pi T}}\, e^{\frac{NT}{8} - i\frac{N\theta}{2} + i\beta} \int_{-\infty}^{\infty} dx\, e^{-Ng(x)}\,, \tag{7.6}$$

$$g(x) = \frac{1}{2T}\big(xe^{i\beta} + iTU(\theta, T)\big)^2 + \log\sinh\frac{i\theta - ixe^{i\beta} + TU(\theta, T)}{2}\,. \tag{7.7}$$

We can now expand $g(x)$ in x. The linear order vanishes by construction, the second order gives a Gaussian integral over x, resulting in

$$\psi^{\text{sym}}_{N,+}(e^{i\theta}, T) \approx e^{\frac{NT}{8} + \frac{NTU^2(\theta,T)}{2}} \frac{\big[e^{-i\theta}(1/4 - U^2(\theta, T))\big]^{N/2}}{\sqrt{1 - T(1/4 - U^2(\theta, T))}}\,. \tag{7.8}$$

Note that the factor $e^{-i\theta}$ cannot be pulled out of the term in square brackets because periodicity in θ would be lost.

There is a potential complication. In principle, $g''(0)$ and therefore the denominator in Eq. (7.8) could be zero, which would mean that the integral over x cannot be performed in Gaussian approximation. For $T > 4$, it is straightforward to show that $g''(0)$ is never zero. For $T \leq 4$, one can use Eq. (7.3) to show that $g''(0) = 0$ only for the saddle points corresponding to the two angles $\theta = \pm\theta_c(T)$ at which the transition from zero to non-zero

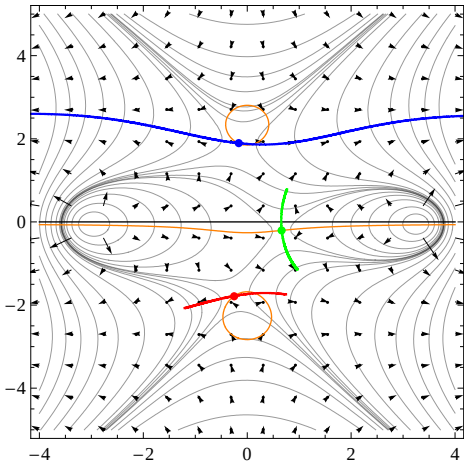

Figure 25: Example for the location of the saddle points and the deformation of the integration contour in the complex-u plane for $T = 5$ and $\theta = 3$ (with small $\varepsilon > 0$). The thin solid lines are lines of constant $\mathrm{Re}\, f(u)$, the arrows point in the direction of increasing $\mathrm{Re}\, f(u)$. On each of the closed orange curves there is one saddle point (red dot and blue dot), and on the open orange curve there are infinitely many saddle points but only one of them in the region shown in the plot (green dot). The thick blue curve is the integration path along the direction of steepest descent through the relevant saddle point.

$\rho_\infty(\theta,T)$ occurs (see Sec. 5.6). This means that the asymptotic expansion in $1/N$ diverges for $|\theta| = \theta_c(T)$, and that it converges ever more slowly as $|\theta| \to \theta_c$ from below.

Note that for $T < 4$ and $\theta_c(T) \le |\theta| \le \pi$, the function $\rho_N^{\mathrm{sym}}(\theta,T)$ is exponentially suppressed in N. The study of the large-N asymptotic behavior in this region requires more work.

7.2 Leading-order result

Equation (7.8) is the leading order in the $1/N$ expansion of $\psi_{N,+}^{\mathrm{sym}}(e^{i\theta},T)$. We now show that it leads to $\rho_N^{\mathrm{sym}}(\theta,T) \to \rho_\infty(\theta,T)$ as $N \to \infty$. We first write Eq. (7.8) in the form

$$\frac{1}{N}\log\psi_{N,+}^{\mathrm{sym}}(z,T) = \frac{T}{8} - f(\bar u(z),z) + \mathcal{O}(1/N) \tag{7.9}$$

with $z = e^{i\theta}$. Note that in this order we do not need the denominator in Eq. (7.8), which corresponds to $g''(0)$ or $f''(\bar u) \equiv \partial_u^2 f(u,z)|_{u=\bar u(z)}$. By construction, we have $f'(\bar u) \equiv \partial_u f(u,z)|_{u=\bar u(z)} = 0$, which results in

$$\begin{aligned} G_{N,+}^{\mathrm{sym}}(z,T) &= -\frac{1}{N}\partial_z \log\psi_{N,+}^{\mathrm{sym}}(z,T) = \partial_u f(u,z)|_{u=\bar u(z)}\partial_z\bar u(z) + \partial_z f(u,z)|_{u=\bar u(z)} + \mathcal{O}(1/N) \\ &= \partial_z f(u,z)|_{u=\bar u(z)} + \mathcal{O}(1/N) = \frac{1}{z - e^{i\bar u(z)}} + \mathcal{O}(1/N)\,. \end{aligned} \tag{7.10}$$

Using $\bar u = iTU$ and the saddle-point equation (7.3), this leads to

$$G_{N,+}^{\mathrm{sym}}(z=e^{i\theta},T) = \frac{1}{e^{i\theta} - e^{-TU(\theta,T)}} + \mathcal{O}(1/N) = \frac{1}{e^{i\theta}}\left(U(\theta,T) + \frac{1}{2}\right) + \mathcal{O}(1/N)\,, \tag{7.11}$$

$$F_{N,+}^{\mathrm{sym}}(z=e^{i\theta},T) = U(\theta,T) + \mathcal{O}(1/N)\,. \tag{7.12}$$

Equation (5.86) then gives

$$\lim_{N\to\infty}\rho_N^{\mathrm{sym}}(\theta,T) = 2\,\mathrm{Re}\,U(\theta,T)\,, \tag{7.13}$$

where $U(\theta,T)$ is the (unique) solution of Eq. (7.3) which is located on the closed contour around $U = \frac{1}{2}$ in the right half-plane (since this is the saddle point which we have to use in the saddle-point approximation of the integral).

In the following, we will show that this result is equivalent to the result of Durhuus and Olesen, i.e., that we have indeed $2\,\mathrm{Re}\,U(\theta,T) = \rho_\infty(\theta,t)$. (In Sec. 4.4, the subscript ∞ has been omitted since we have exclusively considered the infinite-N limit there. For $N = \infty$, we have $t = T$). We have seen that $\rho_\infty(\varphi,t)$ is determined by a function[12] $f(\varphi + i\eta,t)$ through Eq. (4.77), $\rho_\infty(\varphi,t) = 2\lim_{\eta\to 0^-}\mathrm{Im}\,f(\varphi+i\eta,t)$. $f(\theta,t)$ has to fulfill Eq. (4.84) with complex $\theta = \varphi + i\eta$. (In Sec. 4.4, we have used the notation $\theta = \varphi + i\eta$ with $\varphi,\eta \in \mathbb{R}$ and $\eta \le 0$. In the notation of this section, this corresponds to $z = e^{i\varphi+\varepsilon}$ with $\varepsilon = -\eta \ge 0$.) Equation (4.84) can be rewritten as

$$f(\theta,t) = \frac{i}{2}\frac{e^{i(\theta - tf(\theta,t))} + 1}{e^{i(\theta-tf(\theta,t))} - 1} \tag{7.14}$$

or equivalently

$$e^{i(\theta - tf(\theta,t))} = \frac{if(\theta,t) - \frac{1}{2}}{if(\theta,t) + \frac{1}{2}}\,. \tag{7.15}$$

[12] This function $f(\theta,t)$ is not to be confused with $f(u,z)$ defined in Eq. (7.1).

If we identify $-if$ with U, we recover the above saddle-point equation (7.3) (which admits infinitely many solutions).

In Sec. 4.4, we have used the parametrization

$$f(\theta,t)=\frac{\theta-\xi(\theta,t)}{t}\,, \tag{7.16}$$

and by studying the initial condition of the complex Burgers equation which determines $f(\theta,t)$, we have argued that we have to pick the solution ξ with $0\le\mathrm{Re}\,\xi\le\pi$ ($\mathrm{Re}\,\xi(\varphi=0)=0$, $\mathrm{Re}\,\xi(\varphi=\pi)=\pi$) and $\mathrm{Im}\,\xi\le 0$ for $0\le\varphi\le\pi$ ($\varphi\to-\varphi$ results in $\xi\to\xi^*$). As $\varphi=\mathrm{Re}\,\theta$ varies between $-\pi$ and π, the open curve in the complex-ξ plane on which those solutions are located is mapped to a closed curve around $f=\frac{i}{2}$ in the complex-f plane. With the identification $U=-if$, this is precisely the closed curve around $U=\frac{1}{2}$ on which the saddle points are located that we have to use in the approximation of $\psi^{\mathrm{sym}}_{N,+}(z,T)$. These saddle-points determine $\rho^{\mathrm{sym}}_\infty(\theta,T)$. With $z=e^{i\varphi-\eta}$, $\eta\le 0$, this means that

$$f(\varphi+i\eta,T)=iF^{\mathrm{sym}}_{\infty,+}(z,T) \tag{7.17}$$

or, equivalently,

$$\rho^{\mathrm{sym}}_\infty(\varphi,T)=\rho_\infty(\varphi,T)\,. \tag{7.18}$$

Due to the relation (7.13), the location of the saddle point in the complex-U plane directly determines $\rho^{\mathrm{sym}}_\infty(\theta,T)$. For $T>4$, we have $\mathrm{Re}\,U(\theta,T)>0$ for all θ, cf. Fig. 23, which results in non-zero density. For $T<4$, we find $\mathrm{Re}\,U(\theta,T)=0$ for $|\theta|\le\theta_c(T)<\pi$ in the limit $\varepsilon\to 0^+$, i.e., the spectrum has a gap. At $T=4$, only the saddle point for $\theta=\pm\pi$ is located on the imaginary-U axis, $\theta_c(4)=\pi$. This is the point where the Durhuus-Olesen transition occurs and the gap in the eigenvalue density ρ_∞ opens.

7.3 Finite-N correction to $\rho_\infty(\theta,T)$

Higher-order terms in the $1/N$ expansion of $\psi^{\mathrm{sym}}_{N,+}(e^{i\theta},T)$ can be obtained in the standard way by considering higher powers of x in the expansion of $g(x)$, resulting in integrals of the type $\int_{-\infty}^{\infty}dx\,x^{2n}e^{-g''(0)x^2/2}$ with $n\in\mathbb{N}$ (see App. C). However, if we are only interested in the $1/N$ correction to $\rho_\infty(\theta,T)$, the result (7.8) is already sufficient ($1/N$ corrections to this result would give $1/N^2$ corrections to $\rho_\infty(\theta,T)$). Therefore, we now write (with $z=e^{i\theta}$)

$$\frac{1}{N}\log\psi^{\mathrm{sym}}_{N,+}(z,T)=\frac{T}{8}-f(\bar u(z),z)-\frac{1}{2N}\log[Tf''(\bar u(z),z)]+\mathcal{O}(1/N^2)\,, \tag{7.19}$$

where again $f''(\bar u(z),z)\equiv\partial_u^2 f(u,z)|_{u=\bar u(z)}$. Due to

$$f''(\bar u(z),z)=\frac{1}{T}+\frac{ze^{-i\bar u(z)}}{\left(ze^{-i\bar u(z)}-1\right)^2}=\frac{1}{T}+\left(U(\theta,T)-\frac{1}{2}\right)\left(U(\theta,T)+\frac{1}{2}\right)\,, \tag{7.20}$$

we obtain

$$\partial_z\log[Tf''(\bar u(z),z)]=\frac{1}{f''}\left(\partial_U f''\right)\left(\partial_z U\right)=\frac{2U}{\frac{1}{T}+\left(U-\frac{1}{2}\right)\left(U+\frac{1}{2}\right)}\partial_z U\,. \tag{7.21}$$

Differentiating the saddle-point equation (7.3) (with $e^{i\theta+\varepsilon}=z$) w.r.t. z results in

$$-z\partial_z U=\frac{\left(U+\frac{1}{2}\right)\left(U-\frac{1}{2}\right)}{1+T\left(U+\frac{1}{2}\right)\left(U-\frac{1}{2}\right)}\,, \tag{7.22}$$

leading to

$$F_{N,+}^{\mathrm{sym}}(z,T) = U(\theta,T)\left(1+\frac{1}{N}\frac{T(1/4-U(\theta,T)^2)}{[1-T(1/4-U(\theta,T)^2)]^2}\right)+\mathcal{O}(1/N^2) \tag{7.23}$$

and thus to

$$\rho_N^{\mathrm{sym}}(\theta,T) = 2\,\mathrm{Re}\left[U(\theta,T)\left(1+\frac{1}{N}\frac{T(1/4-U(\theta,T)^2)}{[1-T(1/4-U(\theta,T)^2)]^2}\right)\right]+\mathcal{O}(1/N^2)\,. \tag{7.24}$$

Note that for $T \leq 4$ and $|\theta| \to \theta_c(T)$ (from below), the denominator of the $1/N$ term approaches zero, which corresponds to the complication discussed in Sec. 7.1. Note also that for $T \leq 4$ and $|\theta| > \theta_c$ the saddle point $U(\theta,T)$ is purely imaginary so that both the leading order and the $1/N$ term are zero. This confirms that the above saddle-point analysis is not the right tool to compute finite-N effects in this region and more work is needed. Note that finite-N corrections in this region, which are exponentially suppressed in N, cannot be obtained from the contribution of an additional saddle point. The integral is approximated by an integration path which includes only one single saddle point which is passed along a path of steepest descent. (Although, it is possible that the contour of steepest descent through this single saddle point gets close to another saddle point in the limit $\varepsilon \to 0$ (one of the infinitely many that are located on the imaginary axis), this additional saddle point can never be passed along a path of steepest descent and therefore does not provide a local maximum for the absolute value of the integrand.)

In Fig. 26, we show examples for the $1/N$ corrections (obtained from Eq. (7.24)) to $\rho_\infty(\theta,T)$ for $N=10$, $T=2$ and $N=10$, $T=5$ together with the corresponding exact results (which are computed numerically).

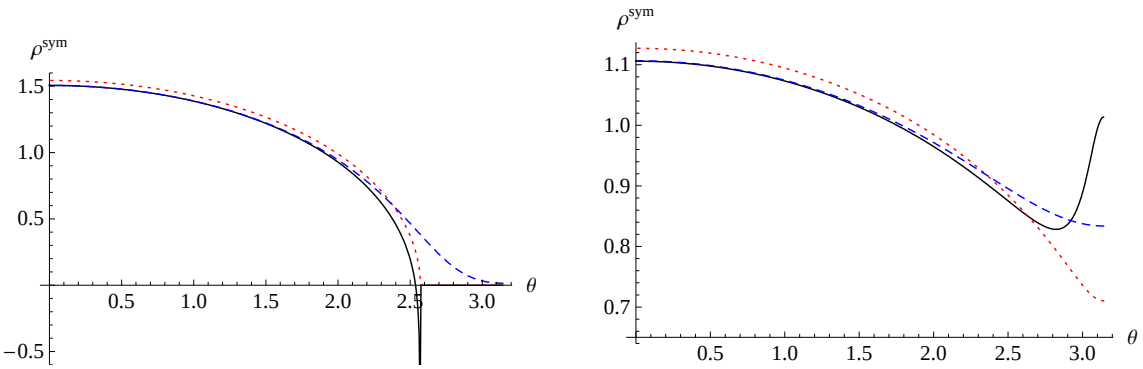

Figure 26: Examples for the $1/N$ corrections to $\rho_\infty(\theta,T)$ for $N=10$ and $T=2$ (left) and $T=5$ (right). Shown are the exact result for $\rho_N^{\mathrm{sym}}(\theta,T)$ (blue dashed curve), the infinite-N result $\rho_\infty(\theta,T)$ (red dotted curve), and the asymptotic expansion of $\rho_N^{\mathrm{sym}}(\theta,T)$ up to order $\mathcal{O}(1/N)$ from Eq. (7.24) (black solid curve). We observe that the asymptotic expansion converges rapidly for small $|\theta|$ and more slowly for larger $|\theta|$.

8 The true eigenvalue density at finite N

In this section, we derive exact formulas for the eigenvalue density $\rho_N^{\rm true}(\theta,t)$ at arbitrary finite N.

8.1 Character expansion

To compute $F_{N,\pm}^{\rm true}(z,t)$, we consider the ratio of determinants

$$R(u,v,W) \equiv \frac{\det(1+uW)}{\det(1-vW)} \tag{8.1}$$

with $|v|<1$ and expand it in SU(N) characters, using (cf. Eqs. (5.30) and (5.74))

$$\det(1+uW) = \sum_{p=0}^{N} u^p \chi_p^{\rm asym}(W)\,, \qquad \frac{1}{\det(1-vW)} = \sum_{q=0}^{\infty} v^q \chi_q^{\rm sym}(W)\,, \tag{8.2}$$

where $\chi_p^{\rm asym}(W)$ (resp. $\chi_q^{\rm sym}(W)$) denotes the character of W in a totally antisymmetric (resp. symmetric) representation whose Young diagram consists of a single column (resp. row) with p (resp. q) boxes. The trivial representation corresponds to $p=0$ and $q=0$, and for SU(N) the antisymmetric representation with $p=N$ boxes is equivalent to the trivial one because of $\chi_N^{\rm asym}(W) = \det W = 1$. This yields

$$R(u,v,W) = \sum_{p=0}^{N}\sum_{q=0}^{\infty} u^p v^q \chi_p^{\rm asym}(W)\chi_q^{\rm sym}(W)\,. \tag{8.3}$$

The task now is to decompose the tensor product $p^{\rm asym}\otimes q^{\rm sym}$ of a p-fold totally antisymmetric and a q-fold totally symmetric representation into irreducible representations. In general, $p^{\rm asym}\otimes q^{\rm sym}$ consists of tensors with $p+q$ indices, where the first p are antisymmetrized and the last q are symmetrized. To decompose into irreducible representations, we take one index from the first p and one from the last q and either symmetrize or antisymmetrize this pair. There are no more symmetrization operations we can perform (this is in agreement with the general method described in Sec. 2.6). Thus, $p^{\rm asym}\otimes q^{\rm sym}$ decomposes into two irreducible representations, except in boundary cases when it is already irreducible. The boundary cases are at $q=0$ or $p=0$ or $p=N$. Away from the boundary cases, $p^{\rm asym}\otimes q^{\rm sym}$ decomposes into two irreducible representations identified by Young diagrams of the form

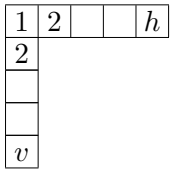

(8.4)

with the top row consisting of h boxes and a left column of v boxes and nothing else. One either has $h=q$ and $v=p+1$ or $h=q+1$ and $v=p$. (Do not confuse the v here with the argument of R.) The first case corresponds to an antisymmetrized pair and the second to a symmetrized pair. For later convenience we shall label the above "hook" diagram by $(v-1,h-1)$ with the understanding that $v=0$ or $h=0$ gives the trivial representation.

In terms of Young diagrams, we have

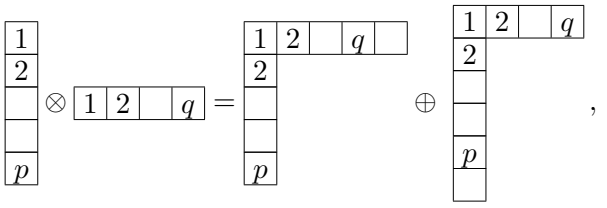

(8.5)

which we write as

$$p^{\text{asym}} \otimes q^{\text{sym}} = (p-1,q) \oplus (p,q-1)\,. \tag{8.6}$$

For the boundary cases, we find

$$p^{\text{asym}} \otimes 0 = (p-1,0)\,, \quad 0 \otimes q^{\text{sym}} = (0,q-1)\,, \quad N^{\text{asym}} \otimes q^{\text{sym}} = (N-1,q) = (0,q-1)\,. \tag{8.7}$$

Taking into account these boundary cases and suppressing the SU(N) matrix argument W, we obtain

$$R(u,v) = 1 + \sum_{p=0}^{N-1}\sum_{q=1}^{\infty} u^p v^q \chi_{(p,q-1)} + \sum_{p=1}^{N}\sum_{q=0}^{\infty} u^p v^q \chi_{(p-1,q)}\,. \tag{8.8}$$

The case $p=0$, $q=0$ is excluded from the sums, every other boundary case appears in exactly one of the two sums above. Every non-trivial pair has one of the two irreducible representations in exactly one of the sums. Changing summation indices $q \to q+1$ in the first sum and $p \to p+1$ in the second sum, we obtain

$$R(u,v) = 1 + (u+v)\sum_{p=0}^{N-1}\sum_{q=0}^{\infty} u^p v^q \chi_{(p,q)}\,, \tag{8.9}$$

which makes it explicit that $R=1$ at $u=-v$.

A consequence of the above result is the character expansion of $\operatorname{Tr} W^k$ for all k. Due to

$$\begin{aligned}\det(1-(v-\varepsilon)W) &= \det(1-vW)\det\left(1+\varepsilon\frac{W}{1-vW}\right) = \det(1-vW)e^{\operatorname{Tr}\varepsilon\frac{W}{1-vW}+\mathcal{O}(\varepsilon^2)} \\ &= \det(1-vW)\left(1+\varepsilon\operatorname{Tr}\frac{W}{1-vW}+\mathcal{O}(\varepsilon^2)\right)\,,\end{aligned} \tag{8.10}$$

we have

$$R(-v+\varepsilon,v) = 1 - \frac{N\varepsilon}{v} + \frac{\varepsilon}{v}\operatorname{Tr}\frac{1}{1-vW} + \mathcal{O}(\varepsilon^2)\,. \tag{8.11}$$

By comparison with Eq. (8.9), this results in

$$\operatorname{Tr}\frac{1}{1-vW} = N + v\sum_{(p,q)}(-1)^p v^{p+q}\chi_{(p,q)}(W)\,, \tag{8.12}$$

where the limits on the double sum are given in Eq. (8.9). Since $|v|<1$, we can expand

$$\operatorname{Tr}\frac{1}{1-vW} = \sum_{k=0}^{\infty} v^k \operatorname{Tr} W^k\,. \tag{8.13}$$

Hence, we obtain for $k>0$ that

$$\operatorname{Tr} W^k = \sum_{\substack{(p,q)\\ p+q=k-1}} (-1)^p \chi_{(p,q)}(W)\,. \tag{8.14}$$

For $k=0$, we have $\operatorname{Tr}\mathbf{1} = N$; the trace of a negative power of W can be obtained from the relation $\operatorname{Tr} W^k = \left(\operatorname{Tr} W^{-k}\right)^*$.

8.2 Performing the average

In analogy to Eqs. (5.34) and (5.77), the average over W with weight (5.4) produces, using character orthogonality,

$$\langle \chi_{(p,q)}(W) \rangle = d(p,q) e^{-\frac{t}{2N} C(p,q)} , \tag{8.15}$$

where $C(p,q)$ is the value of the quadratic Casimir operator in the irreducible representation (p,q), given by [50]

$$C(p,q) = (p+q+1)\left(N - \frac{p+q+1}{N} + q - p \right) , \tag{8.16}$$

and the dimension of the representation labeled by (p,q) is

$$d(p,q) = d_p^{\text{asym}} d_q^{\text{sym}} \frac{(N-p)(N+q)}{N} \frac{1}{p+q+1} \tag{8.17}$$

with

$$d_p^{\text{asym}} = \binom{N}{p} , \qquad d_q^{\text{sym}} = \binom{N+q-1}{q} \tag{8.18}$$

being the dimension of the p-fold antisymmetric and q-fold symmetric irreducible representation.

8.3 Basic combinatorial identities

The expansions of one determinant or one inverse determinant factor (i.e., setting $W = \mathbf{1}$ and $u = \xi$, $v = 0$ or $u = 0$, $v = \eta$ in Eq. (8.9)) provide the identities

$$\begin{aligned} \Sigma^{\text{asym}}(\xi) &\equiv \sum_{p=0}^{N-1} \xi^p d_p^{\text{asym}} (N-p) = (N - \xi\partial_\xi) \sum_{p=0}^{N} \xi^p d_p^{\text{asym}} \\ &= (N - \xi\partial_\xi)(1+\xi)^N = N(1+\xi)^{N-1} , \end{aligned} \tag{8.19a}$$

$$\begin{aligned} \Sigma^{\text{sym}}(\eta) &\equiv \sum_{q=0}^{\infty} \eta^q d_q^{\text{sym}} (N+q) = (N + \eta\partial_\eta) \sum_{q=0}^{\infty} \eta^q d_q^{\text{sym}} = \\ &= (N + \eta\partial_\eta) \frac{1}{(1-\eta)^N} = \frac{N}{(1-\eta)^{N+1}} \end{aligned} \tag{8.19b}$$

with $|\eta| < 1$. These will be needed to carry out the summations over p and q later.

8.4 Factorizing the sums over p and q for the average resolvent at zero area

We now set $u = -v + \varepsilon$ and expand in ε. Up to corrections of order ε^2, we obtain from Eqs. (8.11) and (8.12) with

$$\operatorname{Tr}\left(\frac{1}{1 - vW} \right) - N = \operatorname{Tr} \frac{vW}{1 - vW} = -v \operatorname{Tr} \frac{1}{v - W^\dagger} \tag{8.20}$$

that

$$R(-v+\varepsilon, v, W) = 1 + \varepsilon \sum_{p=0}^{N-1} \sum_{q=0}^{\infty} (-1)^p v^{p+q} \chi_{(p,q)}(W) = 1 - \varepsilon \operatorname{Tr} \frac{1}{v - W^\dagger} . \tag{8.21}$$

Due to $\mathcal{P}(W,t) = \mathcal{P}(W^\dagger,t)$, Eq. (5.13) leads to (we consider $|v|<1$)

$$G^{\rm true}_{N,-}(v,t) = \frac{1}{N}\left\langle \mathrm{Tr}\,\frac{1}{v-W^\dagger}\right\rangle = -\frac{1}{N}\sum_{p=0}^{N-1}\sum_{q=0}^{\infty}(-1)^p v^{p+q} e^{-\frac{t}{2N}C(p,q)} d(p,q)\,. \tag{8.22}$$

Note that the sum can be extended to $p=N$ because of the factor $N-p$ in $d(p,q)$. The true eigenvalue density is obtained from $G^{\rm true}_{N,-}$ through Eq. (5.21), which is repeated here for convenience

$$\rho^{\rm true}_N(\theta,t) = 1 - 2\lim_{\varepsilon\to 0^+}\mathrm{Re}[vG^{\rm true}_{N,-}(v,t)]\,, \qquad v = e^{i\theta-\varepsilon}\,. \tag{8.23}$$

Note that there is no need for the limiting procedure $\varepsilon\to 0^+$ in Eq. (8.23) if we are using the double sum in Eq. (8.22) for $G^{\rm true}_{N,-}(v,t)$, which is well-defined for $|v|=1$.

We now introduce the integral

$$\frac{1}{p+q+1} = \int_0^1 d\rho\,\rho^{p+q} \tag{8.24}$$

to get rid of the denominator in Eq. (8.17), which leads to

$$\begin{aligned} G^{\rm true}_{N,-}(v,t) = -\int_0^1 \frac{d\rho}{N^2}\sum_{p=0}^{N}\sum_{q=0}^{\infty}\left[(-1)^p v^p\rho^p d^{\rm asym}_p(N-p)\right]\left[v^q\rho^q d^{\rm sym}_q(N+q)\right] \\ \times e^{-\frac{t}{2N}(p+q+1)(N-\frac{p+q+1}{N}+q-p)}\,. \end{aligned} \tag{8.25}$$

This achieves factorization of the sums over p and q at $t=0$. The sum in each factor can be performed using Eqs. (8.19a) and (8.19b), leading to

$$\begin{aligned} G^{\rm true}_{N,-}(v,0) &= -\int_0^1 \frac{d\rho}{N^2} N(1-v\rho)^{N-1} N\frac{1}{(1-v\rho)^{N+1}} \\ &= -\int_0^1 d\rho\frac{1}{(1-v\rho)^2} = \frac{1}{v}\left(1-\frac{1}{1-v}\right)\,. \end{aligned} \tag{8.26}$$

As expected, this results in

$$\rho^{\rm true}_N(\theta,0) = \lim_{\varepsilon\to 0^+}\left(-1+\frac{1}{1-e^{i\theta-\varepsilon}}+\frac{1}{1-e^{-i\theta-\varepsilon}}\right) = 2\pi\delta_{2\pi}(\theta)\,. \tag{8.27}$$

8.5 Integral representation at any area

The t-dependent weight factor is the exponent of a bilinear form in p and q. Therefore, the dependence of the exponent on p and q can be made linear by a Hubbard-Stratonovich transformation. After the transformation, the sums over p and q are factorized for every t and can again be done exactly using Eqs. (8.19a) and (8.19b).

We define the complex symmetric matrix

$$B_N = \begin{pmatrix} 1+\frac{1}{N} & \frac{i}{N} \\ \frac{i}{N} & 1-\frac{1}{N}\end{pmatrix}\,, \tag{8.28}$$

which has only one eigenvalue (equal to one) and is non-diagonalizable. We have $\det B_N = 1$ and

$$B_N^{-1} = \begin{pmatrix} 1-\frac{1}{N} & -\frac{i}{N} \\ -\frac{i}{N} & 1+\frac{1}{N}\end{pmatrix}\,. \tag{8.29}$$

The quadratic Casimir form can be written with the help of B_N in the following way:

$$C(p,q) = \begin{pmatrix} ip \\ q \end{pmatrix}^T B_N \begin{pmatrix} ip \\ q \end{pmatrix} + N\left(1-\frac{1}{N^2}\right) + N\left(1+\frac{1}{N}-\frac{2}{N^2}\right)q + N\left(1-\frac{1}{N}-\frac{2}{N^2}\right)p. \tag{8.30}$$

Hence,

$$\begin{aligned} e^{-\frac{t}{2N}C(p,q)} = \frac{N}{t}\, e^{-\frac{t}{2}\left(1-\frac{1}{N^2}\right)} \int_{-\infty}^{\infty}\int_{-\infty}^{\infty} \frac{dxdy}{2\pi}\, \exp\left[-\frac{N}{2t}(x,y)B_N^{-1}\begin{pmatrix} x \\ y \end{pmatrix} - px + iqy\right] \\ \times \exp\left\{-\frac{t}{2}\left[\left(1+\frac{1}{N}-\frac{2}{N^2}\right)q + \left(1-\frac{1}{N}-\frac{2}{N^2}\right)p\right]\right\}. \end{aligned} \tag{8.31}$$

Using Eqs. (8.19a) and (8.19b), we can now perform the sums over p and q,

$$\begin{aligned} G^{\text{true}}_{N,-}(v,t) = -\frac{N}{t}\, e^{-\frac{t}{2}\left(1-\frac{1}{N^2}\right)} \\ \times \int_{-\infty}^{\infty}\int_{-\infty}^{\infty} \frac{dxdy}{2\pi}\, \exp\left[-\frac{N}{2t}[(1-1/N)x^2 + (1+1/N)y^2 - 2ixy/N]\right] \\ \times \int_0^1 d\rho\, \frac{\left[1-v\rho e^{-x-(t/2)(1-1/N-2/N^2)}\right]^{N-1}}{\left[1-v\rho e^{iy-(t/2)(1+1/N-2/N^2)}\right]^{N+1}}. \end{aligned} \tag{8.32}$$

Note that because of $|v|<1$, the denominator in the last line is never zero. The integral over ρ can be done exactly, if one wishes, resulting in

$$\begin{aligned} G^{\text{true}}_{N,-}(v,t) = \frac{1}{t}\, e^{-\frac{t}{2}(1-\frac{1}{N^2})} \int_{-\infty}^{\infty}\int_{-\infty}^{\infty} \frac{dxdy}{2\pi} \left\{\left[\frac{1-v\,e^{-x-(t/2)(1-1/N-2/N^2)}}{1-v\,e^{iy-(t/2)(1+1/N-2/N^2)}}\right]^N - 1\right\} \\ \times \frac{e^{-\frac{N}{2t}[(1-1/N)x^2+(1+1/N)y^2-2ixy/N]}}{v\left[e^{-x-(t/2)(1-1/N-2/N^2)} - e^{iy-(t/2)(1+1/N-2/N^2)}\right]}. \end{aligned} \tag{8.33}$$

The above formula was derived for $|v|<1$, which is sufficient for finding $\rho_N^{\text{true}}(\theta,t)$ via Eq. (8.23). Using symmetries of $\langle R(u,v,W)\rangle$, one can immediately write down also results for $|v|>1$.

8.6 Making sense of negative integer N

Conforming to previous observations (see Ref. [56] and references therein), we extend our result to negative integer N. This may be of relevance to $1/2N$ playing the role of the viscosity term in Burgers' equation [40, 47] and also to approximate equations in Ref. [42].

We first restate the result derived earlier,

$$\begin{aligned} \bar{R}(u,v,N) &\equiv \langle R(u,v,W)\rangle \\ &= 1 + \frac{u+v}{N}\sum_{p=0}^{N-1}\sum_{q=0}^{\infty} \frac{1}{p+q+1} u^p v^q e^{-\frac{t}{2}\hat{C}(p,q,N)} M^A(p,N) M^S(q,N), \end{aligned} \tag{8.34}$$

where

$$\hat{C}(p,q,N) = \frac{C(p,q,N)}{N} = (p+q+1)\left(1 - \frac{p+q+1}{N^2} + \frac{q-p}{N}\right), \tag{8.35a}$$

$$M^A(p,N) = \frac{(N-p)(N-p+1)\cdots N}{(p+1)!}(p+1), \tag{8.35b}$$

$$M^S(q,N) = \frac{(N+q)(N+q-1)\cdots N}{(1+q)!}(q+1). \tag{8.35c}$$

In Eq. (8.35) p and q still are non-negative integers, but N is allowed to be an integer of arbitrary sign (with $N = 0$ excluded).

Note that for $p \geq N$, $M^A(p, N) = 0$. Hence, still keeping $N > 0$, we can remove one of the restrictions on the range of p in the sum in Eq. (8.34),

$$\bar{R}(u, v, N) = 1 + \frac{u+v}{N} \sum_{p,q=0}^{\infty} \frac{1}{p+q+1} u^p v^q e^{-\frac{t}{2}\hat{C}(p,q,N)} M^A(p, N) M^S(q, N) \,. \tag{8.36}$$

We observe that

$$\hat{C}(p, q, -N) = \hat{C}(q, p, N) \,, \tag{8.37a}$$

$$M^A(p, -N) = (-1)^{p+1} M^S(p, N) \,, \tag{8.37b}$$

$$M^S(q, -N) = (-1)^{q+1} M^A(q, N) \,. \tag{8.37c}$$

The entire dependence on N in Eq. (8.36) is explicit, and the function $\bar{R}(u, v, N)$ remains well-defined for $N < 0$, so long as the fixed parameter t is positive. With $N > 0$, this leads to

$$\bar{R}(u, v, N) = 1 + \frac{-u-v}{-N} \sum_{p,q=0}^{\infty} \frac{(-u)^p (-v)^q}{p+q+1} M^S(p, -N) M^A(q, -N) e^{-\frac{t}{2}\hat{C}(q,p,-N)} \,. \tag{8.38}$$

Interchanging the dummy summation labels p and q we get

$$\bar{R}(u, v, N) = \bar{R}(-v, -u, -N) \,. \tag{8.39}$$

Writing

$$\bar{R}(u, v, N) = 1 + \frac{u+v}{N} \Omega(u, v, N) \tag{8.40}$$

results in

$$\Omega(u, v, N) = \Omega(-v, -u, -N) \,. \tag{8.41}$$

Now set $u = -v$. $\Omega(-v, v, N)$ is finite for $t > 0$, and we have

$$\Omega(-v, v, N) = \Omega(-v, v, -N) \,. \tag{8.42}$$

$\Omega(-v, v, N)$ determines $\rho_N^{\text{true}}(\theta, t)$ via Eq. (8.23) because of $\Omega(-v, v, N) = -N^2 G_{N,-}^{\text{true}}(v, t)$, i.e.,

$$\rho_N^{\text{true}}(\theta, t) = 1 + \frac{2}{N^2} \lim_{\varepsilon \to 0^+} \text{Re}\left[v\, \Omega(-v, v, N)\right] , \qquad v = e^{i\theta - \varepsilon} \,. \tag{8.43}$$

At this point we realize that we have defined $\rho_N^{\text{true}}(\theta, t)$ for negative integer N, too:

$$\rho_{-N}^{\text{true}}(\theta, t) = 1 + \frac{2}{N^2} \lim_{\varepsilon \to 0^+} \text{Re}\left[v\, \Omega(-v, v, -N)\right] = \rho_N^{\text{true}}(\theta, t) \,, \tag{8.44}$$

where in the last step we have made use of Eq. (8.42).

8.7 Large-N asymptotics

If one could expand $\rho_N^{\text{true}}(\theta, t)$ in N around $N = 0$, only even powers of N would enter. However, all one can do is an asymptotic expansion in $1/N$, and then odd powers can appear (one can think of the asymptotic expansion as an expansion in $1/|N|$).

We now turn to the integral representation to take the first steps in a $1/N$ expansion of $\rho_N^{\text{true}}(\theta,t)$. Shifting integration variables $x \to x + (t/2)\left(1/N + 2/N^2\right)$ and $y \to y - i(t/2)\left(1/N - 2/N^2\right)$ in Eq. (8.32), we obtain

$$G_{N,-}^{\text{true}}(v,t) = -\frac{N}{t} e^{-\frac{t}{2}} \iint_{-\infty}^{\infty} \frac{dxdy}{2\pi} \int_0^1 d\rho\, e^{\frac{1}{2t}(x+iy)^2 - \frac{N}{2t}(x^2+y^2) - \frac{1}{2}(x-iy)} \frac{\left[1 - v\rho e^{-x-t/2}\right]^{N-1}}{\left[1 - v\rho e^{iy-t/2}\right]^{N+1}} . \tag{8.45}$$

Since this integral representation was derived for $|v| < 1$, we set $v = e^{i\theta-\varepsilon}$ with $|\theta| \le \pi$, $\varepsilon > 0$, and take the limit $\varepsilon \to 0^+$ at the end. We write Eq. (8.45) as

$$\begin{aligned} G_{N,-}^{\text{true}}(v,t) = -\frac{N}{t} e^{-\frac{t}{2}} \iint_{-\infty}^{\infty} \frac{dxdy}{2\pi} \int_0^1 d\rho\, e^{-\frac{N}{2t}\left(x^2+y^2\right) + \frac{1}{2t}(x+iy)^2 - \frac{1}{2}(x-iy)} \\ \times e^{(N-1)\log\left(1-v\rho e^{-x-t/2}\right) - (N+1)\log\left(1-v\rho e^{iy-t/2}\right)} . \end{aligned} \tag{8.46}$$

At large N, the integrals over x and y decouple at leading order and can be done independently by saddle-point approximations. Let us start with the integral over y since it is conceptually simpler. The y-dependent coefficient of the term in the exponent in Eq. (8.46) that is proportional to $-N$ is given by

$$\bar{f}(y) = \frac{1}{2t} y^2 + \log\left[1 - v\rho e^{iy - \frac{t}{2}}\right] . \tag{8.47}$$

Substituting $y = u - it/2 = it(U - 1/2)$ (with $u = itU$ in analogy to Sec. 7) results in exactly the same integrand that was already considered in Sec. 7, with the replacements $T \to t$ and $z \to 1/v\rho$ (with $|v\rho| < 1$) and with an integration over u that is now along the line from $-\infty + it/2$ to $+\infty + it/2$. Since there are no singularities between this line and the real-u axis, we can change the integration path to be along the real-u (or imaginary-U) axis. Now everything goes through as in Sec. 7. The saddle-point equation reads

$$e^{-tU} \frac{U + 1/2}{U - 1/2} = \frac{1}{v\rho} , \tag{8.48}$$

which is equivalent to Eq. (7.3). In Fig. 27 we show the contours in the complex-U plane on which the solutions of the saddle-point equation have to lie. In analogy to Eq. (8.49), those contours are now determined by

$$U_i^2 = U_r \coth(TU_r + \varepsilon - \log\rho) - U_r^2 - \frac{1}{4} . \tag{8.49}$$

(For sufficiently small ρ, we now encounter the case mentioned in Sec. 7.1 where the closed contour in the left half-plane is missing for $t > 4$.) The relevant saddle point, which we denote by $y_0(\theta,t,\rho)$, is again on the closed contour in the right half-plane. For decreasing ρ this contour contracts, but this makes no difference to our analysis. The result for the y-integral is given by an expression similar to Eq. (7.8).

We now turn to the integral over x. The x-dependent coefficient of the term in the exponent in Eq. (8.46) that is proportional to $-N$ is given by

$$\tilde{f}(x) = \frac{1}{2t} x^2 - \log\left[1 - v\rho e^{-x-t/2}\right] = -\bar{f}(ix) . \tag{8.50}$$

Substituting $x = -iu - t/2 = t(U - 1/2)$ (with $u = itU$) again leads to the integral considered in Sec. 7 and the saddle-point equation (8.48), except that the integration is now along the real-U axis. The positions of the saddle points of the x-integral are obtained

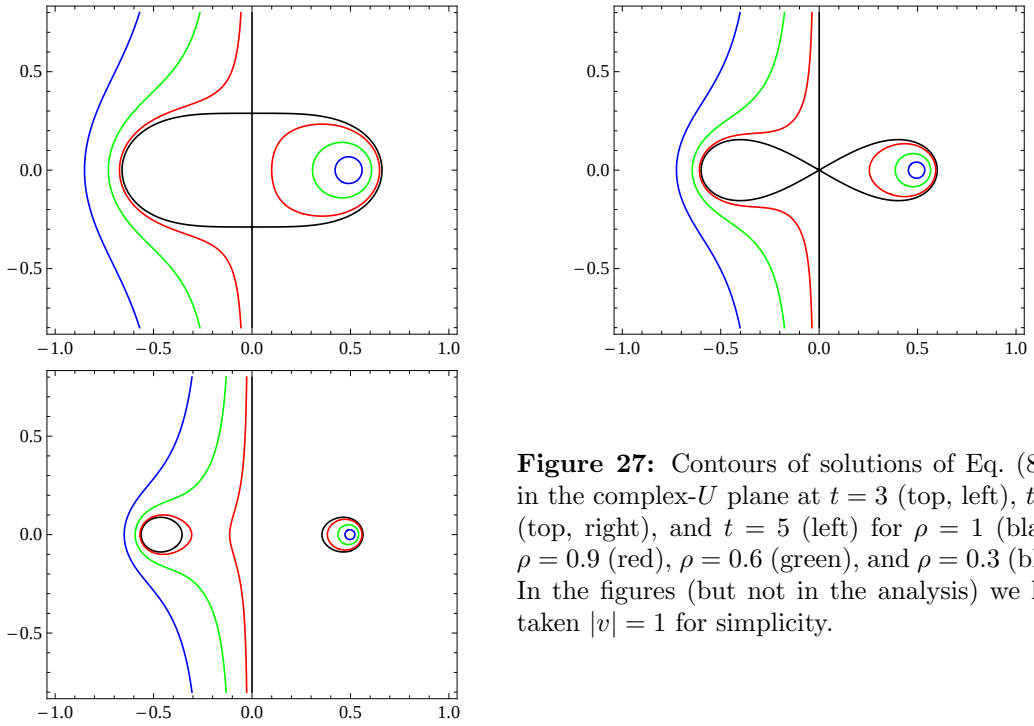

Figure 27: Contours of solutions of Eq. (8.49) in the complex-U plane at $t = 3$ (top, left), $t = 4$ (top, right), and $t = 5$ (left) for $\rho = 1$ (black), $\rho = 0.9$ (red), $\rho = 0.6$ (green), and $\rho = 0.3$ (blue). In the figures (but not in the analysis) we have taken $|v| = 1$ for simplicity.

by rotating the saddles of the y-integral by $-\pi/2$ in the complex-U plane, i.e., $x_s = -iy_s$. At a saddle point, we have

$$\tilde{f}''(x_s) = \frac{1}{t} + \frac{x_s}{t}\left(1 + \frac{x_s}{t}\right) = \bar{f}''(y_s)\,, \tag{8.51}$$

and therefore the directions of steepest descent through a saddle y_s and the corresponding saddle $x_s = -iy_s$ are identical (no rotation). By analyzing the directions along which the phase of the integrand is constant, we find that the integration contour can always be deformed to go through the (single) saddle-point in the right half-plane in the direction of steepest descent. Depending on the parameters ρ, v, and t, there is either one or no additional saddle point on the contour(s) in the left half-plane through which we can also go in the direction of steepest descent. If there is such an additional saddle point, we find that its contribution to the integral is always exponentially suppressed in N compared to the saddle point in the right half-plane and can therefore be dropped from the saddle-point analysis. In addition, there are infinitely many more saddle points on the open contour in the left half-plane. However, we cannot deform the integration path to go through these points in the direction of steepest descent and therefore do not need to include them. An example for the location of the saddle points and the deformation of the integration path is given in Fig. 28. To summarize, the x-integral can be approximated by the contribution of the single saddle point in the right half-plane, which again leads to an expression similar to Eq. (7.8).

Combining the saddle-point approximations for the integrals over x and y, we find that, up to exponentially small corrections in N, the integral in Eq. (8.46) is given by

$$G^{\text{true}}_{N,-}(v,t) = -\frac{N}{t}e^{-t/2}\int_0^1 d\rho\,\frac{1}{2\pi}\left(\frac{2\pi}{N\tilde{f}''(x_0)}\right)\frac{1}{(1-v\rho e^{-x_0-t/2})^2}\,e^{-x_0}\,, \tag{8.52}$$

where $x_0 = x_0(\theta, t, \rho)$ is the dominating saddle point of the x-integral. x_0 is a solution of

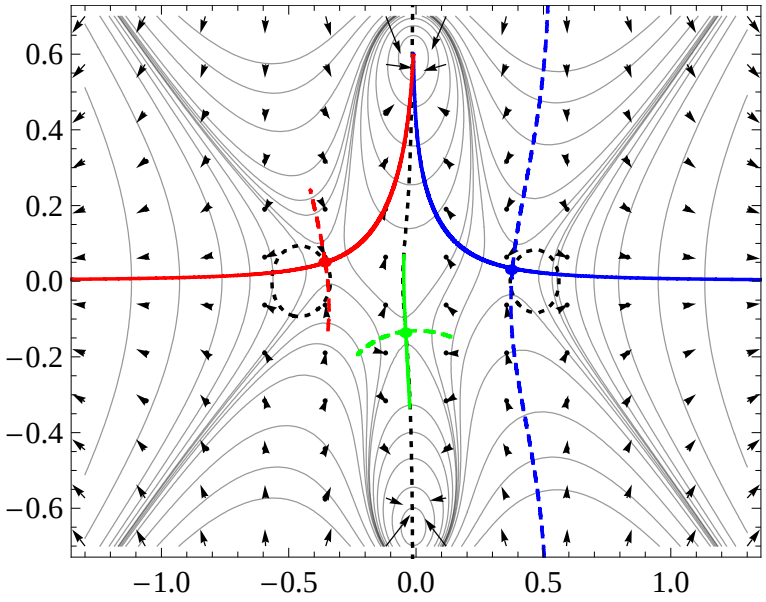

Figure 28: Example for the location of the saddle points and the deformation of the integration path in the complex-U plane for $t = 5$ and $\rho = 0.95$. The dashed black curves (two closed, one open) are the curves on which all saddle points have to lie, cf. (7.5). In this example $\theta = 3.0$. On each of the closed curves there is one saddle point (red dot and blue dot), and on the open curve there are infinitely many saddle points but only one of them in the region shown in the plot (green dot). The thin solid lines are lines of constant $\mathrm{Re}\,\tilde{f}(x)$ and $\mathrm{Re}\,\bar{f}(y)$. The arrows point in the direction of increasing $\mathrm{Re}\,\tilde{f}(x)$ or decreasing $\mathrm{Re}\,\bar{f}(y)$. The dashed blue curve is the integration path for the y-integral along the direction of steepest descent. The solid red-blue curve is the integration path for the x-integral along the direction of steepest descent.

the saddle-point equation obtained by differentiating $\tilde{f}(x)$, which can be written as

$$v\rho e^{-x_0-t/2} = \frac{x_0}{x_0+t} \tag{8.53}$$

and leads to

$$\left(1 - v\rho e^{-x_0-\frac{t}{2}}\right)^2 = \left(\frac{t}{t+x_0}\right)^2 . \tag{8.54}$$

With Eq. (8.51) we obtain

$$\tilde{f}''(x_0)\left(1 - v\rho e^{-x_0-\frac{t}{2}}\right)^2 = \frac{t + x_0\,(t+x_0)}{(t+x_0)^2} \tag{8.55}$$

and

$$G^{\mathrm{true}}_{N,-}(v,t) = -\frac{1}{t}e^{-\frac{t}{2}}\int_0^1 d\rho\,\frac{(t+x_0)^2}{t+x_0\,(t+x_0)}\,e^{-x_0} . \tag{8.56}$$

Differentiating Eq. (8.53) with respect to ρ leads to

$$\frac{\partial x_0}{\partial \rho} = \frac{1}{\rho}\frac{x_0\,(t+x_0)}{t+x_0\,(t+x_0)} = ve^{-x_0-t/2}\frac{(t+x_0)^2}{t+x_0\,(t+x_0)} , \tag{8.57}$$

which yields

$$G^{\mathrm{true}}_{N,-}(v,t) = -\frac{1}{tv}\int_0^1 d\rho\,\frac{\partial x_0}{\partial \rho} = -\frac{1}{tv}\left[x_0(\theta,t,\rho=1) - x_0(\theta,t,\rho=0)\right] . \tag{8.58}$$

We know from Eq. (8.53) that $x_0(\theta, t, \rho = 0) = 0$. Therefore, $G^{\rm true}_{N,-}$ is determined by the saddle point location at $\rho = 1$ only, which we parametrize as $x_0(\theta, t, \rho = 1) = t(U(\theta, t, \rho = 1) - 1/2)$,

$$G^{\rm true}_{N,-}(v, t) = \frac{1}{2v} - \frac{1}{v} U(\theta, t, \rho = 1)\,. \tag{8.59}$$

Here, we need to keep in mind that we have to pick the solution of Eq. (8.48) which corresponds to the dominating saddle point x_0 of the x-integral for $|v\rho| < 1$. For $\rho = 1$, Eq. (8.48) coincides with the saddle point equation (7.3), which determines $\rho^{\rm sym}_\infty(\theta, t)$, if we replace t by T and $1/v$ by z, i.e., $\theta \to -\theta$ (we have always considered $|v| < 1$ and $|z| > 1$; in the infinite-N limit, we have $t = T$). By comparison with Eq. (7.12), we observe that to leading order in $1/N$

$$\begin{aligned} F^{\rm true}_{N,-}(e^{i\theta-\varepsilon}, t) &= e^{i\theta-\varepsilon} G^{\rm true}_{N,-}(e^{i\theta-\varepsilon}, t) - \frac{1}{2} = -U(\theta, t, \rho = 1) \\ &= -F^{\rm sym}_{N,+}(e^{-i\theta+\varepsilon}, t) = -F^{\rm sym}_{N,+}(e^{i\theta+\varepsilon}, t)^* = F^{\rm sym}_{N,-}(e^{i\theta-\varepsilon}, t)\,, \end{aligned} \tag{8.60}$$

where we have used that $U(-\theta) = U(\theta)^*$ and Eq. (5.85), relating $F^{\rm sym}_{N,+}$ and $F^{\rm sym}_{N,-}$. Clearly, this implies that the related densities are equivalent in the infinite-N limit, cf. Eqs. (5.23) and (5.86),

$$\lim_{N\to\infty} \rho^{\rm true}_N(\theta, t) = \lim_{N\to\infty} \rho^{\rm sym}_N(\theta, t)\,, \tag{8.61}$$

which in turn is equal to the Durhuus-Olesen result $\rho_\infty(\theta, t)$, cf. Sec. 7.2. To compute the asymptotic expansion of $\rho^{\rm true}_N(\theta, t)$ in powers of $1/N$ (in regions where this makes sense), one has to keep higher orders in the saddle-point approximation (as explained in Sec. 7.3).

8.8 A partial differential equation for the average of the ratio of characteristic polynomials at different arguments

In the expression for $\Omega(u, v, N)$ that follows from Eq. (8.36), a derivative with respect to t will bring down the Casimir factor from the exponent. Writing

$$u = -e^{X+Y}\,, \qquad v = e^{X-Y}\,, \qquad f_N(X, Y, t) = \Omega(u, v, N)\,, \tag{8.62}$$

we can reconstruct the Casimir by derivatives with respect to X and Y. All that enters is the bilinear structure of the Casimir, and we obtain

$$\frac{\partial f_N}{\partial t} = \frac{1}{2}\left[\frac{1}{N^2}\left(\frac{\partial}{\partial X} + 1\right)^2 - \left(1 - \frac{1}{N}\frac{\partial}{\partial Y}\right)\left(\frac{\partial}{\partial X} + 1\right)\right] f_N\,. \tag{8.63}$$

One can simplify the equation by $f_N \to g_N = e^{X-NY} f_N$,

$$\frac{\partial g_N}{\partial t} = \frac{1}{2}\left(\frac{1}{N^2}\frac{\partial^2}{\partial X^2} + \frac{1}{N}\frac{\partial^2}{\partial Y \partial X}\right) g_N\,. \tag{8.64}$$

Rescaling $X \to NX = Z$ removes all explicit dependence on N in the equation. The equation is linear, so we are free to rescale g_N by any power of N we find convenient. We define

$$h_N(Z, Y, t) \equiv -\frac{1}{N^2} g_N(Z/N, Y, t) \tag{8.65}$$

and now have

$$\frac{\partial h_N}{\partial t} = \frac{1}{2}\left(\frac{\partial^2}{\partial Z^2} + \frac{\partial^2}{\partial Y \partial Z}\right) h_N\,. \tag{8.66}$$

The N-dependence of h_N will then come in only through the initial condition at $t = 0$. We proceed to find the initial condition. Similarly to Eqs. (8.19a) and (8.19b), the combinatorial factors $M^{A,S}$ have the following generating functions:

$$\sum_{p=0}^{\infty} M^A(p,N)A^p = N(1+A)^{N-1}\,, \tag{8.67a}$$

$$\sum_{q=0}^{\infty} M^S(q,N)S^q = \frac{N}{(1-S)^{N+1}}\,. \tag{8.67b}$$

These identities go beyond Eqs. (8.19a) and (8.19b) in that they hold also for negative integer N. Using again

$$\frac{1}{p+q+1} = \int_0^1 d\rho\, \rho^{p+q} \tag{8.68}$$

and the fact that at $t = 0$ we have

$$\Omega(u,v,N)|_{t=0} = \sum_{p,q=0}^{\infty} \frac{u^p v^q}{p+q+1} M^A(p,N) M^S(q,N)\,, \tag{8.69}$$

we obtain

$$\Omega(u,v,N)|_{t=0} = N^2 \int_0^1 d\rho\, \frac{(1+\rho u)^{N-1}}{(1-\rho v)^{N+1}}\,. \tag{8.70}$$

Observing that

$$\frac{\partial}{\partial r}\frac{(1+rA)^N}{(1+rB)^N} = N(A-B)\frac{(1+rA)^{N-1}}{(1+rB)^{N+1}}\,, \tag{8.71}$$

we derive

$$\Omega(u,v,N)|_{t=0} = \frac{N}{u+v}\left[\left(\frac{1+u}{1-v}\right)^N - 1\right]\,. \tag{8.72}$$

From this we now find the initial condition associated with Eq. (8.66),

$$h_N(Z,Y,t=0) = \frac{1}{N}\frac{e^{-NY}}{e^Y - e^{-Y}}\left[\left(\frac{1-e^{\frac{Z}{N}+Y}}{1-e^{\frac{Z}{N}-Y}}\right)^N - 1\right]\,. \tag{8.73}$$

The partial differential equation (8.66) and the associated initial condition (8.73) admit arbitrary N, no longer restricted to integers, although for non-integer N periodicity in θ is lost. However, periodicity in θ was assumed when the relation between $\rho_N^{\rm true}$ and Ω was derived.

One can again check whether there is a symmetry under $N \to -N$. The partial differential equation is linear and invariant under

$$Z \to -Z\,, \quad Y \to -Y\,, \quad N \to -N\,. \tag{8.74}$$

The initial condition is invariant under this transformation, too. Hence,

$$h_N(Z,Y,t) = h_{-N}(-Z,-Y,t)\,. \tag{8.75}$$

For non-integer N, there is some subtlety in defining the cuts in the initial condition so that the above holds. In the original variables, the transformation (8.74) reads $u \to -v$, $v \to -u$, $N \to -N$, so we recover the symmetry (8.41).

By Fourier/Laplace transforms one can derive integral representations, embedding the initial condition at $t \to 0$. To get to the density $\rho_N^{\rm true}(\theta,t)$ via Eq. (8.23) and $\Omega(-v,v,N) = -N^2 G_{N,-}^{\rm true}(v,t)$, one needs to set $u=-v$, which corresponds to $Y=0$ at fixed $Z/N = -\varepsilon + i\theta$, i.e.,

$$\rho_N^{\rm true}(\theta,t) = 1 - 2 \lim_{\varepsilon \to 0^+} {\rm Re}\; h_N(N(-\varepsilon+i\theta),0,t) \tag{8.76}$$

due to

$$h_N(N(-\varepsilon+i\theta),0,t) = -\frac{1}{N^2} v\Omega(-v,v,N) = v G_{N,-}^{\rm true}(v,t)\,, \qquad v = e^{i\theta-\varepsilon}\,. \tag{8.77}$$

At $t>0$, the limit should be smooth, but at $t=0$, one needs to generate a delta-function singularity in $\rho_N^{\rm true}(\theta,t)$ at $\theta = 0 \bmod 2\pi$. We first need the $Y \to 0$ limit of Eq. (8.73), which is

$$h_N(Z,Y=0,t=0) = -\frac{e^{Z/N}}{1-e^{Z/N}} = -\frac{e^{-\varepsilon+i\theta}}{1-e^{-\varepsilon+i\theta}}\,. \tag{8.78}$$

Expanding the denominator in a geometric series and using Eq. (8.76) yields

$$\rho_N^{\rm true}(\theta,t=0) = 1 + e^{i\theta}\sum_{k=0}^{\infty} e^{ik\theta} + e^{-i\theta}\sum_{k=0}^{\infty} e^{-ik\theta} = \sum_{k=-\infty}^{\infty} e^{ik\theta} = 2\pi\delta_{2\pi}(\theta) \tag{8.79}$$

in agreement with Eq. (8.27). Note that the initial distribution $\rho_N^{\rm true}(\theta,t=0)$ is independent of N.

9 Comparison of the three eigenvalue densities

In this section, we compare the true eigenvalue density ρ_N^{true} with the two other densities ρ_N^{asym} and ρ_N^{sym} at finite N.

The antisymmetric density is determined by the zeros of the average of the characteristic polynomial. The average $\langle \det(z - W) \rangle$ is a polynomial of order N in the complex variable z, which is explicitly given by Eq. (5.35). We compute the zeros of this polynomial numerically.

As mentioned in Sec. 5.6, $\rho_N^{\text{sym}}(\theta, T)$ has an explicit form in terms of infinite sums, cf. Eq. (5.90). These sums converge rapidly and can be used to compute $\rho_N^{\text{sym}}(\theta, T)$ to any desired accuracy.

In Sec. 8, we have derived a representation for the true resolvent $G_{N,-}^{\text{true}}(v, t)$ in terms of a double sum, cf. Eq. (8.22). Similar to the symmetric case, we do not need the limiting procedure $\varepsilon \to 0$ ($v = e^{i\theta - \varepsilon}$), the double sum converges for $|v| = 1$ and can be computed numerically. The density $\rho_N^{\text{true}}(\theta, t)$ is then obtained from the resolvent through Eq. (8.23).

Before comparing the three densities with each other, we present a consistency check of our numerical results for $\rho_N^{\text{true}}(\theta, t)$. To this end, we make use of the fact that the probability distribution for the Wilson loop matrix W coincides with the probability distribution generated in the multiplicative random matrix model introduced by Janik and Wieczorek, cf. Sec. 4.4.5. Figure 29 shows that the eigenvalue density obtained from the multiplicative random matrix model is in perfect agreement with our results for ρ_N^{true}.

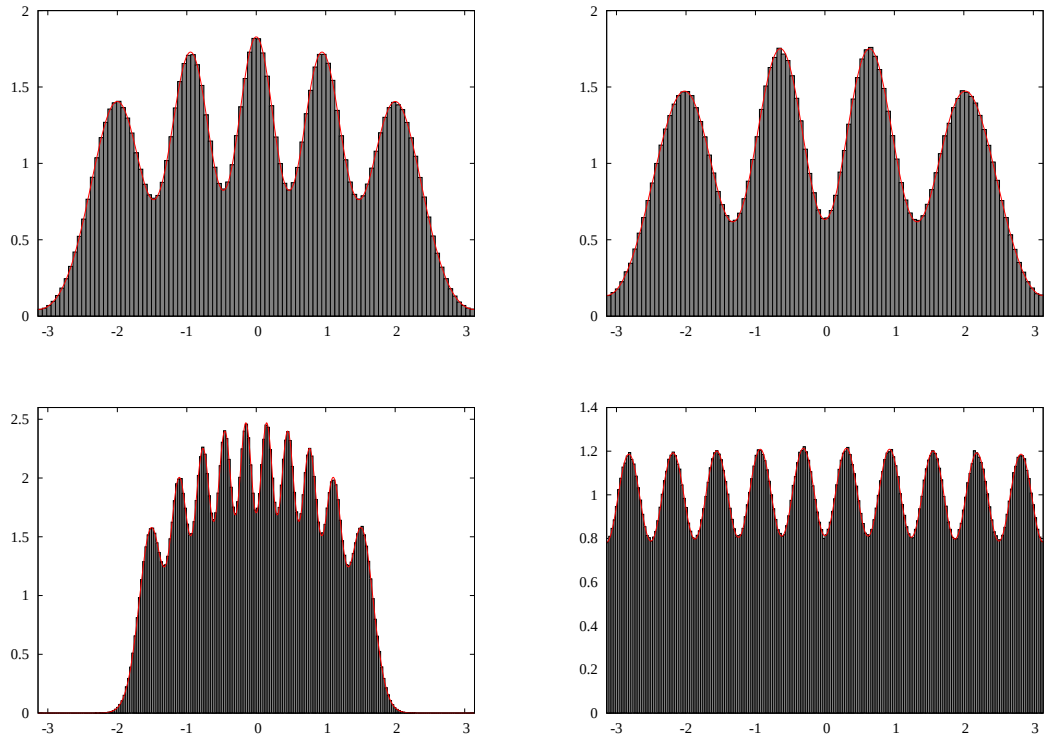

Figure 29: The red curves show plots of ρ_N^{true} as a function of θ, obtained by computing the double sum in Eq. (8.22) for $t = 3$ and $N = 5$ (top, left), $t = 4$ and $N = 4$ (top, right), $t = 1$ and $N = 10$ (bottom, left), and $t = 10$ and $N = 10$ (bottom, right). The histograms show the normalized eigenvalue distributions obtained numerically from the multiplicative random matrix model for the same choices of t and N. In each case, this eigenvalue distribution is obtained by computing the eigenvalues of a set of 5×10^5 product matrices with $n = 10^3$ factors in each product.

9.1 Comparison of $\rho_N^{\text{true}}(\theta, t)$ and $\rho_N^{\text{sym}}(\theta, T)$

If we want to compare $\rho_N^{\text{true}}(\theta, t)$ and $\rho_N^{\text{sym}}(\theta, T)$, we have to take into account the $1/N$ difference between t and T, see Eq. (5.3). At fixed N and t, we have to compare $\rho_N^{\text{true}}(\theta, t)$ and $\rho_N^{\text{sym}}(\theta, T = t(1-1/N))$. The densities ρ_N^{true} and ρ_N^{sym} can be obtained numerically by evaluating the sums in Eq. (8.22) and Eq. (5.89), respectively.

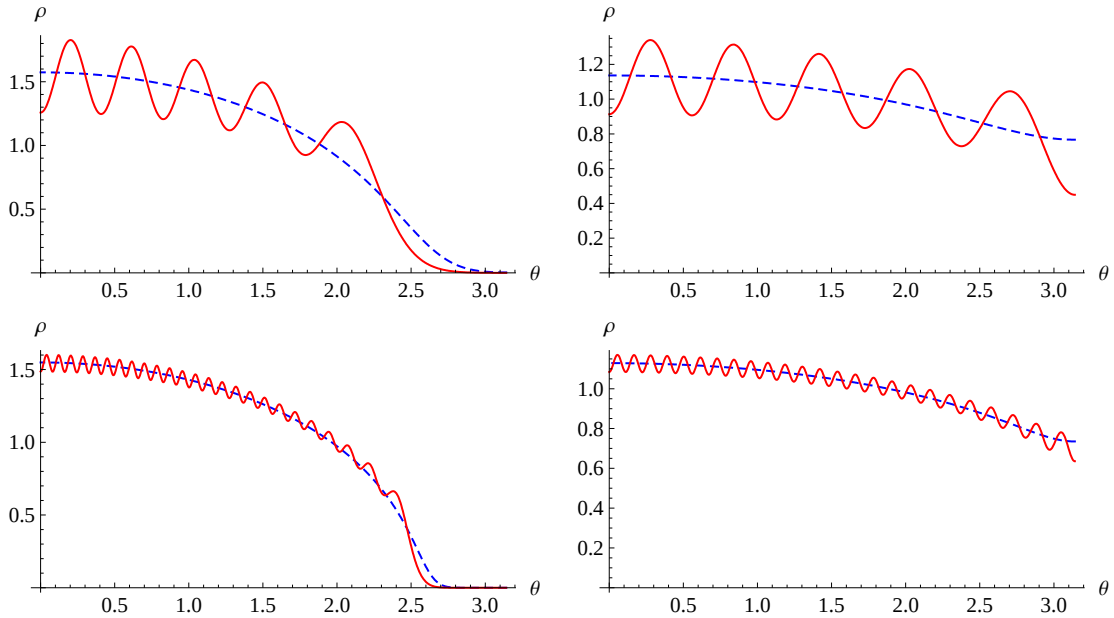

Figure 30: Plots of the densities $\rho_N^{\text{true}}(\theta, t)$ (red, solid) and $\rho_N^{\text{sym}}(\theta, T)$ (blue, dashed) for $t = 2$ (left) and $t = 5$ (right), $N = 10$ (top) and $N = 50$ (bottom).

Figure 30 shows plots of $\rho_N^{\text{true}}(\theta, t) = \rho_N^{\text{true}}(-\theta, t)$ and $\rho_N^{\text{sym}}(\theta, T) = \rho_N^{\text{sym}}(-\theta, T)$ for $t = 2$ and $t = 5$ with $N = 10$ and $N = 50$ in the interval $0 \le \theta \le \pi$. As observed in Sec. 5.6, $\rho_N^{\text{sym}}(\theta, T)$ decreases monotonically in that interval. The true eigenvalue density $\rho_N^{\text{true}}(\theta, t)$ has N peaks (in the complete interval $[-\pi, \pi]$) and oscillates around the non-oscillatory function $\rho_N^{\text{sym}}(\theta, T)$.

9.2 Comparison of $\rho_N^{\text{true}}(\theta, t)$ and $\rho_N^{\text{asym}}(\theta, \tau)$

The density $\rho_N^{\text{asym}}(\theta, \tau)$ is given by a sum of N delta functions, located at the zeros of the average characteristic polynomial, see Sec. 5.5. Figure 31 shows that the locations of these zeros are close to the positions of the N peaks of $\rho_N^{\text{true}}(\theta, t)$. Here we again have to take into account the $1/N$ difference in the definitions of t and τ. For fixed N and t, the peaks of $\rho_N^{\text{true}}(\theta, t)$ have to be compared to the zeros of $\langle \det(e^{i\theta} - W) \rangle$ at $\tau = t(1 + 1/N)$.

Numerical computations of the positions of the peaks and valleys of ρ_N^{true} and the corresponding zeros of the average characteristic polynomial for large N show that the difference in position between a peak and its matching zero vanishes faster than the difference in position between that peak and the next valley. This means that

$$\gamma = \left| \frac{\theta^{(\text{peak})} - \theta^{(\text{matching zero})}}{\theta^{(\text{peak})} - \theta^{(\text{next valley})}} \right| \tag{9.1}$$

decreases with increasing N. Numerically, we find that γ scales as

$$\gamma \propto N^{-\mu} \quad \text{with} \quad \mu > 0 \tag{9.2}$$

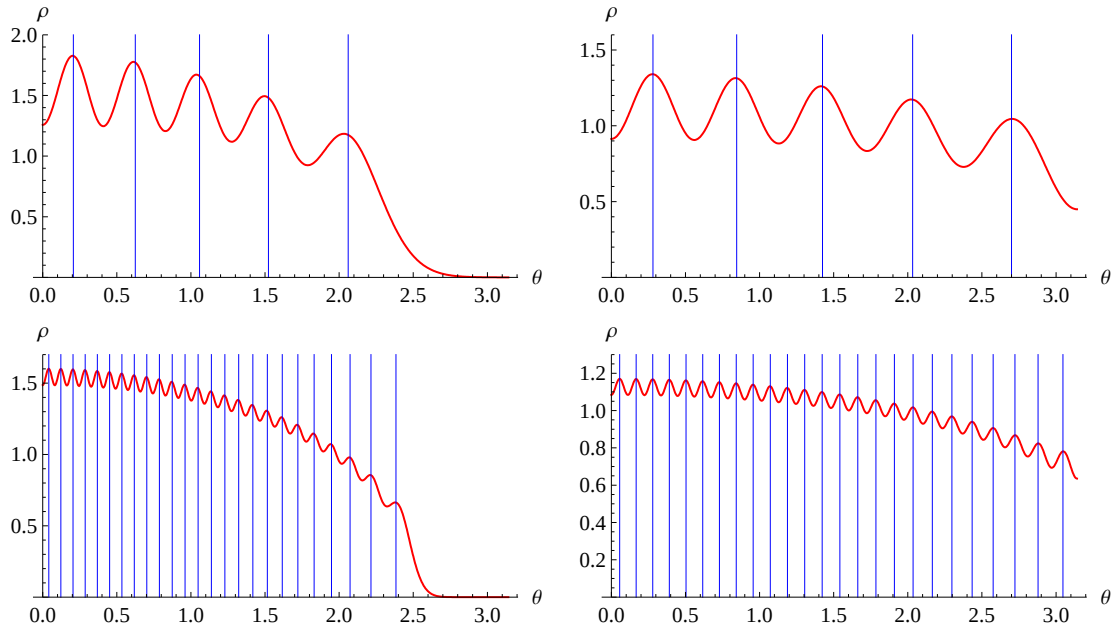

Figure 31: Plots of the density $\rho_N^{\text{true}}(\theta,t)$ (oscillatory red curve) together with the positions of the zeros of $\langle \det(e^{i\theta}-W)\rangle$ (vertical blue lines) for $t=2$ (left) and $t=5$ (right), $N=10$ (top) and $N=50$ (bottom).

for large N. It turns out that the value of the exponent μ depends on t and may be different in different parts of the spectrum, but it is always positive (for large N).

In the bulk of the spectrum, the difference between peak and neighboring valley scales as N^{-1}, whereas the difference between peak and matching zero scales as N^{-2} for all t. This results in $\mu_{\text{bulk}}=1$. Figure 32 shows a plot of $\log\gamma$, computed for the peak closest to $\theta=0$ (for even N), as a function of $\log N$ for $t=5$. The line fitted through the data points has a slope of $-1+\mathcal{O}(10^{-3})$. (The reason for choosing θ close to 0 is that stable fit results can be obtained for lower values of N.)

For $t>4$, the infinite-N limit of the eigenvalue density, $\rho_\infty(\theta,t)$, has no gap. In this case, the scaling behavior does not change as one goes to higher $|\theta|$, but it is necessary to go to large values of N to get stable fit results for μ when $|\theta|$ is close to π. (For $t=5$, e.g., a fit at $N\approx 1000$ results in $\mu\approx 1.04$ for the extremal peak.)

At the transition point, the situation is different. From Eq. (6.65) we know that the difference between the position of the extremal zero (the zero closest to π) and π vanishes as $N^{-\frac{3}{4}}$ (to leading order in $1/N$) for $\tau=4$. Between $N=1800$ and $N=2800$, the scaling of the difference between the extremal zero and its critical-τ approximation is in agreement with the expected $N^{-\frac{5}{4}}$ correction. The difference between that zero and the extremal peak position is found to scale roughly as $N^{-1.11}$, and the difference between the positions of the peak and the next valley (the valley that is closer to $\theta=0$) scales as $N^{-0.83}$. This results in $\mu_{\text{critical}}\approx 0.28$. The plot of $\log\gamma$ for that case (see Fig. 32) indicates that the value of μ_{critical} might slightly increase as one goes to even higher values of N (which would require more computation time).

For $t<4$, there is a gap in the spectrum. In this case, the exponent μ also has different values at the edge and the bulk of the spectrum, but the variation is not as large as it is at the critical point. For $t=3$, e.g., a fit between $N=1000$ and $N=1500$ results in $\mu\approx 0.64$ for the extremal peak. For small $|\theta|$, we find again that $\mu=\mu_{\text{bulk}}=1$.

The numerical estimates for the scaling exponent μ are not very precise, our main

conclusion here is that the ratio γ decreases with increasing N in all investigated cases. Naturally, we expect the exact values of the various exponents of N that enter to be rational numbers with denominators 3 or 4 or 12 (see Sec. 6.1.4).

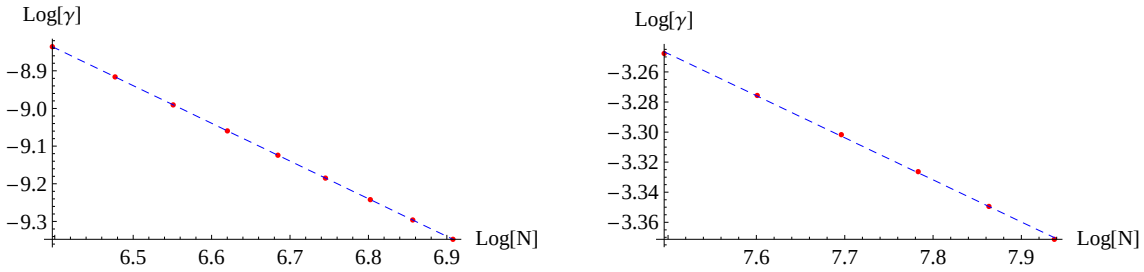

Figure 32: Plots of $\log \gamma$ for the peak closest to $\theta = 0$ at $t = 5$ (left) and for the peak closest to $\theta = \pi$ at $\tau = 4$ (right). Data points (red) are shown together with the fitted line (blue, dashed).

Part III

Large-N transitions for products of random complex matrices

In the previous parts of this thesis, we have seen that Wilson loops in SU(N) gauge theory in two Euclidean dimensions exhibit an infinite-N transition, the Durhuus-Olesen phase transition. The eigenvalue distribution of the untraced Wilson loop unitary matrix expands from a small arc on the unit circle to encompassing the entire unit circle as the size of the underlying spacetime curve is increased. Furthermore, there is numerical evidence from lattice simulations that a similar transition occurs also in three and four spacetime dimensions in eigenvalue distributions of smeared Wilson loops, cf. Sec. 4.4.6. Moreover, it turns out that the universality class of this transition is that of a simple multiplicative ensemble of random unitary matrices, cf. Sec. 4.4.5.

In this part, the unitarity constraint is relaxed and we focus on a multiplicative random complex matrix model, which is similar to the one introduced by Gudowska-Nowak et al. in Ref. [3], where it was also observed that the model leads to an infinite-N phase transition in the eigenvalue spectrum. The results presented in this part of the thesis have been obtained in collaboration with Herbert Neuberger and Tilo Wettig and are published in Ref. [49]. A physical application for this study would be a more general gauge theory, obeying extra symmetries (e.g., in a supersymmetric theory[13]), which would make complex matrix-valued Wilson loop operators natural observables. Moreover, complex matrix transitions may also be relevant to ordinary gauge theories, in dimensions higher than two, since ultraviolet divergences of the bare Wilson loop matrix can be eliminated by a regularization prescription that makes the Wilson loop operator non-unitary, e.g., by introducing an extra scalar field $\Phi = \Phi^\dagger$ transforming as an adjoint under the gauge group, with a mass much heavier than the QCD scale Λ_{QCD}. This means that we could associate with a simple closed curve C in four-dimensional spacetime the operator

$$W_C = P e^{\oint_C [iA_\mu(x)dx_\mu + \Phi(x)|dx|]} , \tag{9.3}$$

where $A_\mu = A_\mu^\dagger$ is the usual gauge field, and $x_\mu(s)$ describes the curve C. By adjusting the normalization of Φ, its contribution could be made to cancel out the linear perimeter divergence associated with the standard Wilson loop operator (cf. Sec. 3.4.3) but otherwise have little impact on smooth loops larger than the QCD scale on account of its large mass. For this to work, Φ must enter the exponent without a $\sqrt{-1}$ prefactor. The regularization would make W a finite operator, but clearly one cannot associate it with a unitary matrix, and its spectrum would be spread somewhat in the complex plane, defining a finite surface eigenvalue density rather than a finite linear eigenvalue density on the unit circle.

If the situation for ordinary gauge theories, where the matrix of the Wilson loop operator is unitary, generalizes to the complex case, the multiplicative random complex matrix model might perhaps capture the universal features of large-N transitions occurring in these non-unitary observables. Multiplicative random matrix models in general are

[13] Although very special Wilson loops can be well described by single-matrix models (cf. Refs. [57, 58]), we think that it is quite possible that non-commutativity will play an essential role in less special cases.

of relevance to a wide range of other physical and non-physical applications, including, e.g., the stability analysis of chaotic and disordered systems (such as spin models with random interaction, wave functions and their localization properties in random potentials, or large economic and social systems), thermal properties of magnetic systems, differential equations with random coefficients, methods of image compression, and communication via antenna arrays (see Refs. [3, 59] and references therein).

Following Ref. [49], we start in Sec. 10 by presenting a set of natural[14] symmetries that we assume the complex Wilson loop matrices to obey. We show that these symmetries, together with the assumption that the complex Wilson loop has a perturbative weak-coupling regime and a non-perturbative "disordered" regime (in analogy to the unitary case studied in part II), already point to a large-N phase transition in the spectrum of the complex Wilson loop matrix W. The support of the eigenvalues of W undergoes a topological change at the transition point, indicating that there might be something universal about the transition (we refer to this hypothetical universality as large-N universality). We then set up a simple multiplicative random complex matrix model which obeys the general symmetry requirements and therefore could be in the same large-N universality class as the above Wilson loops. We proceed by discussing the general properties of the model, where some time is devoted to a technical point: Simplifications occur when one drops the $\det W = 1$ constraint, but it turns out that dropping the constraint has no impact on the infinite-N phase structure. Without actually solving the random matrix model, we find that the shape of the support of the spectrum of W at infinite N is constrained to an annulus in the complex plane. As the loop size of W changes, the spectrum evolves from a simply connected small blob centered at $z = 1$ to a multiply connected region, contained in the annulus confining the spectrum.

A more detailed analysis of the basic multiplicative random complex matrix model is presented in Sec. 11 using the average of the modulus square of the characteristic polynomial of W. The main analytical tool is a representation of this observable in terms of an integral over Grassmann variables. After the introduction of the anticommuting Grassmann variables, the matrix averaging over the individual factors in the random matrix product can be done independently, which eventually makes the entire dependence on N explicit and hence allows for a saddle-point analysis at large N. The analysis is performed only to the extent that it gives the phase structure in the infinite-N limit, global stability questions are dealt with by numerical tests and not by purely analytical methods.

In order to get some feeling for the universal properties of the model, we proceed with a slight generalization in Sec. 12 by introducing extra parameters in the probability distribution of the individual factors of the matrix product. This allows for a smooth interpolation between the complex multiplicative matrix model and the unitary multiplicative matrix model. This generalized model provides further support to the view that in some sense the large-N transition here has a direct relationship to the large-N transition found in pure gauge theories with unitary Wilson loop matrices. It is seen that, similarly to the original complex matrix model and to the unitary matrix model, the inviscid Burgers equation plays a central role also in the generalized model.

Although the infinite-N phase structure indicates that there is a large-N universality class associated with it, it is necessary to go to sub-leading terms in the large-N expansion to make this more concrete. We show in Sec. 13 for arbitrary finite N that the average of the modulus square of the characteristic polynomial of the $N \times N$ complex matrix W can be exactly represented by the solution of an associated multiplicative matrix model, where the matrices are only two-dimensional and the dependence on N is explicit. Unfortunately,

[14] motivated by an Euclidean gauge theory producing the Wilson loops

this still leaves too many variables (albeit a finite, N-independent number), preventing an explicit analysis of the approach to the large-N limit. The 2×2 model can be simplified by focusing on some special cases, and we finally present a case where we end up with only two real variables and show how that model could be solved exactly. However, the solution is in the form of an infinite series, and the study of the large-N limit still presents difficulties.

10 Basic multiplicative random complex matrix model

10.1 General properties of complex Wilson loop matrices

Before we introduce our multiplicative random matrix model, let us imagine that we have some Euclidean field theory providing a probability distribution $\mathcal{P}(W)$ for complex Wilson loop matrices W. Without specifying the details of the theory, we furthermore assume, in analogy to the unitary case, that this distribution possesses the natural properties $\det W = 1$, $\mathcal{P}(W) = \mathcal{P}(W^{-1}) = \mathcal{P}(W^*)$, and $\mathcal{P}(W) = \mathcal{P}(UWU^\dagger)$ for $U \in \mathrm{U}(N)$. A construction of W in terms of traceless double indexed fields and discrete symmetries like parity and charge conjugation could assure the first two properties. Gauge invariance would imply the third property. In the next section, we set up a concrete multiplicative random matrix model for W, leading to a probability distribution satisfying the above requirements. Here, we argue that these symmetry requirements alone already point towards a topological transition in the spectrum of complex Wilson loop matrices.

To study the spectral properties of W, we define

$$Q(z, z^*) = \langle |\det(z - W)|^2 \rangle, \tag{10.1}$$

where $\langle \ldots \rangle$ denotes averaging with respect to $\mathcal{P}(W)$. The general properties of the probability distribution then imply

$$Q(z, z^*) = Q(z^*, z) = |z|^{2N} Q(1/z^*, 1/z) = |z|^{2N} Q(1/z, 1/z^*)\,. \tag{10.2}$$

Motivated by the properties of unitary Wilson loops in $\mathrm{SU}(N)$ Yang-Mills theory, let us assume that the probability distribution $\mathcal{P}$ of the complex matrix W, and consequently also the observable Q, depends on an area variable $t \geq 0$ (maybe defined in terms of a running coupling constant) which allows for scaling the physical (spacetime) size of the loop. Generically, $N \times N$ random matrices have regions in the spectral plane where the eigenvalue density is exponentially suppressed at large N, resulting in vanishing eigenvalue density in these regions at infinite N. Since the surface eigenvalue density at infinite N cannot vanish everywhere, the infinite-N limit induces some lack of smoothness in the eigenvalue density. Typically, the eigenvalue density is guaranteed to be non-zero somewhere in the plane (rather than disappearing at infinity) because for a small loop, W is close to the identity matrix. However, the condition $\det W = 1$ ensures that 0 is not an eigenvalue. We therefore assume that in the $N = \infty$ limit, for any t, the probability of W having eigenvalues within some small finite circle around $z = 0$ is zero. The radius of the circle increases to unity when $t \to 0$ when all the eigenvalues of W are forced into a shrinking region around $z = 1$. Typically, this is reflected in $Q(z, z^*)$ having a holomorphic factorized form for $|z| < \rho(t) < 1$ (cf. Sec. 11.1),

$$Q(z, z^*) = |f(z)|^2\,. \tag{10.3}$$

Due to the inversion symmetry (10.2), the eigenvalue density vanishes also around complex infinity, and we can think of the complex plane as a two-dimensional sphere with the

north and south poles excised. At infinite N, the eigenvalues make up a connected region containing $z = 1$ for any size of the loop. This region is very small and does not wrap around the doubly punctured sphere for small loops.

When t is increased, the dynamics of the particular model become important. We are interested in the case where large loops produce strong disorder in the Wilson loop spectrum because the probability distribution $\mathcal{P}(W)$ becomes less restrictive and the set of eigenvalues can spread widely (this is the case, e.g., in confining theories). Then it makes sense to assume that the spectrum completely surrounds the origin $z = 0$ (as in the case of unitary Wilson loops). As a result, the simply connected domain where the eigenvalues reside for small loops becomes topologically non-trivial on the doubly punctured sphere, becoming multiply connected due to the punctures. In principle, more complicated topology changes could happen, but intuitively, this is the generic way in which eigenvalues would spread out as disorder increases in a model obeying the general symmetries described earlier. (This behavior is also observed, e.g., in generic non-Gaussian and non-Hermitian single random matrix models, cf. Ref. [60].)

As observed above, $z = 1$ will typically be in the domain of eigenvalues. Thus, the unit circle intersects the set of possible eigenvalues and we can look for a signal of the transition on $|z| = 1$. This signal would be the entrance of the point $z = -1$ into the domain of non-vanishing eigenvalue density as the area variable t is increased from zero through the transition point. The points $z = \pm 1$ are special because they are fixed points of the inversion symmetry. The point $z = 1$ is in the domain of eigenvalues for any t, and the topological transition occurs when $z = -1$ also joins. This description makes the similarity with the unitary matrix case clear. The new feature is that as we go from the unitary model to the complex one, the eigenvalues of the product matrix are no longer confined to the unit circle, they spread out from a one-dimensional arc on the unit circle to a "fattened" arc in the complex plane.

10.2 Definition of the model – SL($N, \mathbb{C}$) case

We now introduce a simple random matrix model for complex Wilson loop matrices. Basically, we replace the true $\mathcal{P}(W)$ (produced by some Euclidean field theory) by a much simpler one, obeying the symmetry requirements described in the previous section. The model is almost[15] identical to the one studied by Gudowska-Nowak et al. in Ref. [3].

The integration measure over complex numbers $z = x + iy$ is defined as

$$d\mu(z) = dxdy\,. \tag{10.4}$$

We first consider the space of traceless $N \times N$ complex matrices C and define a normalized probability density over it,

$$P(C)d\mu(C) = e^{-N \operatorname{Tr} C^\dagger C} \pi\delta(\operatorname{Tr} C) \prod_{1\le i,j\le N} \frac{N}{\pi} d\mu(C_{ij})\,, \tag{10.5}$$

where the complex delta function is defined as $\delta(z) = \delta(x)\delta(y)$. For any complex matrices A and B, we find that (see App. B.3)

$$\int P(C)d\mu(C) e^{\operatorname{Tr} C^\dagger A + \operatorname{Tr} B^\dagger C} = e^{\frac{1}{N}\operatorname{Tr}(B^\dagger A) - \frac{1}{N^2}(\operatorname{Tr} A)(\operatorname{Tr} B^\dagger)}\,. \tag{10.6}$$

We define a sequence of n independent and identically distributed (i.i.d.) matrices M_j, $j = 1, \ldots, n$,

$$M_j = e^{\varepsilon C_j}\,, \tag{10.7}$$

[15] The minor difference is irrelevant after all the limits are taken, see Sec. 11.5.

where every C_j is distributed by $P(C_j)$ and $\varepsilon > 0$ is a small number[16]. The delta function in the probability density (10.5) ensures $\det(M_j) = 1$ for all $j = 1, \ldots, n$. The distributions of the C_j's are invariant individually under $C_j \to C_j^*, -C_j$ and $C_j \to U_j^\dagger C_j U_j,\ U_j \in \mathrm{U}(N)$.

We now multiply the M_j's and define

$$W_n = M_1 M_2 \cdots M_n = \prod_{j=1}^{n} M_j \,. \tag{10.8}$$

Due to the symmetries of the probability distribution $P(C_j)$, the matrices M_j, M_j^*, M_j^{-1} and $U^\dagger M_j U$, $U \in \mathrm{U}(N)$, are equally probable. Moreover, any two permuted sequences of M_j's are equally probable since the C_j's are independent and identically distributed. The distribution of the random matrix W_n therefore fulfills the natural complex-Wilson-loop properties listed in the previous section.

We are interested in the limit $n \to \infty$, $\varepsilon \to 0$ with $t = \varepsilon^2 n$ held fixed at a non-negative value. In that limit, the product matrix W will be a finite matrix, and we are interested in the properties of its distribution as a function of the parameter t. (Restricting the matrices C_j to be anti-Hermitian, we would recover the multiplicative unitary random matrix model described in Sec. 4.4.5. In this case, the parameter $n\varepsilon^2$ can be identified with the dimensionless area variable $t = \lambda A$, which determines the probability distribution of unitary Wilson loops in Yang-Mills theory in two Euclidean dimensions. We will return to the unitary case in Sec. 12, where the generalized multiplicative random matrix model is introduced.)

10.3 Definition of the model – GL($N, \mathbb{C}$) case

Above, the matrices W were strictly constrained to have unit determinant. Imposing the linear restriction $\operatorname{Tr} C = 0$ forces $W_n \in \mathrm{SL}(N, \mathbb{C})$ for any sequence M_j. However, little is lost by relaxing the determinant restriction since, as we shall see below (in Secs. 10.4.3 and 11.4), this has no effect on the boundary of the region of non-vanishing eigenvalue density in the infinite-N limit.

Without the restriction on the determinant, we would define a probability density (instead of Eq. (10.5)) by

$$P(C)d\mu(C) = e^{-N \operatorname{Tr} C^\dagger C} \prod_{1 \le i,j \le N} \frac{N}{\pi} d\mu(C_{ij}) \,, \tag{10.9}$$

which would then lead to (see App. B.3)

$$\int P(C)d\mu(C) e^{\operatorname{Tr} C^\dagger A + \operatorname{Tr} B^\dagger C} = e^{\frac{1}{N} \operatorname{Tr} B^\dagger A} \,. \tag{10.10}$$

The single effect of relaxing the restriction $\operatorname{Tr} C_j = 0$ is that we are now left with only the first term in the exponent of the RHS of Eq. (10.6).

10.4 Fokker-Planck equation and determinant restriction

In this section we drop the determinant restriction and argue that this does not affect the $N = \infty$ limit.

[16] For a complex ε, any complex phase could be absorbed in the matrix C due to the invariance of $P(C)$ under $C \to e^{i\phi} C$, leaving us just with $\varepsilon > 0$ as the generic case.

10.4.1 Derivation of the Fokker-Planck equation

In the limit $n \to \infty$ with t fixed, the joint probability distribution of the entries of the matrix W for finite N is $P_N(W_{\alpha\beta};t)d\mu(W)$, where the $W_{\alpha\beta}$'s are N^2 complex numbers and $d\mu(W)$ is some conveniently chosen measure which is independent of t. Since W is a product of i.i.d. matrices, the probability distribution P_N is determined by a Markov chain [61] and will therefore satisfy a partial differential equation of the form [62]

$$\frac{\partial P_N}{\partial t} = \Omega_N P_N \,, \tag{10.11}$$

where Ω_N is a linear partial differential operator of at most second order acting on the $2N^2$ real variables defining the N^2 complex numbers $W_{\alpha\beta}$. The operator Ω_N, which depends explicitly on N but not on t, is determined by the terms of order ε and ε^2 of M_n in the recursion $W_n = W_{n-1}M_n$, higher-order terms do not matter (cf. Sec. 10.4.2 for a simple example illustrating the procedure). Equation (10.11) is an equation of the Fokker-Planck type. Its solution is determined by the initial condition at $t = 0$, which in our case is a delta function with respect to $d\mu(W)$ concentrated at $W = \mathbf{1}$.

The Fokker-Planck equation for P_N is derived by first expressing the step-n probability density $P_N^{(n)}(W;t)d\mu(W)$ in terms of $P_N^{(n-1)}(W';t')d\mu(W')$, where ε^2 is kept fixed (i.e., $t' = (n-1)\varepsilon^2 = t - \varepsilon^2$). The computation is based on the linear recursion

$$W = W'M \,, \tag{10.12}$$

where $M = e^{\varepsilon C}$ with C distributed according to $P(C)d\mu(C)$. The main step is to express $P_N^{(n)}(W;t)d\mu(W)$ in terms of W' and t' going to order ε^2. M acts linearly on the rows of W', and therefore the Jacobian (taking care of the change in the measure) is given by the product of the Jacobians per row, which is $|\det M|^{2N} = e^{2N\varepsilon \operatorname{Re}\operatorname{Tr} C}$. The expansion in W' around W produces first-order derivatives of $P_N^{(n-1)}$ at order ε and ε^2 and second-order derivatives at order ε^2. After averaging over the matrix C, the measure terms of order ε^2 give terms proportional to $P_N^{(n-1)}$, while measure terms of order ε can combine with terms of order ε from the expansion of $P_N^{(n-1)}$, giving first-order derivative terms in $P_N^{(n-1)}$. All second-order derivative terms in $P_N^{(n-1)}$ come from the expansion of $P_N^{(n-1)}$ and not from the measure.

10.4.2 One-dimensional example

Let us consider a simple one-dimensional example to illustrate the derivation of the Fokker-Planck equation which is described in the previous section based on Ref. [62]. To this end, we replace the complex matrices C_j by ordinary real numbers c_j which are distributed with the Gaussian probability distribution

$$p(c) = \frac{1}{\sqrt{\pi}} e^{-c^2} \,. \tag{10.13}$$

We define the step-n probability distribution of the (Abelian) product $w = \prod_j e^{\varepsilon c_j}$ as

$$P^{(n)}(w;t) = \left\langle \delta\left(w - \prod_{j=1}^{n} e^{\varepsilon c_j} \right) \right\rangle_{c_1,\ldots,c_n} \,, \tag{10.14}$$

where we average over all n numbers c_j and set $\varepsilon = \sqrt{t/n}$. Next, we relate $P^{(n)}$ to $P^{(n-1)}$ by averaging over $c_1, c_2, \ldots, c_{n-1}$,

$$P^{(n)}(w;t) = \left\langle e^{-\varepsilon c_n} \delta\left(w e^{-\varepsilon c_n} - \prod_{j=1}^{n-1} e^{\varepsilon c_j} \right) \right\rangle_{c_1,\ldots,c_n} = \left\langle e^{-\varepsilon c_n} P^{(n-1)}(w',t') \right\rangle_{c_n} \tag{10.15}$$

with $w' = e^{-\varepsilon c_n} w$ and $t' = (n-1)\varepsilon^2 = t - t/n$. Following the general procedure described in the previous section, we now expand $P^{(n-1)}(w';t')$ around $P^{(n-1)}(w;t)$ to quadratic order in ε,

$$\begin{aligned} P^{(n-1)}(w';t') = P^{(n-1)}(w;t) - \varepsilon^2 \partial_t P^{(n-1)}(w;t) + \partial_w P^{(n-1)}(w;t) w \left(-\varepsilon c_n + \frac{1}{2}\varepsilon^2 c_n^2 \right) \\ + \frac{1}{2}\partial_w^2 P^{(n-1)}(w;t) \varepsilon^2 w^2 c_n^2 + \mathcal{O}(\varepsilon^3) \,. \end{aligned} \tag{10.16}$$

In combination with the additional measure term $e^{-\varepsilon c_n}$, averaging over c_n results in

$$P^{(n)}(w;t) = P^{(n-1)}(w;t) + \varepsilon^2 \left[\frac{1}{4} - \partial_t + \frac{3}{4} w \partial_w + \frac{1}{4} w^2 \partial_w^2 \right] P^{(n-1)}(w;t) \,. \tag{10.17}$$

Finally, assuming the convergence of $P^{(n)}(w;t)$ to a limiting distribution $P(w;t)$ in the limit $n \to \infty$ leads to the Fokker-Planck equation

$$\partial_t P(w;t) = \frac{1}{4} \left(1 + 3 w \partial_w + w^2 \partial_w^2 \right) P(w;t) \,. \tag{10.18}$$

The solution which reduces to $\delta(w-1)$ for $t \to 0$ is given by

$$P(w;t) = \frac{1}{w\sqrt{\pi t}} e^{-\frac{1}{t}(\log w)^2} \,. \tag{10.19}$$

Due to the Abelian nature of this simple one-dimensional model, we obviously could have computed the step-n probability distribution in Eq. (10.14) directly, simply by integrating over the real and Gaussian-distributed numbers c_j, which immediately (after an $\mathrm{O}(n)$ rotation) results in

$$P^{(n)}(w;t) = \int_{-\infty}^{\infty} \frac{dx}{\sqrt{\pi}} e^{-x^2} \delta\left(w - e^{\varepsilon\sqrt{n} x} \right) = \frac{1}{w\sqrt{\pi n \varepsilon^2}} e^{-\frac{1}{n\varepsilon^2}(\log w)^2} \,. \tag{10.20}$$

With $t = n\varepsilon^2$, we recover Eq. (10.19).

10.4.3 Factorization of the probability distribution

The discussion in Sec. 10.4.1 simplifies if one chooses a measure term that is invariant under the recursion. This is possible in many cases when the evolution is on a group manifold. In our case, it is convenient to parametrize $W \in \mathrm{GL}(N,\mathbb{C})$ as $W = w\tilde{W}$ with $w^N = \det(W)$ and $\tilde{W} \in \mathrm{SL}(N,\mathbb{C})$. Correspondingly, we factorize the measure $d\mu(W) = d\mu(w) d\mu(\tilde{W})$, where $d\mu(\tilde{W})$ is right-invariant on $\mathrm{SL}(N,\mathbb{C})$. By induction in n, we see that the step-n probability distribution $P_N^{(n)}(W;t)$ also factorizes in these variables since if $P_N^{(n-1)}$ is factorized, so is $P_N^{(n)}$, and the initial condition also factorizes. We therefore have

$$P_N^{(n)}(W;t) = P_N^{(n)1}(w;t) P_N^{(n)2}(\tilde{W};t) \,. \tag{10.21}$$

The distribution of the determinant, $P_N^{(n)1}$, is very easy to compute as it comes from an Abelian ensemble (similar to the one discussed in Sec. 10.4.2). Because of the choice for the measure term and because of the invariance of M under conjugation by $\mathrm{SU}(N)$ elements, the Fokker-Planck equation is invariant under $W \to WU$ with $U \in \mathrm{SU}(N)$.

In the limit $\varepsilon \to 0$, $n \to \infty$ at fixed t, we obtain

$$P_N^{(n)}(w, \tilde{W}; t) \to p_N(w; t) P_N(\tilde{W}; t)\,. \tag{10.22}$$

If W were a product of $\mathrm{SU}(N)$ matrices, the form of the operator Ω_N would be uniquely fixed up to an overall constant to being the Laplacian on the $\mathrm{SU}(N)$ group manifold because of the invariance under right multiplication by elements of $\mathrm{SU}(N)$, i.e., the Fokker-Planck equation would become the heat-kernel equation on $\mathrm{SU}(N)$. (If we would require $C_j = -C_j^\dagger$ in the sequence (10.8) defining W, the model would reduce to the unitary model introduced by Janik and Wieczorek, cf. Sec. 4.4.5.)

Using the parametrization $w^N = \det W = e^{u+iv}$ with $u, v \in \mathbb{R}$, we observe that both u and v are normally distributed and their distributions are N-independent: With $\tilde{C}_j = C_j - \frac{1}{N} \operatorname{Tr} C_j$, we have $\operatorname{Tr} \tilde{C}_j = 0$, and the exponent that enters in the probability distribution (10.9) reads

$$-N \operatorname{Tr}\left(C^\dagger C\right) = -N \operatorname{Tr}\left(\tilde{C}^\dagger \tilde{C}\right) - |\operatorname{Tr} C|^2\,. \tag{10.23}$$

Thus, the distribution of $\operatorname{Tr} C_j$ does not depend on N and determines $P_N^{(n)1}(w)$ through the obvious relation

$$w^N = \det W = \det \prod_{j=1}^{n} M_j = \prod_{j=1}^{n} \det\left(e^{\varepsilon C_j}\right) = e^{\varepsilon \sum_{j=1}^{n} \operatorname{Tr} C_j}\,. \tag{10.24}$$

Therefore, replacing W by $\tilde{W}$ in averages of characteristic polynomials (which we will use below to study the spectral properties) only produces an unimportant prefactor in the large-N limit,

$$\begin{aligned} \det(z - W) &= w^N \det\left(\frac{z}{w} - \tilde{W}\right) = e^{u+iv} \det\left(\frac{z}{e^{\frac{1}{N}(u+iv)}} - \tilde{W}\right) \\ &\to e^{u+iv} \det\left(z - \tilde{W}\right)\,, \end{aligned} \tag{10.25}$$

since the probability distribution of $u+iv$ is independent of N. As a result, we see that we can use $\mathrm{GL}(N, \mathbb{C})$ instead of $\mathrm{SL}(N, \mathbb{C})$ without affecting the large-N limit. At subleading order in $1/N$ there are differences, but they are easily determined from $p_N(w; t)$ and little is lost by working with $\mathrm{GL}(N, \mathbb{C})$ instead of $\mathrm{SL}(N, \mathbb{C})$. This result is independently confirmed by the saddle-point analysis presented in Sec. 11.4.

10.5 Bounds for the domain of non-vanishing eigenvalue density

Our objective is to determine the region in the z-plane populated by eigenvalues of W_n in the limit $n \to \infty$, $\varepsilon \to 0$, $t = n\varepsilon^2$ fixed. As a first step, we would like to find some bounds delimiting this region. The region will have a sharp boundary after the $N \to \infty$ limit is taken. Even without the restriction $\det W = 1$, we expect that the inversion symmetry gets restored at large N (since the restriction becomes irrelevant at leading order). Therefore, after all the limits are taken we shall have

$$e^{-\gamma(t)} \le |z| \le e^{\gamma(t)}, \qquad z \in \operatorname{spectrum}(W_n)\,, \tag{10.26}$$

where $\gamma(t)$ is by definition the smallest positive number for which Eq. (10.26) holds almost surely, i.e., with probability 1. The function $\gamma(t)$ is positive for all $t > 0$ and we expect $\gamma(t)$ to be finite for all finite t and to increase monotonically with t because of the associated increase in disorder. The annulus keeps the spectrum of W_n away from the origin and infinity for any finite t. The major structural change that can happen as t is increased from zero is that the spectrum wraps round the annulus. For small t, the spectrum is a small blob around $z = 1$, the inversion and reflection invariance give it a kidney-shaped appearance. As t increases, the blob has a larger annulus available and expands into it, until it eventually reaches completely around it at some finite critical t.

To get some feeling for why there is a $\gamma(t)$ at all and how it behaves, we start from some small ε, large n, and large N, without committing at the moment to any special relations between these numbers, even though we really are interested in the situation $n \propto 1/\varepsilon^2 \gg 1$ and, although $N \gg 1$, we want $n \gg N$.

10.5.1 Bounds for large t

We first fix some $N \gg 1$, take some fixed $\varepsilon^2 \ll 1$, and study what happens as $n \to \infty$. In terms of our true interest, this means that we are trying to understand the asymptotic behavior of $\gamma(t)$ for $t = n\varepsilon^2$ going to infinity. If we take $n \to \infty$ at fixed $\varepsilon^2 > 0$, the theorems of Fürstenberg and Oseledec apply, which provide a generalization of the familiar law of large numbers to the case of independent and identically distributed random matrices (see Refs. [59, 63] and original references therein). For our case, this implies that for a generic matrix norm $\| \dots \|$,

$$\lambda_1 = \lim_{n\to\infty} \frac{1}{n} \log \|W_n\| \tag{10.27}$$

exists with probability 1 and is a non-random quantity (λ_1 is called the maximum characteristic Lyapunov exponent). Furthermore, the matrix

$$\lim_{n\to\infty} \left(W_n^\dagger W_n\right)^{\frac{1}{2n}} \tag{10.28}$$

exists almost surely, too, and has non-random eigenvalues e^{λ_i} ($\lambda_1 \geq \lambda_2 \geq \cdots \geq \lambda_N$ are referred to as the characteristic Lyapunov exponents).

The following discussion is based on the textbooks [59, 63] and Refs. [64, 65]. We start by defining the norm of a vector $v \in \mathbb{C}^N$ by

$$\|v\| = \sqrt{\sum_{a=1}^{N} |v_a|^2} \tag{10.29}$$

and the matrix norm by[17]

$$\|W_n\| = \sup_{\|v\|=1} \|vW_n\|\,, \tag{10.30}$$

identifying it with the square root of the largest eigenvalue of $W_n W_n^\dagger$. For a fixed W_n, we have in general

$$\|W_n\| \geq e^{\gamma_w} \tag{10.31}$$

[17] In Dirac notation, $vW_n \to \langle v|W_n$ and $\|vW_n\|^2 \to \langle v|W_n W_n^\dagger|v\rangle$.

with e^{γ_w} being the spectral radius of W_n, i.e., $|z| \leq e^{\gamma_w}$ for all $z \in \text{spectrum}(W_n)$ (by definition, we have $e^{\gamma_w} \leq e^{\gamma(t)}$ with probability 1, cf. Eq. (10.26)). This is a consequence of the submultiplicativity of the matrix norm [66],

$$\|UW\| = \sup \frac{\|vUW\|}{\|v\|} = \sup \frac{\|vUW\|}{\|vU\|} \frac{\|vU\|}{\|v\|} \leq \sup \frac{\|uW\|}{\|u\|} \sup \frac{\|vU\|}{\|v\|} = \|U\|\|W\|\,, \quad (10.32)$$

where the supremum is taken only over those $v \neq 0$ for which $vU \neq 0$. Let now v_γ be an eigenvector of W_n with eigenvalue z, being the eigenvalue of W_n that has maximum absolute value and defines γ_w, i.e., $W_n v_\gamma = z v_\gamma$ with $|z| = e^{\gamma_w}$. Denoting by V_γ the matrix with all the columns given by the eigenvector v_γ, we have $W_n V_\gamma = z V_\gamma$ and consequently

$$|z|\,\|V_\gamma\| = \|W_n V_\gamma\| \leq \|W_n\|\|V_\gamma\|\,, \quad (10.33)$$

which proves Eq. (10.31).

The above inequality may be sharp because z could in general be associated to an eigenvector that is very different from the maximum eigenvector of $W_n^\dagger W_n$. However, we suppose that our case is sufficiently generic for a conjecture of Ref. [67] (where Lyapunov exponents are analyzed for a broad class of dynamical models) to apply, which would allow us to replace the inequality sign above by an asymptotic equality in the infinite-n limit, resulting in

$$\|W_n\| = e^{\gamma(t)} \quad \text{for} \quad t \to \infty\,. \quad (10.34)$$

This assumption is non-trivial: For example, in the Ginibre ensemble [68], where W_n is not given by a product, but is just a complex matrix C distributed according to the Gaussian distribution $\exp[-N\,\text{Tr}(C^\dagger C)]$, and no non-commutative matrix products are involved, the left-hand side of Eq. (10.31) equals twice the right-hand side (in the limit $N \to \infty$). On the other hand, if the Gaussian distribution of C is replaced by a distribution where each element is real, non-negative, and uniformly drawn from the segment $[0, 1]$ (in which case theorems due to Perron and Frobenius apply, cf. Ref. [66]) Eq. (10.31) does become an equality for large N. A single matrix with Gaussian-distributed elements is of course very different from W_n for large t, however, it is intuitively close to the situation for small t, the case addressed in the next subsection. There, our estimate for $\gamma(t)$ will be more direct, without involving the norm $\|W_n\|$. In any case, that Eq. (10.31) becomes an equality as $t \to \infty$ will be confirmed by both the analytical and numerical results presented below.

To study $\|W_n\|$, we need to know what happens to vW_n for an arbitrary v with $\|v\| \neq 0$. We define v_i, $i = 1, \ldots, n$, by

$$v_i = v \prod_{j=1}^{i} M_j \quad (10.35)$$

and $v_0 = v$. We are only interested in the ray specified by v. Let

$$S_v \equiv \frac{\|vM_1\|}{\|v\|}\,. \quad (10.36)$$

Because of the invariance under conjugation by $\mathrm{U}(N)$ elements, the distribution of S_v induced by that of M_1 is independent of v. We now write

$$\log\|v_n\|^2 - \log\|v\|^2 = \sum_{i=1}^{n} \log \frac{\|v_i\|^2}{\|v_{i-1}\|^2}\,, \quad (10.37)$$

which is a trick used in Ref. [64]. The terms in the sum on the RHS of Eq. (10.37) are i.i.d. real numbers for any fixed values of n, ε^2, N by the same argument as below Eq. (10.36). Therefore, we can calculate the probability distribution of the LHS by calculating the characteristic function $F(k)$ (see Eq. (10.40) below) of one of the terms on the RHS, taking the power n, and taking the inverse Fourier transform of that.

For convenience, we reproduce the equation describing the source of randomness (ignoring the zero trace condition):

$$M = e^{\varepsilon C}, \qquad P(C) = \mathcal{N} e^{-N \operatorname{Tr} C^\dagger C}\,. \tag{10.38}$$

The random variables on the RHS of (10.37) are denoted by x,

$$x = \log \frac{\|vM\|^2}{\|v\|^2}\,, \tag{10.39}$$

and the characteristic function of the identical distributions is

$$F(k) = \langle e^{ikx} \rangle_{P(C)}\,. \tag{10.40}$$

Denoting the random variable on the LHS of Eq. (10.37) by y,

$$y = \log \frac{\|v_n\|^2}{\|v\|^2} = \log \frac{\|vW_n\|^2}{\|v\|^2}\,, \tag{10.41}$$

its probability density is given by

$$P(y) = \int \frac{dk}{2\pi} e^{-iky} [F(k)]^n\,. \tag{10.42}$$

We now expand x in ε to order ε^2 in the calculation of $F(k)$ and assume that the expansion in ε can be freely interchanged with various integrals. An expansion to order ε^2 is assumed to be all that is needed since an alternative treatment of the ensemble, based on the Fokker-Planck equation, would also need only expansions to order ε^2 (cf. Sec. 10.4.1 above).

Because of the U(N) invariance, we can rotate the vector v to point in the 1-direction,

$$x = \log\left(\sum_{j=1}^{N} |M_{1j}|^2 \right). \tag{10.43}$$

Thus, the vector v has dropped out completely (we will reuse the symbol v below). Up to order ε^2, we have

$$x = \log\left(1 + \varepsilon\,(C_{11} + C_{11}^*) + \frac{\varepsilon^2}{2}\left(C^2\right)_{11} + \frac{\varepsilon^2}{2}\left(C^2\right)_{11}^* + \varepsilon^2 \sum_{j=1}^{N} C_{1j} C_{1j}^* \right). \tag{10.44}$$

We now introduce some extra notation,

$$\operatorname{Re} C_{11} = u, \quad C_{j1} = v_j, \quad C_{1j} = w_j \quad \text{for} \;\; j = 2, \ldots, N\,, \tag{10.45}$$

where v and w are $(N-1)$-dimensional complex column vectors. This leads to

$$x = 2\varepsilon u + \frac{\varepsilon^2}{2}(v^T w + v^\dagger w^*) + \varepsilon^2 w^\dagger w + \mathcal{O}(\varepsilon^3)\,. \tag{10.46}$$

To calculate $F(k)$, it is sufficient to know the distribution of u, v, w,

$$P(u,v,w) = \mathcal{N}' e^{-N(u^2+v^\dagger v+w^\dagger w)}\,, \qquad \mathcal{N}' = \frac{1}{\sqrt{\pi}}\left(\frac{\pi}{N}\right)^{-2(N-1)}\,. \tag{10.47}$$

The integral giving $F(k)$ is Gaussian and can be easily done. We have

$$\frac{1}{\sqrt{\pi}}\int_{-\infty}^{\infty} du\, e^{-Nu^2+2\varepsilon iku} = e^{-\frac{\varepsilon^2 k^2}{N}} \tag{10.48}$$

and (with complex numbers v and w)

$$\begin{aligned}\left(\frac{\pi}{N}\right)^{-2}&\int d\mu(v)d\mu(w)e^{-N\left(|v|^2+|w|^2\right)+ik\left(\frac{\varepsilon^2}{2}(vw+v^*w^*)+\varepsilon^2|w|^2\right)}\\ &= \left(\frac{\pi}{N}\right)^{-1}\int d\mu(w)e^{-\left(N-ik\varepsilon^2+\frac{1}{4N}k^2\varepsilon^4\right)|w|^2} = \frac{1}{1-\frac{1}{N}ik\varepsilon^2+\frac{1}{4N^2}k^2\varepsilon^4}\,,\end{aligned} \tag{10.49}$$

resulting in

$$F(k) = e^{-\frac{\varepsilon^2k^2}{N}}\left[\frac{1}{1-\frac{1}{N}ik\varepsilon^2+\frac{1}{4N^2}k^2\varepsilon^4}\right]^{N-1}\,. \tag{10.50}$$

To the level of accuracy in ε^2 at which we are working, we can write

$$F(k) = e^{-\frac{\varepsilon^2k^2}{N}}\, e^{i\frac{\varepsilon^2k(N-1)}{N}}\,. \tag{10.51}$$

The characteristic function of y is therefore given by

$$\langle e^{iky}\rangle = [F(k)]^n = e^{-\frac{n\varepsilon^2k^2}{N}+in\varepsilon^2k(1-\frac{1}{N})}\,. \tag{10.52}$$

Defining

$$\hat{y} = \frac{y}{n}, \tag{10.53}$$

the inverse Fourier transform leads to the probability distribution

$$P(\hat{y}) = n\int\frac{dk}{2\pi}e^{-ik\hat{y}n}[F(k)]^n = \sqrt{\frac{Nn}{4\pi\varepsilon^2}}e^{-\frac{Nn}{4\varepsilon^2}[\hat{y}-\varepsilon^2(1-1/N)]^2}\,. \tag{10.54}$$

Since

$$\hat{y} = \frac{2}{n}\log\frac{\|vW_n\|}{\|v\|}\,, \tag{10.55}$$

the Fürstenberg theorems now tell us that almost surely

$$\lim_{n\to\infty}\frac{1}{n}\log\|W_n\| = \frac{\varepsilon^2}{2}\left(1-\frac{1}{N}\right)\,. \tag{10.56}$$

So far, ε^2 and N have been kept fixed. We therefore conclude that for large enough n,

$$\|W_n\| \approx e^{\frac{n}{2}\varepsilon^2(1-1/N)}\,. \tag{10.57}$$

We now simply replace $n\varepsilon^2$ by the large number t and take $N\to\infty$, which is a relatively harmless limit. Assuming that

$$\|W_n\| = e^{\gamma(t)} \tag{10.58}$$

holds asymptotically, we conclude that

$$\gamma(t) \approx \frac{t}{2} \quad \text{for} \quad t\to\infty\,. \tag{10.59}$$

This asymptotic behavior will be confirmed below by the exact result for $\gamma(t)$ that we obtain from the saddle-point analysis.

10.5.2 Bounds for small t

We now wish to take $\varepsilon \to 0$, keeping n and N large but fixed. In terms of t, this would correspond to the asymptotic regime $t \to 0$. Since ε is very small, we can try to expand to just linear order in ε, keeping n and N finite albeit at large values. To linear order in ε, the non-commutative aspect of the product is lost, and we can write

$$W_n = e^{\varepsilon \sum_{j=1}^n C_j} \equiv e^{\varepsilon\sqrt{n}\hat{C}} \,. \tag{10.60}$$

By an O(n) rotation[18] one can show that the matrix $\hat{C} = \frac{1}{\sqrt{n}} \sum_{j=1}^n C_j$ follows a Gaussian distribution, which is fixed by its average and variance,

$$\langle \hat{C}_{ab} \rangle = 0, \qquad \langle |\hat{C}_{ab}|^2 \rangle = \frac{1}{N} \,. \tag{10.61}$$

Here, $1 \le a, b \le N$ are matrix indices. The matrix $\hat{C}$ is distributed exactly like in the Ginibre ensemble [68]. For $N \to \infty$, we have

$$\text{spectrum}(\hat{C}) = \{z; |z| \le 1\} \,, \tag{10.62}$$

giving

$$\max_w \{|w|; w \in \text{spectrum}(W_n)\} = e^{\varepsilon\sqrt{n}} = e^{\sqrt{t}} \,. \tag{10.63}$$

We are therefore led to

$$\gamma(t) \approx \sqrt{t} \qquad \text{for} \quad t \to 0 \,. \tag{10.64}$$

10.5.3 Bounds for all t

Our subsequent work confirms the findings in Ref. [3], which, in turn, imply the existence of an annulus with a $\gamma(t)$ obeying our considerations. For $N = \infty$, we will show below (see Eq. (11.45)) that the inverse function to $\gamma(t)$, which we call $T(\gamma)$ with $\gamma > 0$, is given by

$$T(\gamma) = 2\gamma \tanh \frac{\gamma}{2} \,, \qquad T(\gamma(t)) = t \,. \tag{10.65}$$

The previously presented asymptotic results are recovered since

$$T(\gamma) \approx \gamma^2 \qquad \text{for} \quad \gamma \to 0 \,, \tag{10.66}$$

$$T(\gamma) \approx 2\gamma \qquad \text{for} \quad \gamma \to \infty \,. \tag{10.67}$$

Figure 33 shows a plot of $\gamma(t)$ together with the approximations for small and large t. The approximations in the two regimes $t \to 0$ and $t \to \infty$ differ in the order in ε one goes to. With either choice, one obtains a finite expression if t is finite, so the truncation of the expansion in ε is self-consistent. When the full limit $n \to \infty$, $\varepsilon \to 0$ is studied at fixed arbitrary t, going to order ε^2 should reproduce both asymptotic results in t, and we shall see that this indeed happens. Note that the crossover between the two asymptotic regimes occurs roughly where $\sqrt{t} = t/2$, which means $t = 4$. It will turn out that as t increases, the spectrum encircles the origin first at a critical value of $t = 4$ (as in the unitary case). In some rough sense, this is the point where the lack of commutativity among the factors in the product of matrices becomes qualitatively important.

[18] The O(n) rotation matrix is given by the matrix S introduced in App. B.3 (with the replacement $N \to n$).

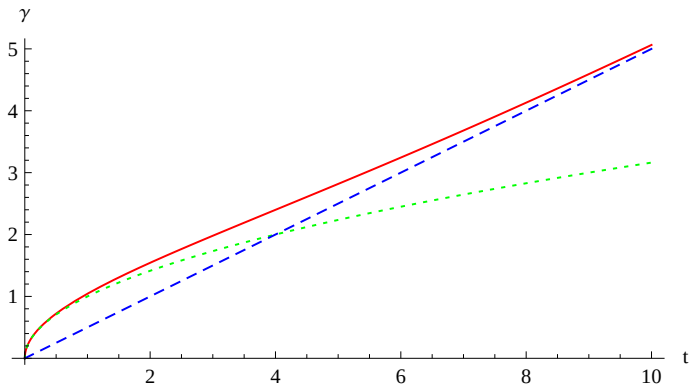

Figure 33: The red curve shows $\gamma(t)$ obtained by solving Eq. (10.65) numerically, the blue (dashed) curve shows the large-t approximation (10.59), the green (dotted) curve corresponds to the small-t approximation (10.64).

11 Saddle-point analysis for the basic model

11.1 Average of products of characteristic polynomials

It is difficult to derive a closed formula for the distribution of all the matrix entries of the product matrix W for general N. We are interested in just the spectral properties of W, however, even this is difficult to obtain for arbitrary finite N. The main complication in the analysis of the multiplicative random complex matrix model is due to the fact that the matrix product is non-commutative and that the eigenvalues populate two-dimensional domains in the complex plane, rather than one-dimensional line segments.

The natural definition of the spectral (surface) density in the complex plane is given by

$$\rho(z) = \frac{1}{N} \left\langle \sum_{i=1}^{N} \delta\left(z - z_i(W)\right) \right\rangle , \tag{11.1}$$

where the eigenvalues of a fixed matrix W are denoted by $z_i(W)$, $i = 1, \ldots, N$, and $\langle \ldots \rangle$ denotes the average over the matrices C_j defining W. Since a representation of the complex delta function is given by

$$\delta(z) = \frac{1}{\pi} \lim_{\varepsilon \to 0} \frac{\varepsilon^2}{\left(|z|^2 + \varepsilon^2\right)^2} , \tag{11.2}$$

the surface eigenvalue density can be obtained from (cf. Ref. [3])

$$\begin{aligned} F_\varepsilon(z, z^*) &= \frac{1}{N} \operatorname{Tr} \log \left[(z - W)(z^* - W^\dagger) + \varepsilon^2 \right] \\ &= \frac{1}{N} \log \det \left[(z - W)(z^* - W^\dagger) + \varepsilon^2 \right] . \end{aligned} \tag{11.3}$$

Due to

$$\frac{\partial^2}{\partial z \partial z^*} F_\varepsilon(z, z^*) = \frac{1}{N} \operatorname{Tr} \left(\frac{\varepsilon^2}{\left[(z - W)(z^* - W^\dagger) + \varepsilon^2 \right]^2} \right) = \frac{1}{N} \sum_{i=1}^{N} \frac{\varepsilon^2}{\left(|z - z_i(W)|^2 + \varepsilon^2 \right)^2} , \tag{11.4}$$

the eigenvalue density is given by

$$\rho(z) = \frac{1}{\pi} \left\langle \lim_{\varepsilon \to 0} \partial_z \partial_{z^*} F_\varepsilon(z, z^*) \right\rangle . \tag{11.5}$$

Rather than calculating $\rho(z)$ directly, we will focus on the averages of characteristic polynomials related to W in the following sections. In the unitary case, we have seen that partial information about the distribution of eigenvalues of the unitary matrix W can be obtained from $\langle \det(z - W) \rangle$. (We have found that the locations of the zeros of the average characteristic polynomial provide good approximations for the peaks of the true eigenvalue distribution on the unit circle and that this approximation becomes more and more accurate with increasing N, cf. Sec. 9.)

In analogy to the unitary model, we expect that information about the surface eigenvalue density in the multiplicative random complex matrix model can be extracted from averages of characteristic polynomials, too. These polynomials are generating functionals for various moments of the eigenvalue distribution. It turns out that the calculation of some simple characteristic polynomials is feasible. Below, we will first show that the

results obtained in Ref. [3] for the basic random matrix model can be reproduced with the help of averages of characteristic polynomials. Then, we will carry over this approach to the generalized model, which allows for a smooth interpolation between the unitary and the basic complex model. In both cases, our findings are confirmed with extensive numerical simulations.

In contrast to the unitary case, $\langle \det(z - W) \rangle$ carries no information in the complex model: Due to the invariance of $P(C)$ under $C \to Ce^{i\Phi}$, we obtain for $k \in \mathbb{N}_0$

$$\begin{aligned} \left\langle C_{ab}^k \right\rangle &= \int d\mu(C) P(C) C_{ab}^k = \frac{N}{\pi} \int d\mu(C_{ab}) e^{-N|C_{ab}|^2} C_{ab}^k \\ &= \frac{N}{\pi} \int_0^{2\pi} d\phi \int_0^\infty r dr e^{-Nr^2} r^k e^{i\phi k} = \delta_{k0} \,, \end{aligned} \tag{11.6}$$

i.e., averages of products of an arbitrary number of factors C_j vanish (as long as there is no contribution from a $C_j^\dagger$). Hence, expanding the matrix elements W_{ab} in powers of matrix elements of the factors C_j leads to

$$\langle (W_n)_{ab} \rangle = \delta_{ab} \,. \tag{11.7}$$

In averages involving only W_n (or $W_n^\dagger$, bot not both), we can therefore make the replacement $W_n \to \mathbf{1}$. The average of the characteristic polynomial, e.g., is simply given by

$$\langle \det(z - W_n) \rangle = (z - 1)^N \,. \tag{11.8}$$

The first non-trivial case is

$$Q(z, z^*) = \left\langle |\det(z - W_n)|^2 \right\rangle \,, \tag{11.9}$$

and from now on we focus on the calculation of the above observable in the limit $n \to \infty$, $\varepsilon \to 0$ with $t = \varepsilon^2 n$ held fixed (sometimes referred to as "the limit" in the following).

If one applies large-N factorization to $\left\langle |\det(z - W_n)|^2 \right\rangle$ (i.e., assuming that the average of the product can be replaced by the product of the averages, see Sec. 3.6.2) one gets holomorphic factorization, $\left\langle |\det(z - W_n)|^2 \right\rangle = |z - 1|^{2N}$, and all eigenvalues seem to have to be unity. For any $t > 0$, holomorphic factorization will hold for z-values close to 0 and z-values close to ∞. These two regions are outside the annulus defined by $\gamma(t)$ (cf. Eq. (10.26)). We will observe below that the full holomorphic factorized regime penetrates the annulus and is connected for sufficiently small t but splits into two disconnected components for t larger than a critical value. There are two disconnected components when the eigenvalue support, always contained within the annulus defined by $\gamma(t)$, fully encircles the origin $z = 0$.

We wish to calculate $Q(z, z^*)$ as a function of t and confirm that at infinite N the transition we are looking for indeed occurs. As a first step, we need to find a way to disentangle the non-Abelian product defining W. Then, we can make the N-dependence explicit by integrating out all degrees of freedom whose multiplicity is N-dependent. This allows us to take $N \to \infty$ which, as usual, becomes a saddle-point problem. In the following, we analyze the saddle-point problem partially, only to the point where we can identify the transition we are interested in.

11.2 Grassmann-integral representation of characteristic polynomials for matrix products

Let $X_1, X_2, \ldots, X_n$ be n $N \times N$ square matrices of general structure. We are interested in the characteristic polynomial of

$$W = X_1 X_2 \cdots X_n \,. \tag{11.10}$$

We first introduce $n \cdot N$ pairs of Grassmann variables: $\{\bar\psi_j, \psi_j\}_{j=1,\ldots,n}$, where each ψ_j and $\bar\psi_j$ has N components (ψ_j and $\bar\psi_j$ are independent variables). With the convention that $\psi_{n+1} \equiv \psi_1$ and $\bar\psi_{n+1} \equiv \bar\psi_1$, we define

$$I_n(X_1, X_2, \ldots, X_n) = \int \prod_{j=1}^{n} [d\psi_j d\bar\psi_j] e^{w \sum_{j=1}^n \bar\psi_j \psi_j - \sum_{j=1}^n \bar\psi_j X_j \psi_{j+1}} \,. \tag{11.11}$$

It can be proved by induction in n, see App. D.2, that

$$I_n(X_1, X_2, \ldots, X_n) = \det(w^n - W) \,. \tag{11.12}$$

Obviously, $\det(w^n - W)$ is invariant under cyclic permutations of the matrices X_j. In the Grassmann-integral representation, this invariance can be seen by shifting the Grassmann pairs in their index j.

11.3 Making the dependence on N explicit

We start by defining a complex variable σ which depends on n and z such that

$$z = e^{n\sigma}, \quad z = |z| e^{i\Psi}, \quad \sigma = \frac{1}{n} \log|z| + i \frac{\Psi}{n} \tag{11.13}$$

with $-\pi \le \Psi < \pi$. We now introduce $4n$ N-component Grassmann vectors $\bar\psi_j, \psi_j, \bar\chi_j, \chi_j$ and write

$$|\det(z - W_n)|^2 = \int \prod_{j=1}^{n} [d\bar\psi_j d\psi_j d\bar\chi_j d\chi_j] e^{\sum_{j=1}^n (e^\sigma \bar\psi_j \psi_j + e^{\sigma^*} \bar\chi_j \chi_j)} e^{-\sum_{j=1}^n (\bar\psi_j M_j \psi_{j+1} + \bar\chi_j M_j^* \chi_{j+1})} \,, \tag{11.14}$$

where $\psi_{n+1} = \psi_1$ and $\chi_{n+1} = \chi_1$. This can be rewritten as

$$|\det(z - W_n)|^2 = \int \prod_{j=1}^{n} [d\bar\psi_j d\psi_j d\bar\chi_j d\chi_j] e^{\sum_{j=1}^n (e^\sigma \bar\psi_j \psi_j + e^{\sigma^*} \bar\chi_j \chi_j)} e^{-\sum_{j=1}^n (\bar\psi_j M_j \psi_{j+1} - \chi_{j+1} M_j^\dagger \bar\chi_j)} \,. \tag{11.15}$$

We now perform several integration variable changes. We first switch the sign of χ_j. Keeping the symbols $\bar\chi, \chi$ for the new variables, we then replace χ_j by $\bar\chi_{j-1}$ (with the understanding that $\chi_1 \to \bar\chi_n$) and also replace $\bar\chi_j$ by χ_{j-1} (again with the understanding that $\bar\chi_1 \to \chi_n$). When the integration measure for the new variables is written in canonical order (cf. App. D), two $(-1)^N$ signs cancel and we are left with

$$|\det(z - W_n)|^2 = \int \prod_{j=1}^{n} [d\bar\psi_j d\psi_j d\bar\chi_j d\chi_j] e^{\sum_{j=1}^n (e^\sigma \bar\psi_j \psi_j + e^{\sigma^*} \bar\chi_j \chi_j)} e^{-\sum_{j=1}^n (\bar\psi_j M_j \psi_{j+1} + \bar\chi_j M_j^\dagger \chi_{j-1})} \,. \tag{11.16}$$

The integral over the matrices $C_1, \ldots, C_n$ now factorizes and can be calculated explicitly to sufficient accuracy in ε to produce the correct t-dependent limit. The following equalities ought to be understood in the sense that they hold up to terms which vanish as $n \to \infty$, $\varepsilon \to 0$ with $t = \varepsilon^2 n$ kept fixed. In general, we need to keep expressions correct to order ε^2, but not higher. However, we need to expand M only to linear order in ε as the next term in the expansion does not contribute after the C integration because of its phase invariance, and we obtain (indices a, b are used to label the N components of the vectors ψ, $\bar{\psi}$, etc.)

$$\begin{aligned}\left\langle e^{-\bar{\psi}M\psi' - \bar{\chi}M^\dagger\chi'}\right\rangle &= e^{-\bar{\psi}\psi' - \bar{\chi}\chi'} \int d\mu(C) P(C) e^{-\sum_{a,b=1}^N (\varepsilon\bar{\psi}_a\psi'_b) C_{ab} - \sum_{a,b=1}^N (\varepsilon\bar{\chi}_a\chi'_b)(C^\dagger)_{ab}} \\ &= e^{-\bar{\psi}\psi' - \bar{\chi}\chi'} \int d\mu(C) P(C) e^{\sum_{a,b=1}^N (\varepsilon\psi'_b\bar{\psi}_a) C_{ab} + \sum_{a,b=1}^N (\varepsilon\chi'_b\bar{\chi}_a)(C^\dagger)_{ab}} .\end{aligned} \tag{11.17}$$

We can now use the general formula (10.6) with $\left(B^\dagger\right)_{ba} \to \varepsilon\psi'_b\bar{\psi}_a$ and $A_{ba} \to \varepsilon\chi'_b\bar{\chi}_a$, which leads to

$$\begin{aligned}\left\langle e^{-\bar{\psi}M\psi' - \bar{\chi}M^\dagger\chi'}\right\rangle &= e^{-\bar{\psi}\psi' - \bar{\chi}\chi'} e^{\frac{\varepsilon^2}{N}\sum_{a,b=1}^N \psi'_b\bar{\psi}_a\chi'_a\bar{\chi}_b - \frac{\varepsilon^2}{N^2}\sum_{a,b=1}^N \psi'_b\bar{\psi}_b\chi'_a\bar{\chi}_a} \\ &= e^{-\bar{\psi}\psi' - \bar{\chi}\chi' - \frac{\varepsilon^2}{N}(\bar{\psi}\chi')(\bar{\chi}\psi') - \frac{\varepsilon^2}{N^2}(\bar{\psi}\psi')(\bar{\chi}\chi')} ,\end{aligned} \tag{11.18}$$

where the extra minus sign results from moving a Grassmann variable through an odd number of other Grassmann variables. Taking the average of Eq. (11.16) leads to n factors of the above type.

We now separate the quartic Grassmann terms into bilinears by introducing scalar complex bosonic multipliers, ζ and λ,

$$e^{-\frac{\varepsilon^2}{N}(\bar{\psi}\chi')(\bar{\chi}\psi')} = \mathcal{N}_a \int d\mu(\zeta) e^{-N|\zeta|^2} e^{-\varepsilon(\zeta\bar{\psi}\chi' - \zeta^*\bar{\chi}\psi')} , \tag{11.19a}$$

$$e^{-\frac{\varepsilon^2}{N^2}(\bar{\psi}\psi')(\bar{\chi}\chi')} = \mathcal{N}_b \int d\mu(\lambda) e^{-N^2|\lambda|^2} e^{-\varepsilon(\lambda\bar{\psi}\psi' - \lambda^*\bar{\chi}\chi')} \tag{11.19b}$$

with

$$\mathcal{N}_a = \frac{N}{\pi} \qquad \text{and} \qquad \mathcal{N}_b = \frac{N^2}{\pi} . \tag{11.20}$$

The relative minus sign is needed to get the right sign in front of the quartic Grassmann term. The integration measure is $d\mu(\zeta) = d\,\mathrm{Re}\,\zeta\, d\,\mathrm{Im}\,\zeta$. The net effect of this procedure is that the average over the complex matrices C_j is replaced by an average over complex numbers ζ_j and λ_j. This prepares the scene for making the dependence on N explicit.

To separate all quartic Grassmann terms in $\langle|\det(z - W_n)|\rangle$, we need n integrals of the form (11.19a) and (11.19b). The limit we are after can be obtained from

$$\begin{aligned}\left\langle|\det(z - W_n)|^2\right\rangle = \mathcal{N}_a^n\mathcal{N}_b^n \int \prod_{j=1}^n [d\bar{\psi}_j d\psi_j d\bar{\chi}_j d\chi_j d\mu(\zeta_j) d\mu(\lambda_j)] e^{-N\sum_{j=1}^n |\zeta_j|^2 - N^2\sum_{j=1}^n |\lambda_j|^2} \\ \times e^{-\sum_{j=1}^n (\bar{\psi}_j\psi_{j+1}(1+\varepsilon\lambda_j) + \bar{\chi}_j\chi_{j-1}(1-\varepsilon\lambda_j^*))} e^{\sum_{j=1}^n (e^\sigma\bar{\psi}_j\psi_j + e^{\sigma^*}\bar{\chi}_j\chi_j)} \\ \times e^{-\varepsilon\sum_{j=1}^n (\zeta_j\bar{\psi}_j\chi_{j-1} - \zeta_j^*\bar{\chi}_j\psi_{j+1})} .\end{aligned} \tag{11.21}$$

One further change of Grassmann variables reduces the number of terms that are not diagonal in the index j. To this end, we introduce $\psi_{j+1} = \psi'_j$ and $\chi_{j-1} = \chi'_j$. Again, canonical

ordering of integration measures leads to two $(-1)^N$ factors which cancel. Dropping the primes on the new variables, we obtain

$$\begin{aligned}\left\langle |\det(z-W_n)|^2\right\rangle = \mathcal{N}_a^n\mathcal{N}_b^n \int\prod_{j=1}^n [d\bar\psi_j d\psi_j d\bar\chi_j d\chi_j d\mu(\zeta_j) d\mu(\lambda_j)] e^{-N\sum_{j=1}^n|\zeta_j|^2 - N^2\sum_{j=1}^n|\lambda_j|^2} \\ \times e^{-\sum_{j=1}^n(\bar\psi_j\psi_j(1+\varepsilon\lambda_j)+\bar\chi_j\chi_j(1-\varepsilon\lambda_j^*))} e^{\sum_{j=1}^n(e^\sigma\bar\psi_j\psi_{j-1}+e^{\sigma^*}\bar\chi_j\chi_{j+1})} \\ \times e^{-\varepsilon\sum_{j=1}^n(\zeta_j\bar\psi_j\chi_j-\zeta_j^*\bar\chi_j\psi_j)}\,. \end{aligned} \tag{11.22}$$

Since the Grassmann variables enter only quadratically in the exponent, we can now carry out the Grassmann integrals. Each ψ_j, χ_j, $\bar\psi_j$, $\bar\chi_j$ $(j=1,\dots,n)$ is an N-dimensional vector with components $(\psi_j)_a$ $(a=1,\dots,N)$ etc., and the exponent consists only of (implicit) scalar products of those vectors, e.g.,

$$\bar\psi_j\psi_j \equiv \sum_{a=1}^N \left(\bar\psi_j\right)_a (\psi_j)_a\,. \tag{11.23}$$

Due to the basic identity (D.9), this means that the integration will result in the N-th power of a determinant,

$$\left\langle |\det(z-W_n)|^2\right\rangle = \mathcal{N}_a^n\mathcal{N}_b^n \int\prod_{j=1}^n [d\mu(\zeta_j) d\mu(\lambda_j)] e^{-N\sum_{j=1}^n|\zeta_j|^2 - N^2\sum_{j=1}^n|\lambda_j|^2} \det{}^N \begin{pmatrix} A & B \\ C & D\end{pmatrix}, \tag{11.24}$$

where

$$A = e^\sigma T^\dagger - 1 - \varepsilon\Lambda\,,\quad D = e^{\sigma^*}T - 1 + \varepsilon\Lambda^\dagger\,,\quad B = -\varepsilon Z\,,\quad C = \varepsilon Z^\dagger \tag{11.25}$$

with

$$T = \begin{pmatrix} 0 & 1 & 0 & \cdots & 0 & 0 \\ 0 & 0 & 1 & \cdots & 0 & 0 \\ \vdots & \vdots & \vdots & \dots & \vdots & \vdots \\ 0 & 0 & 0 & \cdots & 0 & 1 \\ 1 & 0 & 0 & \cdots & 0 & 0 \end{pmatrix},\quad Z = \mathrm{diag}(\zeta_1,\dots,\zeta_n)\,,\quad \Lambda = \mathrm{diag}(\lambda_1,\dots,\lambda_n)\,. \tag{11.26}$$

Using known formulas on determinants of block matrices, we have

$$\det\begin{pmatrix} A & B \\ C & D\end{pmatrix} = \det(AD - ACA^{-1}B) = \det A\det D\det(1+\varepsilon^2 Z^\dagger A^{-1} Z D^{-1})\,. \tag{11.27}$$

11.4 The trivial large-N saddle point and its domain of local stability

Since the N-dependence of the λ-integral is of the form

$$\mathcal{N}_b^n \int\prod_{j=1}^n [d\mu(\lambda_j)] e^{-N^2\sum_{j=1}^n|\lambda_j|^2} \det{}^N \begin{pmatrix} A & B \\ C & D\end{pmatrix}, \tag{11.28}$$

we evidently get a trivial saddle point $\lambda_j = 0$, $j=1,\dots,n$, for large N due to the dominance of the N^2 term. In this limit, we can therefore focus on the remaining ζ-integration with the replacements

$$A \to A_0 = e^\sigma T^\dagger - 1\,,\qquad D \to D_0 = e^{\sigma^*}T - 1 = A_0^\dagger\,, \tag{11.29}$$

which yields

$$\left\langle |\det(z-W_n)|^2 \right\rangle \to \mathcal{N}_a^n \int \prod_{j=1}^{n} [d\mu(\zeta_j)] e^{-N\sum_{j=1}^{n}|\zeta_j|^2} \det{}^N \begin{pmatrix} A_0 & B \\ C & D_0 \end{pmatrix}. \tag{11.30}$$

This expression is exactly equal to the result which we would obtain without restricting the determinant of W_n. Integrals over complex λ-variables were needed to decouple quartic Grassmann terms arising from the second term in the exponent of Eq. (10.6), which simply does not occur in Eq. (10.10). This confirms that the boundary of non-vanishing eigenvalue density is indeed identical for $W_n \in \mathrm{GL}(N,\mathbb{C})$ and $W_n \in \mathrm{SL}(N,\mathbb{C})$ in the large-N limit.

Reemploying the labels A and D for A_0 and D_0, we have

$$\det \begin{pmatrix} A & B \\ C & D \end{pmatrix} = \det(AD - ACA^{-1}B) = |\det A|^2 \det(1 + \varepsilon^2 Z^\dagger A^{-1} Z (A^\dagger)^{-1}). \tag{11.31}$$

The matrix T implements cyclical one-step shifts and obeys $T^n = 1$ and $T^{n-1} = T^\dagger = T^{-1}$. Hence, we can write

$$\begin{aligned} A^{-1} &= \frac{1}{e^\sigma T^\dagger - 1} = e^{-\sigma} T \sum_{r=0}^{\infty} \sum_{s=0}^{n-1} \left(e^{-\sigma} T\right)^{rn+s} = e^{-\sigma} T \sum_{s=0}^{n-1} \left(e^{-\sigma} T\right)^s \sum_{r=0}^{\infty} \left(e^{-n\sigma}\right)^r \\ &= \frac{1}{1-e^{-n\sigma}} \sum_{s=1}^{n} e^{-s\sigma} T^s . \end{aligned} \tag{11.32}$$

Each entry in A^{-1} gets a contribution from exactly one single term in the sum over s above. A^{-1} is a circulant matrix, which means that it has each row vector circularly shifted by one element to the right relative to the preceding row vector.

The large-N limit will obviously lead to saddle-point equations which will be satisfied at $\zeta_j = 0$ since the integration variables ζ_j, ζ_j^* enter only bilinearly in the integrand of Eq. (11.30). If this saddle dominated at infinite N, we could replace W_n by a unit matrix,

$$\left\langle |\det(z-W_n)|^2 \right\rangle = |\det A|^{2N} = |e^{n\sigma} - 1|^{2N} = |z-1|^{2N} . \tag{11.33}$$

This means that there are no eigenvalues at any $z \neq 1$ in the complex plane. In particular, the eigenvalue density in the complex plane, scaled to be finite at infinite N, is zero everywhere (except at the singularity $z = 1$). We shall refer to this saddle as saddle A. For those z for which saddle A gives the correct answer, $\left\langle |\det(z-W_n)|^2 \right\rangle = |z-1|^{2N}$ is the absolute value square of a holomorphic function in z and there is no finite eigenvalue surface density. An eigenvalue surface density will develop in regions of the complex plane where saddle A is displaced by another saddle, saddle B, which destroys holomorphic factorization. To find the regime where saddle B must take over, we determine where saddle A is no longer locally stable (we call the saddle locally stable if the Gaussian integral, that is obtained by truncating at second order the expansion in the integration variables ζ_j, ζ_j^* around zero, is convergent). A comparison with results of numerical simulations shows that saddle A is always dominating whenever it is locally stable and that saddle B indeed produces non-zero surface eigenvalue density. Thus, at the boundary of the domain of stability of saddle A, one has a continuous transition to regions with non-zero surface eigenvalue density. We do not calculate saddle B explicitly.

11.4.1 Determination of the boundary of the domain of stability of the trivial saddle point

To determine the domain of local stability of the trivial saddle point, we need to calculate the Gaussian form of the integrand around saddle A. To quadratic order in ζ_j, ζ_j^*, we can

write Eq. (11.31) as

$$\det \begin{pmatrix} A & B \\ C & D \end{pmatrix} = |\det A|^2 e^{\mathrm{Tr}\log\left(1+\varepsilon^2 Z^\dagger A^{-1} Z (A^\dagger)^{-1}\right)} = |\det(1-e^\sigma T^\dagger)|^2 e^{\varepsilon^2 F} \tag{11.34}$$

with

$$F = \mathrm{Tr}\, Z^\dagger A^{-1} Z (A^\dagger)^{-1} = \sum_{j,l=1}^{n} \zeta_j^* |(A^{-1})_{jl}|^2 \zeta_l \equiv \sum_{j,l=1}^{n} \zeta_j^* K_{jl} \zeta_l \,. \tag{11.35}$$

Since A^{-1} is a circulant matrix, the matrix K is also circulant. Thus, its eigenvalues are determined by the discrete Fourier transform of one row of the matrix K, which defines the entire matrix in terms of an n-term series, e.g., $K_j = K_{nj}$, with

$$K_j = |(A^{-1})_{nj}|^2 = \left|\frac{1}{1-e^{-n\sigma}}\right|^2 e^{-j(\sigma+\sigma^*)} \,. \tag{11.36}$$

The eigenvalues of the matrix K are therefore given by (cf. Eqs. (6.36) and (6.37))

$$\lambda_k = e^{-i\frac{2\pi k}{n} l} \sum_{j=1}^{n} K_{lj} e^{i\frac{2\pi k}{n} j} \,, \tag{11.37}$$

where the RHS is independent of l because K is circulant. This results in

$$\lambda_k = \left|\frac{1}{1-e^{-n\sigma}}\right|^2 \sum_{j=1}^{n} e^{-j(\sigma+\sigma^*)} e^{i\frac{2\pi k}{n} j} = \left|\frac{1}{1-e^{-n\sigma}}\right|^2 \frac{1-e^{-n(\sigma+\sigma^*)}}{1-e^{i\frac{2\pi k}{n}} e^{-(\sigma+\sigma^*)}} e^{-(\sigma+\sigma^*)} e^{i\frac{2\pi k}{n}} \,. \tag{11.38}$$

From Eqs. (11.30) and (11.34), we obtain that the condition for local stability is given by

$$\mathrm{Re}\left(-1+\varepsilon^2\lambda_k\right) < 0 \qquad \text{for all } k = 1, \ldots, n \,. \tag{11.39}$$

If this condition is fulfilled, the integral in Eq. (11.30) is convergent when we truncate the expansion in the integration variables ζ_j, ζ_j^* around the trivial saddle point (at $\zeta_j = \zeta_j^* = 0$) at quadratic order. Going back to the original variables, the above condition reads

$$\varepsilon^2 \frac{1}{|z-1|^2} \,\mathrm{Re}\left(\frac{|z|^2-1}{|z|^{\frac{2}{n}} e^{-\frac{2\pi i}{n}k} - 1}\right) < 1 \tag{11.40}$$

for all $k = 1, \ldots, n$. Since

$$\mathrm{Re}\,\frac{1}{|z|^{\frac{2}{n}} e^{-i\phi_k} - 1} = \frac{|z|^{\frac{2}{n}} \cos\phi_k}{|z|^{\frac{4}{n}} + 1 - 2|z|^{\frac{2}{n}} \cos\phi_k} \tag{11.41}$$

has a maximum (resp. minimum) at $\phi_k = 0 \mod 2\pi$ for $|z| > 1$ (resp. $|z| < 1$), the above inequality is strongest for the $k = n$ case. Hence, the condition holds also for all $k < n$ if it holds for $k = n$. We end up with a determination of the region of local stability of saddle A by the single inequality

$$\varepsilon^2 \frac{1}{|z-1|^2} \left(\frac{|z|^2-1}{|z|^{\frac{2}{n}} - 1}\right) < 1 \,. \tag{11.42}$$

With

$$|z|^{\frac{2}{n}} - 1 = \frac{2}{n} \log |z| + \mathcal{O}(n^{-2}), \tag{11.43}$$

taking $n \to \infty$ at constant $t = n\varepsilon^2$ in Eq. (11.42) leads to

$$1 > \frac{t}{2|z-1|^2} \frac{|z|^2 - 1}{\log |z|} \,. \tag{11.44}$$

Hence, the eigenvalue density for fixed t vanishes at a point z in the complex plane if this inequality is satisfied. The above result is in agreement with Eq. (83) of Ref. [3].

It is easy to see that the points on the boundary, separating charged[19] and chargeless regions, having maximal or minimal absolute values are located on the positive real axis. This means that the function $\gamma(t)$, defined in Sec. 10.5, has to fulfill

$$\gamma(t) = \frac{t}{2} \left(\frac{e^{\gamma(t)} + 1}{e^{\gamma(t)} - 1} \right) , \tag{11.45}$$

which is equivalent to Eq. (10.65).

Note that the exact invariance under inversion and complex conjugation of z has been restored in the limit, although it was lost at finite n because of the truncation in the expansion in ε to second order (which was all that is needed to get the correct limit). Therefore, as explained earlier, one can look for the transition point by just focusing on the unit circle. The portion of the unit circle which resides in the chargeless region is

$$t < |z-1|^2, \quad |z| = 1 \,. \tag{11.46}$$

For $t < 4$, there is an arc centered at $z = -1$ which resides in the chargeless region. The endpoints of this arc are at the the two angles $\theta = \pm\theta_c$ with $\theta_c > 0$ satisfying

$$\cos(\theta_c) = 1 - t/2 \,. \tag{11.47}$$

Figure 34 shows a plot of $\theta_c(t)$. When $t \geq 4$, the charged region contains the whole unit circle. The region of non-vanishing eigenvalue density becomes multiply connected at the transition point $t = t_c = 4$ (we explicitly see from Eq. (11.44) that there is a region around $z = 0$ where the eigenvalue density has to be zero). The last point (on the unit circle) to be engulfed by the charged region as t increases is the point $z = -1$.

11.4.2 More detailed study of the neighborhood of the critical point

To study the shape of the boundary on both sides of the transition point $t = 4$, it is useful to employ the following map,

$$z(u) = \frac{u + \frac{1}{2}}{u - \frac{1}{2}} \,, \quad u(z) = \frac{1}{2} \left(\frac{z+1}{z-1} \right) . \tag{11.48}$$

Under this map, $z = 0$ and $z = \infty$ map into $u = \mp\frac{1}{2}$, and $z = 1$ maps into $u = \infty$. The eigenvalue density is always non-zero at $z = 1$, so the charged region extends to infinity in the complex-u plane. The circle $|z| = 1$ maps into the imaginary axis in the u-plane, and $z = -1$ maps into the origin $u = 0$. Inversion in z becomes $u \to -u$. The real-z

[19] We sometimes refer to the regions of vanishing (resp. non-vanishing) surface eigenvalue density as charged (resp. chargeless) regions.

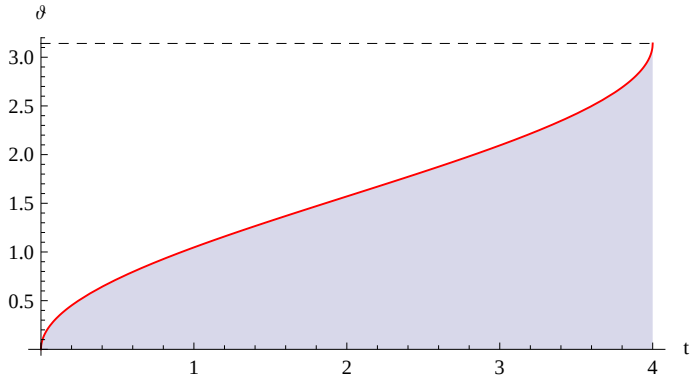

Figure 34: Plot of the endpoint $\theta_c = \arccos(1 - t/2)$ of the arc on the unit circle that is located in the chargeless region. The surface eigenvalue density is non-zero if (θ, t) lies below the red curve (in the blue area), $\rho(e^{i\theta}, t) > 0$ for $\theta < \theta_c(t)$. For $t = 4$, the whole unit circle belongs to the charged region (the horizontal dashed line corresponds to $\theta = \pi$).

axis maps into the real-u axis. The region $\{\mathrm{Im}\, z > 0\} \cap \{|z| > 1\}$ maps into the region $\{\mathrm{Im}\, u < 0\} \cap \{\mathrm{Re}\, u > 0\}$. Reflection about the real axis ($z \to z^*$) maps into reflection about the real axis in the u-plane ($u \to u^*$), and reflection with respect to the unit circle ($z \to 1/z^*$) corresponds to reflection about the imaginary axis in the u-plane ($u \to -u^*$). Our problem has these symmetries in the z-variable, so it suffices to analyze one of the four quadrants in the u-plane; results for the other quadrants are then obtained by reflections through common axes in the u-plane.

We have seen that the eigenvalues are restricted to the annulus

$$e^{-\gamma(t)} \leq |z| \leq e^{\gamma(t)}\,. \tag{11.49}$$

Therefore, the complement of this annulus is contained in the chargeless region. Under the map (11.48), the two circles $|z| = e^{\pm\gamma(t)}$ go into two circles with non-overlapping interiors in the u-plane,

$$\left| u - \frac{1}{2}\coth\left(\pm\gamma(t)\right)\right|^2 = \frac{1}{(2\sinh\gamma(t))^2}\,. \tag{11.50}$$

The eigenvalues are restricted to the exterior of these two circles (the image of the annulus) and therefore the chargeless region (11.44) includes the interior of these two circles.

Denoting $\mathrm{Re}\, u = u_r$ and $\mathrm{Im}\, u = u_i$, the chargeless region is found to be determined by

$$0 \leq u_i^2 \leq u_r \coth(t u_r) - u_r^2 - 1/4\,. \tag{11.51}$$

As mentioned before, we observe that the boundary between charged and chargeless region in the complex-u plane is determined by an equation that is equivalent to Eq. (7.5) with $\varepsilon = 0$, which is related to the eigenvalue density in the unitary case. Therefore, the black curves (with $u_r \neq 0$) in Fig. 23 correspond to the boundary of the chargeless region in the u-plane as obtained from Eq. (11.51). Note that the imaginary axis is not part of this boundary; there are at most two isolated points on the boundary which have $u_r = 0$. The eigenvalue density vanishes in the interior of the closed curves encircling the points $u = \pm\frac{1}{2}$ (cf. also Fig. 36 below).

For u_r^2 sufficiently large, the above inequalities self-contradict, showing that the chargeless region is bounded in the u-plane.

The chargeless region in the positive quadrant of the u-plane determines the entire chargeless region by reflections from quadrant to quadrant through a common axis. When $u_r \to 0$ we have

$$u_i^2 \leq \frac{1}{t} - \frac{1}{4} + \left(\frac{t}{3} - 1\right) u_r^2 + \mathcal{O}(u_r^4)\,. \tag{11.52}$$

For $t < 4$, there is a portion of the imaginary-u axis inside the chargeless region; hence, the charged portion of the imaginary-u axis has a break around the origin, and this maps into the unit circle in the z-plane having a gap around $z = -1$. There is only one connected chargeless region for $t < 4$, which contains the two circles from Eq. (11.50). For $t > 4$, $u_r = 0$ is not in the chargeless region. Consequently, the entire imaginary axis is in the charged region. The domain of zero eigenvalue density is split into two disconnected regions, each containing exactly one of the two circles of Eq. (11.50).

Exactly at the transition, when $t = 4$, the boundary in the vicinity of the origin is given by the two lines

$$u_i = \pm\frac{1}{\sqrt{3}} u_r + \dots\,. \tag{11.53}$$

The critical contour (separating charged and chargeless regions) at $t = 4$ is a slightly deformed figure-8, laying horizontally along the real-u axis and symmetrically with respect to the imaginary-u axis. The midpoint of the 8, which is located at the origin of the u-plane, separates along the real-u axis as t is increased from $t = 4$ (splitting the chargeless region into two disconnected regions) and separates along the imaginary-u axis as t is decreased from $t = 4$ (with the chargeless region becoming one single connected region), see Fig. 36.

11.4.3 Connection to the inviscid Burgers equation

The formula (11.44) for the boundary of the chargeless region leads us to introduce the following map from the complex plane onto itself,

$$Z(u,t) = \frac{u + \frac{1}{2}}{u - \frac{1}{2}} e^{-tu}\,. \tag{11.54}$$

For $\operatorname{Re} u \neq 0$, Eq. (11.44) is equivalent to

$$|Z(u,t)| \begin{cases} > 1 & \text{for } \operatorname{Re} u(z) > 0\,, \\ < 1 & \text{for } \operatorname{Re} u(z) < 0\,, \end{cases} \tag{11.55}$$

and the boundary between the charged and chargeless regions is given by

$$|Z(u,t)| = 1, \quad \operatorname{Re} u \neq 0\,. \tag{11.56}$$

For $\operatorname{Re} u = 0$, isolated points on the boundary are found using Eq. (11.52).

The map $Z(u,t)$ is one-to-one only at $t = 0$. For non-zero t, $Z(u,t)$ has an essential singularity at $u = \infty$ which prevents an analytic definition of an inverse, $U(z,t)$. One is therefore led to look for a local definition of the map by a partial differential equation. We differentiate the equation

$$Z(U(w,t),t) = w \tag{11.57}$$

with respect to w at fixed t and with respect to t at fixed w. We find then that $U(w,t)$ obeys

$$\frac{\partial U}{\partial t} = Uw\frac{\partial U}{\partial w}\,. \tag{11.58}$$

This is the inviscid complex Burgers equation, up to a change of variables $w = e^{-x}$. We have seen above (cf. Sec. 4.4) that equations of this type play a central role in two-dimensional Yang-Mills theory: Durhuus and Olesen found the transition in the eigenvalue density of SU(N) Wilson loop matrices by studying the inviscid Burgers equation (4.72). In fact, as mentioned already in Sec. 7.1, Eq. (11.54) is equivalent to Eq. (7.3) (when we make the replacements $Z \to z = e^{i\theta+\varepsilon}$, $u \to U$, $t \to T$), which determines the eigenvalue density $\rho_\infty(\theta,t)$ in the unitary case. Here, the complex Burgers equation (11.58) comes with the initial condition

$$U(w,0) = \frac{1}{2}\left(\frac{w+1}{w-1}\right) \equiv u(w)\,. \tag{11.59}$$

Equation (11.56) identifies the boundary separating the charged region from the chargeless one with the image of the circle $|w| = 1$ in the u-plane under the map $u = U(w,t)$ for $\operatorname{Re} u \neq 0$. It is well-known that as t increases from zero, depending on the initial condition, singularities can be generated at finite $t > 0$. In our case, we have seen explicitly that at $t = 4$ a singularity is generated. This is the point where the domain of non-vanishing eigenvalue density becomes multiply connected. In the unitary model, the closure of the gap in the eigenvalue distribution (confined to the unit circle) occurs at $t = 4$, too. In Sec. 12 we will introduce a generalized multiplicative random matrix model that allows for a smooth interpolation between the unitary and the complex case.

11.5 Precise relation to the model of Gudowska-Nowak et al.

In Sec. 10, we have introduced a probability distribution for the complex matrices C_j, leading to a distribution for the product matrix W_n through the definition $W_n = \prod_{j=1}^n M_j$ with $M_j = \exp(\varepsilon C_j)$. To study the limit $n \to \infty$, $\varepsilon \to 0$ with $t = n\varepsilon^2$ kept fixed, we have expanded M_j in powers of ε and observed that an expansion to linear order is sufficient.

Instead of Eq. (10.7), we could therefore define

$$M_j = 1 + \varepsilon C_j \tag{11.60}$$

from the beginning. This is the exact form of the model introduced in Ref. [3]. It looses the inversion symmetry in z at finite n. With this definition, our formulas become exact even for finite n. The limit $n \to \infty$, $\varepsilon \to \infty$ with $t = n\varepsilon^2$ held fixed will not change if Eq. (10.8) is replaced by Eq. (11.60) and the inversion symmetry is recovered. However, with Eq. (11.60) we can explicitly work out a few low-n cases and test them either numerically or by more direct analytical means (we did this for $n = 1, 2$ and obtained agreement with Ref. [3], providing an additional check on our method, which relies only on information captured by the observable Q).

This "linear" model (as opposed to the previous "exponential" version) is more convenient for numerical simulations because one does not need to exponentiate a large matrix.

11.6 Numerical results

Since we have focused only on the local stability properties of our trivial saddle point (we have not identified explicitly the competing non-trivial saddles), we need a bit more

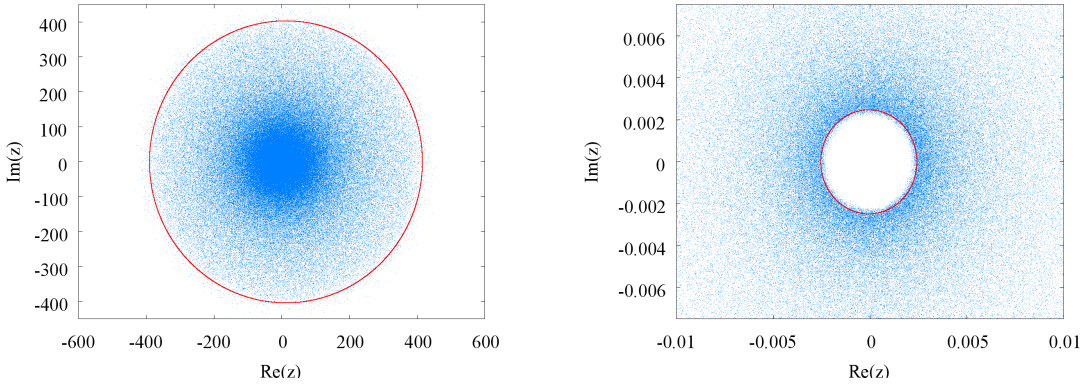

Figure 35: Plots of the eigenvalues of W in the z-plane for $t = 12$. The plot on the right is an enlarged version of the plot on the left.

evidence to establish the transition. We do this numerically (some numerical checks were also carried out by Gudowska-Nowak et al. in Ref. [3], and we confirm their results).

We obtain from Eq. (11.51) that the boundaries between domains with vanishing and non-vanishing surface eigenvalue density in the complex-u plane are determined by the equation

$$u_i^2 = u_r \coth(tu_r) - u_r^2 - 1/4\,, \tag{11.61}$$

which explicitly gives u_i as a function of u_r. The boundaries in the u-plane are then easily mapped to the boundaries in the original z-plane through the transformation (11.48).

All numerical simulations were performed with $n = 2000$ and $N = 2000$ for ensembles consisting of about 500 matrices (for the linear version of the model). In the following figures, the solid lines correspond to the analytically derived boundaries (obtained from Eq. (11.61)), which are in very good agreement with the numerical data. Figure 36 shows eigenvalue distributions in the z- and u-plane for $t = 3$, $t = 4$, and $t = 5$. Our numerical tests confirm that the topological transition of the domain of non-vanishing eigenvalue density occurs at $t = 4$, when the domain becomes multiply connected at $z = -1$. This corresponds to the imaginary-u axis completely lying in the domain of eigenvalues. Note also that the eigenvalue density in the u-plane is indeed symmetric under reflections at the real and imaginary axis, which is related to the inversion symmetry in z.

Figure 35 shows eigenvalues for $t = 12$ and affirms that the boundary for large t approximately consists of two circles with center at $z = 0$ and radii $\exp(\pm t/2)$.

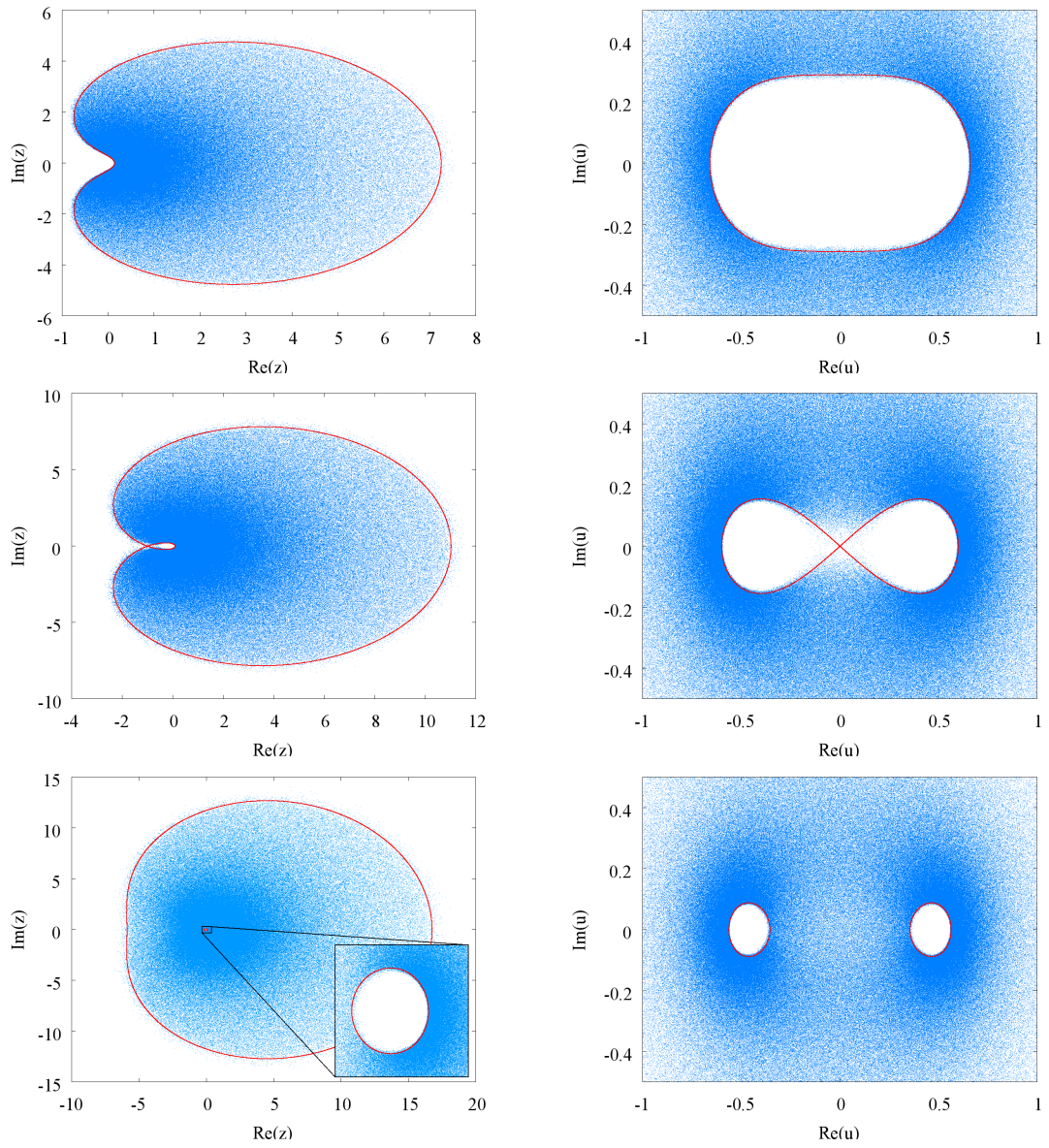

Figure 36: Scatter plot of the eigenvalues of W in the z-plane (left) and in the u-plane (right) for $t = 3$ (top), $t = 4$ (center), and $t = 5$ (bottom). The red curves show the boundaries of the domains of non-vanishing eigenvalue density obtained from Eq. (11.61).

12 Generalized multiplicative random matrix model

12.1 Definition and general properties

The basic complex matrix model can be generalized to interpolate between the case in which the individual factors are unitary and the case in which they are Hermitian. Writing the matrix C of each factor M in the product (10.8) as $C = H_1 + iH_2$ with $H_{1,2}$ being Hermitian and traceless, we take the generalized probability distribution of $H_{1,2}$ to be

$$P(H_1, H_2) = \mathcal{N} e^{-N\left(\frac{1}{2\omega_1}\operatorname{Tr} H_1^2 + \frac{1}{2\omega_2}\operatorname{Tr} H_2^2\right)} \tag{12.1}$$

with $\omega_{1,2} > 0$. For $\omega_1 = \omega_2 = \frac{1}{2}$, the exponent is given by

$$-N \operatorname{Tr}\left(H_1^2 + H_2^2\right) = -N \operatorname{Tr}\left((H_1 + iH_2)(H_1 - iH_2)\right) = -N \operatorname{Tr}\left(CC^\dagger\right), \tag{12.2}$$

and we recover the probability distribution of the basic complex model introduced in Sec. 10. In the limit $\omega_1 \to 0$ (with ω_2 kept fixed) the probability distribution produces a delta function for the matrix H_1 and M reduces to $e^{i\varepsilon H_2}$, i.e., we are in the unitary case, $M \in \mathrm{SU}(N)$ and $W_n \in \mathrm{SU}(N)$. Similarly, for $\omega_2 \to 0$ we have $M = e^{\varepsilon H_1}$ which means that $M = M^\dagger$. However, multiplication of n Hermitian matrices M_j in general results in a complex non-Hermitian product matrix $W_n = \prod_{j=1}^n M_j$ with $W_n^\dagger \neq W_n$.

The generalized probability distribution (12.1) produces the following correlation functions,

$$\left\langle (H_1)_{ij} (H_1)_{lk} \right\rangle = \frac{\omega_1}{N}\delta_{ik}\delta_{jl} - \frac{\omega_1}{N^2}\delta_{ij}\delta_{lk}\,, \tag{12.3}$$

$$\left\langle (H_2)_{ij} (H_2)_{lk} \right\rangle = \frac{\omega_2}{N}\delta_{ik}\delta_{jl} - \frac{\omega_2}{N^2}\delta_{ij}\delta_{lk}\,, \tag{12.4}$$

$$\left\langle (H_1)_{ij} (H_2)_{lk} \right\rangle = 0\,, \tag{12.5}$$

and therefore

$$\langle C_{ij} C_{lk} \rangle = \langle C_{ij}^* C_{lk}^* \rangle = \frac{1}{N}(\omega_1 - \omega_2)\delta_{ik}\delta_{jl} - \frac{1}{N^2}(\omega_1 - \omega_2)\delta_{ij}\delta_{lk} \tag{12.6}$$

and

$$\langle C_{ij} C_{lk}^\dagger \rangle = \frac{1}{N}(\omega_1 + \omega_2)\delta_{ik}\delta_{jl} - \frac{1}{N^2}(\omega_1 + \omega_2)\delta_{ij}\delta_{lk}\,. \tag{12.7}$$

The terms of order N^{-2} are due to the restrictions on the traces, $\operatorname{Tr} H_1 = \operatorname{Tr} H_2 = 0$. As a consequence of the above correlation functions, we have

$$\left\langle \left[e^{\varepsilon C} e^{\varepsilon C^\dagger}\right]_{ij} \right\rangle = \left(1 + 2\omega_1\left(1 - \frac{1}{N^2}\right)\varepsilon^2 + O(\varepsilon^4)\right)\delta_{ij}\,. \tag{12.8}$$

Using the same analysis as in the original model, we learn (see below) that the spectrum of W_n, in the limit $n \to \infty$, $\varepsilon \to 0$ with $t = \varepsilon^2 n$ held fixed, will now be restricted at any N to the annulus[20]

$$e^{-\frac{2\omega_1}{\omega_1+\omega_2}\gamma(t(\omega_1+\omega_2))} \leq |z| \leq e^{\frac{2\omega_1}{\omega_1+\omega_2}\gamma(t(\omega_1+\omega_2))}\,, \tag{12.9}$$

where the function γ is defined in Sec. 10.5 and fulfills Eq. (10.65). As $\omega_1 \to 0$, we are in the unitary case and the spectrum is restricted to the unit circle $|z| = 1$. For $\omega_1 = \omega_2 = 1/2$, we are in the original model and the above equation reduces to Eq. (10.26).

[20] Now it would be meaningful to make ε complex since for $\omega_1 \neq \omega_2$ the phase invariance $C \to e^{i\Phi}C$ has been eliminated. One still has invariance under a sign switch of C and only ε^2 enters. A complex ε would produce a complex t.

12.2 Large-N factorized average

For $\omega_1 \neq \omega_2$,

$$\langle \det(z - W_n) \rangle = J(z) \tag{12.10}$$

is no longer equal to $(z-1)^N$ but to a more complicated polynomial in z. The polynomial $J(z)$ is completely determined by the two-point function of the matrix C.

Where factorization holds, we have

$$\langle |\det(z - W_n)|^2 \rangle = |J(z)|^2 \tag{12.11}$$

and expect vanishing surface eigenvalue density.

The polynomial $J(z)$ can be read off from previous work of R. Narayanan and H. Neuberger, cf. Ref. [2], on the product of random unitary matrices (cf. also Sec. 5.5 above). Let us first take $\omega_1 < \omega_2$. The correlation functions in Eq. (12.6) tell us that the polynomial $J(z)$ depends only on the difference $\omega_2 - \omega_1$, so we could simply set $\omega_1 = 0$, and then we obviously are in the unitary case with $C = iH_2$. So for $\omega_2 - \omega_1 > 0$, the dependence on $\omega_2 - \omega_1$ can be absorbed in t by a rescaling,

$$t_\pm \equiv t(\omega_2 \pm \omega_1), \qquad t_+ \geq |t_-| \,. \tag{12.12}$$

Therefore, we get from Eq. (5.35) that

$$J(z) = \sum_{k=0}^{N} \binom{N}{k} z^{N-k} (-1)^k e^{-\frac{\tau_- k(N-k)}{2N}} \,, \tag{12.13}$$

where $\tau_- = t_-(1 + 1/N)$. For large N, nothing is lost by ignoring the difference between τ_- and t_-. From now on we set $\tau_- = t_-$,

$$J(z) = \sum_{k=0}^{N} \binom{N}{k} z^{N-k} (-1)^k e^{-\frac{t_- k(N-k)}{2N}} \,. \tag{12.14}$$

We also have an integral representation,

$$J(z) = \sqrt{\frac{Nt_-}{2\pi}} \int_{-\infty}^{\infty} d\lambda \, e^{-\frac{N}{2} t_- \lambda^2} \left[z - e^{-t_-(\lambda + \frac{1}{2})} \right]^N \,. \tag{12.15}$$

As mentioned in Sec. 5.5, it was shown in Ref. [2] that for $t_- > 0$ the above polynomial has all its roots on the unit circle.

For $\omega_2 - \omega_1 < 0$, we need to analytically continue to negative t_-. As observed in Ref. [2], this is evidently possible in the polynomial form. However, it no longer is true that all zeros are on the $|z| = 1$ circle. One can also analytically continue the integral expression,

$$J(z) = \sqrt{-\frac{Nt_-}{2\pi}} \int_{-\infty}^{\infty} d\lambda e^{\frac{N}{2} t_- \lambda^2} \left[z - e^{-t_-(i\lambda + \frac{1}{2})} \right]^N \,, \tag{12.16}$$

where, by Eq. (12.12), now $t_- < 0$.

Equations (12.15) and (12.16) can be combined into one line-integral expression,

$$J(z) = \sqrt{\frac{Nt_-}{2\pi}} \int_{\mathcal{L}} d\lambda \, e^{-\frac{N}{2} t_- \lambda^2} \left[z - e^{-t_-(\lambda + \frac{1}{2})} \right]^N \,. \tag{12.17}$$

Here, t_- is real of either sign and $\mathcal{L}$ is the real axis (from $-\infty$ to ∞) for $t_- > 0$ and the imaginary axis (from $-i\infty$ to $+i\infty$) for $t_- < 0$. For $t_- > 0$, we take $\sqrt{t_-} > 0$, and for $t_- < 0$, we take $\sqrt{t_-} = -i\sqrt{-t_-}$ with $\sqrt{-t_-} > 0$.

12.3 An exact representation of the generalized Gaussian model

We need the analogue of Eq. (11.24) to determine for which values of z the factorized formula (12.11) no longer holds and one expects non-zero surface eigenvalue density as a result of the loss of holomorphic factorization. The method of getting at this formula is the same as for the basic model; the one complication is that, in addition to the complex integrals over ζ_j and λ_j, one needs to introduce additional integrals over real variables ξ_j and θ_j, $j = 1, \ldots, n$. Still, at the end the dependence on N is made explicit.

These extra integrals are needed because more quadrilinear Grassmann interaction terms need to be decoupled. For the generalized model, the analogue of Eq. (11.18) reads (up to order ε^2)

$$\left\langle e^{-\bar\psi M\psi' - \bar\chi M^\dagger \chi'} \right\rangle = e^{\left(-\bar\psi\psi' - \bar\chi\chi'\right)\left[1 - \frac{\omega_-^2}{2}\left(1 - \frac{1}{N^2}\right)\right] - \frac{\omega_+^2}{N}(\bar\psi\chi')(\bar\chi\psi') - \frac{\omega_+^2}{N^2}(\bar\psi\psi')(\bar\chi\chi')} \times e^{\frac{\omega_-^2}{2N}\left(1+\frac{1}{N}\right)\left[(\bar\psi\psi')^2 + (\bar\chi\chi')^2\right]}, \tag{12.18}$$

where we introduced the notation

$$\omega_+ = \sqrt{\varepsilon^2(\omega_1 + \omega_2)}\,, \tag{12.19}$$

$$\omega_- = \begin{cases} \sqrt{|\varepsilon^2(\omega_2 - \omega_1)|} & \text{for } \omega_2 > \omega_1\,, \\ i\sqrt{|\varepsilon^2(\omega_2 - \omega_1)|} & \text{for } \omega_2 < \omega_1\,. \end{cases} \tag{12.20}$$

For $\omega_1 = \omega_2 = \frac{1}{2}$, we have $\omega_- = 0$ and $\omega_+ = \varepsilon^2$. In this case, the expectation value (12.18) reduces to the result for the basic model given in Eq. (11.18). We can decouple the terms that are quadratic in $\bar\psi\psi'$ and $\bar\chi\chi'$ by introducing integrals over real variables θ and ξ,

$$e^{\frac{\omega_-^2}{2N}\left(1+\frac{1}{N}\right)(\bar\psi\psi')^2} = \sqrt{\mathcal{N}_c}\int_{-\infty}^{\infty} d\xi\, e^{-\frac{N}{2}\xi^2} e^{\omega_- \sqrt{1+\frac{1}{N}}\,\xi(\bar\psi\psi')}\,, \tag{12.21}$$

$$e^{\frac{\omega_-^2}{2N}\left(1+\frac{1}{N}\right)(\bar\chi\chi')^2} = \sqrt{\mathcal{N}_c}\int_{-\infty}^{\infty} d\theta\, e^{-\frac{N}{2}\theta^2} e^{\omega_- \sqrt{1+\frac{1}{N}}\,\theta(\bar\chi\chi')} \tag{12.22}$$

with $\mathcal{N}_c = \frac{N}{2\pi}$. As for the basic complex model, we introduce integrals over complex variables ζ and λ to separate the remaining terms that are quartic in the Grassmann variables, cf. Eq. (11.19),

$$e^{-\frac{\omega_+^2}{N}(\bar\psi\chi')(\bar\chi\psi')} = \mathcal{N}_a \int d\mu(\zeta) e^{-N|\zeta|^2} e^{-\omega_+(\zeta\bar\psi\chi' - \zeta^*\bar\chi\psi')}\,, \tag{12.23}$$

$$e^{-\frac{\omega_+^2}{N^2}(\bar\psi\psi')(\bar\chi\chi')} = \mathcal{N}_b \int d\mu(\lambda) e^{-N^2|\lambda|^2} e^{-\omega_+(\lambda\bar\psi\psi' - \lambda^*\bar\chi\chi')}\,, \tag{12.24}$$

where $\mathcal{N}_a = \frac{N}{\pi}$ and $\mathcal{N}_b = \frac{N^2}{\pi}$.

As before, we can now integrate over the Grassmann variables ψ_j, $\bar\psi_j$, χ_j, $\bar\chi_j$ which makes the dependence on N explicit, cf. Eq. (11.24). The additional integrals over the variables θ_j and ξ_j, $1 \le j \le n$ (we need to decouple n expectation values of the type (12.18)) lead to a modification of the matrices A and D, which now depend on these integration variables (see below).

Since the integral over the variables λ_j is again of the form (11.28), it can be trivially approximated by a saddle point at the origin in the large-N limit. This results in

$$\langle |\det(z - W_n)|^2 \rangle = \mathcal{N}_a^n \mathcal{N}_c^n \int \prod_{j=1}^{n} [d\mu(\zeta_j) d\xi_j d\theta_j]\, e^{-N\sum_{j=1}^n \left(|\zeta_j|^2 + \frac{1}{2}\xi_j^2 + \frac{1}{2}\theta_j^2\right)} \det{}^N \begin{pmatrix} A & B \\ C & D \end{pmatrix}, \tag{12.25}$$

where

$$A = -\left(1 - \frac{1}{2}\omega_-^2\left(1 - \frac{1}{N^2}\right) - \omega_-\sqrt{1+\frac{1}{N}}\Xi\right) + e^{\sigma}T^\dagger\,, \tag{12.26}$$

$$D = -\left(1 - \frac{1}{2}\omega_-^2\left(1 - \frac{1}{N^2}\right) - \omega_-\sqrt{1+\frac{1}{N}}\Theta\right) + e^{\sigma^*}T\,, \tag{12.27}$$

$$B = -\omega_+ Z = -C^\dagger \tag{12.28}$$

with

$$T = \begin{pmatrix} 0 & 1 & 0 & \cdots & 0 & 0 \\ 0 & 0 & 1 & \cdots & 0 & 0 \\ \vdots & \vdots & \vdots & \ldots & \vdots & \vdots \\ 0 & 0 & 0 & \cdots & 0 & 1 \\ 1 & 0 & 0 & \cdots & 0 & 0 \end{pmatrix} \tag{12.29}$$

and

$$Z = \mathrm{diag}(\zeta_1, \ldots, \zeta_n)\,, \quad \Xi = \mathrm{diag}(\xi_1, \ldots, \xi_n)\,, \quad \Theta = \mathrm{diag}(\theta_1, \ldots, \theta_n)\,. \tag{12.30}$$

Equation (12.25) is the analogue of Eq. (11.30) for the basic complex model. As for the basic model, setting $\lambda_j = 0$ (and ignoring terms of order N^{-1} and N^{-2} in A and D) is equivalent to abandoning the restriction $\mathrm{Tr}\, C = 0$ from the beginning. We observe that this restriction does not affect the boundaries of the charged region for the generalized model in the infinite-N limit, too.

12.4 Region of stability of the factorized saddle

The identity

$$\det\begin{pmatrix} A & B \\ C & D \end{pmatrix} = \det(A)\det(D)\det(1 - D^{-1}CA^{-1}B) \tag{12.31}$$

shows that the variables ζ_j and ζ_j^* only enter as bilinears $\zeta_j\zeta_k^*$. At large N, the ζ-integral will be dominated by some saddle point, and $\zeta_j = 0$ is a trivial solution to the ζ saddle-point equations, for any Θ, Ξ. Where this saddle point dominates, z is always in the region of vanishing eigenvalue density. The reason is that we have $C = B = 0$ at this saddle, and then the remaining Ξ and Θ integrals factorize, which results in

$$\begin{aligned} \langle|\det(z - W_n)|^2\rangle &= \mathcal{N}_c^n \int \prod_{j=1}^n [d\xi_j d\theta_j]\, e^{-N\sum_{j=1}^n\left(\frac{1}{2}\xi_j^2 + \frac{1}{2}\theta_j^2\right)}\det{}^N(AD) \\ &= \left|\mathcal{N}_c^{\frac{n}{2}} \int \prod_{j=1}^n [d\xi_j]\, e^{-N\sum_{j=1}^n\left(\frac{1}{2}\xi_j^2\right)}\det{}^N(A)\right|^2 . \end{aligned} \tag{12.32}$$

Since

$$\det(A) = (-1)^{n-1}\left[z - \prod_{j=1}^n\left(1 - \frac{1}{2}\omega_-^2\left(1 - \frac{1}{N^2}\right) - \omega_-\sqrt{1+\frac{1}{N}}\xi_j\right)\right] \tag{12.33}$$

depends only on z, and not on z^*, we have holomorphic factorization. Therefore, it is just the structure of the ζ-saddle which determines if z is in a chargeless region. The

holomorphic factor in Eq. (12.32), however, is relevant to the local stability of the trivial saddle point. At the $\zeta = 0$ saddle, we have to compute

$$K(z) = (-1)^{N(n-1)} \mathcal{N}_c^{\frac{n}{2}} \int \prod_{j=1}^{n} [d\xi_j]\, e^{-N\sum_{j=1}^{n}\left(\frac{1}{2}\xi_j^2\right)} \det{}^N(A)$$
$$= \mathcal{N}_c^{\frac{n}{2}} \int \prod_{j=1}^{n} [d\xi_j]\, e^{-N\sum_{j=1}^{n}\left(\frac{1}{2}\xi_j^2\right)} \left[z - \prod_{j=1}^{n} \left(1 - \frac{1}{2}\omega_-^2 \left(1 - \frac{1}{N^2} \right) - \omega_- \sqrt{1 + \frac{1}{N}}\xi_j \right) \right]^N , \tag{12.34}$$

which determines the holomorphic factorized form of $\langle |\det(z - W_n)|^2 \rangle$. This integral has been performed in Ref. [2] (cf. Sec. 2.1.4 therein) by an $O(n)$ transformation of the integration variables ξ_j, introducing polar-coordinates for $n-1$ integration variables, integrating over the associated angular variables, and performing a saddle-point approximation for the radial variable in the limit $n \to \infty$ (with t kept finite). This reduces the n-dimensional integral above to a single one-dimensional integral. In the large-N limit, this leads to

$$K(z) = J(z) \tag{12.35}$$

with $J(z)$ defined in Eqs. (12.15) and (12.16). This means that we indeed have

$$\langle |\det(z - W_n)|^2 \rangle = |K(z)|^2 = |J(z)|^2 \tag{12.36}$$

whenever the integral over the ζ variables can be approximated by the trivial saddle point at $|\zeta_j|^2 = 0$. To determine the local stability of this saddle point, we need the saddle point which dominates the integral over the ξ_j variables in the integral (12.34). In the following, we consider the case $\omega_2 > \omega_1$; with obvious changes, a similar story holds for $\omega_2 < \omega_1$. The derivation leading from Eq. (12.34) to Eq. (12.15) shows that the saddle-point equation, translated back to the original integration variables (before the $O(n)$ rotation), is simply given by $\xi_j = \xi$ for all j, where

$$\xi = \sqrt{\frac{t_-}{n}} \lambda_s \tag{12.37}$$

with finite (n-independent) λ_s. Here, λ_s is a saddle point of the integrand in Eq. (12.15) and has to satisfy

$$\lambda_s = \frac{1}{z e^{t_-(\lambda_s + \frac{1}{2})} - 1} . \tag{12.38}$$

The appropriate contour $\mathcal{L}$ in Eq. (12.17), whose endpoints at infinity are fixed, will be deformed to λ_s, and we assume that the integral will be dominated by one single saddle point as long as one is in the chargeless region (i.e., the mapping between z and λ_s is one-to-one).

To leading order in N, we then have

$$\det(A) \to (-1)^{n-1} \left[z - \prod_{j=1}^{n} \left(1 - \frac{t_-}{2n} - \sqrt{\frac{t_-}{n}}\xi \right) \right] = (-1)^{n-1} \left[z - e^{-t_-(\lambda_s + \frac{1}{2})} \right] \tag{12.39}$$

in the limit $n \to \infty$ with t kept finite. We end up with the following expression for the matrices A and D needed for the analysis of the stability of the trivial saddle under variations of ζ,

$$A = -\left[1 - \frac{t_-}{n} \left(\lambda_s + \frac{1}{2} \right) \right] \mathbf{1} + e^{\sigma} T^{\dagger} , \qquad D = A^{\dagger} . \tag{12.40}$$

It is now convenient to define $\hat{u} = \lambda_s + \frac{1}{2}$. From Eq. (12.38), we obtain that the relation between $\hat{u}$ and z can be written as

$$z \equiv z(u) = \frac{\hat{u} + \frac{1}{2}}{\hat{u} - \frac{1}{2}} e^{-t_- \hat{u}} \equiv Z(\hat{u}, t_-)\,, \tag{12.41}$$

where $Z(u,t)$ is introduced in Eq. (11.54) and z is defined in terms of u in Eq. (11.48),

$$z(u) = \frac{u + \frac{1}{2}}{u - \frac{1}{2}}\,. \tag{12.42}$$

In terms of the map $U(w,t)$, we have

$$\hat{u} = U(z, t_-)\,, \tag{12.43}$$

where we also allow for $t_- < 0$, corresponding to "backward evolution".

The stability of the trivial saddle is now determined by $\hat{u}$ from

$$\det\left[1 + \omega_+^2 Z^\dagger A^{-1} Z (A^\dagger)^{-1}\right] \tag{12.44}$$

with

$$A = -e^{-\frac{t_- \hat{u}}{n}}\, \mathbf{1} + e^\sigma T^\dagger = e^{-\frac{t_- \hat{u}}{n}} \left(-\mathbf{1} + e^{\sigma + \frac{t_- \hat{u}}{n}} T^\dagger\right)\,, \tag{12.45}$$

where, as before, $e^{n\sigma} = z$. We can drop the prefactor $e^{-\frac{t_- \hat{u}}{n}}$ because there is an extra ε^2 prefactor in the determinant. We therefore end up with

$$\det\left[1 + \frac{t_+}{n} Z^\dagger \hat{A}^{-1} Z (\hat{A}^\dagger)^{-1}\right]\,, \tag{12.46}$$

where

$$\hat{A} = -\mathbf{1} + e^{\hat{\sigma}} T^\dagger \tag{12.47}$$

and

$$\hat{z} = e^{n\hat{\sigma}} = e^{n\sigma + t_- \hat{u}} = z e^{t_- \hat{u}} = \frac{\hat{u} + \frac{1}{2}}{\hat{u} - \frac{1}{2}}\,. \tag{12.48}$$

Comparison with the $\omega_1 = \omega_2 = \frac{1}{2}$ case (see Eqs. (11.29), (11.31), and (11.44)) now immediately leads to a condition determining the region of stability of the trivial saddle point in terms of the $\hat{z}$ variable,

$$1 > \frac{t_+}{2|\hat{z} - 1|^2} \frac{|\hat{z}|^2 - 1}{\log|\hat{z}|}\,. \tag{12.49}$$

The variable $\hat{z}$ is defined by the complex number $\hat{u}$ which in turn is determined by z and t_- in Eq. (12.41). Since the relation between $\hat{z}$ and $\hat{u}$ is the same as the one between z and u, the region of vanishing eigenvalue density in the $\hat{u}$-plane is given by (see Eq. (11.51))

$$0 \le \hat{u}_i^2 \le \hat{u}_r \coth(t_+ \hat{u}_r) - \hat{u}_r^2 - 1/4\,, \tag{12.50}$$

where $\hat{u}_r = \operatorname{Re}\hat{u}$ and $\hat{u}_i = \operatorname{Im}\hat{u}$. The boundary separating charged and chargeless region in the complex-$\hat{u}$ plane can then be mapped to the boundary in the original z-plane through Eq. (12.41).

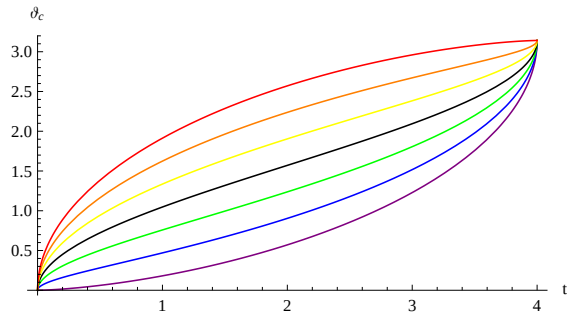

Figure 37: Plots of $\theta_c(t_+ = t, t_- = t(1-2\omega_1))$ as a function of t for $\omega_1 = 1$ (purple), $\omega_1 = \frac{5}{6}$ (blue), $\omega_1 = \frac{2}{3}$ (green), $\omega_1 = \frac{1}{2}$ (black), $\omega_1 = \frac{1}{3}$ (yellow), $\omega_1 = \frac{1}{6}$ (orange), $\omega_1 = 0$ (red). We have $\theta_c = \pi$ at $t = 4$ for all ω_1 since we have set $\omega_2 = 1 - \omega_1$ resulting in $t_+ = t$. The basic complex model is obtained for $\omega_1 = \frac{1}{2}$, the unitary case corresponds to $\omega_1 = 0$. For fixed t, θ_c increases as we go from the Hermitian model to the unitary model, cf. also Figs. 38 and 39 below.

Using the maps Z and U, this can be written in a more compact form: Let the unit circle $|w| = 1$ be parametrized by $|s| \leq \pi$, with $w = e^{is}$. For $|z| \neq 1$, the boundary separating the charged and chargeless region is defined in the z-plane by $z = f(s)$, given by

$$f(s) = Z(U(e^{is}, t_+), t_-) \quad \text{for} \quad \operatorname{Re} U(e^{is}, t_+) \neq 0\,. \tag{12.51}$$

Note that $t_+ \geq |t_-|$. For $t_+ < 4$, the boundary intersects the unit circle in the z-plane at the points

$$z = Z\left(\pm i\sqrt{\frac{1}{t_+} - \frac{1}{4}}, t_-\right). \tag{12.52}$$

For $t_+ < 4$, the maximum angle for which the eigenvalue density is non-zero is therefore given by

$$\theta_c(t_+, t_-) = \arccos\left(1 - \frac{t_+}{2}\right) + t_-\sqrt{\frac{1}{t_+} - \frac{1}{4}}\,. \tag{12.53}$$

For $t_+ = t_- = t$, W is unitary and we recover Eq. (4.92) derived for the unitary case in Sec. 4.4. For $t_- = 0$, we are in the basic complex model and the above equation reduces to Eq. (11.47). See Fig. 37 for plots of $\theta_c(t_+, t_-)$.

From Eq. (12.49) we obtain, by comparison with the basic model, that the domain of non-vanishing eigenvalue density is confined to

$$e^{-\gamma(t_+)} \leq |\hat{z}| \leq e^{\gamma(t_+)} \tag{12.54}$$

with $\gamma(t)$ defined in Eq. (10.65). This is mapped to

$$e^{-\gamma(t_+)\left(1-\frac{t_-}{t_+}\right)} \leq |z| \leq e^{\gamma(t_+)\left(1-\frac{t_-}{t_+}\right)}\,, \tag{12.55}$$

which is equivalent to Eq. (12.9).

The topological transition from a simply connected to a multiply connected domain of non-vanishing eigenvalue density in the complex-z plane occurs at $t_+ = 4$. In complete analogy to the basic model, setting aside the restriction $\det(W_n) = 1$ does not affect the boundary in the infinite-N limit.

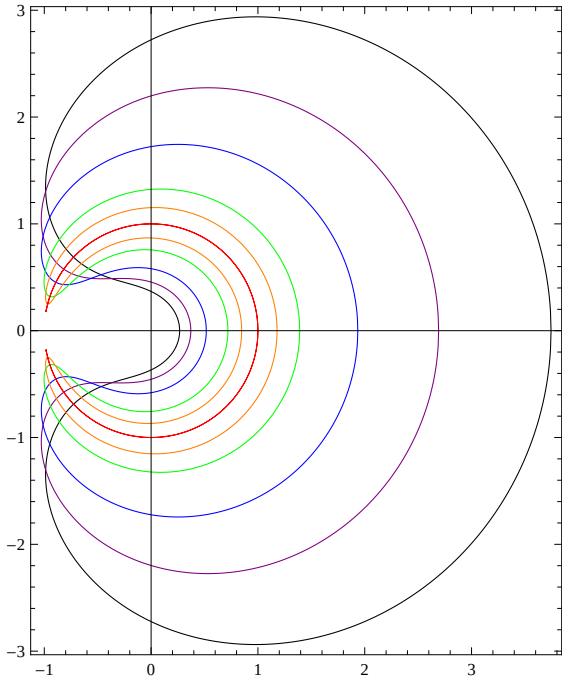

Figure 38: Plots of the boundary separating charged and chargeless region in the complex-z plane for $t_+ = 3$ fixed and $t_- = 1$ (black), $t_- = 1.5$ (purple), $t_- = 2$ (blue), $t_- = 2.5$ (green), $t_- = 2.75$ (orange), and $t_- = 3$ (red). As t_- increases, the domain of non-vanishing eigenvalue density (given by the interior of the closed curves) shrinks towards the unit circle, and the intersection point of the boundary with the unit circle moves closer to $z = -1$. However, since t_+ is below the critical value ($t_+ < 4$), the domain of non-vanishing eigenvalue density remains simply connected for all t_-. For $t_- = t_+ = 3$, we are in the unitary case and the eigenvalues are confined to the unit circle $|z| = 1$.

Figures 38 and 39 show plots of the boundary separating the domain of non-vanishing eigenvalue density and the domain of vanishing eigenvalue density in the complex-z plane for fixed t_+ and different values of t_-. Since $t_- = 0$ is equivalent to $\omega_2 = \omega_1$, the generalized model reduces to the basic model for vanishing t_-. For $t_- = t_+$, we are in the unitary case, $\omega_1 = 0$, and all eigenvalues are located on the unit circle $|z| = 1$. For $t_- = -t_+$, we have $\omega_2 = 0$, which means that the individual factors $M_j = e^{\varepsilon C_j}$ are Hermitian.

12.5 Numerical results

12.5.1 Linear version of the generalized model

As mentioned above, the linear model is much more convenient for numerical simulations than the exponential one. Performing a similar stability analysis for the linear version of the generalized model, it turns out that the boundaries of the domains with non-vanishing eigenvalue density for the two models (exponential and linear) are equivalent up to a simple scaling factor.

For the linear (generalized) model, we take again $M_j = \mathbf{1} + \varepsilon C_j$ for each factor in the product defining W_n (as in Sec. 11.6). In this case, we have to replace Eq. (12.18) by

$$\left\langle e^{-\bar\psi M\psi' - \bar\chi M^\dagger \chi'} \right\rangle = e^{\left(-\bar\psi\psi' - \bar\chi\chi'\right) - \frac{\omega_+^2}{N}\left(\bar\psi\chi'\right)\left(\bar\chi\psi'\right) - \frac{\omega_+^2}{N^2}\left(\bar\psi\psi'\right)\left(\bar\chi\chi'\right)} \times e^{\frac{\omega_-^2}{2N}\left(1+\frac{1}{N}\right)\left[\left(\bar\psi\psi'\right)^2 + \left(\bar\chi\chi'\right)^2\right]}. \tag{12.56}$$

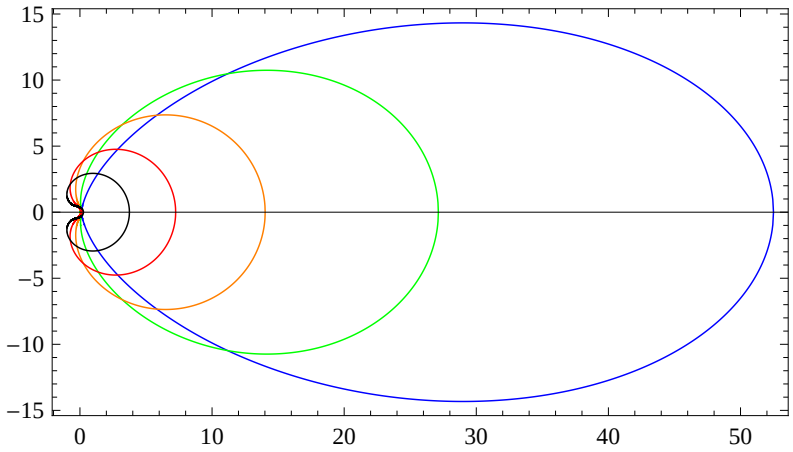

Figure 39: Plots of the boundary separating charged and chargeless region in the complex-z plane for $t_+ = 3$ fixed and $t_- = -3$ (blue), $t_- = -2$ (green), $t_- = -1$ (orange), $t_- = 0$ (red), and $t_- = 1$ (black). For $t_- = 0$, the generalized model reduces to the basic complex model; for $t_- = -t_+$ we are in the Hermitian case (only the factors M_j are Hermitian, but the product matrix W is non-Hermitian and the eigenvalues are not confined to the real axis).

This expression differs from Eq. (12.18) only in the coefficient of the $\bar{\psi}\psi' + \bar{\chi}\chi'$ term. The procedure presented in detail for the exponential model has to be modified by replacing the expression for $\det A$ in Eq. (12.33) with

$$\det(A) = (-1)^{n-1} \left[z - \prod_{j=1}^{n} \left(1 - \omega_- \sqrt{1 + \frac{1}{N}\xi_j} \right) \right] , \tag{12.57}$$

i.e., the term of order ω_-^2 has to be discarded. This means that the "linear" versions of Eqs. (12.38) and (12.40) read

$$A = -\left[1 - \frac{t_-}{n} \bar{\lambda}_s \right] \mathbf{1} + e^{\sigma} T^{\dagger} , \tag{12.58}$$

where $\bar{\lambda}_s$ has to satisfy

$$\bar{\lambda}_s = \frac{1}{z e^{t_- - \bar{\lambda}_s} - 1} . \tag{12.59}$$

If we now define

$$\hat{\bar{z}} = z e^{t_- - \bar{\lambda}_s} , \tag{12.60}$$

substituting the relation $\hat{z} = z e^{t_- \left(\lambda_s - \frac{1}{2}\right)}$ for the exponential model, then the domain of vanishing eigenvalue density in the $\hat{\bar{z}}$-plane is again given by Eq. (12.49) with the replacement $\hat{z} \to \hat{\bar{z}}$. However, the relation between $\hat{\bar{z}}$ and the original variable z is different from the relation between $\hat{z}$ and z. For the exponential model, we have

$$\lambda_s = \frac{1}{\hat{z} - 1} , \qquad z = \hat{z} e^{-t_- \left(\lambda_s + \frac{1}{2}\right)} = \hat{z} e^{-t_- \left(\frac{1}{\hat{z}-1} + \frac{1}{2} \right)} . \tag{12.61}$$

For the linearized form of the model, the corresponding equations read

$$\bar{\lambda}_s = \frac{1}{\hat{\bar{z}} - 1} , \qquad z = \hat{\bar{z}} e^{-t_- \bar{\lambda}_s} = \hat{\bar{z}} e^{-t_- \frac{1}{\hat{\bar{z}}-1}} . \tag{12.62}$$

Since the domain of vanishing eigenvalue density for the linear model in the $\hat{\tilde{z}}$-plane is identical to the domain of vanishing eigenvalue density for the exponential model in the $\hat{z}$-plane, the boundary of the chargeless region in the z-plane for the exponential model is identical to the boundary for the linear model scaled with a factor of $e^{-t_-/2}$. (For the basic model, we have $t_- = 0$ and the boundaries become identical, see also Sec. 11.5.)

12.5.2 Numerical results for the linear model

The following figures show perfect agreement between numerically obtained eigenvalue domains and analytically determined boundaries for the linear model (data points as well as predicted boundaries are scaled by the corresponding factor of $e^{-t_-/2}$, i.e., the plots show the expected behavior for the exponential model). Therefore, we expect that the stability analysis gives the correct boundary for the exponential model, too.

Figure 41 shows results of numerical simulations for $\omega_1 = 1/10$, $\omega_2 = 1/2$, with all other parameters as in Sec. 11.6. The topological transition occurs at $t = 20/3$, which corresponds to $t_+ = \frac{20}{3}\left(\frac{1}{2} + \frac{1}{10}\right) = 4$ in agreement with the prediction for the transition point.

Figure 40 is generated with $\omega_2 = 1$ and $\omega_1 = 1/2000$ for $t = 1$. Since this is already close to the unitary model, the eigenvalues are restricted to the vicinity of the unit circle in the z-plane, which corresponds to the imaginary axis in the u-plane. As t_+ is below the critical value, we get vanishing eigenvalue density around $z = -1$ or $u = 0$.

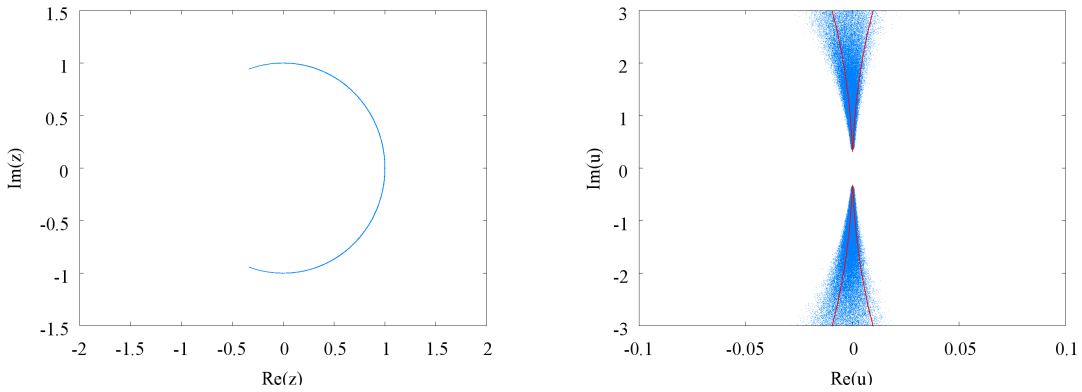

Figure 40: Scatter plot of the eigenvalues of W in the z-plane (left) and in the u-plane (right) for $\omega_1 = 1/2000$, $\omega_2 = 1$ and $t = 1$.

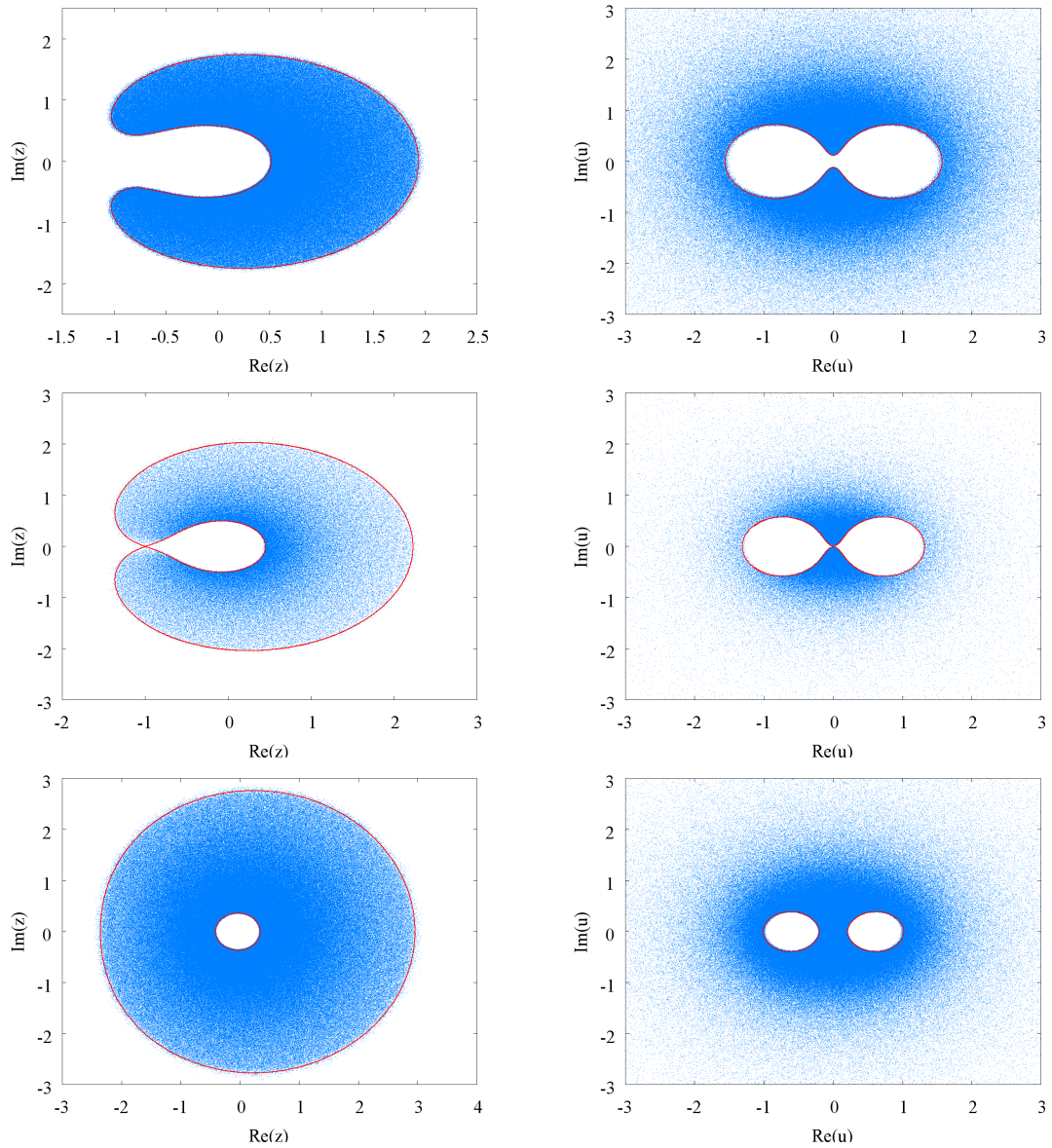

Figure 41: Scatter plot of the eigenvalues of W in the z-plane (left) and in the u-plane (right) for $\omega_1 = 1/10$, $\omega_2 = 1/2$ and $t = 5$ (top), $t = 20/3$ (center), $t = 10$ (bottom).

13 Beyond infinite N and the associated saddle-point approximation

Our motivation for re-analyzing and generalizing the model introduced in Ref. [3] is the guess that it might be a universal representative of the large-N phase structure of large classes of complex matrix Wilson loops[21]. Like in the unitary case, we would like to study in more detail the approach to infinite N and see what the matrix model universal features of this transition are. To do this, we need a more convenient finite-N representation of the average of the product of two characteristic polynomials we have been looking at. More precisely, we would like to first take the continuum limit $\varepsilon \to 0$, $n \to \infty$ without making any assumptions about how large N is and only later take N large. (This is in contrast to the analysis of the previous sections, where we used the saddle-point method to approximate n-dimensional integrals at large N to derive an equation for the boundary of the domain of non-vanishing eigenvalue density in the infinite-N limit at finite n.) In this section, an outline of how one could achieve this is presented, however, this approach has not been carried to completion yet because, as will become clear, a full analysis keeping exact N-dependence is complicated. We hope that using the presented technique one could learn which subleading terms in the large-N limit can be dropped without changing the universal properties of the approach to the large-N limit. We start with the unitary case for which the problem has been studied in Ref. [2] and present an alternative approach leading to the same results. This alternative way can be generalized to the complex matrix case, where we first look at the simplest complex matrix model and then at the more general one.

13.1 The unitary case

As before, we consider the SU(N) case but drop some irrelevant $\mathcal{O}(1/N)$ corrections to keep the formulas simple. We have seen that in the unitary case it is sufficient to look at the average of the characteristic polynomial, and there is no need to calculate the average of its absolute value squared, which is a significant simplification. Employing Grassmann integrals, one can derive the following representation of the average characteristic polynomial (cf. Eq. (12.34) and Ref. [2])

$$\langle \det(z-W)\rangle = \int \prod_{i=1}^{n} \left[\frac{\sqrt{N}d\lambda}{\sqrt{2\pi}}\right] \left(z - \prod_{j=1}^{n}\left(1-\frac{\varepsilon^2}{2}-\varepsilon\lambda_j\right)\right)^N e^{-\frac{N}{2}\sum_{i=1}^{n}\lambda_i^2}\,. \tag{13.1}$$

Here, W is the product of n unitary matrices all close to the identity matrix. We introduce the notation

$$\rho(\lambda)d\lambda = \sqrt{\frac{N}{2\pi}}e^{-\frac{N}{2}\lambda^2}d\lambda \tag{13.2}$$

and

$$a_n = \prod_{j=1}^{n}\left(1-\frac{\varepsilon^2}{2}-\varepsilon\lambda_j\right)\,. \tag{13.3}$$

We are only interested in the limit $n \to \infty$, $\varepsilon \to 0$ with $t = n\varepsilon^2$ kept fixed. We eliminate the λ-independent term without affecting the limit by introducing new variables

$$\hat{a}_n = \prod_{j=1}^{n}(1-\varepsilon\lambda_j), \qquad a_n = e^{-\frac{t}{2}}\hat{a}_n\,. \tag{13.4}$$

[21] We shall refer to this hypothetical class as the large-N universality class.

We now proceed by finding the probability distribution for the variable $\hat{a}_n$. In other words, we look for a way to perform the integral over all λ-variables keeping the product we are interested in fixed at some arbitrary value $\hat{a}$. This can be done in the limit we are interested in, where the probability density for $\hat{a}$ would be $P(\hat{a};t)d\hat{a}$. $P(\hat{a};t)d\hat{a}$ is obtained from the $P^{(n)}(\hat{a};t)d\hat{a}$, the probability densities governing the variables $\hat{a}_n$ at step n. We can use the method of Sec. 10.4 to derive $P(\hat{a};t)$. In fact, the product defining $\hat{a}_n$ is just a linear version of the model studied in detail in Sec. 10.4.2. The basic step is to derive a recursion relation for the $P^{(n)}(\hat{a};t)$ and take the limit on that recursion relation. In complete analogy to the calculation of Sec. 10.4.2, we obtain (up to order ε^2)

$$P^{(n)}(\hat{a};t) = P^{(n-1)}(\hat{a};t) + \frac{\varepsilon^2}{N}\left[1 - N\partial_t + 2\hat{a}\partial_{\hat{a}} + \frac{1}{2}\hat{a}^2\partial_{\hat{a}}^2\right] P^{(n-1)}(\hat{a};t), \tag{13.5}$$

which is the analogue of Eq. (10.17) above.

In the limit, the recursion relation leads to a partial differential equation which is of the Fokker-Planck type,

$$N\frac{\partial P(\hat{a};t)}{\partial t} = P(\hat{a};t) + 2\hat{a}\frac{\partial P(\hat{a};t)}{\partial \hat{a}} + \frac{1}{2}\hat{a}^2\frac{\partial^2 P(\hat{a};t)}{\partial \hat{a}^2}\,. \tag{13.6}$$

In conjunction with the boundary condition $\lim_{t\to 0^+} P(\hat{a};t) = \delta(\hat{a}-1)$, this equation determines $P(\hat{a};t)$ completely. The above equation can also be written in the form

$$N\partial_t P = \partial_{\hat{a}}(\hat{a}P) + \frac{1}{2}\partial_{\hat{a}}\hat{a}^2\partial_{\hat{a}}P\,, \tag{13.7}$$

showing explicitly that the integral $\int P d\hat{a}$ is time-independent and therefore equal to unity, its initial value.

The equation with the delta function initial condition has the following solution (see Ref. [62]), describing a log-normal distribution,

$$P(\hat{a};t) = \sqrt{\frac{N}{2\pi t}}e^{-\frac{N}{2t}(\log\hat{a}+\frac{t}{2N})^2}\,. \tag{13.8}$$

We can now write an expression for the average characteristic polynomial in terms of an integral over the variable $\hat{a}$,

$$\langle\det(z-W)\rangle = \int d\hat{a}\left(z - \hat{a}e^{-\frac{t}{2}}\right)^N P(\hat{a};t)\,. \tag{13.9}$$

Changing the integration variables,

$$\hat{a} = e^{-t\mu - \frac{t}{2N}}\,, \tag{13.10}$$

we finally arrive at

$$\langle\det(z-W)\rangle = \sqrt{\frac{Nt}{2\pi}}\int d\mu\left(z - e^{-t\left(\frac{1}{2}+\mu+\frac{1}{2N}\right)}\right)^N e^{-\frac{N}{2}t\mu^2}\,. \tag{13.11}$$

Dropping the $t/2N$ term in the exponent inside the parenthesis in the integrand, this reproduces the result of Eq. (12.15).

One does not need to solve the Fokker-Planck equation exactly in order to get the large-N limit because N plays a role in Eq. (13.7) which is analogous to $1/\hbar$. With $P = e^{NS}$, the Fokker-Planck equation reduces to a Hamilton-Jacobi equation for S at large N,

$$\frac{\partial S}{\partial t} = \frac{1}{2}\hat{a}^2\left(\frac{\partial S}{\partial \hat{a}}\right)^2 + \mathcal{O}(1/N)\,. \tag{13.12}$$

The solution that satisfies the initial condition is particularly simple,

$$S = -\frac{1}{2t}\log^2 \hat{a}\,. \tag{13.13}$$

As usual, there is a prefactor to e^{NS} which contains additional t-dependence, but this factor is not needed for the large-N limit.

In the expression for the average characteristic polynomial (cf. Eq. (13.9)), we now have two terms that are exponential in N,

$$e^{N\left[\log\left(z-e^{-\frac{t}{2}}\hat{a}\right)-\frac{1}{2t}\log^2\hat{a}\right]}\,, \tag{13.14}$$

and the saddle-point equation therefore is

$$-\frac{e^{-\frac{t}{2}}}{z-e^{-\frac{t}{2}}\hat{a}} = \frac{1}{t}\frac{\log\hat{a}}{\hat{a}}\,. \tag{13.15}$$

With $\hat{a} = e^{-t\lambda}$, this reproduces the saddle-point equation we had before,

$$\lambda = \frac{1}{ze^{t\left(\lambda+\frac{1}{2}\right)}-1}\,. \tag{13.16}$$

The main conclusion is that, as it often is the case in the context of large-N models, one has a "quantum"-like equation for finite N with $1/N$ playing a role analogous to $\hbar$. The large-N limit is then "semiclassical", with the "quantum" equation being replaced by a classical one, in a variant of the WKB method. This is what we would like to duplicate in the complex matrix case.

13.2 The basic product of random complex matrices

13.2.1 An exact map to a product of random 2 × 2 matrices

In the following, we do not restrict the determinant of W_n to keep the analysis as simple as possible. As explained in Sec. 11, we can then start from Eq. (11.21) without the λ-integrals,

$$\begin{aligned}\left\langle|\det(z-W_n)|^2\right\rangle = \mathcal{N}_a^n \int\prod_{j=1}^{n}[d\bar{\psi}_j d\psi_j d\bar{\chi}_j d\chi_j d\mu(\zeta_j)]e^{-\varepsilon\sum_{j=1}^{n}(\zeta_j\bar{\psi}_j\chi_{j-1}-\zeta_j^*\bar{\chi}_j\psi_{j+1})}\\ \times e^{-\sum_{j=1}^{n}(\bar{\psi}_j\psi_{j+1}+\bar{\chi}_j\chi_{j-1})}e^{\sum_{j=1}^{n}(e^{\sigma}\bar{\psi}_j\psi_j+e^{\sigma^*}\bar{\chi}_j\chi_j)}e^{-N\sum_{j=1}^{n}|\zeta_j|^2}\,.\end{aligned} \tag{13.17}$$

We now change the notation by introducing two-component Grassmann variables Φ_j, $\bar{\Phi}_j$,

$$\Phi_j = \begin{pmatrix}\psi_j\\ \chi_{j-1}\end{pmatrix}, \qquad \bar{\Phi}_j = \left(\bar{\psi}_j,\,\bar{\chi}_j\right)\,, \tag{13.18}$$

where each component, e.g., ψ_j, has in turn N components (scalar products are implicitly denoted by $\bar{\psi}_j\psi_j \equiv \sum_{a=1}^{N}\left(\bar{\psi}_j\right)_a\left(\psi_j\right)_a$, cf. Sec. 11.3). Equation (13.17) can then be written as

$$\begin{aligned}\left\langle|\det(z-W_n)|^2\right\rangle = (-1)^{N(n-1)}\mathcal{N}_a^n\int\prod_{j=1}^{n}[d\bar{\Phi}_j d\Phi_j d\mu(\zeta_j)]e^{-N\sum_{j=1}^{n}|\zeta_j|^2}\\ \times\exp\left[\sum_{j=1}^{n}\left(\bar{\Phi}_j\begin{pmatrix}e^{\sigma} & -\varepsilon\zeta_j\\ 0 & -1\end{pmatrix}\Phi_j+\bar{\Phi}_j\begin{pmatrix}-1 & 0\\ \varepsilon\zeta_j^* & e^{\sigma^*}\end{pmatrix}\Phi_{j+1}\right)\right],\end{aligned} \tag{13.19}$$

where the factor $(-1)^{N(n-1)}$ results from bringing the integration measures for the new variables Φ_j and $\bar{\Phi}_j$ in canonical order (cf. Eq. (D.8)) after the index shift in χ_j.

We can again change integration variables from $\bar{\Phi}_j$ to $\bar{\Phi}_j \begin{pmatrix} e^{\sigma} & -\varepsilon\zeta_j \\ 0 & -1 \end{pmatrix}$. This variable change produces an additional factor of (each Φ_j has in total $2N$ Grassmann components)

$$\left[\prod_{j=1}^{n} \det \begin{pmatrix} e^{\sigma} & -\varepsilon\zeta_j \\ 0 & -1 \end{pmatrix}\right]^N = (-1)^{nN} z^N \tag{13.20}$$

since $e^{n\sigma} = z$. This results in

$$\begin{aligned}\left\langle |\det(z - W_n)|^2 \right\rangle = (-z)^N \mathcal{N}_a^n \int \prod_{j=1}^{n} [d\bar{\Phi}_j d\Phi_j d\mu(\zeta_j)] e^{-N\sum_{j=1}^{n} |\zeta_j|^2} \\ \times \exp\left[\sum_{j=1}^{n} \left(\bar{\Phi}_j \Phi_j - e^{-\sigma} \bar{\Phi}_j \begin{pmatrix} -1 & \varepsilon\zeta_j \\ 0 & e^{\sigma} \end{pmatrix} \begin{pmatrix} -1 & 0 \\ \varepsilon\zeta_j^* & e^{\sigma^*} \end{pmatrix} \Phi_{j+1}\right)\right].\end{aligned} \tag{13.21}$$

Now, we can use the identity (11.12) to integrate over all the Grassmann variables, which results in an expression containing another random matrix product, but this time the matrices are just 2×2,

$$\left\langle |\det(z - W_n)|^2 \right\rangle = (-z)^N \mathcal{N}_a^n \int \prod_{j=1}^{n} [d\mu(\zeta_j)] e^{-N\sum_{j=1}^{n} |\zeta_j|^2} \det{}^N \left(1 - \frac{1}{z} \prod_{j=1}^{n} Q_j\right) \tag{13.22}$$

with

$$Q_j = \begin{pmatrix} 1 + \varepsilon^2 |\zeta_j|^2 & \varepsilon e^{\sigma^*} \zeta_j \\ \varepsilon \zeta_j^* e^{\sigma} & e^{\sigma + \sigma^*} \end{pmatrix}. \tag{13.23}$$

Absorbing the phase factor $\exp\left(\frac{\sigma^* - \sigma}{2}\right)$ into the variables ζ_j, the matrices Q_j can be further simplified to

$$Q_j = e^{\frac{\sigma + \sigma^*}{2}} \begin{pmatrix} (1 + \varepsilon^2 |\zeta_j|^2) e^{-\frac{\sigma + \sigma^*}{2}} & \varepsilon\zeta_j \\ \varepsilon\zeta_j^* & e^{\frac{\sigma + \sigma^*}{2}} \end{pmatrix}. \tag{13.24}$$

The matrix after the prefactor is an $\mathrm{SL}(2, \mathbb{C})$ matrix. Hence, the product of Q_j matrices will be, up to a simple multiplicative factor, also in $\mathrm{SL}(2, \mathbb{C})$ and the two-dimensional multiplicative random matrix model defines a stochastic process on the $\mathrm{SL}(2, \mathbb{C})$ manifold. Unlike the $N \times N$ matrix ensemble, the new 2×2 matrix ensemble has no inversion symmetry and only a restricted conjugation symmetry.

With the parametrization $z = e^{n\sigma} = |z| e^{i\Psi}$, we can write

$$\left\langle |\det(z - W_n)|^2 \right\rangle = (-z)^N \mathcal{N}_a^n \int \prod_{j=1}^{n} [d\mu(\zeta_j)] e^{-N\sum_{j=1}^{n} |\zeta_j|^2} \det{}^N \left(1 - e^{-i\Psi} \Delta_n\right), \tag{13.25}$$

where $\Delta_n = \prod_{j=1}^{n} Y_j$ and

$$Y_j = \begin{pmatrix} |z|^{-1/n} (1 + \varepsilon^2 |\zeta_j|^2) & \varepsilon\zeta_j \\ \varepsilon\zeta_j^* & |z|^{1/n} \end{pmatrix}. \tag{13.26}$$

The new multiplicative matrix ensemble has $\det Y_j = 1$, so Δ_n is restricted to $\mathrm{SL}(2,\mathbb{C})$, which in turn implies

$$(-z)\det\left(1-e^{-i\Psi}\Delta_n\right) = (-z)e^{-i\Psi}\det\left(e^{i\frac{\Psi}{2}}-e^{-i\frac{\Psi}{2}}\Delta_n\right) = -|z|\left(2\cos\Psi-\mathrm{Tr}\,\Delta_n\right) \tag{13.27}$$

and

$$\left\langle|\det(z-W_n)|^2\right\rangle = |z|^N\mathcal{N}_a^n\int\prod_{j=1}^n[d\mu(\zeta_j)]e^{-N\sum_{j=1}^n|\zeta_j|^2}\left(\mathrm{Tr}\,\Delta_n-2\cos\Psi\right)^N\,. \tag{13.28}$$

In the new ensemble, we have invariance under complex conjugation and conjugation by a U(1) subgroup,

$$Y_j \to \begin{pmatrix} e^{i\theta_j} & 0 \\ 0 & e^{-i\theta_j}\end{pmatrix} Y_j \begin{pmatrix} e^{-i\theta_j} & 0 \\ 0 & e^{i\theta_j}\end{pmatrix}\,, \tag{13.29}$$

since this conjugation results only in a phase factor for the ζ_j variables,

$$\begin{pmatrix} e^{i\theta_j} & 0 \\ 0 & e^{-i\theta_j}\end{pmatrix} Y_j \begin{pmatrix} e^{-i\theta_j} & 0 \\ 0 & e^{i\theta_j}\end{pmatrix} = \begin{pmatrix} |z|^{-1/n}(1+\varepsilon^2|\zeta_j|^2) & \varepsilon\zeta_j e^{2i\theta_j} \\ \varepsilon\zeta_j^* e^{-2i\theta_j} & |z|^{1/n}\end{pmatrix}\,. \tag{13.30}$$

Therefore, the probability density of Δ_n will be invariant under

$$\Delta_n \to \begin{pmatrix} e^{i\theta} & 0 \\ 0 & e^{-i\theta}\end{pmatrix}\Delta_n\begin{pmatrix} e^{-i\theta} & 0 \\ 0 & e^{i\theta}\end{pmatrix}. \tag{13.31}$$

Hence, the Fokker-Planck equation for this case (see Sec. 10.4 for a general description of the derivation),

$$\frac{\partial\Sigma_N}{\partial t} = \Theta_N\Sigma_N\,, \tag{13.32}$$

is an equation for a function Σ_N of six real variables including t (z is a parameter), i.e., Θ_N is a linear partial differential operator of second degree in five real variables. There are no terms from the measure if we pick the latter to be $\mathrm{SL}(2,\mathbb{C})$ invariant.

The dependence on N is explicit, the integration over the ζ variables produces

$$\mathcal{N}_a\int d\mu(\zeta)e^{-N|\zeta|^2} = \mathcal{N}_a\frac{\pi}{N} = 1\,, \qquad \mathcal{N}_a\int d\mu(\zeta)e^{-N|\zeta|^2}|\zeta|^2 = \frac{1}{N} \tag{13.33}$$

and

$$\mathcal{N}_a\int d\mu(\zeta)e^{-N|\zeta|^2}\zeta = \mathcal{N}_a\int d\mu(\zeta)e^{-N|\zeta|^2}\zeta^* = 0\,, \tag{13.34}$$

$$\mathcal{N}_a\int d\mu(\zeta)e^{-N|\zeta|^2}\zeta^2 = \mathcal{N}_a\int d\mu(\zeta)e^{-N|\zeta|^2}\zeta^{*2} = 0\,. \tag{13.35}$$

Since all terms in Y_j that are linear in ε come with a factor of ζ_j or ζ_j^*, cf. Eq. (13.26), all second-order derivative terms in the differential operator Θ_N carry a $1/N$ factor. Among the first-order derivative terms some have a $1/N$ factor and others are N-independent because Y_j contains terms of order ε^2 which are multiplied with $|\zeta_j|^2$, resulting in a $1/N$ factor when integrated out, as well as terms of order ε^2 which are independent of ζ_j (coming from $|z|^{\frac{1}{n}} = 1+\frac{\varepsilon^2}{t}\log|z|+\mathcal{O}(\varepsilon^4)$) resulting in N-independent terms.

One can write down an exact integral expression for $Q(z, z^*)$ in terms of $\Sigma_N(\Delta_n; |z|, t)$,

$$Q(z, z^*; t) = |z|^N \int d\mu(\Delta_n) \Sigma_N(\Delta_n; |z|; t) (\mathrm{Tr}\, \Delta_n - 2\cos\Psi)^N \,. \tag{13.36}$$

In the infinite-N limit, $Q(z, z^*)$ would be given by a dominating saddle point, and subleading corrections would identify the relevant large-N universality class.

An analysis of the Fokker-Planck equation for arbitrary z seems to be too complicated to attack directly, so in the following, we restrict our attention to the unit circle, $|z| = 1$.

13.2.2 Simplifications for $|z| = 1$ and large N

Setting $|z| = 1$ simplifies the operator Θ_N, eliminating the first-order derivative terms that had no N-dependence. Consequentially, at $|z| = 1$, one has

$$N \frac{\partial \Sigma_N}{\partial t} = \Theta \Sigma_N \,, \tag{13.37}$$

where Θ is independent of N.

We are looking for solutions having the structure

$$\Sigma_N \sim \exp\left[-\frac{N}{t} S + \ldots \right], \tag{13.38}$$

where the dots stand for terms subleading in t/N. Due to the structure of the Fokker-Planck equation, all terms which are linear in the derivatives can be ignored at large N, as long as we keep $|z| = 1$. This leads us to replace the $|z| = 1$ model, defined by the factors

$$Y_j = \begin{pmatrix} (1 + \varepsilon^2 |\zeta_j|^2) & \varepsilon \zeta_j \\ \varepsilon \zeta_j^* & 1 \end{pmatrix}, \tag{13.39}$$

by a new model, defined by the factors

$$Y_j' = \frac{1}{\sqrt{1 - \varepsilon^2 |\zeta_j|^2}} \begin{pmatrix} 1 & \varepsilon \zeta_j \\ \varepsilon \zeta_j^* & 1 \end{pmatrix}. \tag{13.40}$$

The Y' model preserves the U(1) symmetry of the Y model and differs from it only in the first-order derivative terms, while the powers of N appear in the same places as before. Therefore, the leading large-N behavior of the two models is the same. The advantage of the new model is that the factors are now restricted to an SU(1, 1) subgroup of SL(2, $\mathbb{C}$), which forces also the product Δ' into SU(1, 1). This implies that the solution $\Sigma_N'(\Delta'; t)$ depends on only two real variables in addition to t.

We observe now that with the right choice of variables, the second-order derivatives acting on $\Sigma_N(\Delta; t)$ only attack two of the five real arguments (on which Σ_N depends, in addition to t) also in the Y model. Therefore, in the large-N limit, one can again look for a solution of the form (13.38). Furthermore, this discussion indicates that significant simplifications will occur at large N even for $|z| \neq 1$, when first-order derivative terms that matter also in the large-N limit appear.

13.2.3 Fokker-Planck equation for the new ensemble at $|z| = 1$

We now focus on the SU(1, 1) model and for notational convenience drop the primes, which now get a different use. The recursion relation determining the Fokker-Planck equation is

$$\Delta = \Delta' Y \tag{13.41}$$

with

$$Y = \frac{1}{\sqrt{1-|\omega|^2}} \begin{pmatrix} 1 & \omega \\ \omega* & 1 \end{pmatrix}, \quad \omega = \varepsilon\zeta\,. \tag{13.42}$$

The structure of the Fokker-Planck equation will be simpler in a well-chosen parametrization. The best choice of parameters is determined by the symmetries obeyed both by the equation and by our particular initial condition. To derive the Fokker-Planck equation, it is convenient to parametrize Δ by

$$\Delta = \begin{pmatrix} a & b \\ b^* & a^* \end{pmatrix}, \quad |a|^2 - |b|^2 = 1\,, \tag{13.43}$$

with

$$a = \sqrt{u}e^{i\phi}, \quad b = \sqrt{u-1}e^{i\psi}, \quad \infty \geq u \geq 1, \ -\pi \leq \phi, \psi \leq \pi\,. \tag{13.44}$$

In these variables, the invariant measure on SU(1, 1) is $dud\phi d\psi$, up to a constant. The recursion relation for Δ is

$$\begin{pmatrix} a' & b' \\ b'* & a'* \end{pmatrix} = \begin{pmatrix} a-\delta a & b-\delta b \\ b^*-\delta b^* & a^*-\delta a^* \end{pmatrix} = \begin{pmatrix} a & b \\ b^* & a^* \end{pmatrix} Y^{-1}\,, \tag{13.45}$$

where $\delta a = a - a'$ and $\delta b = b - b'$. Working out the algebra, and keeping only terms up to second order in ω and among those only terms that could contribute to a term of the form $|\omega|^2$, we find that

$$\delta a = b\omega^* - \frac{1}{2}a|\omega|^2\,, \qquad \delta b = a\omega - \frac{1}{2}b|\omega|^2\,, \tag{13.46}$$

due to $u - \delta u = |a - \delta a|^2$, $i(\phi - \delta\phi) = \log\frac{a-\delta a}{|a-\delta a|}$, results in

$$\delta u = -(2u-1)|\omega|^2 + \sqrt{u(u-1)}\left(e^{i(\psi-\phi)}\omega^* + e^{-i(\psi-\phi)}\omega\right)\,, \tag{13.47}$$

$$\delta\phi = \frac{i}{2}\sqrt{\frac{u-1}{u}}\left(e^{i(\phi-\psi)}\omega - e^{i(\psi-\phi)}\omega^*\right)\,. \tag{13.48}$$

Because of the invariance under conjugation with a $U(1)$ subgroup, cf. Eq. (13.31), the probability distribution of Δ does not depend on the angular variable ψ. Integrating over ω, ω^*, the Fokker-Planck equation is found to be

$$N\frac{\partial\Sigma_N(u,\phi;t)}{\partial t} = -H\Sigma_N(u,\phi;t)\,, \tag{13.49}$$

where H is given by

$$H = -\frac{\partial}{\partial u}u(u-1)\frac{\partial}{\partial u} - \frac{u-1}{4u}\frac{\partial^2}{\partial\phi^2}\,. \tag{13.50}$$

Transforming variables to $u = (1+x)/2$, $x \geq 1$, we get

$$H = -\frac{\partial}{\partial x}(x^2-1)\frac{\partial}{\partial x} - \left(\frac{x}{2(x+1)} - \frac{1}{4}\right)\frac{\partial^2}{\partial\phi^2}\,. \tag{13.51}$$

This equation is almost identical to Eq. (28) in Ref. [62], the difference is the 1/4 term in the prefactor of the second derivative with respect to ϕ. The invariances of the equations

are the reason for the similarity (in Ref. [62], the multiplicative random ensemble consists of real 2×2 matrices of the form $1+\varepsilon X$, where X is real and drawn from identical Gaussian distributions for each of its four entries).

The initial condition $\lim_{t\to0^+}\Sigma_N(u,\phi;t) = 2\delta(u-1)\delta_{2\pi}(\phi)$ ($\delta_{2\pi}(\phi) = \frac{1}{2\pi}\sum_{n\in\mathbb{Z}} e^{in\phi}$) is N-independent, and we take the integration measure to be $dud\phi$. Taking into account Eq. (13.49), we conclude that the dependence of Σ_N on N and t is of the form

$$\Sigma_N(u,\phi;t) = \Sigma\left(u,\phi;\frac{t}{N}\right). \tag{13.52}$$

Therefore, the large-N limit is dominated by the short time ($\hat{t} = t/N$) behavior of the probability distribution $\Sigma(u,\phi;\hat{t})$.

In Ref. [62], the authors solve their equation by separation of variables. The ϕ-dependence must be periodic and is labeled by an integer $m \in \mathbb{Z}$. In each sector, H is replaced by

$$H_m = -\frac{\partial}{\partial x}(x^2-1)\frac{\partial}{\partial x} + m^2\left(\frac{x}{2(x+1)} - \frac{1}{4}\right). \tag{13.53}$$

The eigenfunctions and eigenvalues of H_m are known exactly. We see that our problem will be solved in an identical way, only the eigenvalues have to be shifted by $(m/2)^2$. This shift does not affect the matching onto the initial condition, which is the same here as in Ref. [62]. Therefore a formula for $\Sigma(u,\phi;\hat{t})$ is available, and we know that, although explicit, it is difficult to do much with it at the analytic level.

13.2.4 Large-N limit from the Fokker-Planck equation at $|z| = 1$

For the modified model, Eq. (13.36) looks as follows for $z = e^{i\Psi}$,

$$Q(z,z^*;t) = \int_1^\infty du \int_{-\pi}^{\pi} d\phi \Sigma\left(u,\phi;\frac{t}{N}\right) 2^N(\sqrt{u}\cos\phi - \cos\Psi)^N. \tag{13.54}$$

As $t/N \to 0$, Σ must become a delta function in u and ϕ. Therefore, for small t/N we expect $\Sigma(u,\phi;t/N)$ to drop rapidly as u increases beyond 1 and ϕ departs from 0. Looking at H, we realize that the ϕ-derivative term is suppressed for u close to 1. This leads us to the simple ansatz

$$\Sigma\left(u,\phi;\frac{t}{N}\right) \sim \frac{N}{t}\delta_{2\pi}(\phi)e^{-\frac{N}{t}(u-1)}. \tag{13.55}$$

When this is inserted into the expression for Q, the integral over ϕ is trivial, leaving only the integral over u,

$$Q(z,z^*;t) = \frac{N}{t}\int_1^\infty du\, e^{-\frac{N}{t}(u-1)}(2\sqrt{u} - 2\cos\Psi)^N. \tag{13.56}$$

This integral will be dominated by a saddle point or by the endpoint $u = 1$. When the endpoint dominates, we get the holomorphically factorized answer $(2-2\cos\Psi)^N = |1-e^{i\Psi}|^{2N}$ we have seen before (resulting in vanishing eigenvalue density). Thus, "saddle A" (introduced in the analysis of Sec. 11.4) corresponds to endpoint dominance in the integral (13.56).

The saddle-point equation for u is

$$\frac{t}{2} = \left(\sqrt{u} - \cos\Psi\right)\sqrt{u}, \tag{13.57}$$

and its positive solution is given by

$$\sqrt{u_s} = \frac{1}{2}\left(\cos\Psi + \sqrt{\cos^2\Psi + 2t}\right). \tag{13.58}$$

We see that this saddle is available for $z = e^{i\Psi}$ on the unit circle only when

$$\sqrt{u_s} > 1, \quad \cos\Psi > 1 - \frac{t}{2}, \tag{13.59}$$

in agreement with our findings earlier (see Eq. (11.46)): when the integral is not dominated by the endpoint, holomorphic factorization no longer holds, which results in non-zero eigenvalue density on the unit circle for $\cos\Psi > 1 - \frac{t}{2}$. However, once the saddle is away from the endpoint, the ansatz form of Σ is no longer plausible, and a more complete analysis is needed.

13.3 The generalized Gaussian model: Exact map to a random multiplicative model of 2×2 matrices

When $\omega_1 \neq \omega_2$, i.e., in the generalized case, one can again reduce the problem to a product of random 2×2 matrices, albeit of a slightly more complicated structure than the one we have seen in the $\omega_1 = \omega_2$ case discussed above. Using similar manipulations, one can derive the representation

$$\begin{aligned}\langle|\det(z - W_n)|^2\rangle = \mathcal{N}_a^n \mathcal{N}_c^n (-z)^N \int \prod_{j=1}^{n} [d\mu(\zeta_j) d\xi_j d\theta_j e^{-N\sum_{j=1}^{n}(|\zeta_j|^2 + \frac{1}{2}\xi_j^2 + \frac{1}{2}\theta_j^2)} \\ \times \left[\prod_{j=1}^{n}(d_j)\right]^N \left[\det\left(\mathbf{1} - \prod_{j=1}^{n}(A_j^{-1}B_j)\right)\right]^N,\end{aligned} \tag{13.60}$$

where

$$d_j = 1 - \frac{1}{2}\omega_-^2 - \omega_-\theta_j \tag{13.61}$$

and

$$A_j = \begin{pmatrix} e^{\sigma} & \omega_+\zeta_j \\ 0 & 1 - \frac{1}{2}\omega_-^2 - \omega_-\theta_j \end{pmatrix}, \qquad B_j = \begin{pmatrix} 1 - \frac{1}{2}\omega_-^2 - \omega_-\xi_j & 0 \\ -\omega_+\zeta_j^* & e^{\sigma^*} \end{pmatrix}. \tag{13.62}$$

Now, one can proceed to take the $\varepsilon \to 0$ limit, deriving a Fokker-Planck equation for the new 2×2 random matrix product of $A_j^{-1}B_j$. The structure is similar to the one in the special case analyzed before, and it seems that no progress can be made before the special case is fully solved.

13.4 Large-N universality

The main objective of the attempt to go beyond the infinite-N saddle-point approximation is to identify a universality class for the large-N phase transition, its exponents and its associated relevant perturbations. For the unitary case, this can be achieved by studying $\langle\det(z-W)\rangle$, however, for complex matrices we need the more complicated object $\langle|\det(z-W)|^2\rangle$, which both has a large-N phase transition and a region where large-N factorization does not hold (i.e., $\langle|\det(z-W)|^2\rangle \neq |\langle\det(z-W)\rangle|^2$), and probably the large-N universal region will have to deal with both of these issues. Although one can make simplifications that do not matter at large N without loosing the universal properties, we have not yet

learned how to do this effectively. A simpler case might be when $\omega_1 t \ll 1$. In that case, we are close to the unitary model, with the unit circle slightly expanded into a strip of similar shape in the complex plane. This case might be easier to treat, in the sense of establishing large-N universal properties in an appropriately defined regime of "weak non-unitarity" (analogous to the regime of weak non-Hermiticity in non-multiplicative random complex matrix ensembles, see, e.g., Ref. [69]).

Part IV

Numerical computation of entanglement entropy in free QFT

The following discussion is somewhat unrelated to the previous parts of this thesis. The results presented here are published in Ref. [70] and have been obtained in collaboration with Herbert Neuberger, Adam Schwimmer, and Stefan Theisen.

Recently, there has been a lot of interest in entanglement entropy in quantum field theories, associated with certain regions of the underlying spacetime: For a $(d+1)$-dimensional QFT, this entanglement entropy is defined as the von Neumann entropy of the reduced density matrix which is obtained by tracing out the degrees of freedom residing inside a d-dimensional submanifold of the underlying spacetime. It turns out that for a free massless scalar field in four-dimensional Euclidean spacetime, the entropy associated with an imaginary sphere is at leading order proportional to the area of the sphere, a result which is similar to the area law found for the intrinsic entropy of a black hole [71]. Since existing analytical calculations of subleading terms rely on some non-trivial assumptions (e.g., the replica trick, cf. Ref. [72]), we have determined the next-order correction to the area law in four dimensions, a logarithmic term which might be universal, by numerical means. Using the regularization introduced by M. Srednicki in Ref. [71], we have found numerically that the coefficient of the logarithm is $-1/90$ to 0.2 percent accuracy (cf. Sec. 15), which is in agreement with an existing analytical result (cf. Ref. [72]).

14 Entanglement entropy

14.1 Entanglement for simple quantum mechanical systems

Quantum entanglement is one of the fascinating features distinguishing the quantum theory from classical physics, formulated, e.g., in the famous Einstein-Podolsky-Rosen paradox and Bell's inequalities. The essential property of an entangled quantum system is that a local measurement of one part of the system can instantaneously determine the outcome of a second measurement, which may be performed far away. Measures of entanglement in general play an important role, e.g., in quantum information theory, quantum cryptography, and quantum computation. The concept of entanglement entropy provides a convenient way to quantify how closely entangled a given state of a composite quantum system is.

Let us consider first a quantum mechanical system consisting of two subsystems A and B with associated Hilbert spaces H_A and H_B of dimension n_A and n_B, respectively. With $n = \min\{n_A, n_B\}$, any pure state $|\psi\rangle \in H_A \otimes H_B$ of the composite system can be written in the so-called Schmidt decomposition

$$|\psi\rangle = \sum_{j=1}^{n} c_j \, |\psi_j^A\rangle \otimes |\psi_j^B\rangle \ , \tag{14.1}$$

where $\{|\psi_1^A\rangle, \ldots, |\psi_{n_A}^A\rangle\}$ and $\{|\psi_1^B\rangle, \ldots, |\psi_{n_B}^B\rangle\}$ are appropriate orthonormal bases in H_A and H_B, and the coefficients c_j can be made real and non-negative by adjusting the phases

of the states in the two bases. The set of numbers $\{c_1, \ldots, c_n\}$ is uniquely determined by the state $|\psi\rangle$; a proper normalization of $|\psi\rangle$ can ensure $\sum_j c_j^2 = 1$.

The state $|\psi\rangle$ is said to be *entangled* if (and only if) it cannot be represented by a single direct product of two states contained in H_A and H_B, i.e., if there is more than one non-vanishing coefficient c_j in the sum (14.1) above.

The *entanglement entropy* of the pure state, which is described by the density matrix

$$\rho = |\psi\rangle \langle\psi| \ , \tag{14.2}$$

is defined as the von Neumann entropy $S(\rho_A) = S(\rho_B)$ of the density matrix associated with one of the subsystems by tracing out the degrees of freedom of the other subsystem,

$$\rho_A = \mathrm{Tr}_B \, |\psi\rangle \langle\psi| = \sum_{j=1}^{n} c_j^2 \, |\psi_j^A\rangle \langle\psi_j^A| \ , \tag{14.3}$$

$$\rho_B = \mathrm{Tr}_A \, |\psi\rangle \langle\psi| = \sum_{j=1}^{n} c_j^2 \, |\psi_j^B\rangle \langle\psi_j^B| \ , \tag{14.4}$$

see, e.g., Ref. [73] and references therein. The von Neumann entropy is defined as

$$S(\rho_A) = -\,\mathrm{Tr}\, \rho_A \log \rho_A = -\sum_{j=1}^{n} c_j^2 \log c_j^2 = S(\rho_B) \tag{14.5}$$

and can be interpreted as the entropy measured by an observer who can only access subsystem A (resp. B) and is completely isolated from subsystem B (resp. A). The eigenvalues of ρ_A and ρ_B are identical, up to additional zeros (for $n_A \neq n_B$), which results in $S(\rho_A) = S(\rho_B)$.

If the pure state $|\psi\rangle$ is not entangled, there is only one non-vanishing coefficient c_j and the entanglement entropy vanishes (the non-zero coefficient has to be equal to unity). For an entangled state, the entropy is non-zero and assumes its maximum value of $\log n$ if $c_j^2 = \frac{1}{n}$ for all $j = 1, \ldots, n$. In this case, the density matrices ρ_A and ρ_B describe mixed systems with an additional degree of uncertainty (beyond that due to quantum mechanics), and the entanglement entropy quantifies the lack of knowledge of the respective inaccessible subsystem.

For the "classical" example of two coupled spin-$\frac{1}{2}$ states, a maximally entangled state of the composite system is, e.g., given by the singlet state

$$\frac{1}{\sqrt{2}} \left(|\uparrow\rangle \otimes |\downarrow\rangle - |\downarrow\rangle \otimes |\uparrow\rangle \right) \tag{14.6}$$

(the coefficients can be made non-negative, e.g., by taking $-\,|\downarrow\rangle$ as a basis state in the first basis). The density matrix obtained by tracing out one of the two spins is given by

$$\rho_A = \rho_B = \begin{pmatrix} \frac{1}{2} & 0 \\ 0 & \frac{1}{2} \end{pmatrix} \ , \tag{14.7}$$

resulting in maximum entropy $S(\rho_A) = S(\rho_B) = \log 2$.

Note that the entanglement entropy defined in this way does not provide a good measure for the entanglement of a composite system that is in a mixed state, i.e., a system which is described by a statistical mixture of pure quantum states (in general, this case requires a minimization procedure over decompositions of the associated mixed state density matrix; see, e.g., Ref. [73]).

In Ref. [71], Srednicki outlines a calculation for the entanglement entropy of a system of N coupled harmonic oscillators described by the Hamiltonian

$$H = \frac{1}{2}\sum_{j=1}^{N} p_j^2 + \frac{1}{2}\sum_{i,j=1}^{N} x_i K_{ij} x_j \tag{14.8}$$

with K being a real, symmetric matrix that has only positive eigenvalues. The ground state wave function ψ_0 of the composite system is obtained by diagonalizing the matrix K,

$$\psi_0(x_1,\ldots,x_N) = \pi^{-\frac{N}{4}}\,(\det K)^{\frac{1}{8}}\, e^{-x^T\sqrt{K}x}\,. \tag{14.9}$$

Tracing out the first $n < N$ oscillators results in a density matrix for the remaining $N-n$ oscillators,

$$\begin{aligned}&\rho_{\text{out}}(x_{n+1},\ldots,x_N;x'_{n+1},\ldots,x'_N)\\ &\quad= \int dx_1\cdots dx_n \psi_0(x_1,\ldots,x_n,x_{n+1},\ldots,x_N)\psi_0^*(x_1,\ldots,x_n,x'_{n+1},\ldots,x'_N)\,.\end{aligned} \tag{14.10}$$

The Gaussian integral can be performed by decomposing $\sqrt{K}$ into blocks according to the separation of $x_1,\ldots,x_N$ into "inside" degrees of freedom $x_1,\ldots,x_n$ and "outside" degrees of freedom $x_{n+1},\ldots,x_N$,

$$\sqrt{K} = \begin{pmatrix} A & B \\ B^T & C \end{pmatrix}\,, \tag{14.11}$$

where A is an $n\times n$ matrix, C is an $(N-n)\times(N-n)$ matrix, and B is an $n\times(N-n)$ matrix. By a suitable change of variables from $x_{n+1},\ldots,x_N$ to $z_1,\ldots,z_{N-n}$, the density matrix ρ_{out} can be brought into a factorized form

$$\rho_{\text{out}}(z,z') \propto \prod_{j=1}^{N-n} e^{-\frac{1}{2}\left(z_j^2+z_j'^2\right)+\beta'_j z_j z'_j}\,, \tag{14.12}$$

where the β'_j, $j=1,\ldots,N-n$, denote the eigenvalues of the matrix

$$\beta' = \frac{1}{\sqrt{C-\beta}}\beta\frac{1}{\sqrt{C-\beta}} \tag{14.13}$$

with

$$\beta = \frac{1}{2}B^T A^{-1} B\,. \tag{14.14}$$

The entropy of ρ_{out} is determined by the eigenfunctions and eigenvalues of the $N-n$ independent factors in the product (14.12). It is found to be given by

$$S(\rho_{\text{out}}) = \sum_{j=1}^{N-n}\left(-\log(1-\xi_j) - \frac{\xi_j}{1-\xi_j}\log\xi_j\right)\,, \tag{14.15}$$

where

$$\xi_j = \frac{\beta'_j}{1+\sqrt{1-\beta'^2_j}}\,. \tag{14.16}$$

This can be written as

$$S(\rho_{\text{out}}) = -\operatorname{Tr}\left[\log(1-\Xi) + \frac{\Xi}{1-\Xi}\log\Xi\right], \qquad \Xi = \frac{\beta'}{1+\sqrt{1-\beta'^2}}. \tag{14.17}$$

All square roots and inversions are well-defined and the eigenvalues of Ξ, ξ_j, obey $0 \leq \xi_j \leq 1$ for all $j = 1, \ldots, N-n$.

It is also shown in Ref. [71] that the above result for N coupled harmonic oscillators can be generalized to the case of a free quantum field theory (cf. Sec. 15 below).

14.2 Entanglement entropy in quantum field theory

We now consider a free massless real field $\phi(t, \vec{x})$ defined in four-dimensional spacetime (with t denoting time). We work in the Hamiltonian formalism and assume that at $t = 0$ the system is in its ground state, the vacuum. We wish to eliminate the quantum degrees of freedom associated with $\phi(\vec{x})$ and its conjugate momentum $\pi(\vec{x})$ located in the spherical region $|\vec{x}| \leq R$ in space. We eliminate these degrees of freedom by tracing over all wave functionals of $\phi(\vec{x})$ with $|\vec{x}| \leq R$. Vacuum expectation values of operators $\mathcal{O}$ depending only on $\phi(\vec{x})$ and $\pi(\vec{x})$ with $|\vec{x}| > R$, denoted as ϕ_{out}, π_{out}, respectively, can be expressed with the help of the density matrix operator $\rho_{\text{out}}(\phi_{\text{out}}, \phi'_{\text{out}})$,

$$\langle \mathcal{O} \rangle = \operatorname{Tr}\left(\mathcal{O}\rho_{\text{out}}\right). \tag{14.18}$$

The reduced density matrix ρ_{out} represents a mixed state and a measure of its "distance" from a pure state may again be taken as the von Neumann entropy

$$S_{\text{out}} = S(\rho_{\text{out}}) = -\operatorname{Tr}\rho_{\text{out}}\log\rho_{\text{out}}. \tag{14.19}$$

One can trace out the outside degrees of freedom instead which results in an entropy $S_{\text{in}} = S(\rho_{\text{in}})$ that is equal to S_{out} since the reduced density matrices ρ_{in} and ρ_{out} are obtained from a pure state (the ground state) and therefore have the same eigenvalues, up to zeros that do not contribute to the entropy (cf. also Eq. (14.5) above). Hence, it is not surprising that the entanglement entropy is not an extensive quantity and in general depends only on the geometric properties of the surface separating the regions "in" and "out".

The entropy $S_{\text{in}} = S_{\text{out}}$ is non-zero because the operators $\phi(\vec{x})$ are coupled for points $\vec{x}$ infinitesimally close to the two sides of the surface $|\vec{x}| = R$. Were it not for the spatial derivative terms in the Hamiltonian, the ground state would be a single tensor product over $\vec{x}$ of functionals of $\phi(\vec{x})$ and the elimination of the degrees of freedom inside the sphere would leave a pure state describing the outside degrees of freedom. Thus, one can view S_{out} as an entanglement entropy where the reference basis is made out of single tensor products of functionals of $\phi(\vec{x})$. Since the reason for $S_{\text{in}} = S_{\text{out}} \neq 0$ is due to the coupling of the fields at the surface of the sphere, this also indicates that the entropy should depend only on the surface of the sphere and its embedding in flat spacetime. As the coupling causing the entanglement occurs at infinitesimal separation, it is natural that a complete definition of the entropy will require, at the least, an ultraviolet cutoff, i.e., a small distance a. Without any cutoff, there could be no dependence on R since the entropy is a pure number. For the same reason, only a logarithmic dependence on R can have an a-independent meaning. The main result presented in Ref. [70] is a numerical estimate for this coefficient of $\log R$ in S_{out} (cf. Sec. 15 below).

In Ref. [74], a general formula for S_{out} is derived for Hamiltonians that are quadratic in the fields. Furthermore, it is shown that with the addition of a mass term to the

Hamiltonian, the entropy per unit surface for a cavity of the form of a three-dimensional slab of finite thickness is finite in the $a \to 0$ limit after the subtraction of a divergent term which does not depend on the thickness. First, ultraviolet and infrared cutoffs are introduced, and then, the appropriate limits are taken.

Ref. [74] also outlines the calculation for more general cavities. In the spherical case with massless free fields, the entropy cannot be finite and R-dependent because R is the single available scale. The spherical case was first studied numerically by Srednicki in Ref. [71]. Srednicki independently arrived at the same setting of the problem as Bombelli et al. in Ref. [74] and took the next step and evaluated $S_{\rm out}$ for the case of the sphere with a specific regularization. It turns out that one only needs to discretize the spatial radial direction and that there are no infrared divergences. The short distance structure in the spatial angular directions does not require any ultraviolet regularization, in agreement with the expectation that only the coupling in the normal direction to the sphere surface is relevant. If the lattice spacing in the radial direction is denoted by a, the leading term in $S_{\rm out}$ is proportional to $(R/a)^2$ for $R/a \to \infty$. The coefficient of this leading term was computed numerically in Ref. [71], but it clearly is not a universal number, i.e., it is not independent of the regularization procedure.

The spherical case is particularly interesting since tracing out the degrees of freedom inside the imaginary sphere (in the vacuum of flat space) results in an entanglement entropy that is somewhat reminiscent of the Bekenstein-Hawking entropy $S_{\rm BH}$ of a black hole, being proportional to the area A of the event horizon, $S_{\rm BH} = \frac{1}{4} M^2_{\rm Planck} A$. (The classical law that the surface area of the event horizon of a black hole can only increase with time led Bekenstein to the suggestion that it might be related to an entropy. This interpretation was supported by other analogies between classical black holes and thermodynamics found by Bardeen, Carter, and Hawking, and finally by Hawking's discovery that applying quantum mechanics to matter fields in the background geometry of a black hole metric leads to the emission of particles corresponding to a thermal spectrum with a certain temperature (determined by the mass of the black hole), which enables the black hole to remain in equilibrium with thermal radiation at the same temperature, see, e.g., Ref. [75].) The observation that the entanglement entropy in free field theory is also proportional to the area of the (imaginary) boundary surface led to the interpretation that the amount of missing information in the black hole case, quantified by the entropy $S_{\rm BH}$, can be viewed in analogy to the entropy resulting from restricting the access of an observer to the outside of a sphere in flat spacetime [71, 74].

In Ref. [70], we have followed Srednicki and pushed his numerical analysis further, looking for terms in $S_{\rm out}$ that are subleading in R/a. We found subleading terms of the form

$$c \log(R/a) + d \,. \tag{14.20}$$

We determined the values $c = -1/90$ and $d = -0.03537$ with a precision of about two tenths of a percent (cf. Sec. 15 below). Like the coefficient of the leading $(R/a)^2$ term, the constant d is non-universal, but the value $-1/90$ for c is expected to be a universal number (cf. Sec. 15.4 for a more detailed discussion).

Since c might be universal, there ought to be other, analytical, ways to derive it. An attractive method to do this is based on an analogue of the so-called replica method, using the identity

$$S_{\rm out} = -\frac{\partial}{\partial n} \operatorname{Tr} \rho_{\rm out}^n \big|_{n=1} \,. \tag{14.21}$$

First, the vacuum wave functional is represented by a functional integral over the Euclidean half space $t < 0$. The reduced density matrix $\rho_{\rm out}$ is then obtained by gluing two copies of the half space along the space region complementary to the "outside" region (the interior

of the sphere) at $t = 0$. For integer n, the trace operation can then be implemented by taking n copies of the Euclidean space, which are cut along the complement of the imaginary sphere, and cyclically gluing together successive copies along the two sides of the cut. At the end, $\mathrm{Tr}\,\rho_{out}^n$ is obtained from a partition function on a complicated Riemann surface, an n-sheeted manifold with conical singularities located at the boundary of the sphere (see Ref. [72] for details). One advantage of this method is that the universal term can be obtained from the conformal anomaly, perhaps in closed form and for arbitrarily shaped cavities, not just a spherical one. However, handling the singularity and the needed analytic continuation in n make the application of this method somewhat uncertain.

In the 't Hooft large-N limit of a conformal field theory, one may try to use the AdS/CFT correspondence in order to calculate the entanglement entropy for various cavities in the context of strongly interacting conformal field theories. One needs a prescription for the quantity corresponding to S_{out}. An ansatz that seems to work is reviewed in Ref. [76]. This ansatz can be applied to $\mathcal{N} = 4$ U(N) supersymmetric YM theory and leads to an entropy given by $-N^2 \log R$ for the sphere.

The result of applying the replica method to the spherical case for a real scalar field in flat four-dimensional spacetime is quoted in the review [72] and relevant references are given. The answer they quote is $c = -1/90$ (cf. Eq. (281) in Ref. [72]). In this calculation, originally presented in Ref. [77], a missing coefficient in the generic four-dimensional case is calibrated by comparing the replica method to the holographic ansatz of Ref. [76] for the entanglement entropy in superconformal gauge theories (based on the assumption that the coefficient does not depend on the field content).

The result $c = -1/90$ is in agreement with the numerical result presented below. Our numerical work is presented in greater detail in the next section since the application of the replica method in conjunction with conformal anomaly calculations encounters some subtleties in the case that the surface enclosing the cavity has extrinsic curvature, as is the case for the sphere, cf. Ref. [78]. Our numerical work is a check of the logarithmic coefficient for a real scalar field in the free case using a specific regularization (introduced in Ref. [71]). We expect that a similar approach could be used to determine the coefficients for electromagnetic fields and massless Weyl fermions (for which the predictions of the replica method are $c = -62/90$ and $c = -11/180$, respectively, cf. Ref. [72]). Any general conclusions about the validity of the replica method, the associated conformal anomaly calculation, and the related AdS/CFT correspondence prescription for entanglement entropy in four dimensions, in the presence of cavities with surfaces possessing extrinsic curvature, are left for future work. More examples might have to be numerically worked out before matters can be clarified. In this context, we conclude that reasonable numerical results can be obtained in sufficiently simple cases with the accuracy attainable in reasonable amounts of time on today's consumer-level desktop computers.

15 Numerical computation for a sphere

15.1 Setup of the problem

In the following, we summarize the setup of the problem in Ref. [71], which is the starting point for our numerical approach. The Hamiltonian of the free and massless scalar field is

$$H = \frac{1}{2}\int d^3x[\pi^2(\vec{x}) + |\nabla\phi(\vec{x})|^2]\,. \tag{15.1}$$

It is convenient to expand π and ϕ in spherical harmonics, labeled by integers $l \geq 0$ and $m = -l, \ldots, l$, which amounts to a canonical transformation to

$$[\phi_{lm}(x), \pi_{l'm'}(x')] = i\delta_{ll'}\delta_{mm'}\delta(x - x')\,, \tag{15.2}$$

where $x \equiv |\vec{x}| \geq 0$. The new variables can still be separated into "inside" and "outside" sets. Now $H = \sum_{lm} H_{lm}$, with

$$H_{lm} = \frac{1}{2}\int_0^\infty dx \left\{\pi_{lm}^2(x) + x^2\left[\frac{\partial}{\partial x}\left(\frac{\phi_{lm}(x)}{x}\right)\right]^2 + \frac{l(l+1)}{x^2}\phi_{lm}^2(x)\right\}. \tag{15.3}$$

The variable x is discretized to $j \cdot a$, where a is our short distance cutoff and $j = 1, 2, \ldots, N$. The number N provides an infrared cutoff which will be taken to infinity at the end. The range of l is kept infinite and it will be shown that the sum over l and m converges for fixed N. This means that one does not need to discretize also the angular degrees of freedom; no ultraviolet divergences are generated in the directions tangential to the surface of the sphere. The finite, regularized H_{lm} is given by

$$H_{lm} = \frac{1}{2a}\sum_{j=1}^{N}\left[\pi_{lm,j}^2 + \left(j + \frac{1}{2}\right)^2\left(\frac{\phi_{lm,j}}{j} - \frac{\phi_{lm,j+1}}{j+1}\right)^2 + \frac{l(l+1)}{j^2}\phi_{lm,j}^2\right], \tag{15.4}$$

where we set $\phi_{lm,N+1} \equiv 0$. Focusing on a specific (lm)-sector, we drop the l, m indices of the field variables and write

$$H_{lm} = \frac{1}{2a}\sum_{i,j=1}^{N}(\delta_{ij}\pi_j^2 + \phi_j K_{ji}^{(l)}\phi_i)\,. \tag{15.5}$$

The real, symmetric, semipositive, tridiagonal $N \times N$ matrix $K^{(l)}$ is independent of m and has non-vanishing entries given by

$$K_{11}^{(l)} = \frac{9}{4} + l(l+1)\,, \tag{15.6a}$$

$$K_{jj}^{(l)} = 2 + \frac{1}{j^2}\left(\frac{1}{2} + l(l+1)\right), \qquad 2 \leq j \leq N\,, \tag{15.6b}$$

$$K_{j,j+1}^{(l)} = K_{j+1,j}^{(l)} = -\frac{\left(j + \frac{1}{2}\right)^2}{j(j+1)}, \qquad 1 \leq j \leq N-1\,. \tag{15.6c}$$

This means that we can proceed exactly as in the simple example of N coupled harmonic oscillators for every l and m independently (see Sec. 14.1). We trace out the degrees of freedom at radial coordinates $1 \leq j \leq n$, which corresponds to a separation into "inside" and "outside" regions by a sphere of radius $R = \left(n + \frac{1}{2}\right)a$.

We use again the block decomposition

$$\sqrt{K^{(l)}} = \begin{pmatrix} A^{(l)} & B^{(l)} \\ B^{(l)T} & C^{(l)} \end{pmatrix} , \tag{15.7}$$

where $A^{(l)}$ is an $n \times n$ matrix with $n < N$, which determines the dimensions of $B^{(l)}$ and $C^{(l)}$. Let

$$\beta^{(l)} = \frac{1}{2} B^{(l)T} \frac{1}{A^{(l)}} B^{(l)} , \qquad \beta^{(l)\prime} = \frac{1}{\sqrt{C^{(l)} - \beta^{(l)}}} \beta^{(l)} \frac{1}{\sqrt{C^{(l)} - \beta^{(l)}}} , \tag{15.8}$$

then the $(N-n) \times (N-n)$ matrix $\beta^{(l)\prime}$ determines the entropy for fixed l and m in complete analogy to Eq. (14.17). The entropy per fixed angular momentum, $S_l(n,N)$, is given by

$$S_l(n,N) = -\operatorname{Tr}\left[\log(1-\Xi^{(l)}) + \frac{\Xi^{(l)}}{1-\Xi^{(l)}} \log \Xi^{(l)} \right] \tag{15.9}$$

with

$$\Xi^{(l)} = \frac{\beta^{(l)\prime}}{1 + \sqrt{1 - \left(\beta^{(l)\prime}\right)^2}} , \tag{15.10}$$

where $\Xi^{(l)}$ depends on l through the matrix $K^{(l)}$, cf. Eq. (15.6). $S_l(n,N)$ is determined by the eigenvalues of $\Xi^{(l)}$. Again, all square roots and inversions are well-defined and the eigenvalues of $\Xi^{(l)}$, $\xi_j^{(l)}$, obey $0 \le \xi_j^{(l)} \le 1$, $j = 1, \ldots, N-n$, for every l.

The total entropy is obtained by summing over l and m because the ground state is a direct product of the ground states of the different (l,m)-sectors. Since H_{lm} does not depend on m, the total entropy is given by [71]

$$S(n,N) = \sum_{l=0}^{\infty} (2l+1) S_l(n,N) . \tag{15.11}$$

Srednicki shows that the sum over l converges for fixed n and N because the l-dependent terms in $K^{(l)}$ dominate for $l \gg N > n$ and one can compute $S_l(n,N)$ perturbatively in this case. At leading order, only a single eigenvalue of $\beta^{(l)\prime}$ contributes, which results in

$$S_l(n,N) = \xi_1^{(l)}(n)[-\log \xi_1^{(l)}(n) + 1] , \qquad \xi_1^{(l)}(n) = \frac{n(n+1)(2n+1)^2}{64 l^2 (l+1)^2} + \mathcal{O}(l^{-6}) \tag{15.12}$$

and shows that the sum over l converges.

15.2 Numerical details

The calculation of the eigenvalues ξ_j for any l can be done in a straightforward manner using *Mathematica*. The choice of *Mathematica* is motivated by its ability to carry out calculations at arbitrary precision, a feature that is costly in computer time for precisions different from ordinary double float (*MachinePrecision*).

One starts by choosing a value of n, which determines the radius R of the sphere. We find that looking at values of n in the range of 10 to 60 suffices for extracting from $S(n,\infty)$ the term proportional to $\log R$.

We first take the large-N limit at fixed l. Next, the sum over l is performed. This sum is truncated at a point from where on the remainder can be computed to sufficiently high accuracy by employing the large-l approximation (15.12), including also the first subleading term, which we determine numerically (cf. Sec. 15.2.2).

One needs to make sure that the process preserves sufficiently high precision. Our ultimate goal is to get $S(n,\infty)$ with an absolute accuracy of about 10^{-8}.

15.2.1 The infinite-N limit

By computing $S_l(n, N)$ numerically, we find that at least for values of l up to $l \approx 15$, the large-N limit of $S_l(n, N)$ is approached as

$$S_l(n, N) = a_l(n) + \frac{b_l(n)}{N^{2l+2}} \,. \tag{15.13}$$

For larger l, it is difficult to determine the exponent of N accurately, but it is of the order of $2l$ and therefore finite-N corrections vanish very fast.

The coefficient $b_l(n)$ was found to be negative in all investigated cases. Figure 42 shows plots of $\Delta S_l(n, N) = S_l(n, N) - S_l(n, N_0)$ as a function of N^{-2l-2} for $n = 20$, $l = 0, 1, 2$, and $l = 10$ (N_0 is the smallest value of N in the plotted data set).

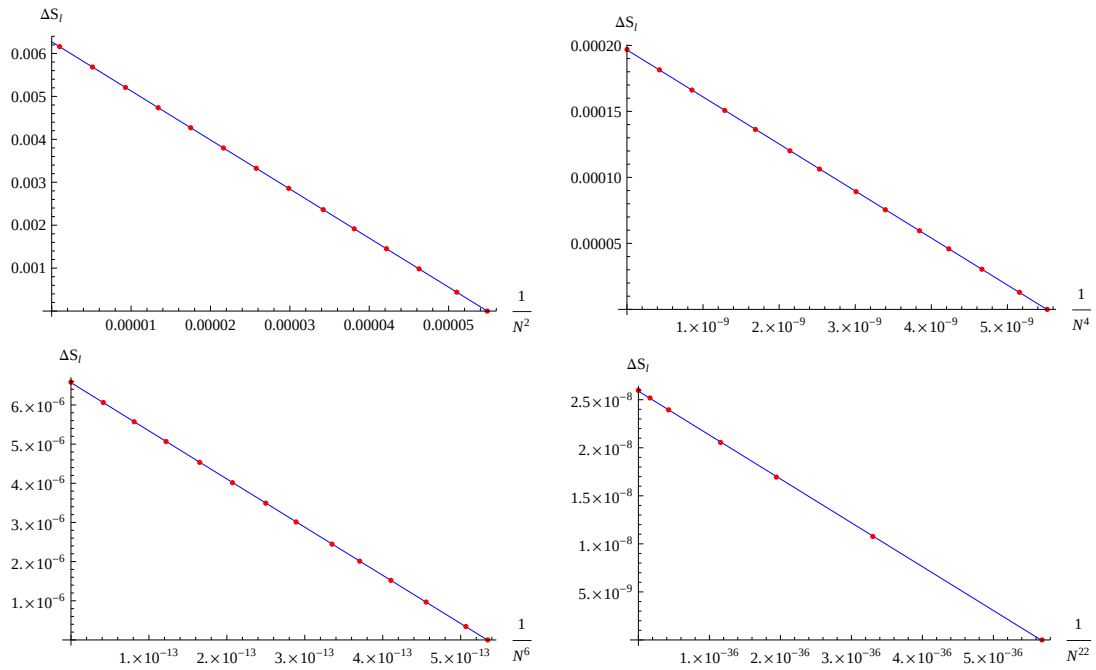

Figure 42: Plots of $\Delta S_l(n, N) = S_l(n, N) - S_l(n, N_0)$ as a function of N^{-2l-2} for $n = 20$ and $l = 0$ (top, left), $l = 1$ (top, right), $l = 2$ (bottom, left), and $l = 10$ (bottom, right). The blue lines are straight line fits through the data points (red dots).

For $n = 20$, $l = 20$, and $N \geq N_0 = 60$, $\Delta S_{l=20}(n = 20, N)$ is already of the order of 10^{-21} (when computed with precision 40 in *Mathematica*). Only for small l do we have to go to N-values as large as a few thousands in order to be able to extrapolate to infinite N with sufficiently small errors.

The cases $0 \leq l \leq 2$ and $l \geq 3$ are treated somewhat differently. For $l = 0, 1, 2$, we extrapolate $S_l(n, N)$ linearly in $1/N^{2l+2}$ to $N = \infty$, applying a least square fit to determine the parameters $a_l(n)$ and $b_l(n)$ in Eq. (15.13) from evaluations at five large values of N. Varying the number of points used for the fit, we obtain estimates for the errors on the infinite-N limit, see table 1 for examples.

We observe that the errors are dominated by the $l = 0$ contribution. We have therefore also allowed the power of $\frac{1}{N}$ to become a fit parameter for $l = 0$. Although the fit result for the exponent has always been close to the expected value, this slightly increased the error estimate in a few cases (error estimates given in table 1 already include these larger errors; for $l = 1, 2$, the correction is irrelevant).

n	$a_0(n)$	Δ	$a_1(n)$	Δ	$a_2(n)$	Δ
10	0.4779764889	$0.8 \cdot 10^{-9}$	0.3218551631505	$1.0 \cdot 10^{-12}$	0.24324853242244	$1.1 \cdot 10^{-14}$
20	0.5892154049	$3.0 \cdot 10^{-9}$	0.4316043027242	$1.9 \cdot 10^{-12}$	0.35065320435835	$2.6 \cdot 10^{-14}$
30	0.6553795277	$6.2 \cdot 10^{-9}$	0.4974300032432	$9.9 \cdot 10^{-12}$	0.41592189386854	$8.8 \cdot 10^{-14}$
40	0.7026231983	$9.9 \cdot 10^{-9}$	0.544542664951	$3.0 \cdot 10^{-11}$	0.46281476449290	$3.4 \cdot 10^{-13}$
50	0.739392926	$1.3 \cdot 10^{-8}$	0.581247646267	$6.9 \cdot 10^{-11}$	0.4994098682251	$1.1 \cdot 10^{-12}$
60	0.769499767	$1.6 \cdot 10^{-8}$	0.61131758758	$1.3 \cdot 10^{-10}$	0.5294166892935	$3.0 \cdot 10^{-12}$

Table 1: Results of extrapolations to infinite N (and corresponding absolute error bounds $\Delta(n,l)$) for $l = 0, 1, 2$. Ranges of N used to extrapolate: $3000 \leq N \leq 5000$ for $l = 0$, $1500 \leq N \leq 3000$ for $l = 1$, and $1000 \leq N \leq 2000$ for $l = 2$. For a fixed set of values of N at which full calculations are made, the error decreases with increasing l. Although smaller N-values are used for $l = 1, 2$, the estimates on the errors in these cases are smaller than those for $l = 0$.

The computation of $S_l(n, N)$ with increased precision in *Mathematica* is only possible if N is not too large. The limitation is either the length of time the computation would take or the available amount of memory. For small l, the extrapolations to infinite N were all performed with $MachinePrecision$. At smaller values of N, results obtained with $MachinePrecision$ and results computed with increased precision did not differ significantly (between $N = 600$ and $N = 900$, the relative error is below 10^{-14} for $l = 0$). Therefore, extrapolations obtained with $MachinePrecision$ are reliable within the estimated error bounds, which are of the order 10^{-8}.

For $l \geq 3$, we have carried out full computations at only two large N-values. Based on these two numbers we build various estimates to ensure that even if the correction for large N goes only as $\frac{1}{N^{2l}}$, rather than $\frac{1}{N^{2l+2}}$, the large-N limit is still recovered with sufficiently high precision.

15.2.2 The infinite sum over l

Having taken the infinite-N limit for finite values of l, we now turn to performing the infinite sum over l. For every n, we can compute, as described above, the value of $S_l(n, N = \infty)$. We do this for $l = 0, 1, 2, \ldots, l_{\max}$ and then use the leading term in Eq. (15.12) to estimate the remainder of the sum, stemming from contributions starting at $l = l_{\max} + 1$ and all the way to $l = \infty$. This procedure can be further improved by performing some calculations at a few selected very large values of $l > l_{\max}$ and looking at the difference between the leading asymptotic form and the numerical result. In this way we get an assessment for the subleading term in Eq. (15.12). With this method, we convince ourselves that the values of $l_{\max}$ we use in conjunction with the asymptotic result provide an absolute accuracy on the final numbers of approximately 10^{-8} (we have to increase $l_{\max}$ with n in order to get a similar absolute accuracy for all n).

15.3 Asymptotics at large R

15.3.1 Fit results for subleading coefficients

We end up with a set of numbers for

$$S(R = (n + 1/2)a) \equiv \lim_{N\to\infty} S\,(n, N) = \lim_{N\to\infty} \sum_{l=0}^{\infty} (2l + 1) S_l(n, N) \tag{15.14}$$

for $(R/a)^2$ up to about $3.7 \cdot 10^3$. The results for $S(R)$ vary from order one to a few hundreds and are accurate to about 10^{-8}, i.e., to at least eight digits (see table 2).

n	$S(n,\infty)$	Δ_n
5	8.882458402	$3.6 \cdot 10^{-9}$
10	32.509818844	$1.4 \cdot 10^{-8}$
15	70.911615387	$4.4 \cdot 10^{-9}$
20	124.086187971	$5.4 \cdot 10^{-9}$
25	192.033006873	$6.1 \cdot 10^{-9}$
30	274.751830288	$7.8 \cdot 10^{-9}$
35	372.242527052	$8.9 \cdot 10^{-9}$
40	484.505017950	$1.1 \cdot 10^{-8}$
45	611.539251453	$1.2 \cdot 10^{-8}$
50	753.345192156	$1.4 \cdot 10^{-8}$
55	909.922814676	$1.5 \cdot 10^{-8}$
60	1081.272100199	$1.7 \cdot 10^{-8}$

Table 2: Some numerical results for $\lim_{N\to\infty} S\,(n,N)$ together with the corresponding estimate for the total absolute error Δ_n.

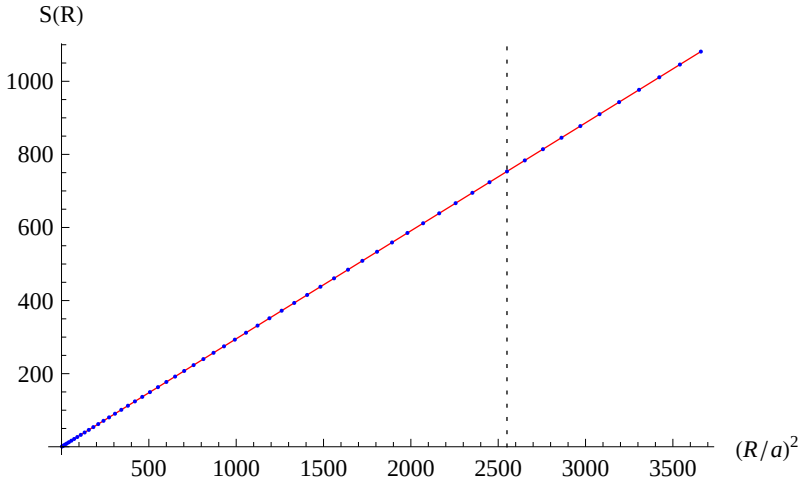

Figure 43: Plot of $S(R)$ as a function of $(R/a)^2$, the red line is obtained from a fit through the last 10 points.

Figure 43 shows a plot of $S(R)$ as a function of $(R/a)^2$, confirming the area law found in Ref. [71]. The red line through the data points (obtained from a fit through the last 10 points, to the right of the vertical dashed line) is given by

$$S_{\rm lin}(R) = 0.295406\,(R/a)^2\,. \tag{15.15}$$

Srednicki quotes a slope of 0.30, so we confirm the two digits he has found.

Next, we fit the data points to the functional form

$$S_{\log}(R) = s(R/a)^2 + c'\log(R/a)^2 + d\,. \tag{15.16}$$

A least square fit over the last 16 data points, $45 \le n \le 60$, results in

$$s = 0.295431\,, \qquad c' \equiv c/2 = -0.005545\,, \qquad d = -0.03537\,. \tag{15.17}$$

Note the change in s by $2.5 \cdot 10^{-5}$.

To estimate the quality of our fit, we compute

$$\chi^2 = \sum_{i=45}^{60} \frac{[S(R=(i+1/2)a) - S_{\log}(R=(i+1/2)a)]^2}{\Delta_i^2} \approx 2.93\,, \tag{15.18}$$

where Δ_i denotes the estimate for the error bound for the numerical value of $S(R = (i+1/2)a)$ (these estimates are all of the order of 10^{-8}, cf. table 2). Dividing by the number of degrees of freedom $N_{\text{d.o.f.}} = 16 - 3 = 13$, we obtain

$$\frac{\chi^2}{N_{\text{d.o.f.}}} \approx 0.23\,, \tag{15.19}$$

which indicates that the error estimates Δ_i might even be a little bit too conservative.

When we change the range of the data points used in the fit, the result for s does not change to the given precision, variations in c' are of the order 10^{-5}, and variations in d are of the order 10^{-4}. The fit results can be confirmed within this accuracy by fitting even further subleading terms (with two more subleading terms a fit in the same range of R leads to coefficients $s = 0.295431$, $c' = -0.0055549$, $d = -0.03529$). Therefore, we expect that our numerical result for the coefficient of the logarithmic term is correct within an accuracy of 0.2 percent.

Figure 44 shows a plot of the difference between the two fits, $S_{\log}(R) - S_{\text{lin}}(R)$, as a function of $(R/a)^2$ together with the corresponding data points. Figure 45 shows a similar plot, but this time the linear term $S_{\text{lin, corr}}(R) = 0.295431(R/a)^2$ obtained from the fit result (15.17) is subtracted. Both plots show that the numerical results are well described by the functional form (15.16) with coefficients (15.17) in the entire range of R (only the last 16 points are used for the fit).

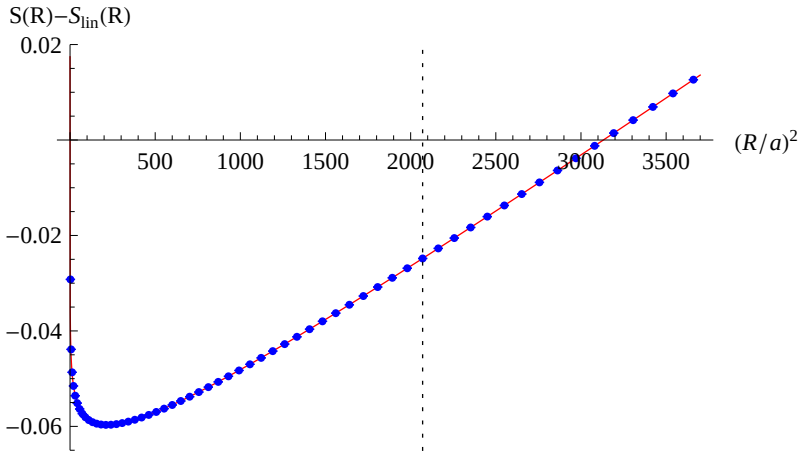

Figure 44: Plot of $S_{\log}(R) - S_{\text{lin}}(R) = 2.5 \cdot 10^{-5}(R/a)^2 - 0.005545\log(R/a)^2 - 0.03537$ as a function of $(R/a)^2$ (solid red curve) and numerically computed data points $S(R) - S_{\text{lin}}(R) = S(R) - 0.295406(R/a)^2$ (blue dots). $S_{\log}(R)$ is obtained from a fit over the last 16 data points (to the right of the vertical dashed line). Error bounds are of the order 10^{-8} and are not visible in the plot.

15.3.2 Discretized derivative

Based on the results presented above, we have good reason to believe that $S(R)$ is indeed given by the functional form of Eq. (15.16), up to terms that vanish in the limit $R \to \infty$.

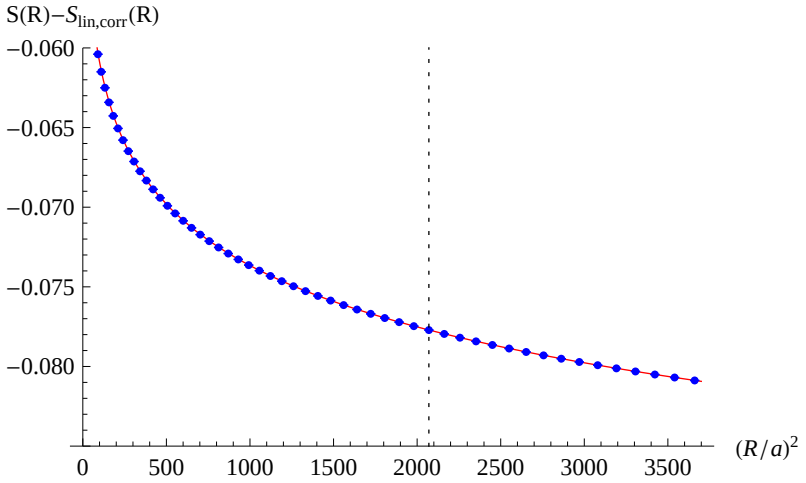

Figure 45: Plot of $S_{\log}(R) - 0.295431(R/a)^2 = -0.005545\log(R/a)^2 - 0.03537$ as a function of $(R/a)^2$ (solid red curve) and numerically computed data points $S(R) - 0.295431(R/a)^2$ (blue dots). $S_{\log}(R)$ is obtained from a fit over the last 16 data points (to the right of the vertical dashed line). Error bounds are of the order 10^{-8} and are not visible in the plot.

This means that the coefficient c' of the logarithmic term could also be obtained by taking the third derivative w.r.t. R,

$$\partial^3_{(R/a)} S(R) = 4c' \frac{a^3}{R^3} + \dots \tag{15.20}$$

and consequently

$$c' = \lim_{R/a\to\infty} \frac{R^3}{4a^3} \partial^3_{(R/a)} S(R)\,. \tag{15.21}$$

Therefore, we now use our numerical data to compute the discretized version of the third derivative

$$\Delta^3_R S(R) = \frac{1}{8}\left(S(R+3a) - 3S(R+a) + 3S(R-a) - S(R-3a)\right)\,. \tag{15.22}$$

Then, an estimate for the coefficient of the logarithmic term is obtained from

$$\frac{R^3}{4a^3}\Delta^3_R S(R) \tag{15.23}$$

for large R/a.

Figure 46 shows a plot of $\frac{R^3}{4a^3}\Delta^3_R S(R)$ as a function of R/a. The data points seem to be quite stable on a horizontal line, indicating again that the error bounds might be too pessimistic (the error bars in the plot increase with increasing R/a due to the multiplication with $(R/a)^3$). The occurrence of a plateau confirms that there is indeed a subleading logarithmic correction to the area law $S(R) \propto (R/a)^2$. The numerical value for the coefficient of the logarithm found in the previous section is confirmed and is in agreement with the prediction of $-1/180$ within an error of 0.2 percent (the red horizontal line in Fig. 46 shows this predicted value).

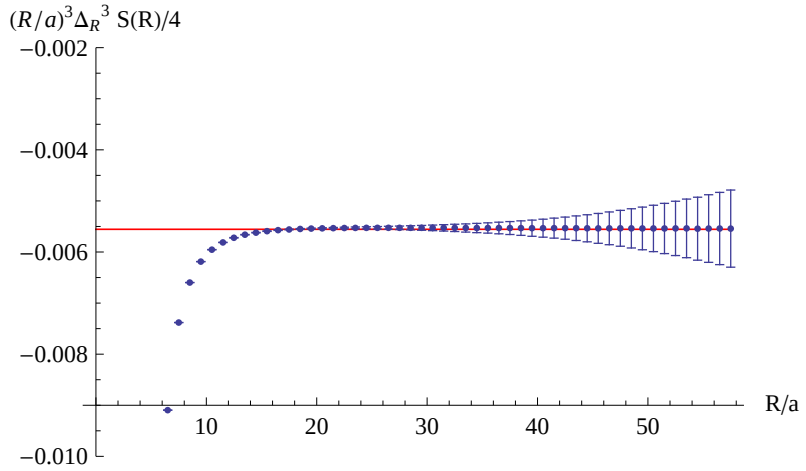

Figure 46: Plot of the discretized third derivative, multiplied by $R^3/(4a^3)$ (blue points). The horizontal red line is not a fit, it corresponds to the predicted value of $-1/180$ for the coefficient of $\log(R/a)^2$.

This agreement can be confirmed by an additional plot of $\log\left|\Delta_R^3 S(R)\right|$ as a function of $\log(R/a)$. The straight line in the plot shown in Fig. 47 is not a fit, it shows the predicted relation

$$\log|\partial^3_{(R/a)} S(R)| = -\log 45 - 3\log(R/a)\,, \tag{15.24}$$

corresponding to $c = -1/90$ and $c' = -1/180$.

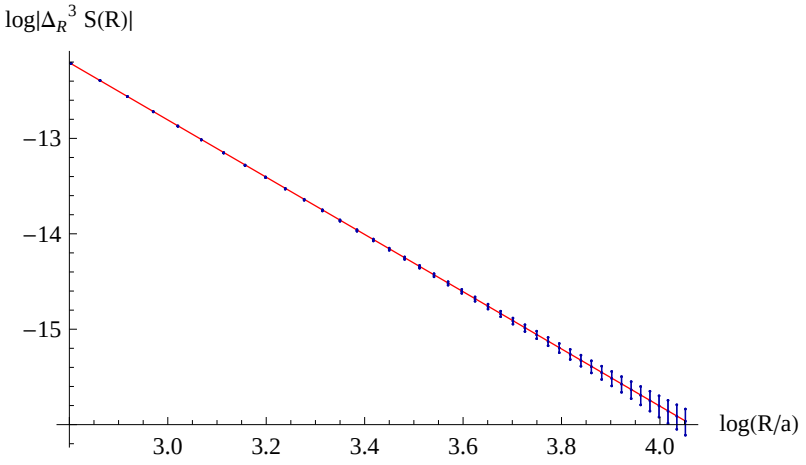

Figure 47: Double-logarithmic plot of the discretized third derivative. The red line through the data points (blue) is not a fit, it corresponds to the predicted relation $\log|\partial^3_{(R/a)} S(R)| = -\log 45 - 3\log(R/a)$, which is in good agreement with the data.

15.4 Universality of the numerical result

Equations (15.2) and (15.3) are somewhat formal because the Hamiltonian has to be regularized. At this level, one could also make a formal canonical transformation and

afterward discretize the resulting expression. In this case, there is no guarantee that the coefficient c of $\log R$ in the entropy will again come out as $-1/90$.

Let us sketch an example which works in the same way in every (l, m)-sector (then, for brevity, we can again drop the l, m indices). We make the canonical transformation

$$q(\xi) = \phi(e^{\xi}), \quad p(\xi) = e^{\xi}\pi(e^{\xi}), \tag{15.25}$$

which leads to

$$[q(\xi), p(\xi')] = i\delta(\xi - \xi'). \tag{15.26}$$

In terms of the new variables q and p, we get

$$H = \frac{1}{2}\int_{-\infty}^{\infty} d\xi e^{-\xi}\left[p^2(\xi) + \left(\frac{dq}{d\xi} - q(\xi)\right)^2 + l(l+1)q^2(\xi)\right]. \tag{15.27}$$

A further canonical transformation $p(\xi) \to p(\xi - \xi_0)$, $q(\xi) \to q(\xi - \xi_0)$ results in $H \to e^{\xi_0}H$. The entropy depends only on the ground state of H and therefore remains invariant under a rescaling of H by a positive number. It now seems that we can always absorb R in ξ and S will be R-independent. If we want to preserve the simple behavior of H under $\xi \to \xi - \xi_0$, we would need to discretize ξ on a regular lattice, $\xi \to ja$, $-N < j < N$. We expect that taking the various limits then will lead to an entropy that does not depend on R at all.

The set of regularizations under which the coefficient of $\log R$ is fixed at $-1/90$ must then be, at the least, restricted by some additional requirements. Assuming that c is indeed determined by an anomaly, it becomes apparent that the true consequence of being forced to employ a regularization is that there are several symmetries which cannot be simultaneously preserved in the quantum continuum limit. If we insist on maintaining scale invariance, some other symmetry will have to be violated. The most likely candidate in our example is the $\vec{x} \to \vec{x} - \vec{x}_0$ three-dimensional translational invariance of the Hamiltonian in Eq. (15.1). Although broken at finite spacing a in Srednicki's regularization, we expect that in this case it gets restored in the limit $a \to 0$.

In order to clarify matters, it might also be interesting to study the effect of a generalization of the canonical transformation (15.25) to

$$q(\xi) = \phi(\tau(\xi)), \quad p(\xi) = \tau'(\xi)\pi(\tau(\xi)) \tag{15.28}$$

with an arbitrary monotonic function $x = \tau(\xi)$. Under this transformation, the Hamiltonian is replaced by

$$H = \frac{1}{2}\int d\xi \frac{1}{\tau'(\xi)}\left[p^2(\xi) + \left(q'(\xi) - \frac{\tau'(\xi)}{\tau(\xi)}q(\xi)\right)^2 + l(l+1)\left(\frac{\tau'(\xi)}{\tau(\xi)}\right)^2 q^2(\xi)\right]. \tag{15.29}$$

Discretizing ξ, one could repeat the numerical procedure and study the dependence of the coefficient c, if any, on the discrete values $\tau_1, \tau_2, \ldots$ parametrizing the function $\tau(\xi)$. In principle, one should then be able to decide if the dependence survives in the continuum limit. In the four-dimensional path integral obtained via the replica method, a conformal anomaly appears. Specifically, Ref. [78] suggests that the anomaly is intrinsically four-dimensional, i.e., implying for our case that c depends on the entire function $\tau(\xi)$. On the other hand, the ansatz of Ref. [76] seems to predict that the nature of the anomaly is two-dimensional, i.e., c would not depend on $\tau(\xi)$.

To us it seems likely that requiring three-dimensional translational invariance in the continuum limit would fix c to $-1/90$. Allowing this invariance to break may result

in different values for c, among them even 0 if scaling becomes fully preserved in the continuum limit. We have certainly not shown this here and substantially more work would be needed to achieve a convincing numerical argument for the universality of c and its limitations.

Part V

Epilogue

16 Summary and conclusions

Durhuus and Olesen discovered in 1981 that the infinite-N limit of the eigenvalue density of Wilson loops in SU(N) pure gauge theory in two Euclidean dimensions undergoes a phase transition at a critical size of the loop, where a gap in the eigenvalue density closes. A similar behavior occurs also in higher dimensions and the transition seems to have universal properties. In part II of this thesis, we have focused on the distribution of the eigenvalues of the unitary Wilson loop matrix in the two-dimensional case at arbitrary finite N. The starting point of this study has been the representation of the probability distribution of the Wilson loop matrix by a simple sum over all inequivalent irreducible representations of SU(N), where only dimensions, the values of the quadratic Casimir operator, and the characters of the matrix in the irreducible representations enter. To characterize the distribution of the eigenvalues, we have introduced three density functions (the "symmetric", the "antisymmetric", and the "true" eigenvalue density[22]) which differ at finite N but possess the same infinite-N limit, exhibiting the Durhuus-Olesen phase transition. These densities are related to the average of the characteristic polynomial, the average of the inverse of the characteristic polynomial, and the average of the ratio of characteristic polynomials at different arguments. Using expansions of determinants and inverse determinants in characters of totally symmetric or totally antisymmetric representations of SU(N), the densities at finite N can be expressed in terms of simple sums involving only dimensions and quadratic Casimir invariants of certain irreducible representations of SU(N), allowing for a numerical computation of the densities at arbitrary N to any desired accuracy. We have found that the true eigenvalue density, adding N oscillations to the monotonic symmetric density, is in some sense intermediate between the symmetric and the antisymmetric density, which in turn is given by a sum of N delta peaks located at the zeros of the average of the characteristic polynomial. We have studied in detail the area dependence of these zeros and found that they provide a good approximation for the location of the peaks in the true eigenvalue density, i.e., that with increasing N, the distance between peaks and matching zeros vanishes faster than the difference between peaks and closest valleys. Furthermore, we have shown that the dependence on N can be made explicit by deriving integral representations for the resolvents associated to the three eigenvalue densities. In each case, the parameter N enters only in the exponent of the integrand, which means that the infinite-N limit can be studied by a saddle-point analysis. With these saddle-point approximations, we have confirmed that all three densities reduce to the Durhuus-Olesen result in the infinite-N limit. In a detailed study of the symmetric case, we have found that finite-N corrections can be obtained easily with our saddle-point approach in the region where the infinite-N density is non-zero, however, it turned out that this method is not the right tool to compute finite-N effects in the region where the density vanishes for infinite N and corrections are exponentially suppressed in N.

[22] The symmetric (resp. antisymmetric) density is related to averages of characters of the Wilson loop matrix in totally symmetric (resp. antisymmetric) irreducible representations. Only the true eigenvalue density has a natural interpretation at finite N.

In part III, we have studied an exponential form of the multiplicative random complex matrix model introduced by Gudowska-Nowak et al. (cf. Ref. [3]). Varying a parameter[23] which can be identified with the area of the Wilson loop in the unitary case, the region of non-vanishing eigenvalue density of the N-dimensional complex product matrix undergoes a topological change at a transition point in the infinite-N limit. For the complex model, eigenvalues are no longer confined to the unit circle, they spread out on a fattened arc in the complex plane. At the transition point, the domain of non-zero surface eigenvalue density becomes multiply connected (below the transition point, it is simply connected). We have studied the transition by a detailed analysis of the average of the modulus square of the characteristic polynomial. In an intermediate step, we have used a representation of this observable by a multi-dimensional integral over anticommuting Grassmann variables, which allows for averaging over the factors in the matrix product independently. We ended up with a representation by an integral over ordinary complex numbers, where the dependence on N is explicit. Supported by results of high-statistics numerical simulations, we have observed that the boundary of the domain of non-zero eigenvalue density follows from the stability properties of a trivial saddle point of this integral representation. With this analysis, we have confirmed the expectation that restricting the determinant to unity does not affect the boundary in the infinite-N limit. Furthermore, the basic complex matrix model has been generalized by introducing extra parameters in the probability distributions of the individual matrix factors allowing for a smooth interpolation between the original model and the two extreme cases where the factors in the product are Hermitian or unitary. Although the shape of the domain of non-vanishing infinite-N eigenvalue density is modified, the generalized model always leads to a transition in the topology of this domain. This transition can be viewed as a natural generalization of the Durhuus-Olesen transition occurring in the unitary case. Even though more integrals are needed in the general case, it turned out that the boundary separating domains of vanishing and non-vanishing eigenvalue density in the infinite-N limit can again be obtained from a saddle-point analysis. Furthermore, we have found that the inviscid Burgers equation plays a central role for both the original model and its generalization. We have presented our first attempt to go to sub-leading terms in a systematic large-N expansion of the average of the modulus square of the characteristic polynomial in order to identify the universality class of the transition in the eigenvalue density. We have shown for arbitrary finite N that the model can be mapped to an equivalent ensemble of 2×2 matrices, making the dependence on N explicit. Although simplifications occur in some special cases, we ended up being forced to leave further work on the large-N universal properties to the future, but feel that we have made substantial progress towards achieving a complete understanding of the universal nature of the large-N transition.

In part IV, we have presented a numerical study of the entanglement entropy which is obtained by tracing out the degrees of freedom residing inside an imaginary sphere for a free massless scalar field in four-dimensional Euclidean spacetime. Since existing analytical calculations of subleading terms to the area law rely on some non-trivial assumptions (e.g., the replica trick), we have determined the next order correction, a logarithmic term which might be universal, by numerical means. Using the regularization introduced by Srednicki in Ref. [71], we have found numerically that the coefficient of the logarithm is $-1/90$ to 0.2 percent accuracy. This is in agreement with an existing analytical result. In order to clarify the universality of this result, additional numerical computations for different regularization schemes have to be performed in the future.

[23] This parameter is $t = n\varepsilon^2$, where n is the number of factors in the matrix product and ε determines the deviation from the identity matrix in the probability distribution for each factor. We are interested in the limit $n \to \infty$, $\varepsilon \to 0$ with t kept fixed.

Acknowledgements

First of all, I would like to thank Tilo Wettig for his encouraging support and advice, for many interesting and stimulating discussions, for providing an enjoyable working environment, and also for initiating the long-term collaboration with Herbert Neuberger. I have highly benefited from this collaboration, especially from three long visits at Rutgers University. I would like to thank Herbert Neuberger for his hospitality, for proposing many interesting projects, and for countless interesting and beneficial discussions. I am also very grateful to Andreas Schäfer for his support during my participation in the "Elitestudiengang Physik" at the University of Regensburg in the past five years. Furthermore, I would like to thank Rajamani Narayanan for making possible two visits at Florida International University and for very beneficial discussions. I would also like to thank my collaborators Adam Schwimmer and Stefan Theisen. I am very grateful to Christoph Lehner for many interesting discussions, not only about physics, and for proof-reading this thesis. I acknowledge financial support by BayEFG and by the US DOE under grant number DE-FG02-01ER41165. Finally, I would like to thank my family for their unlimited support.

Appendices

A Gauge-field propagator in position space

We want to calculate the integral (over Euclidean momenta k_μ)

$$D_{\mu\nu}(x) = \int \frac{d^dk}{(2\pi)^d} \left(\frac{\delta_{\mu\nu}}{k^2} + (\xi - 1) \frac{k_\mu k_\nu}{k^4} \right) e^{ikx} \,, \tag{A.1}$$

where $k^4 \equiv (k^2)^2$. Let us start with the Fourier transform

$$\begin{aligned} D^{(A)}(x) &= \int \frac{d^dk}{(2\pi)^d} \frac{1}{k^2} e^{ikx} = \int \frac{d^dk}{(2\pi)^d} \int_0^\infty dt^{-tk^2} e^{ikx} \\ &= \int_0^\infty dt \prod_{\mu=1}^{d} \left[\int \frac{dk_\mu}{2\pi} e^{-tk_\mu^2 + ik_\mu x_\mu} \right] , \end{aligned} \tag{A.2}$$

where in the last exponent no sum over μ is implied. Performing the Gaussian integral

$$\int \frac{dk_\mu}{2\pi} e^{-tk_\mu^2 + ik_\mu x_\mu} = \int \frac{dk_\mu}{2\pi} e^{-t\left(k_\mu - \frac{ix_\mu}{2t}\right)^2} e^{-\frac{1}{4t}x_\mu^2} = \sqrt{\frac{\pi}{t}} e^{-\frac{1}{4t}x_\mu^2} \tag{A.3}$$

leads to

$$D^{(A)}(x) = \int_0^\infty dt \prod_{\mu=1}^{d} \frac{1}{2\sqrt{\pi t}} e^{-\frac{1}{4t}x_\mu^2} = \frac{1}{2^d \pi^{\frac{d}{2}}} \int_0^\infty dt\, t^{-\frac{d}{2}} e^{-\frac{1}{4t}x^2} \,. \tag{A.4}$$

Changing the integration variable from t to $u = \frac{1}{4t}x^2$ finally leads to

$$\begin{aligned} D^{(A)}(x) &= \frac{1}{2^d \pi^{\frac{d}{2}}} \int_0^\infty du \left(\frac{x^2}{4u^2} \right) \left(\frac{4u}{x^2} \right)^{\frac{d}{2}} e^{-u} = \frac{1}{4\pi^{\frac{d}{2}}} \frac{1}{(x^2)^{\frac{d}{2}-1}} \int_0^\infty u^{\frac{d}{2}-2} e^{-u} \\ &= \frac{\Gamma\left(\frac{d}{2} - 1\right)}{4\pi^{\frac{d}{2}} (x^2)^{\frac{d}{2}-1}} \,. \end{aligned} \tag{A.5}$$

Consider next the integral

$$\begin{aligned} D^{(B)}_{\mu\nu}(x) &= \int \frac{d^dk}{(2\pi)^d} \frac{k_\mu k_\nu}{k^4} e^{ikx} = -\frac{\partial^2}{\partial x_\mu \partial x_\nu} \int \frac{d^dk}{(2\pi)^d} \frac{1}{k^4} e^{ikx} \\ &= -\frac{\partial^2}{\partial x_\mu \partial x_\nu} \int_0^\infty dt \int \frac{d^dk}{(2\pi)^d} t e^{-tk^2 + ikx} = -\frac{\partial^2}{\partial x_\mu \partial x_\nu} \int_0^\infty dt\, t \frac{1}{2^d \pi^{\frac{d}{2}} t^{\frac{d}{2}}} e^{-\frac{1}{4t}x^2} \\ &= \int_0^\infty dt \left(\frac{1}{2}\delta_{\mu\nu} - \frac{1}{4t} x_\mu x_\nu \right) \frac{1}{2^d \pi^{\frac{d}{2}} t^{\frac{d}{2}}} e^{-\frac{1}{4t}x^2} = \left(\frac{1}{2}\delta_{\mu\nu} + x_\mu x_\nu \frac{\partial}{\partial x^2} \right) D^{(A)}(x) \\ &= \left(\frac{1}{2}\delta_{\mu\nu} + x_\mu x_\nu \left(1 - \frac{d}{2} \right) \frac{1}{x^2} \right) D^{(A)}(x) \end{aligned} \tag{A.6}$$

which leads to

$$\begin{aligned} D_{\mu\nu}(x) &= \delta_{\mu\nu} D^{(A)}(x) + (\xi - 1) D^{(B)}(x) \\ &= \left(\delta_{\mu\nu} + (\xi - 1)\frac{1}{2}\delta_{\mu\nu} + \frac{1}{2}(\xi - 1)(2 - d)\frac{x_\mu x_\nu}{x^2} \right) D^{(A)}(x) \\ &= \left(\frac{1 + \xi}{2}\delta_{\mu\nu} + \frac{1 - \xi}{2}(d - 2)\frac{x_\mu x_\nu}{x^2} \right) \frac{\Gamma\left(\frac{d}{2} - 1\right)}{4\pi^{\frac{d}{2}}} \frac{1}{(x^2)^{\frac{d}{2}-1}} \,. \end{aligned} \tag{A.7}$$

B Gaussian integrals

B.1 One-dimensional real Gaussian integral

The basic identity is

$$\int_{-\infty}^{\infty} dx\, e^{-Nx^2+xz} = \sqrt{\frac{\pi}{N}}\, e^{\frac{z^2}{4N}}\,, \tag{B.1}$$

which holds for any complex number z (and $N > 0$). This identity follows immediately from

$$\left(\int_{-\infty}^{\infty} dx\, e^{-x^2}\right)^2 = \int_0^{2\pi} d\phi \int_0^{\infty} r dr\, e^{-r^2} = \pi\,. \tag{B.2}$$

B.2 Multi-dimensional integrals

The above identity can easily be generalized to higher dimensional integrals (see, e.g., Ref. [11]). Let $x = (x_1, \ldots, x_n) \in \mathbb{R}^n$ and $A = (A_{ij})$ be a real, symmetric, positive matrix. In this case, A can be decomposed into $A = S^T \operatorname{diag}(\lambda_1, \ldots, \lambda_n) S$ with $S^T = S^{-1}$ and λ_i real and positive for all $i = 1, \ldots, n$. The integral

$$I = \int d^n x\, e^{-\sum_{i,j=1}^n x_i A_{ij} x_j} = \int d^n x\, e^{-x^T A x} \tag{B.3}$$

can then be calculated by changing integration variables to $y = Sx$, which leads to the factorized integral

$$I = \int d^n y\, e^{-y^T \operatorname{diag}(\lambda_1,\ldots,\lambda_n) y} = \prod_{i=1}^n \int dy_i\, e^{-y_i \lambda_i y_i} = \prod_{i=1}^n \sqrt{\frac{\pi}{\lambda_i}} = \frac{\pi^{\frac{n}{2}}}{(\det A)^{\frac{1}{2}}}\,. \tag{B.4}$$

Including an additional linear term, we can generalize Eq. (B.3) to

$$\begin{aligned} I(j_1, \ldots, j_n) &= \int d^n x\, e^{-x^T A x + x^T j} = \int d^n y\, e^{-y^T \operatorname{diag}(\lambda_1,\ldots,\lambda_n) y + y^T (Sj)} \\ &= \prod_{i=1}^n \int dy_i\, e^{-y_i \lambda_i y_i + y_i (Sj)_i} = \prod_{i=1}^n \sqrt{\frac{\pi}{\lambda_i}}\, e^{\frac{1}{4}(j^T S^T)_i \lambda_i^{-1} (Sj)_i} \\ &= \frac{\pi^{\frac{n}{2}}}{(\det A)^{\frac{1}{2}}}\, e^{\frac{1}{4} j^T A^{-1} j} = I(0, \ldots, 0)\, e^{\frac{1}{4} j^T A^{-1} j}\,. \end{aligned} \tag{B.5}$$

B.3 Integrals over complex matrices

We want to calculate the Gaussian integrals in Eqs. (10.6) and (10.10). The integration measure over complex numbers $z = x + iy$ is defined as $d\mu(z) = dxdy$, $\int d\mu(z) = \int_{-\infty}^{\infty} \int_{-\infty}^{\infty} dxdy$. From Eq. (B.1), we obtain for any complex numbers a and b

$$\int d\mu(z)\, e^{-N|z|^2 + z^* a + z b} = \int_{-\infty}^{\infty} \int_{-\infty}^{\infty} dxdy\, e^{-N(x^2+y^2) + x(a+b) + y(ib - ia)} = \frac{\pi}{N}\, e^{\frac{ab}{N}}\,. \tag{B.6}$$

B.3.1 GL($N, \mathbb{C}$) case

Let us start with the integral in Eq. (10.10), which we can write in the factorized form

$$\left(\frac{N}{\pi}\right)^{N^2} \prod_{i,j} \int d\mu(C_{ij})\, e^{-NC_{ij}C_{ij}^* + C_{ij}\left(B^\dagger\right)_{ji} + C_{ij}^* A_{ij}} \,. \tag{B.7}$$

We have N^2 integrals of the type (B.6), resulting in

$$\int P(C) d\mu(C)\, e^{\mathrm{Tr}\, C^\dagger A + \mathrm{Tr}\, B^\dagger C} = \prod_{i,j} e^{\frac{1}{N} A_{ij}\left(B^\dagger\right)_{ji}} = e^{\frac{1}{N}\,\mathrm{Tr}\, B^\dagger A} \,, \tag{B.8}$$

where $P(C)$ is the probability distribution defined in Eq. (10.9).

B.3.2 SL($N, \mathbb{C}$) case

Due to the presence of the delta function, the integral in Eq. (10.6) is slightly more complicated. Obviously, the integral over the off-diagonal matrix elements can be performed as before, leading to

$$\prod_{i \neq j} \frac{N}{\pi} \int d\mu(C_{ij})\, e^{-NC_{ij}C_{ij}^* + C_{ij}\left(B^\dagger\right)_{ji} + C_{ij}^* A_{ij}} = e^{\frac{1}{N}\left(\mathrm{Tr}\left[B^\dagger A\right] - \sum_i A_{ii} B_{ii}^*\right)} \,. \tag{B.9}$$

To perform the integral over the diagonal elements, we define $C_{ii} = c_i$, $B_{ii} = b_i$, $A_{ii} = a_i$, and $c^T = (c_1, \ldots, c_N)$, $b^T = (b_1, \ldots, b_N)$, $a^T = (a_1, \ldots, a_N)$. We have to calculate the integral

$$I = \int \left(\prod_{i=1}^N d\mu(c_i)\right) \delta\left(\sum_{i=1}^N c_i\right) e^{-Nc^\dagger c + c^\dagger a + b^\dagger c} \tag{B.10}$$

with the complex delta function $\delta(z) = \delta(\mathrm{Re}(z))\delta(\mathrm{Im}(z))$ and $a^\dagger b = \sum_{i=1}^N a_i^* b_i$, etc. We now change the integration variables to $d_i = \sum_{j=1}^N S_{ij} c_j$ with a real matrix S such that

$$d_1 = \frac{1}{\sqrt{N}}(1, 1, \ldots, 1)c = \frac{1}{\sqrt{N}} \sum_{i=1}^N c_i \,, \tag{B.11}$$

$$d_k = \frac{1}{\sqrt{k(k-1)}}(\underbrace{1, 1, \ldots, 1}_{(k-1)}, -(k-1), 0, \ldots, 0)c = \frac{1}{\sqrt{k(k-1)}} \sum_{i=1}^{k-1} c_i - \sqrt{1 - \frac{1}{k}}\, c_k \tag{B.12}$$

for $2 \leq k \leq N$. Since the matrix S, defined through Eqs. (B.11) and (B.12), obeys $S^{-1} = S^T = S^\dagger$, we obtain

$$\begin{aligned} I &= \int \left(\prod_{i=1}^N d\mu(d_i)\right) \delta\left(\sqrt{N} d_1\right) e^{-Nd^\dagger d + d^\dagger S a + b^\dagger S^T d} \\ &= \frac{1}{N} \int \left(\prod_{i=2}^N d\mu(d_i)\right) e^{-N\sum_{i=2}^N d_i^* d_i + \sum_{i=2}^N \left(d_i^* (Sa)_i + (b^\dagger S^T)_i d_i\right)} \\ &= \frac{1}{N} \left(\frac{\pi}{N}\right)^{N-1} e^{\frac{1}{N}\sum_{i=2}^N (b^\dagger S^T)_i (Sa)_i} \,, \end{aligned} \tag{B.13}$$

where we have again made use of Eq. (B.6). Due to

$$\begin{aligned}\frac{1}{N}\sum_{i=2}^{N}(b^\dagger S^T)_i(Sa)_i &= \frac{1}{N}\sum_{i=1}^{N}(b^\dagger S^T)_i(Sa)_i - \frac{1}{N}(b^\dagger S^T)_1(Sa)_1 \\ &= \frac{1}{N}b^\dagger S^T Sa - \frac{1}{N}\left(\sum_{k=1}^{N}S_{1k}a_k\right)\left(\sum_{j=1}^{N}b_j^* S_{1j}\right) \\ &= \frac{1}{N}b^\dagger a - \frac{1}{N^2}\left(\sum_{k=1}^{N}a_k\right)\left(\sum_{j=1}^{N}b_j^*\right) \\ &= \frac{1}{N}\sum_i B_{ii}^\dagger A_{ii} - \frac{1}{N^2}\operatorname{Tr}A\operatorname{Tr}B^\dagger\,, \end{aligned} \tag{B.14}$$

we finally arrive at

$$\int P(C)d\mu(C)\,e^{\operatorname{Tr}C^\dagger A+\operatorname{Tr}B^\dagger C} = e^{\frac{1}{N}\operatorname{Tr}B^\dagger A-\frac{1}{N^2}\operatorname{Tr}A\operatorname{Tr}B^\dagger}\,, \tag{B.15}$$

where $P(C)$ is defined in Eq. (10.5).

C Saddle-point approximation

Consider first a real function $f(u)$ which has a global (non-degenerate) minimum at $u = u_0 \in \mathbb{R}$, i.e., $f'(u_0) = 0$ and $f''(u_0) > 0$. We want to calculate the integral

$$\begin{aligned} I &= \int_{-\infty}^{\infty} du\, e^{-Nf(u)} \\ &= e^{-Nf(u_0)}\int_{-\infty}^{\infty} du\, e^{-N\left(\frac{1}{2}f''(u_0)(u-u_0)^2+\frac{1}{3!}f^{(3)}(u_0)(u-u_0)^3+\frac{1}{4!}f^{(4)}(u_0)(u-u_0)^4+\ldots\right)}\,. \end{aligned} \tag{C.1}$$

Rescaling the integration variable according to

$$u - u_0 = \frac{x}{\sqrt{N}} \tag{C.2}$$

leads to

$$I = e^{-Nf(u_0)}N^{-\frac{1}{2}}\int_{-\infty}^{\infty} dx\, e^{-\frac{1}{2}f''(u_0)x^2}e^{-\frac{1}{3!\sqrt{N}}f^{(3)}(u_0)x^3-\frac{1}{4!N}f^{(4)}(u_0)x^4+\ldots}. \tag{C.3}$$

By expanding the second exponential factor in a power series, we obtain a systematic expansion of the integral in inverse powers of N. To compute the coefficients in this expansion, we have to evaluate integrals of the form

$$\int_{-\infty}^{\infty} dx\, e^{-\alpha x^2}x^{2k} = \left(-\frac{\partial}{\partial\alpha}\right)^k\int_{-\infty}^{\infty} dx\, e^{-\alpha x^2} = \sqrt{\pi}\,\frac{\prod_{j=1}^{k}(2j-1)}{2^k}\alpha^{-\frac{1}{2}-k}\,. \tag{C.4}$$

If $f'(u)$ is non-zero on the real axis, the method may still be used when the function f is analytic in some region of the complex plane (including the original integration domain along the real axis) since the integration contour can then be deformed in the complex plane due to Cauchy's integral theorem (see, e.g., Ref. [79]).

Let us now consider a path γ in the complex plane, $\gamma : (a, b) \to \mathbb{C}$, and the integral

$$\int_\gamma dz\, e^{-NF(z)} = \int_a^b dt \dot{\gamma}(t) e^{-NF(\gamma(t))} \tag{C.5}$$

with an analytic function $F(z)$.

If $u(t) = \operatorname{Re} F(\gamma(t))$ has an absolute (non-degenerate) minimum at $t_0 \in (a, b)$ with $\partial_t^2 u(t_0) < 0$, i.e., $F(z)$ has a saddle point[24] at $z = z_0 = \gamma(t_0)$ ($F'(z_0) = 0$ and $F''(z_0) \neq 0$), and if in addition $v(t) = \operatorname{Im} F(\gamma(t))$ is constant in the vicinity of t_0, then we can proceed as before and obtain to leading order[25] in $\frac{1}{N}$

$$\int_\gamma dz\, e^{-NF(z)} = e^{-NF(z_0)} \sqrt{\frac{2\pi}{NF''(z_0)}} + \mathcal{O}\left(N^{-\frac{3}{2}}\right), \tag{C.6}$$

where we have to choose the square root which points in the direction of $\dot{\gamma}(t_0)$. The requirement $\operatorname{Im} F(\gamma(t)) = \text{const}$ in some finite interval around t_0 is equivalent to the condition that $\gamma(t)$ is a path of steepest descent for $\operatorname{Re} F(\gamma(t))$ through the saddle point z_0. In the vicinity of the saddle point, $\operatorname{Re} F(\gamma(t))$ decreases as fast as possible for $t < t_0$ and increases as fast as possible for $t > t_0$. Therefore, the saddle-point approximation method is often referred to as the method of steepest descent.

The saddle-point method can be used to evaluate integrals along every other path $\alpha(t)$ that can be deformed to the special path $\gamma(t)$ (satisfying the above conditions) if the deformation leaves the integral unchanged due to Cauchy's integral theorem,

$$\int_\alpha dz\, e^{-NF(z)} = \int_\gamma dz\, e^{-NF(z)}. \tag{C.7}$$

Obviously, the deformation from α to γ has to take place in the domain where $F(z)$ is analytic. For Cauchy's integral theorem to apply, the endpoints of α and γ have to be identical, however, since we are using the saddle-point method to approximate the integral along the path γ, it is sufficient in this case that the end points of α and γ are located in the same valleys[26] of $-\operatorname{Re} F(z)$. (In this case, the paths connecting the end points of α and γ are irrelevant.)

D Grassmann integrals

D.1 Basic properties of Grassmann numbers

The basic feature of Grassmann variables is that they anticommute. This means that for any two Grassmann numbers θ and η, we have

$$\theta\eta = -\eta\theta. \tag{D.1}$$

Addition of Grassmann numbers and multiplication with ordinary complex numbers fulfill all the requirements of an ordinary vector space. Obviously, the square of any Grassmann number is zero, and a product of two Grassmann numbers commutes with any other Grassmann number. If we consider a general function f which can be expanded in a Taylor series, then $f(\theta)$ terminates after the linear term in θ.

[24] $\operatorname{Re} F$ and $\operatorname{Im} F$ cannot have a local maximum or minimum at z_0, only saddle points are possible due to the analyticity of F.

[25] Subleading terms can also be obtained as before.

[26] A region with $\operatorname{Re} F(z) > \operatorname{Re} F(z_0) - \delta$ for some finite $\delta > 0$.

Therefore, integration over a Grassmann variable θ is completely defined by requiring

$$\int d\eta = 0 \tag{D.2a}$$

and

$$\int d\eta\, \eta = 1\,. \tag{D.2b}$$

Integrals over Grassmann numbers are invariant under linear shifts $\eta \to \eta + \theta$.

For a multiple integral over more than one Grassmann number, we use the convention that the innermost integral is performed first,

$$\int d\theta d\eta\ \eta\theta = 1\,. \tag{D.3}$$

D.2 Multi-dimensional integrals

Let α and $\bar{\alpha}$ be N-dimensional vectors with (independent) components α_j and $\bar{\alpha}_j$, $1 \leq j \leq N$. Scalar products are implicitly assumed in expressions like

$$\bar{\alpha}\alpha = \sum_{i=1}^{N} \bar{\alpha}_i \alpha_i = -\alpha\bar{\alpha} \tag{D.4}$$

and (with a complex $N \times N$ matrix A)

$$\bar{\alpha}A\alpha = \sum_{i,j=1}^{N} \bar{\alpha}_i A_{ij} \alpha_j = -\alpha A^T \bar{\alpha}\,. \tag{D.5}$$

We use the following conventions for integration measures in integrals over vectors of Grassmann numbers:

$$[d\alpha] = d\alpha_N d\alpha_{N-1} \dots d\alpha_1\,, \tag{D.6}$$

$$[d\bar{\alpha}] = d\bar{\alpha}_N d\bar{\alpha}_{N-1} \dots d\bar{\alpha}_1\,, \tag{D.7}$$

$$[d\alpha d\bar{\alpha}] = d\alpha_N d\bar{\alpha}_N d\alpha_{N-1} d\bar{\alpha}_{N-1} \dots d\alpha_1 d\bar{\alpha}_1 = (-1)^{\frac{1}{2}N(N-1)} [d\alpha][d\bar{\alpha}]\,. \tag{D.8}$$

With these conventions, we obtain for an arbitrary complex $N \times N$ matrix A,

$$\int [d\alpha d\bar{\alpha}] e^{\bar{\alpha}A\alpha} = \int [d\alpha d\bar{\alpha}] e^{\sum_{1\leq i,j\leq N} \bar{\alpha}_i A_{ij} \alpha_j} = \det A\,. \tag{D.9}$$

The above identity follows by expanding the exponential in powers of $\bar{\alpha}A\alpha$. Due to the definition of Grassmann integrals, cf. Eq (D.2), only the term of order N in this expansion can contribute to the integral. Furthermore, a non-vanishing result is only obtained for those terms where each component α_i, $\bar{\alpha}_j$ appears exactly once,

$$\begin{aligned}
\int [d\alpha d\bar{\alpha}] e^{\bar{\alpha}A\alpha} &= \int [d\alpha d\bar{\alpha}] \frac{1}{N!} (\bar{\alpha}A\alpha)^N \\
&= \int [d\alpha d\bar{\alpha}] \sum_{\text{perm.}\ p\in S_n} \bar{\alpha}_1 A_{1,p(1)} \alpha_{p(1)} \cdots \bar{\alpha}_N A_{N,p(N)} \alpha_{p(N)} \\
&= \sum_{p\in S_n} \operatorname{sign}(p) A_{1,p(1)} \cdots A_{N,p(N)} \int [d\alpha d\bar{\alpha}] \bar{\alpha}_1 \alpha_1 \cdots \bar{\alpha}_N \alpha_N \\
&= \sum_{p\in S_n} \operatorname{sign}(p) A_{1,p(1)} \cdots A_{N,p(N)} = \det(A)\,,
\end{aligned} \tag{D.10}$$

where sign(p) results from bringing the integration variables into the canonical order $\bar{\alpha}_1\alpha_1\cdots\bar{\alpha}_N\alpha_N$.

Next, we calculate the integral

$$J(w;\alpha,\beta) = \int [d\psi d\bar{\psi}] e^{w\bar{\psi}\psi - \bar{\psi}\beta - \alpha\psi}\,, \tag{D.11}$$

where w is a complex number and ψ, $\bar{\psi}$, α, β are N-dimensional Grassmann vectors. Since we can shift the integration variables ψ_i and $\bar{\psi}_j$, and pairs of Grassmann numbers commute with each other, we obtain

$$\begin{aligned} J(w;\alpha,\beta) &= \int [d\psi d\bar{\psi}] e^{w\left(\bar{\psi}-\frac{1}{w}\alpha\right)\left(\psi-\frac{1}{w}\beta\right)-\frac{1}{w}\alpha\beta} \\ &= \int [d\psi d\bar{\psi}] e^{w\bar{\psi}\psi} e^{-\frac{1}{w}\alpha\beta} = w^N e^{-\frac{1}{w}\alpha\beta}\,. \end{aligned} \tag{D.12}$$

Finally, we provide a proof for Eq. (11.12), which reads

$$I_n(X_1, X_2, \ldots, X_n) = \det(w^n - W)\,, \tag{D.13}$$

where

$$I_n(X_1, X_2, \ldots, X_n) = \int \prod_{j=1}^{n} [d\psi_j d\bar{\psi}_j] e^{w\sum_{j=1}^{n}\bar{\psi}_j\psi_j - \sum_{j=1}^{n}\bar{\psi}_j X_j \psi_{j+1}}\,. \tag{D.14}$$

One can prove this by induction in n. For $n = 1$ the result is trivial, cf. Eq. (D.9). Assuming $n \geq 2$, we integrate over the pair $\bar{\psi}_n\psi_n$. With Eq. (D.12) we obtain

$$\int \left[d\psi_n d\bar{\psi}_n\right] e^{w\bar{\psi}_n\psi_n - \bar{\psi}_n(X_n\psi_1) - \left(\bar{\psi}_{n-1}X_{n-1}\right)\psi_n} = w^N e^{-\frac{1}{w}\bar{\psi}_{n-1}X_{n-1}X_n\psi_1}\,. \tag{D.15}$$

This leads to the recursion relation

$$w^N I_{n-1}\left(X_1, X_2, \ldots, X_{n-2}, \frac{X_{n-1}X_n}{w}\right) = I_n(X_1, X_2, \ldots, X_n)\,. \tag{D.16}$$

Assuming that the claim holds for $n-1$, we get

$$\begin{aligned} I_n(X_1, X_2, \ldots, X_n) &= w^N \det\left(w^{n-1} - X_1X_2\cdots X_{n-2}\frac{X_{n-1}X_n}{w}\right) \\ &= \det\left(w^n - X_1X_2\cdots X_n\right)\,, \end{aligned} \tag{D.17}$$

which means that it also holds for n, and this concludes the proof.

References

[1] B. Durhuus and P. Olesen, *The spectral density for two-dimensional continuum QCD*, Nucl. Phys. B184 (1981) 461.

[2] R. Narayanan and H. Neuberger, *Universality of large N phase transitions in Wilson loop operators in two and three dimensions*, JHEP 12 (2007) 066, `arXiv:0711.4551 [hep-th]`.

[3] E. Gudowska-Nowak, R. A. Janik, J. Jurkiewicz, and M. A. Nowak, *Infinite Products of Large Random Matrices and Matrix-valued Diffusion*, Nucl. Phys. B670 (2003) 479, `arXiv:math-ph/0304032`.

[4] H. Georgi, *Lie Algebras in Particle Physics*. Westview Press, Boulder, Co., 1999.

[5] T. Wettig, *Group theory for physicists*. Lecture notes, Regensburg, 2006.

[6] M. Hamermesh, *Group theory and its application to physical problems*. Addison-Wesley Publishing Company, Reading, Massachusetts, 1962.

[7] M. Peskin and D. Schroeder, *An Introduction to Quantum Field Theory*. Westview Press, Boulder, Co., 1995.

[8] A. Zee, *Quantum field theory in a nutshell*. Princeton University Press, Princeton, NJ, 2003.

[9] M. Maggiore, *A Modern Introduction to Quantum Field Theory*. Oxford University Press, Oxford, 2005.

[10] L. Ryder, *Quantum Field Theory*. Cambridge University Press, Cambridge, 2006.

[11] I. Montvay and G. Münster, *Quantum Fields on a Lattice*. Cambridge University Press, Cambridge, 1997.

[12] H. Rothe, *Lattice Gauge Theories, An Introduction*. World Scientific, Singapore, 1997.

[13] F. Halzen and A. Martin, *Quarks and Leptons: An Introductory Course in Modern Particle Physics*. John Wiley & Sons, New York, 1984.

[14] J. Zinn-Justin, *Quantum field theory and critical phenomena*. Clarendon Press, Oxford, 2003.

[15] H. Neuberger, *Large N phase transitions under scaling and their uses*, `arXiv:0906.5299 [hep-th]`.

[16] V. S. Dotsenko and S. N. Vergeles, *Renormalizability of Phase Factors in the Nonabelian Gauge Theory*, Nucl. Phys. B169 (1980) 527.

[17] Y. M. Makeenko, *Methods of contemporary gauge theory*. Cambridge University Press, Cambridge, 2002.

[18] G. S. Bali, *QCD forces and heavy quark bound states*, Phys. Rept. 343 (2001) 1, `arXiv:hep-ph/0001312`.

[19] G. 't Hooft, *A planar diagram theory for strong interactions*, Nucl. Phys. B72 (1974) 461.

[20] Y. M. Makeenko, *Large-N gauge theories*, arXiv:hep-th/0001047.

[21] M. Teper, *Large N*, PoS LAT2008 (2008) 022, arXiv:0812.0085 [hep-lat].

[22] R. Narayanan, *Continuum reduction in large N gauge theories*, arXiv:0910.3711 [hep-lat].

[23] E. Witten, *The 1/N expansion in atomic and particle physics.* Recent developments in gauge theories, eds. G. 't Hooft et al. Plenum Press, New York, 1980.

[24] S. Coleman, *Asepcts of symmetry.* Cambridge Univ. Press, Cambridge, 1988.

[25] R. Gopakumar, *The master field revisited*, Nucl. Phys. Proc. Suppl. 45B (1996) 244.

[26] Y. M. Makeenko and A. A. Migdal, *Exact Equation for the Loop Average in Multicolor QCD*, Phys. Lett. B88 (1979) 135.

[27] G. 't Hooft, *A Two-Dimensional Model for Mesons*, Nucl. Phys. B75 (1974) 461.

[28] D. J. Gross and E. Witten, *Possible third-order phase transition in the large-N lattice gauge theory*, Phys. Rev. D 21 (1980) 446.

[29] M. Abramowitz and I. Stegun, *Pocketbook of mathematical functions.* Verlag Harri Deutsch, Thun/Frankfurt am Main, 1984.

[30] I. Bars and F. Green, *Complete integration of U(N) lattice gauge theory in a large N limit*, Phys. Rev. D20 (1979) 3311.

[31] P. Menotti and E. Onofri, *The action of SU(N) lattice gauge theory in terms of the heat kernel on the group manifold*, Nucl. Phys. B190 (1981) 288.

[32] J. M. Drouffe, *Transitions and duality in gauge lattices systems*, Phys. Rev. D18 (1978) 1174.

[33] A. A. Migdal, *Recursion equations in gauge field theories*, Sov. Phys. JETP 42 (1975) 413.

[34] B. Durhuus and P. Olesen, *Eigenvalues of the Wilson operator in mutlticolor QCD*, Nucl. Phys. B184 (1981) 406.

[35] J.-P. Blaizot and M. A. Nowak, *Large N_c Confinement, Universal Shocks and Random Matrices*, arXiv:0911.3683 [hep-th].

[36] P. Olesen, *A Linear Equation for Wilson Loops*, Phys. Lett. B660 (2008) 597, arXiv:0712.0923 [hep-th].

[37] P. Rossi, *Continuum QCD in two-dimensions from a fixed point lattice action*, Ann. Phys. 132 (1981) 463.

[38] V. A. Kazakov and I. K. Kostov, *Nonlinear strings in two-dimensional U(∞) gauge theory*, Nucl. Phys. B176 (1980) 199.

[39] P. Olesen, *Tunneling in two dimensional QCD*, Nucl. Phys. B752 (2006) 197, arXiv:hep-th/0606153.

[40] H. Neuberger, *Burgers' equation in 2D SU(N) YM*, Phys. Lett. B666 (2008) 106, arXiv:0806.0149 [hep-th].

[41] J.-P. Blaizot and M. A. Nowak, *Large N_c confinement and turbulence*, Phys. Rev. Lett. 101 (2008) 102001, arXiv:0801.1859 [hep-th].

[42] J.-P. Blaizot and M. A. Nowak, *Universal shocks in random matrix theory*, arXiv:0902.2223 [hep-th].

[43] R. A. Janik and W. Wieczorek, *Multiplying unitary random matrices – universality and spectral properties*, J. Phys. A: Math. Gen. 37 (2004) 6521.

[44] D. Voiculescu, K. Dykema, and A. Nica, *Free random variables, CRM Monograph Series, Volume 1.* American Mathematical Society, 2002.

[45] R. Narayanan and H. Neuberger, *Infinite N phase transitions in continuum Wilson loop operators*, JHEP 03 (2006) 064, arXiv:hep-th/0601210.

[46] R. Narayanan, H. Neuberger, and E. Vicari, *A large N phase transition in the continuum two dimensional SU(N) X SU(N) principal chiral model*, JHEP 04 (2008) 094, arXiv:0803.3833 [hep-th].

[47] H. Neuberger, *Complex Burgers' equation in 2D SU(N) YM*, Phys. Lett. B670 (2008) 235, arXiv:0809.1238 [hep-th].

[48] R. Lohmayer, H. Neuberger, and T. Wettig, *Eigenvalue density of Wilson loops in 2D SU(N) YM*, JHEP 05 (2009) 107, arXiv:0904.4116 [hep-lat].

[49] R. Lohmayer, H. Neuberger, and T. Wettig, *Possible large-N transitions for complex Wilson loop matrices*, JHEP 11 (2008) 053, arXiv:0810.1058 [hep-th].

[50] A. M. Perelomov and V. M. Popov, *Casimir operators for the unitary group*, JETP Letters 1 (1965) 160.

[51] R. Lohmayer, *Eigenvalue density of Wilson loops in 2D SU(N) YM at large N*, Acta Physica Polonica B Proceedings Supplement 2 (2009) 473, arXiv:0910.3264 [hep-th].

[52] M. L. Mehta, *Random Matrices.* Academic Press, San Diego, 2nd ed., 1991.

[53] H. S. Wilf, *Mathematics for the Physical Sciences.* Dover, 1978.

[54] G. Szegö, *Orthogonal Polynomials.* American Mathematical Society, Providence, RI, 1991.

[55] D. Senouf, *Asymptotic and numerical approximations of the zeros of Fourier integrals*, SIAM J. Math. Anal. 27 (1996) 1102.

[56] G. V. Dunne, *Negative dimensional groups in quantum physics*, J. Phys. A22 (1989) 1719.

[57] V. Pestun, *Localization of gauge theory on a four-sphere and supersymmetric Wilson loops*, arXiv:0712.2824 [hep-th].

[58] J. K. Erickson, G. W. Semenoff, and K. Zarembo, *Wilson loops in N = 4 supersymmetric Yang-Mills theory*, Nucl. Phys. B582 (2000) 155, arXiv:hep-th/0003055.

[59] A. Crisanti, G. Paladin, and A. Vulpiani, *Products of Random Matrices.* Springer-Verlag, Berlin, 1993.

[60] J. Feinberg, R. Scalettar, and A. Zee, *Single ring theorem and the disk-annulus phase transition*, J. Math. Phys. 42 (2001) 5718.

[61] C. W. Gardiner, *Handbook of Stochastic Methods for Physics, Chemistry and the Natural Sciences*. Springer-Verlag, Berlin, 1990.

[62] A. D. Jackson, B. Lautrup, P. Johansen, and M. Nielsen, *Products of Random Matrices*, Phys. Rev. E 66 (2002) 066124, `arXiv:physics/0202037`.

[63] P. Bougerol and J. Lacroix, *Products of Random Matrices with Applications to Schrödinger Operators*. Birkhäuser, Boston, 1985.

[64] J. E. Cohen and C. M. Newman, *The Stability of Large Random Matrices and Their Products*, The Annals of Probability 12 (1984) 283.

[65] J. E. Cohen, *Subadditivity, Generalized Products of Random Matrices and Operations Research*, SIAM Review 30 (1989) 69.

[66] R. A. Horn and D. R. Johnson, *Matrix Analysis*. Cambridge University Press, Cambridge, 1999.

[67] I. Goldhirsch, P.-L. Sulem, and S. A. Orszag, *Stability and Lyapunov Stability of Dynamical Systems: A Differential Approach and a Numerical Method*, Physica 27D (1987) 311.

[68] J. Ginibre, *Statistical Ensembles of Complex, Quaternion, and Real Matrices*, J. Math. Phys. 6 (1965) 440.

[69] Y. V. Fyodorov, B. A. Khoruzhenko, and H.-J. Sommers, *Almost Hermitian Random Matrices: Crossover from Wigner-Dyson to Ginibre Eigenvalue Statistics*, Phys. Rev. Lett. 79 (1997) 557.

[70] R. Lohmayer, H. Neuberger, A. Schwimmer, and S. Theisen, *Numerical determination of entanglement entropy for a sphere*, Phys. Lett. B685 (2010) 222, `arXiv:0911.4283 [hep-lat]`.

[71] M. Srednicki, *Entropy and area*, Phys. Rev. Lett. 71 (1993) 666, `arXiv:hep-th/9303048`.

[72] H. Casini and M. Huerta, *Entanglement entropy in free quantum field theory*, J. Phys. A42 (2009) 504007, `arXiv:0905.2562 [hep-th]`.

[73] W. Wootters, *Entanglement of formation and concurrence*, Quantum Information and Computation Vol. 1, No. 1 (2001) 27.

[74] L. Bombelli, R. K. Koul, J. Lee, and R. D. Sorkin, *Quantum source of entropy for black holes*, Phys. Rev. D34 (1986) 373.

[75] S. W. Hawking and W. Israel, eds., *General Relativity: An Einstein Centenary Survey*. Cambridge University Press, Cambridge, 1979.

[76] T. Nishioka, S. Ryu, and T. Takayanagi, *Holographic entanglement entropy: an overview*, J. Phys. A42 (2009) 504008, `arXiv:0905.0932 [hep-th]`.

[77] S. N. Solodukhin, *Entanglement entropy, conformal invariance and extrinsic geometry*, Phys. Lett. B665 (2008) 305–309, `arXiv:0802.3117 [hep-th]`.

[78] A. Schwimmer and S. Theisen, *Entanglement entropy, trace anomalies and holography*, Nucl. Phys. B801 (2008) 1, arXiv:0802.1017 [hep-th].

[79] K. Jäenich, *Analysis für Physiker und Ingenieure*. Springer-Verlag, Berlin, 2001.